

SOME STUDIES ON OPTICAL PROPERTIES  
OF THIN FILMS

A Thesis submitted to the  
UNIVERSITY OF POONA  
for the degree of  
DOCTOR OF PHILOSOPHY  
IN PHYSICS

By

B. Venkatesha Rao, M. Sc.

Electron Diffraction and Thin Film Laboratory

NATIONAL CHEMICAL LABORATORY

POONA 8

September 1973

C O N T E N T S

<u>Chapter</u>	<u>Title</u>	<u>Page No.</u>
I.	<u>GENERAL INTRODUCTION</u>	
	(A) Thin films, their nature, structures and properties. ..	1
	(B) Electromagnetic theory of wave propagation. ..	5
	(C) Dispersion theory. ..	10
	(D) Absorption. ..	15
	(E) Optical constants of thin films ..	18
	(F) Theory of reflection and transmission by a single film. ..	20
	(G) Principle methods for determining optical constants. ..	25
II.	<u>EXPERIMENTAL TECHNIQUES</u>	
	(A) Preparation of thin films. ..	31
	(B) Substrates. ..	32
	(C) Deposition at higher substrate temperatures. ..	33
	(D) Annealing of films in vacuo. ..	34
	(E) Measurement of film thickness. ..	34
	(F) Spectrophotometer. ..	36
	(G) Measurement of transmittance, reflectance, etc. ..	39
	(H) Measurement of optical constants. ..	40
	(I) Absorption coefficient. ..	43

<u>Chapter</u>	<u>Title</u>	<u>Page No.</u>
II.	(J) Dielectric constant. ..	44
	(K) Electron diffraction studies. ..	45
III.	<u>STUDIES ON COPPER AND CHROMIUM FILMS</u>	
	(A) Introduction. ..	48
	(B) Experimental. ..	55
	(C) Results.	
	(a) Copper films. ..	56
	(b) Chromium films. ..	57
	(D) Discussion. ..	59
IV.	<u>STUDIES ON SELENIUM AND TELLURIUM FILMS</u>	
	(A) Introduction. ..	67
	(B) Experimental. ..	76
	(C) Results.	
	(a) Selenium films. ..	77
	(b) Tellurium films. ..	79
	(D) Discussion. ..	81
V.	<u>STUDIES ON OXIDES OF COPPER FILMS</u>	
	(A) Introduction. ..	86
	(B) Experimental. ..	92
	(C) Results.	
	(a) Cuprous oxide films. ..	94

<u>Chapter</u>	<u>Title</u>		<u>Page No.</u>
V.	(b) Copper oxide films.	..	97
	(c) Cupric oxide films.	..	100
	(D) Discussion.	..	103
VI.	<u>STUDIES ON SULPHIDES OF COPPER FILMS</u>		
	(A) Introduction.	..	110
	(B) Experimental.	..	114
	(C) Results.		
	(a) Cuprous sulphide films.	..	115
	(b) Copper sulphide films.	..	119
	(D) Discussion.	..	122
VII.	<u>STUDIES ON CUPROUS SELENIDE AND CUPROUS TELLURIDE FILMS</u>		
	(A) Introduction.	..	129
	(B) Experimental.	..	136
	(C) Results.		
	(a) Cuprous selenide films.	..	139
	(b) Cuprous telluride films.	..	142
	(D) Discussion.	..	146
VIII.	<u>STUDIES ON INDIUM ARSENIDE FILMS</u>		
	(A) Introduction.	..	153
	(B) Experimental.	..	158
	(C) Results	..	159
	(D) Discussion.	..	161



<u>Chapter</u>	<u>Title</u>	<u>Page No.</u>
IX.	<u>SUMMARY AND CONCLUSIONS</u>	.. 166
	<u>ACKNOWLEDGEMENT</u>	
	<u>REFERENCES</u>	

## CHAPTER I

### GENERAL INTRODUCTION

#### (A) THIN FILMS, THEIR NATURE, STRUCTURES AND PROPERTIES

In recent years a keen interest has developed in thin films of metals, semiconductors and dielectrics owing to a number of practical applications in various fields and also because of modern trends towards the microminiaturisation of electronic devices. Thin films are extensively used in the preparations of reflectors, antireflection coatings, protective layers, fluorescent screens, optical interference filters, polarisers, photocells and in many semiconducting devices e.g. field triodes, thin film transistors, thin film integrated circuits, switching circuits, etc. Intensive researches are still in progress to find out newer and better materials with desirable properties for newer applications.

In the ideal case of a solid film, matter is uniformly distributed between two parallel planes extended infinitely in these two directions, however the dimension of the material is restricted along the third direction i.e. along thickness ( $d$ ). Thickness can however vary from the limit  $d \sim 0$  to several times

the wavelength of light, but always less than the other two dimensions. In reality these solid films deviate from the idealised cases since these two planes in most cases are not exactly parallel as a result of the surface asperities due to the growth conditions and further there may also be present voids, discontinuities, dislocations, stacking faults, grain boundaries, new phases, etc. in the films thus causing uneven distribution of matter in these films.

Solid thin films may be prepared by various methods namely, chemical deposition, electrodeposition, anodic oxidation, cathode sputtering reactive or otherwise, vacuum evaporation, etc. The vacuum evaporation method is most commonly used because of the ease with which the process may be controlled. The properties such as structural, electrical, optical, etc. of vacuum deposited films are generally dependent upon the evaporation conditions viz. nature and presence of the residual gas, the rate of deposition, substrate temperatures, the purity of the sample, new phase formation, etc. It is now well known that materials in the thin film state behave differently from the bulk. Even highly conducting materials like sodium, potassium, rubidium and cesium showed negative temperature coefficient of resistance, when they are in the thin

film state, similar to semiconductors (Mayer, 1959, 1961). Similarly thin bismuth films unlike the bulk showed superconductivity (Buckel and Hilsch, 1954).

During the last two decades interest in the optical and other properties of thin films has grown considerably. Developments in the technique of producing and studying thin films have enabled better understanding of the nature of films, conduction mechanism, optical behaviour, etc. The results of early workers on the optical properties of films often showed large difference from those of bulk materials. This was particularly true for absorbing materials such as metallic films thus suggesting that the physical state of the metallic films may be different from the bulk. Very thin films are often agglomerated to form discrete islands. This has been shown by the electron microscopic studies (Piccard and Duffendeck, 1943; Hass, 1942; Senett and Scott, 1960; Pashley, 1959).

Investigations on optical properties of thin films deal primarily with optical transmission, reflection and absorption properties and their dependence on film thickness and the wavelength of the incident light. The reflected, transmitted and interferometric properties of thin films made it possible to evaluate

the optical constants viz. refractive index ( $n$ ) and extinction coefficient ( $k$ ) or the real ( $\epsilon_1$ ) and imaginary ( $\epsilon_2$ ) parts of the complex dielectric constant ( $\epsilon^*$ ) which is a basic and essential parameter to obtain the information concerning the electronic structure of the material. The refractive index is also needed for the analysis of the photoemissive properties to get the information about the electronic structure (Kroliskowski, 1969). Refractive index is an important quantity for understanding the chemical bonding (Van Vachten, 1969; Wemple and Didomenico, 1971). From the absorption studies it is possible to determine the absorption edge, optical energy band gap, optical transitions direct or indirect, allowed or forbidden and in fact this is comparatively a simpler technique to study band structures than by the electrical methods. The interaction of electromagnetic wave in the present case optical waves with matter may cause several transition processes such as band to band, between sub-bands, between impurities and band, transition by free carriers, transition of free carriers within a band, resonance due to lattices vibration impurities, etc. Hence a detailed study of the absorption band spectra is likely to give a wealth of information about the band structure of the thin film material. Since

these pictures and band structures are the consequence of the interaction of electromagnetic wave with the solid material modifying the wave propagation in the process, in the subsequent paragraphs a brief summary of the above pertaining to our work is given.

(B) ELECTROMAGNETIC THEORY OF WAVE PROPAGATION

Maxwells mathematical treatment of the electromagnetic field showed a connection between electromagnetism and optics. The space and time derivatives of the different vectors are related by the Maxwell's material equations.

$$\text{Curl } \bar{E} = - \frac{1}{c} \frac{\partial \bar{D}}{\partial t} \quad \dots \quad (1a)$$

$$\text{Curl } \bar{H} = \frac{1}{c} \frac{\partial \bar{D}}{\partial t} + \frac{4\pi}{c} \bar{J} \quad \dots \quad (1b)$$

$$\text{div } \bar{D} = 4\pi \rho \quad \dots \quad (1c)$$

$$\text{div } \bar{B} = 0 \quad \dots \quad (1d)$$

where vector  $\bar{E}$  is the electric field,  $\bar{H}$ , magnetic field;  $\bar{D}$ , displacement caused by  $\bar{E}$ ;  $\bar{B}$ , magnetic induction and  $\bar{J}$  electric current density; the scalar  $\rho$  is the electric charge density and  $c$ , the velocity of light in vacuo. The above vectors are further related to others by

$$\bar{J} = \sigma \bar{E}, \bar{D} = \epsilon \bar{E} \text{ and } \bar{B} = \mu \bar{H}$$

where  $\sigma$  is the specific conductivity,  $\epsilon$ , the permittivity (dielectric constant) and  $\mu$ , the magnetic permeability. For a nonconducting medium  $\sigma = 0$  and  $\bar{J} = 0$ , hence we have

$$\text{Curl } \bar{E} = \frac{\mu}{c} \frac{\partial \bar{H}}{\partial t} \quad \dots \quad (2a)$$

$$\text{Curl } \bar{H} = \frac{\epsilon}{c} \frac{\partial \bar{E}}{\partial t} \quad \dots \quad (2b)$$

$$\text{div } \bar{D} = 0 \quad \dots \quad (2c)$$

$$\text{div } \bar{B} = 0 \quad \dots \quad (2d)$$

From the above simplified relations it can be shown that for a homogeneous and isotropic medium, the propagation of electromagnetic wave can be represented by

$$\nabla^2 \bar{E} - \frac{\epsilon \mu}{c^2} \frac{\partial^2 \bar{E}}{\partial t^2} = 0 \quad \dots \quad (3a)$$

and

$$\nabla^2 \bar{H} - \frac{\epsilon \mu}{c^2} \frac{\partial^2 \bar{H}}{\partial t^2} = 0 \quad \dots \quad (3b)$$

In the case of non magnetic materials  $\mu = 1$   $v = c/\sqrt{\epsilon}$   
 where the wave velocity  $v = c/\sqrt{\epsilon}$  since  $\mu = 1$ . In

vacuo  $\epsilon = 1$  and hence the wave velocity will be  $c$ . Since refractive index ( $n$ ) is given by the ratio of the velocity of electromagnetic wave in vacuo to that in the medium, then

$$n = c/v = \sqrt{\epsilon} \quad \dots \quad (4)$$

It has so far been assumed that the refractive index is a real quantity. But this is not so and it depends on the dielectric constant which is a complex quantity. Hence the equation (4) should be modified to

$$n^* = n - ik = \sqrt{\epsilon^*} = \sqrt{\epsilon_1 - i\epsilon_2} \quad \dots \quad (5)$$

and  $n$  is the real part of complex refractive index  $k$  is the imaginary part of the refractive index and called the extinction coefficient/index. Hence

$$n^2 - k^2 = \epsilon_1 \quad \dots \quad (6a)$$

$$2nk = \epsilon_2 \quad \dots \quad (6b)$$

The extinction coefficient ( $k$ ) is also related to absorption coefficient ( $\alpha$ ) by the equation

$$k = \frac{\lambda \alpha}{4\pi} \quad \dots \quad (7)$$



Further,  $\alpha$  is related to intensity of light by the Lambert's law.

$$I = I_0 \exp(-\alpha x) \quad \dots \quad (8)$$

where  $x$  is the distance through which the electromagnetic waves travel to change its intensity from  $I_0$  to  $I$ .

For the time varying fields the wave equation can be written as

$$\nabla^2 \bar{E} + \frac{\omega^2 \epsilon \mu}{c^2} \bar{E} = 0 \quad \dots \quad (9a)$$

or

$$\nabla^2 \bar{E} + K^2 \bar{E} = 0 \quad (9b)$$

where  $\partial^2 / \partial t^2$  is replaced by  $-\omega^2$  and  $K = \frac{\omega}{c} (\epsilon \mu)^{\frac{1}{2}}$ ;  $\omega/c$ , called wave number and  $\bar{E}$  is a complex quantity which is dependent on the  $x$  component of the scalar equation

$$\frac{\partial^2 E}{\partial x^2} + K^2 E_x = 0 \quad \dots \quad (10)$$

The solution of  $E$  takes the form

$$E = E_0 \exp(iK(\bar{r} \cdot \bar{s}) - t) \quad \dots \quad (11)$$

In the case of the conducting medium,  $\text{div } \bar{E} = 0$   
since  $\rho$  is zero,

Hence the equation (3a) takes the form

$$\nabla^2 \bar{E} + \frac{\mu \epsilon \partial^2 \bar{E}}{c^2 \partial t^2} + \frac{4\pi \mu \sigma}{c^2} \frac{\partial \bar{E}}{\partial t} = 0 \dots \quad (12)$$

the last term in the equation is a damping factor  
indicating the attenuation of the electromagnetic wave.  
The above equation (12) can be represented by

$$\nabla^2 \bar{E} + K^2 \bar{E} = 0 \quad \dots \quad (13)$$

$$\text{where } K^2 = \frac{\omega^2 \mu}{c^2} \left( \epsilon + \frac{1}{\omega} \frac{4\pi \sigma}{\omega} \right)$$

This equation is identical with the previous equation (4)  
where  $\epsilon$  is replaced  $\epsilon^*$  given by

$$\epsilon^* = \epsilon + \frac{1}{\omega} \frac{4\pi \sigma}{\omega} \quad \dots \quad (14)$$

$$\text{In this case, } n^* = \sqrt{\mu \epsilon^*} = \frac{c}{\omega} K \quad \dots \quad (14a)$$

$$n^2 - k^2 = \mu \epsilon \quad \dots \quad (15a)$$

$$nk = - \frac{2\pi \mu \sigma}{\omega} = \frac{\mu \sigma}{\nu} \quad \dots \quad (15b)$$

As  $\sigma \rightarrow 0$ ,  $k \rightarrow 0$ , and  $n^2 = \mu \epsilon$

(C) DISPERSION THEORY

In the above relation it is seen that the refractive index  $n^*$  is a complex quantity depending on the frequency ( $\omega$ ).

No material is transparent in all frequencies and hence there will be some sort of absorptions in the same region of the spectrum. Insulating materials have lower absorption than the metallic films in the visible region except for the narrow region of selective absorptions. The interactions of electromagnetic waves with the band electron of the dielectric medium result in the displacements from the equilibrium position causing some loss of the energy of the electromagnetic waves during its passage through the dielectric medium. This later effect in the dielectric material has been assumed to be represented by a damping force given by the quantity  $mg \cdot dx/dt$  in the equation of motion

$$m \frac{d^2 x}{dt^2} + mg \frac{dx}{dt} + m \omega_0^2 x = eEe^{i\omega t} \quad \dots (16)$$

where  $m \omega_0^2 x$  is the restoring force and  $\omega_0$  is the natural frequency of the electron. The solution of the above equation in the frequency  $\omega_0$  is given by

$$x = \frac{eE/m}{\omega_0^2 + \omega^2 + i\omega g} \quad \dots \quad (17)$$

It is seen that the above is sinusoidal with the applied frequency.

Now correlating the polarisability (P) with x is given by the relation

$$P = Nex/E$$

where N is the number of electrons per unit volume. The complex dielectric constant is then given by (Moss, 1959).

$$\epsilon^* = 1 + P/\epsilon \quad \dots \quad (18)$$

$$\epsilon^* = (n-ik)^2 = \frac{Ne^2/m\epsilon}{\omega_0^2 - \omega^2 + i\omega g} + 1 \quad \dots \quad (19)$$

$$n^2 - k^2 = \frac{Ne^2}{m\epsilon} \left\{ \frac{\omega_0^2 - \omega^2}{(\omega_0^2 - \omega^2)^2 + \omega^2 g^2} \right\} + 1 \quad \dots \quad (20a)$$

$$2nk = \frac{Ne^2}{m\epsilon} \left\{ \frac{\omega g}{(\omega_0^2 - \omega^2)^2 + \omega^2 g^2} \right\} \quad \dots \quad (20b)$$

These equations relate the variation of  $n$  and  $k$  with frequency and is usually known as dispersion relations. The consequences of these are that when  $\omega$  is nearly equal to  $\omega_0$  the absorption is maximum and that on decreasing  $\omega_0$  through this region,  $n$  increases rapidly. It then passes through a maximum and falls asymptotally as the frequency is moved away from  $\omega_0$ .

Similar results can also be derived with a detailed quantum mechanical treatment of dispersion relation (Rosenfield, 1951; Mott and Jones, 1936 and Nozieres and Pines, 1958) by taking into account the interaction of the field with the absorbing atoms. These equations can, however, be modified as shown below:

$$n^2 - k^2 - 1 = \sum_f \frac{(Ne^2 f / m\epsilon) (\omega_j^2 - \omega^2)}{(\omega_j^2 - \omega^2)^2 + \omega_g^2} \quad \dots \quad (21a)$$

$$2nk = \sum_f \frac{(Ne^2 f / m\epsilon) \omega g}{(\omega_j^2 - \omega^2)^2 + \omega_g^2} \quad \dots \quad (21b)$$

where  $f$  is the oscillator strength. From these it is also possible to calculate the static dielectric constant of material from optical data alone (Moss, 1959). Since at a long wavelength ( $\omega_0 \rightarrow 0$ )  $k$  becomes

insignificant. Hence

$$n^2 - 1 = Ne^2 f / m \epsilon \omega_0^2 \quad \dots \quad (22)$$

According to Bode (1945) the real part,  $n^2 - k^2$  and the imaginary part,  $2nk$  at any frequency are given in the case of many oscillators by the equations

$$(n^2 - k^2)_a - 1 = \frac{2}{\pi} \int_0^{\infty} \frac{2nk\omega - a (2nk)_a}{\omega^2 - a^2} d\omega \quad \dots \quad (23a)$$

$$(2nk)_a = \frac{-2a}{\pi} \int_0^{\infty} \frac{n^2 - k^2 - (n^2 - k^2)_a}{\omega^2 - a^2} d\omega \quad \dots \quad (23b)$$

where  $a$  is the specific frequency. For  $k = 0$  i.e. for the non-conducting dielectric case the above equation leads us to

$$n^2 - 1 = \frac{2}{\pi} \int_0^{\infty} 2nk \frac{d\lambda}{\lambda} \quad \dots \quad (24)$$

when  $n = 0$

It is also possible to correlate the reflectivity maximum or minimum amplitude and phase of reflection from the above dispersion equation. The most important process viz. absorption can also be related with the refractive index in the following way. Polarizability (P)

is given by the equation

$$P = (nk)^2 - 1 = \beta \exp(-i\alpha) \quad \dots \quad (25)$$

In the case of metals it is generally assumed that natural frequency ( $\omega_0$ ) of electron is zero. Since all electrons are free to move giving rise to conductivity, there is no longer any restoring force, the equation (20a) reduce to

$$n^2 - k^2 - 1 = - (Ne^2/m\epsilon) / (\omega^2 + g^2) \quad \dots \quad (26a)$$

$$2nk\omega = (gNe^2/m\epsilon) / (\omega^2 + g^2) \quad \dots \quad (26b)$$

In the case of the steady field  $dx/dt = uE$  where  $u$  is the mobility of electron at the frequency, then  $g = e/um$  and hence equation (26b) becomes

$$2nk\omega = (\sigma/\epsilon) \left[ 1 + (\omega um/e)^2 \right] \quad \dots \quad (26c)$$

In the cases of semiconductors both bound and free electrons contribute and the complex expression for  $n^2 - k^2$  and  $nk$  would be then similar to (21b) together with terms as above (26c).

(D) ABSORPTION

The most direct and perhaps the simplest method of finding the band structure of a material is by the optical method. Electrical measurements are, however, less valuable mostly because of the fact that the effective mass influences of most of the electrical parameters through the mobility of the charge carriers and the measurement of effective charge is not always reliable since it is coupled with many other parameters. Optical phenomenon is, however, less ambiguous. Parameters like transmittance (T) and Reflectance (R) are related to  $n$ ,  $k$  and  $\alpha$  by the relations

$$R = \frac{(n-1)^2 + k^2}{(n+1)^2 + k^2} \quad \dots \quad (27a)$$

$$T = \frac{(1-R)^2 \exp(-\alpha x)}{1-R^2 \exp(-2\alpha x)} \quad \dots \quad (27b)$$

where  $x$  is the thickness of the material.

When light is absorbed by a solid two processes may take place viz. (i) the energy can be used to lift the electrons from the valence band to conduction band or (ii) it may excite the lattice vibration of the material. Consequently, the latter process (ii) gives



information regarding the bond strength of the lattice, effective charge of the lattice atoms and characteristic of the frequency of lattice vibration. By the former process (i) however it is possible to find out the band structure and consequently information about the band model.

The above process of absorption can also induce different types of transitions viz. band to band, between sub-bands, between impurities and bands, interaction with free carriers within a band, resonance due to vibrational state of lattice and impurities, etc. These lead to the appearance of absorption band in absorption spectra at or appearance of absorption peak. Hence the characteristic of the energy difference in the band can be determined by the absorption process.

The transitions especially between the valence band and conduction band can be direct or indirect. In both the cases, however, the transition can either be allowed as permitted by the transition probability or forbidden where such probability does not exist. Thus the transition probability can be related by the equation (Brooks, 1955; Dexter, 1956; Bardeen et al. 1956).

$$\alpha = A (h\nu - E_g)^p \quad \dots \quad (28)$$

where  $p$  have discrete values like  $1/2$ ,  $3/2$ ,  $2$  or more depending on whether the transitions were direct or indirect and allowed or forbidden. In the direct and allowed cases the index  $p = 1/2$  whereas for direct forbidden case it is  $3/2$ . For indirect transitions it will be  $2$  for allowed cases and  $3$  or more for forbidden ones. It is, therefore, possible to estimate the types of transition by the interaction of light quanta with electrons from the magnitude of exponent  $p$ . The value of  $p$  often depends on the presence or absence of other factors such as impurities, doping agents and in fact also on the nature of the crystallites.

In the case of indirect absorption, the absorption coefficient  $\alpha$  can be expressed in terms of light energy, energy band gap, etc., as given by the following equation (Macfarlane and Roberts, 1955).

$$\alpha = A \left[ \frac{h\nu - E_g + k\theta}{\exp \theta/T - 1} + \frac{(h\nu - E_g - k\theta)^2}{(1 - \exp(-\theta/T))} \right] \quad \dots (28a)$$

where  $E_g$  is the minimum energy gap,  $k\theta$  is the phonon energy and  $A$ , a material dependent constant. The two terms refer to the contribution due to absorption and emission respectively. In an  $\alpha^{1/2}$  vs.  $h\nu$  plot, these two terms give separate contributions with the

intercept on the energy axis equal to  $2K\theta$  and the intersection point gives approximately the value of  $E_g$ .

#### (E) OPTICAL CONSTANTS OF THIN FILMS

As mentioned before, the optical properties of any material are characterised by two parameters  $n$ , the refractive index and  $k$ , the extinction coefficient. They form the real and imaginary part of complex refractive index  $n^* = n - ik$ . The optical constants of thin films are, however, influenced by various factors, such as the rate of evaporation, the substrate temperature, crystallinity and otherwise, etc. which generally affect the electrical properties. It has been shown by several workers that the optical constants of thin films are often different from the bulk material from which it is prepared.  $n$  and  $k$  were also found to vary with film thickness and the wavelength of incident light. Druce (1894) first applied the electron theory of metal to explain the optical properties of bulk material/metal.

Maxwell-Garnett (1904) showed that the change in the optical constants of thin films from those of the bulk metal could be explained by assuming that the thinner films were composed of small aggregates comprising of spherical crystallites having diameters

smaller compared to the film dimensions and (ii) spherical particles were distributed at random and the density of the film being characterised by a packing factor  $q$ . The optical constants  $n_f$  and  $k_f$  of the films are related to  $n_b$  and  $k_b$  of the bulk material through  $q$  which is defined as the volume of metal per unit volume of the film

Then

$$k_f^2 - n_f^2 = 2 - \frac{3(1-qa)}{(1-qa)^2 + 4q^2 b^2} \quad \dots \quad (30a)$$

$$n_f k_f = \frac{3qb}{(1-qa)^2 + 4q^2 b^2} \quad \dots \quad (30b)$$

where

$$a = \frac{(k_b^2 - n_b^2 + 1)(k_b^2 - n_b^2 - 2) + 4n_b^2 k_b^2}{(k_b^2 - n_b^2 - 2) + 4k_b^2 n_b^2}$$

$$b = \frac{3n_b k_b}{(k_b^2 - n_b^2 - 2)^2 + 4n_b^2 k_b^2}$$

The value  $n_f k_f$  gives a measure of absorption

of the film. The packing factor  $q$  may be estimated by a direct examination of the electron micrographs and the theoretical value of  $n_f k_f$  may be calculated.

Male (1950, 54), Schopper (1957) and others used Maxwell-Garnett theory to explain the experimental results for the variation of the optical constants of thin film with thickness. In order to explain the variation of  $n$  with film thickness Rouard (1952) assumed the presence of air particles in the metallic films. The proportion of air particles increases as the thickness gets smaller and the value of  $n$  therefore tends to that of air as  $d \rightarrow 0$ .

(F) THEORY OF REFLECTION AND TRANSMISSION BY A SINGLE FILM

The progress of a plane wave in the medium may also be written as

$$E = E_0 \exp \left[ i \omega \left( t - \frac{n^*}{c} \cdot x \right) \right] \quad \dots \quad (31)$$

where  $n^*$  is complex, the amplitude of the wave decreases with distance which corresponds to the absorption.

Considering a parallel beam of light of unit amplitude and of wavelength  $\lambda$  falling on a plane, parallel sided homogeneous isotropic film of thickness

$d$  and refractive index  $n$  supported on a substrate  $n_2$ . Incident beam on the film is divided into reflected and transmitted parts at each time the beam strikes an interface. The transmitted and reflected beams are obtained by summing the multiple internal transmitted and reflected elements. The amplitudes of the successive reflected beams are

$r_1, t_1 t_1' r_2, -t_1 t_1' r_1 r_2^2 \dots$  and the transmitted

amplitudes are  $t_1 t_2, -t_1 t_2 r_1 r_2 \dots$ , and  $\delta$  is the

phase change on traversing the film is given by

$$= \frac{2\pi}{\lambda} n d \cos \phi \dots \quad (32)$$

The reflectance and transmittance are defined as the ratios of reflected and transmitted energy to the incident energy and are given by summing multiply reflected and transmitted beams

$$R = \frac{r_1^2 + 2r_1 r_2 \cos 2\delta + r_2^2}{1 + 2r_1 r_2 \cos 2\delta + r_1^2 r_2^2} \dots \quad (33a)$$

$$T = \frac{n_2}{n_0} \cdot \frac{t_1^2 t_2^2}{(1 + 2r_1 r_2 \cos 2\delta + r_1^2 r_2^2)} \quad \dots \quad (33b)$$

For normal incidence, Fresnel coefficients are

$$r_1 = \frac{n_0 - n_1}{n_0 + n_1}, \quad t_1 = \frac{2n_0}{n_0 + n_1}$$

$$r_2 = \frac{n_1 - n_2}{n_1 + n_2}, \quad t_2 = \frac{2n_1}{n_1 + n_2}$$

The reflectance and transmittance are given by

$$R = \frac{(n_0^2 + n_1^2)(n_1^2 + n_2^2) - 4n_0 n_1 n_2 + (n_0^2 - n_1^2)(n_1^2 - n_2^2) \cos 2\delta}{(n_0^2 + n_1^2)(n_1^2 + n_2^2) + 4n_0 n_1 n_2 + (n_0^2 - n_1^2)(n_1^2 - n_2^2) \cos 2\delta} \quad \dots \quad (34a)$$

$$T = \frac{8n_0 n_1 n_2}{(n_0^2 + n_1^2)(n_1^2 + n_2^2) + 4n_0 n_1 n_2 + (n_0^2 - n_1^2)(n_1^2 - n_2^2) \cos 2\delta} \quad \dots \quad (34b)$$

In the case of an absorbing film on a transparent substrate  $n_1$  is replaced by  $n-ik$  and the resulting expression is complicated and cumbersome and  $n$  and  $k$  are generally evaluated by programming in a

computer.

For non-normal incidence, Fresnel coefficients are

$$r_{1p} = \frac{n_0 \cos \varphi_1 - n_1 \cos \varphi_0}{n_0 \cos \varphi_1 + n_1 \cos \varphi_0} \quad \dots \quad (35a)$$

$$r_{1s} = \frac{n_0 \cos \varphi_0 - n_1 \cos \varphi_1}{n_0 \cos \varphi_0 + n_1 \cos \varphi_1} \quad \dots \quad (35b)$$

$$t_{1p} = \frac{2n_0 \cos \varphi_0}{n_0 \cos \varphi_1 + n_1 \cos \varphi_0} \quad \dots \quad (35c)$$

$$t_{1s} = \frac{2n_0 \cos \varphi_0}{n_0 \cos \varphi_0 + n_1 \cos \varphi_1} \quad \dots \quad (35d)$$

For an absorbing film  $n_1 = n - ik$  and  $\sin \varphi_1$

$$= \frac{n_0 \sin \varphi_0}{n - ik}$$

For the normal incidence case  $\varphi_0 = \varphi_1 = 0$

$$r_{1p} = r_{1s} = \frac{n_0 - n + ik}{n_0 + n - ik} \quad \dots \quad (36)$$

and the reflectance is given by



$$R_p = R_s = \frac{(n_o - n)^2 + k^2}{(n_o + n)^2 + k^2} \dots \quad (37)$$

For the non-normal incidence, exact expressions for the reflectance are complex. The reflectance expressions according to Hass (1964) are then,

$$R_g = \frac{n_o^2 \cos^2 \phi_o + (n^2 + k^2)(a^2 + b^2) - 2n_o \cos \phi_o (na - kb)}{n_o^2 \cos^2 \phi_o + (n^2 + k^2)(a^2 + b^2) + 2n_o \cos \phi_o (nb - kb)} \dots (38a)$$

$$R_p = \frac{n_o^2 (a^2 + b^2) + (n^2 + k^2) \cos^2 \phi_o - 2n_o \cos \phi_o (na + kb)}{n_o^2 (a^2 + b^2) + (n^2 + k^2) \cos^2 \phi_o + 2n_o \cos \phi_o (na + kb)} \dots (38b)$$

where

$$a = \sqrt{\frac{\sqrt{p^2 + q^2} + p}{2}}, \quad b = \sqrt{\frac{\sqrt{p^2 + q^2} - p}{2}}$$

$$p = 1 + (k^2 - n^2) \left( \frac{n_o \sin \phi_o}{n^2 + k^2} \right)^2,$$

$$q = -2nk \left( \frac{n_o \sin \phi_o}{n^2 + k^2} \right)^2$$

Since these expressions are very difficult to solve,

certain approximations are made for absorbing materials particularly metals in the visible region namely  $n^2+k^2 \gg 1$ , then the reflectances reduce to a simpler form (Heavens, 1955).

$$R_{\text{sp}} = \frac{(n^2+k^2) \cos^2 \varphi_0 - 2n \cos \varphi_0 + 1}{(n^2+k^2) \cos^2 \varphi_0 + 2n \cos \varphi_0 + 1} \quad \dots (39a)$$

$$R_{\text{s}} = \frac{(n^2+k^2) - 2n \cos \varphi_0 + \cos^2 \varphi_0}{(n^2+k^2) + 2n \cos \varphi_0 + \cos^2 \varphi_0} \quad \dots (39b)$$

For semiconductors  $n$  can be several times unity while  $k$  is about unity or less. Hence  $n^2 \gg k^2$  and  $n^2 \gg \sin^2 \varphi_0$ . The above equations are then applicable according to Moss (1959).

#### (G) PRINCIPLE METHODS FOR DETERMINING OPTICAL CONSTANTS

There are various methods for determining the optical constants of thin films. Only the important techniques described here in brief.

##### (i) Spectrophotometric methods

Spectrophotometric methods are of general applications where intensity measurements only are required.

(a) Normal Incidence:

Reflectance and transmittance at normal incidence or near normal incidence are measured and optical constants may be evaluated as described earlier. A rough estimate of  $n$  may be made from the expression

$$R = \frac{(n-1)^2 + k^2}{(n+1)^2 + k^2} \dots \quad (40)$$

knowing  $k$  from transmission measurements.

(b) Murmann's Method:

In this method, reflectance ( $R$ ) and the reflectance at the substrate side ( $R'$ ) of the film are measured.  $R$  and  $R'$  are calculated for a range of values of  $n$  and  $k$  knowing the film thickness and wavelength of the incident beam, and then a graph of  $R$  and  $R'$  vs.  $n$  for various values of  $k$  is plotted. For the observed  $R$  and  $R'$  the values of  $n$  for each value of  $k$  may be read. On plotting  $n$  vs.  $k$  which gives the value of  $R$  and  $R'$  obtained with the film, yields two pairs of values for  $n$ ,  $k$ , the correct one may be then distinguished.

(c) Male's Method:

The optical constants  $n$  and  $k$  and the film

thickness  $d$  can be determined from transmittance  $T$ , reflectance  $R$  and reflectance on the substrate side  $R'$ . The procedure involves heavy computations.

Both these  $R$ ,  $R'$  and  $T$  methods could not be adopted in the present work. A simple method due to Wolter (1937) and David (1937) was used to evaluate the optical constants of very thin films. Transmittance  $T$ , reflectance  $R$  and  $R'$  were measured at near normal incidence i.e. at about  $8^\circ$ .  $n$  and  $k$  are then evaluated from the expression

$$n_1^2 - k_1^2 = \frac{n_0^2 + n_2^2}{2} \pm \frac{\lambda}{2\pi d} \left\{ 2n_0 n_2 \frac{R+R'}{T} - (n_2 - n_0)^2 - \left( \frac{4\pi n_1 k_1 d_1}{\lambda} \right)^2 + \frac{n_1^2 k_1^2}{4} \left( \frac{4\pi d}{\lambda} \right)^4 (|n_1^2 - k_1^2| + n_0 n_2) \right\}^{1/2} \quad \dots (41a)$$

$$n_1 k_1 = \frac{\lambda}{4\pi d} n \frac{1-T-R}{T} = \frac{\lambda}{4\pi d} \frac{n_0 n_2}{n_2 - n_0} \frac{R-R'}{T} \quad \dots (41b)$$

(11) Oblique incidence method:

The optical constants may be determined from the reflectance measurements using polarised radiation

at a non-normal incidence. The two components of the reflected light  $R_p$ , the reflectance light parallel to the plane of incidence and  $R_s$  the reflectance perpendicular to the plane of incidence are measured at an angle of incidence  $\theta$ , then  $n$  and  $k$  may be evaluated as described earlier. In this method two reflectance measurements  $R_s$  and  $R_p$  at one angle of incidence or one reflectance measurement at two angle of incidence are required. The sensitivities of these methods have been discussed by Humphreys-Owen (1960). Avery (1952) employed the ratio of  $R_p/R_s$  at two angle of incidence. This method has an advantage that a ratio of reflectance rather than absolute values is required.

In the present work, two measurements of  $R_s$  and  $R_p$  at an angle of incidence  $\theta = 45^\circ$ , were made and the optical constants were evaluated. Abeles (1957) has shown that  $R_s^2 = R_p$  at  $45^\circ$  for homogeneous films. This relation confirms the absolute measurements of  $R_s$  and  $R_p$  and the results are not affected by inhomogeneities due to structure. Schulz and Taugherlini (1954), Robin (1952) have employed this method to determine the refractive index of evaporated films of metals.

(iii) Polarimetric method:

In this method, incident light plane polarised

parallel to the plane of incidence is reflected by the film. The reflected light is generally elliptically polarised and the angle of incidence is varied until a crossed analyser in the reflected light extinguishes the beam. The optical constants are calculated from the observed values of  $\psi$ , azimuth and  $\Delta$ , phase difference by well established procedures (P. Drude, 1891; Voigt, 1910; Minor, 1904; Vasclieck, 1947; Avery, 1952).

(iv) Abele's method:

The refractive index of a thin film on a smooth substrate is measured by the Brewster angle method using parallel polarised light. The angle of incidence is measured at which the filmed and unfiled surfaces have equal reflectance. The refractive index of the film is given by  $n = \tan \theta$ . The Brewster angle is the angle at which the reflectance of the p-component is a minimum. The equal reflectance condition is independent of film thickness.

(v) Interferometric methods:

Fochs (1950) used Michelson interferometer to measure the film thickness and refractive index of self supporting films and films supported on transparent

substrate. Stewart (1948) determined refractive index from equal chromatic order interference fringes formed between the film surface and the flat and obtained an accuracy of  $\sim 0.01$ .

Present work:

The interaction of electromagnetic wave with the thin film material gives us valuable information concerning its electronic structure. From the absorption studies it is possible to determine absorption edge, optical energy band gap, band structure, optical transitions, etc. Further it is likely that optical properties may considerably be affected by the deposition conditions such as substrate temperature, annealing, etc. and film thickness which have been generally observed for semiconducting films. The present work was therefore undertaken to study these parameters for various films of materials such as metals, semiconductors and their compounds.

## CHAPTER II

### EXPERIMENTAL TECHNIQUES

To measure the optical parameters of thin films, various experimental techniques some of which have been developed in this laboratory are described in the subsequent paragraphs. The optical behaviour of a film often depends on the conditions of preparations. Special care has been taken during the preparation of these films for their homogeneity, isotropy, uniformity in thickness, structure, etc. To remove stress, strain, inhomogeneity, etc. these films were annealed in vacuo at suitable temperatures and sometime ageing of these films in a vacuum dessicator was also carried out. The annealing temperature was such that there was no loss of material due to the reevaporation. Films after deposition were transferred to a vacuum dessicator and kept there till the optical measurements were carried out.

#### (A) PREPARATION OF THIN FILMS

For the present investigation all the films were prepared from the bulk materials by the thermal evaporation technique in a vacuum coating unit which was capable of giving vacuum of the order of  $10^{-5}$  mm.



of mercury. The bulk samples which were either procured or made from the constituent elements, were then taken in a tungsten boat or a conical silica basket surrounded by helical coil of tungsten. The boat or coil of tungsten was initially flashed to remove surface impurities. The substrates used were generally glass. These substrates were symmetrically placed above the source on a horizontal plane, keeping the distance between the source and substrates to about 10-15 cms. Six samples were usually prepared in each set of evaporation. It was possible to get films of different thickness at the same evaporating conditions by shifting the evaporating source to one side. This technique was found very suitable to make films of different thicknesses made under the same evaporation conditions.

#### (B) SUBSTRATES

The glass substrates were obtained by cutting microslides to dimensions of about 3.75x1.5 cms, the covered area being about 3.0x1.5 cms. Before deposition all the substrates were cleaned with a mixture of chromic acid and sulphuric acid and washed with distilled water. These were dried with distilled acetone and wiped with clean tissue papers. Substrates

were always handled with a pair of tweezers to avoid contamination.

(C) DEPOSITION AT HIGHER SUBSTRATE TEMPERATURES

Films were also deposited at higher substrate temperatures. A thick copper sheet, which was heated by means of an insulated heater was placed in contact with the back side of substrate surfaces, and the temperature of copper sheet was measured by means of an alumel-chromel thermocouple. The temperature was measured only when the thermal equilibrium was established between the films and the copper sheet. Since the films were normally thin the equilibrium was reached very quickly. The temperature of the heater was controlled with the help of a variac. When the desired temperature was reached the substrates were kept at that temperature for about half an hour to attain the equilibrium condition. The deposition was then carried out at a suitable rate. The rate of deposition was determined by knowing the time of the evaporation and the thickness of the films deposited. It may be mentioned here that the heating of the substrates was carried out only when the required vacuum was attained. Even after the deposition the temperature was maintained for about half an hour. The deposited films were then

Fig. 2

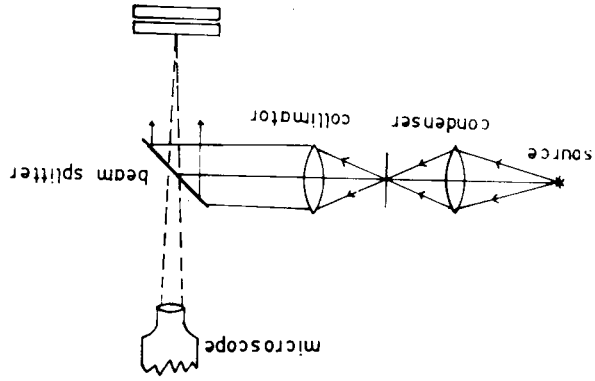
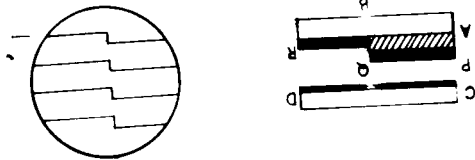


Fig. 1



cooled slowly in vacuo inside the chamber. The rate of deposition and the thickness were controlled either by adjusting the current passed through the filament or by varying the distance between the source and the substrate.

(D) ANNEALING OF FILMS IN VACUO

Films were heated in vacuum to remove stress, strain, inhomogeneity, etc. The maximum temperature of heating varied depending on the nature of the films. This was however always less than the temperature of discontinuity  $T_d$  (Goswami and Jog, 1964). Once this temperature was attained, these samples were kept at that temperature for about one hour and then cooled also in vacuo.

(E) MEASUREMENT OF FILM THICKNESS

Since a knowledge of film thickness is necessary for the computation of the optical constants  $n$  and  $k$ , hence it should be known very precisely. An accurate measurement of the film thickness involves many difficulties since they are rarely uniform and they contain many voids, discontinuities especially for ultra thin films. Film-thickness can however be determined in the following ways i.e. (a) from the

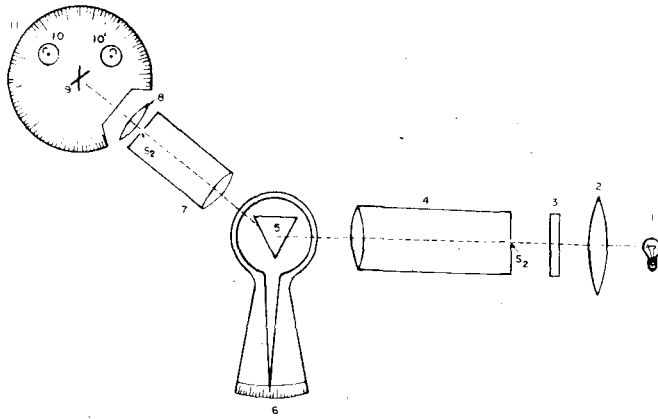
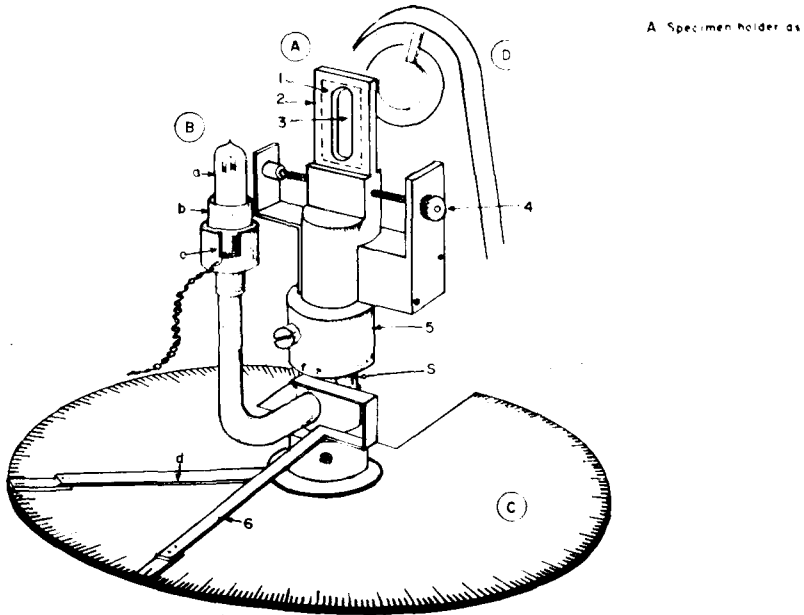


fig. 3.



SAMPLE HOLDER AND PHOTO CELL ASSEMBLY ETC. OF SPECTROPHOTOMETER

fig 4.

knowledge of the mass of the material evaporated from the filament (Williams and Backus, 1949; Ramazanev, 1962); (b) from the knowledge of the mass of the film deposited and the area of the deposit film (Wait, 1922; Brattain and Briggs, 1949; Moss, 1952) and (c) by multiple beam interferometry (Tolansky, 1948). Last two methods were employed in the present investigations.

Film-thickness was calculated in the method (b) is by using the relation  $d = \frac{m}{gA}$  where  $d$  was the thickness of the film,  $m$  the mass deposited on the substrate in gms,  $g$  the density of the film assuming it to be equal to the bulk and  $A$  the area of the film ( $\text{cm}^2$ ). Method (c) was developed by Tolansky (1948) by making use of the reflection-multiple beam fringes for measuring accurately the thickness of films. The principle of this technique is briefly described below.

Any film (AB Fig. 1) whose thickness is to be determined is deposited on an optically flat surface covering only a portion of it. Over this is deposited an opaque film of silver/aluminium (PQR) about 500 Å thickness. Between the heights PQ and QR there is now a step which is of same height as that of the film AB. This composite surface is now matched against a

\*

transparent silvered/aluminium optically flat CD. The experimental arrangement is shown in Fig. (2). A monochromatic light (sodium lamp) was allowed to fall on the film from above so that multiple beam fringes are observed. A step appears in the fringes due to the wedge and can be measured with a good accuracy by a travelling microscope. A film thickness as small as  $100 \text{ \AA}$  can be measured accurately. The thickness of the film can then be calculated from the formula

$$d = \frac{\lambda}{2} \frac{\text{fringe displacement}}{\text{fringe width}}$$

#### (F) SPECTROPHOTOMETER

(i) A spectrophotometer was designed by (Goswami to be published) and fabricated in this laboratory was used to measure reflectance, transmittance, etc. of deposit films for various angles of incidence of monochromatic light in the visible region. Fig. 3 & 4 shows the basic elements of the apparatus. The salient features are as follows:

It consists of a light source 1, a condensing lens 2, a polaroid 3, a collimator 4, a prism 5 and a rotating table moving over a graduated scale 6, a telescope 7, a second lens 8, a sample holder 9, a

photocell 10 and a graduated disc 11. The light source consisted of a tungsten lamp (10 V, 7.5 Amp.) which was excited by a high capacity 12 V accumulator or a stabilized power source. Both the collimator and the telescope were provided with adjustable slits ( $S_1$  and  $S_2$ ). The prism 5 can be rotated on the graduated base 6 so as to select the suitable monochromatic light. The sample holder 9 placed nearly at the focus of the second lens 8 can be rotated freely around its vertical axis coinciding with the central shaft of disc 11 and its position over the disc (not shown) read by a pointer. The photocell placed very close to the sample holder can similarly be rotated around the sample axis say to position 10' and its position similarly read (not shown). The intensity of light incident on the photocell (Phillips 90 CV or 92 AV) was measured by the deflection of a sensitive galvanometer (Pye, England) using lamp and scale arrangement. The polaroid can alternately be placed between the sample holder and second lens. Necessary precautions were taken for eliminating extraneous light falling on the samples, photocells or other parts of the above equipment. The whole instrument was enclosed in a light proof case.

Two types of photocells were used i.e. 90 CV,



sensitive in the red region and 92 AV, in the blue region. Necessary care was taken to see that the same portion of the photocell was exposed at all angle of incidence.

(ii) Standardisation

The equipment was initially aligned and the constant emission of the lamp was tested by noting the deflection of the galvanometer due to the photo current with time without using any sample in the sample holder. When this was achieved the prism position as indicated by the scale 6 was standardised with respect to the wavelength by inserting suitable filters in position 3 after removing the polaroid. By keeping the photocell at position 10 which was in line with the optical axis and without inserting any specimen the position of the prism was slightly moved to and fro to get the maximum deflection of the galvanometer. The reading of the prism on the scale 6 corresponded to the wavelength of light passing through the filter. Similar procedure was also followed with different filters and the scale readings standardised. The slits  $S_1$  and  $S_2$  however controlled the band width and the intensity of the emergent monochromatic (approximate) beam falling on the sample.

(G) MEASUREMENT OF TRANSMITTANCE, REFLECTANCE, ETC.

This was carried out both for polarised and unpolarised light of different wavelengths. Deposits formed on glass substrates ( $n = 1.52$ ) was placed vertically on the sample holder in such a way that the monochromatic beam was transmitted and caught on the photocell at position 10. This was, however, achieved by suitable adjustment of the positions of the sample holder and also of the photocell so as to obtain maximum deflection of the galvanometer. This corresponds to the normal incidence of the beam and the zero position of the photocell. The position of the samples as well as the photocell were read from the graduated disc 11. Necessary precautions were also taken so that the deposit surface-normal was parallel to the incident beam. In order to avoid the internal reflection the uncoated surface of the glass slide was covered with a matt black paper (Hall and Fergusson, 1955).

For measurement of reflectance the glass slide along with the film was rotated by an angle  $\theta$  around its axis. The photocell when rotated to a position say  $10'$  corresponding to  $2\theta$  would then give the maximum deflection of the galvanometer. It was in fact found to be so thus ensuring the satisfactory

alignment of the instrument, sample holder, photocell, etc. Similar procedure was also followed for measuring reflectance, etc. at various wavelengths of light.

$R_s$  and  $R_p$  components of light were obtained by rotating the polaroid through  $90^\circ$ .

#### (H) MEASUREMENT OF OPTICAL CONSTANTS

(i) Optical constants viz. refractive index ( $n$ ) and extinction coefficient ( $k$ ) of the films were evaluated from  $R_s$  and  $R_p$ , the intensity reflectances corresponding to light polarised perpendicular and parallel to the plane of incidence, using the relations as already mentioned in Chapter I given below: (Hass and Thun, 1964)

$$R_s = \frac{n_o^2 \cos^2 \varphi + (n^2 + k^2) (a^2 + b^2) - 2n_o \cos \varphi (na - kb)}{n_o^2 \cos^2 \varphi + (n^2 + k^2) (a^2 + b^2) + 2n_o \cos \varphi (na - kb)} \dots(1)$$

$$R_p = \frac{n_o^2 (a^2 + b^2) + (n^2 + k^2) \cos^2 \varphi - 2n_o \cos \varphi (na + kb)}{n_o^2 (a^2 + b^2) + (n^2 + k^2) \cos^2 \varphi + 2n_o \cos \varphi (na + kb)} \dots(2)$$

where  $n_o$  is the refractive index of the medium (air) and the quantities  $a$  and  $b$  are given by the expressions

$$a = \sqrt{\frac{\sqrt{p^2 + q^2} + p}{2}}; \quad b = \sqrt{\frac{\sqrt{p^2 + q^2} - p}{2}} \quad \dots \quad (3)$$

$$p = 1 - (k^2 - n^2) \left( \frac{n_0 \sin \phi}{n^2 + k^2} \right)^2; \quad q = -2nk \left( \frac{n_0 \sin \phi}{n^2 + k^2} \right)^2$$

When  $n^2 + k^2 \gg 1$ , the term  $\left( \frac{n_0 \sin \phi}{n^2 + k^2} \right)^2$  can be

neglected and the above equations (1) and (2) reduce to simpler forms as given by Heavens (1955) namely

$$R_s = \frac{\cos^2 \phi + (n^2 + k^2) - 2nk \cos \phi}{\cos^2 \phi + (n^2 + k^2) + 2nk \cos \phi} \quad \dots \quad (4)$$

$$R_p = \frac{1 + (n^2 + k^2) \cos^2 \phi - 2n \cos \phi}{1 + (n^2 + k^2) \cos^2 \phi + 2n \cos \phi} \quad \dots \quad (5)$$

It has been found that the conditions  $n^2 + k^2 \gg 1$  was generally valid for the compounds studied.

From the above equations (4) and (5)  $n$  is given below in terms of  $R_s$  and  $R_p$  and

$$n = \frac{(1-R_s)(1-R_p) - (1-R_s)(1-R_p) \cos^4 \phi}{2 \cos \phi \left\{ (1+R_p)(1-R_s) - (1+R_s)(1-R_p) \cos^2 \phi \right\}} \quad \dots(6)$$

The homogeneity of the films was generally tested by making use of the fact that, at an angle of incidence of  $45^\circ$ , the reflectances for the p and s components are related by the expression  $R_s^2 = R_p$ . All the measurements of  $R_s$  and  $R_p$  were mostly carried out at an angle of incidence of  $45^\circ$  not only to check homogeneity criteria but also to evaluate the optical constants. The homogeneity criteria  $R_s^2 = R_p$  ensured that the values of  $R_s$ ,  $R_p$  and  $\phi$  were correct.

When  $k$  was much less than unity, its estimation from  $R_s$  and  $R_p$  components was often associated with a large error (Avery, 1953; Moss, 1959). In such cases it was estimated from the absorption coefficient.

(ii) R, R', T method

For very thin films where  $d$  is known also small as compared with the wavelength used then the optical constants can be also evaluated from the values of  $R$  (reflectance on the air side) and  $R'$  (reflectance at the substrate side) and  $T$ , the transmittance using the following equations (Walter, 1937;

David, 1937)

$$\begin{aligned}
 n_1 k_1 &= \frac{\lambda}{4\pi d} \quad n \frac{1-T-R}{T} \\
 &= \frac{\lambda}{4\pi d} \quad \frac{n_0 n_2}{n_2 - n_0} \frac{R-R'}{T} \quad \dots \quad (7)
 \end{aligned}$$

and

$$\begin{aligned}
 n_1^2 - k_1^2 &= \frac{n_0^2 + n_2^2}{2} \pm \frac{\lambda}{2\pi d} \left[ 2n_0 n_2 \frac{R+R'}{T} - (n_2 - n_0)^2 \right. \\
 &\quad \left. - \left( \frac{4\pi n_1 k_1 d}{\lambda} \right)^2 + \frac{n_1^2 k_1^2}{4} \left( \frac{4\pi d}{\lambda} \right)^4 \left\{ |n_1^2 - k_1^2| + n_0 n_2 \right\} \right]^{1/2} \dots (8)
 \end{aligned}$$

$n_0$  is the refractive index of medium (air) and  $n_2$  is the refractive index of glass ( $n_2 = 1.52$ ). The last two terms in the equation (8) were neglected as they were small compared with the other terms in the bracket.

Thickness of the film was measured accurately by interference method.  $R$ ,  $R'$  and  $T$  were measured at near normal incidence i.e. at about  $8^\circ$  and the optical constants were evaluated from the above equations.

#### (I) ABSORPTION COEFFICIENT

The absorption coefficient ( $\alpha$ ) was deduced from  $\log T$  vs. thickness ( $d$ ) curves for various

wavelengths in the visible spectral region using the relation

$$= \frac{2.303 (\log T_1 - \log T_2)}{d_2 - d_1} \text{ in cm}^{-1} \quad \dots (9)$$

where  $T_1$  and  $T_2$  are transmittance corresponding to thickness  $d_1$  and  $d_2$  respectively. The extinction coefficient  $k$  was also evaluated from the absorption coefficient from the relation

$$k = \frac{\alpha \lambda}{4\pi}$$

$$= \frac{0.1832 (\log T_1 - \log T_2)}{(d_2 - d_1)} \quad \dots (10)$$

#### (J) DIELECTRIC CONSTANT

Real ( $\epsilon_1$ ) and imaginary part ( $\epsilon_2$ ) of the complex dielectric constant are related to the optical parameters.

$$\epsilon^* = \epsilon_1 - i \epsilon_2 = (n - ik)^2$$

hence

$$\epsilon_1 = n^2 - k^2$$

$$\text{and } \epsilon_2 = 2nk$$

$\epsilon_1$  and  $\epsilon_2$  are evaluated from optical data for different wavelengths.

(L) ELECTRON DIFFRACTION STUDIES

The electron diffraction method has great advantage over the X-rays especially for thin films because electrons are scattered about  $10^7$  times more effectively by atoms than by X-rays and the depth of penetration of electrons is also small. Consequently this is a powerful tool for identifying the vacuum deposited films for their structure, phase transitions, etc. Films used for optical studies were examined simultaneously or separately in a Finch type electron diffraction camera fabricated in this laboratory in order to identify the nature of the films and their composition. For the identification of compounds the net plane spacings calculated from the electron diffraction patterns were compared with the data obtained by X-ray diffraction from bulk material. In addition to being a means of identification, electron diffraction patterns give much useful information about the crystal size, shape and orientation of thin films, etc.



(i) Preparation of substrate/specimen

For identification of the nature of the deposit vacuum deposits obtained on various substrates such as glass, collodion or polycrystalline NaCl tablets were studied both by reflection and transmission electron diffraction technique.

(ii) Collodion

Thin films of collodion were prepared by putting a drop of about 0.25% solution of collodion on the surface of distilled water taken in a petri dish. The uniform films of collodion floating on water were then picked up on a clean stainless steel wire mesh and dried. Vapour phase deposits were made on collodion support and examined by transmission method in the electron diffraction camera.

(iii) Polycrystalline NaCl tablet

Polycrystalline sodium chloride tablets were ground with emery paper down to 0000 grade. The loose particles were removed by a camel hair brush and the smooth surface was etched with distilled alcohol and dried. Thus prepared these substrates were then used for film deposition. The sodium chloride tablet along

with the film was slowly dipped in a petri dish containing water keeping the deposit film surface horizontal. Water slowly dissolved the top layers of the substrate in contact with the film thus leaving the film to float on water. The deposits were then collected carefully on a collodion support and examined by the transmission technique.

The electron diffraction pattern obtained were interpreted by the method described by previous workers (Finch and Wilman, 1937; Thomson and Cochrane, 1939; Pinsker, 1953 and others).

CHAPTER IIISTUDIES ON COPPER AND CHROMIUM FILMSINTRODUCTIONCopper

Copper has a face centred cubic structure with  $a = 3.607 \text{ K x}$  at  $20^{\circ}\text{C}$  (Rose, 1946; Lu and Chang, 1941). Copper is a monovalent metal and its important properties are interpreted by the free electron model. Its optical properties especially in the red and infrared wavelengths range are of interest as they are attributed to the free electrons.

Optical properties of copper metal and evaporated films have been investigated by many workers. Tool (1910) determined optical constants of polished copper mirror by polarimetric method and also studied the time effect on  $n$  and  $k$ . He found that  $n$  varied from 1.18 to 0.615 and  $k$  varied from 2.29 to 3.58 for  $\lambda_{460-640 \text{ m}\mu}$ . Meir (1910) determined the absorptive and refractive indices of copper in the visible and ultraviolet region  $250-700 \text{ m}\mu$  using the photographic polarisation method. Bor et al. (1939) found  $n$  and  $k$  in the range of  $4000-11,000 \text{ \AA}$ . The refractive index

obtained differ slightly in magnitude from those previously reported but the  $n$ -wavelength curves were parallel. Kretzmann (1940) computed optical constants from the relative intensities of polarised components of the metal copper in the region  $\lambda$  5000 Å<sup>o</sup> to 10,000 Å<sup>o</sup>. Avery (1950) measured the relative phase change on reflection at a number of layers of copper and also the ellipticity of the light reflected at these layers and evaluated optical constants.

Senett and Scott (1950) studied the structure of evaporated films of copper ( $d \simeq 30$  to 500 Å<sup>o</sup>) in electron microscope and correlated with their optical properties. They used Maxwell-Garnet theory (1904) to explain the peculiar variation with the thickness of the optical properties in terms of the observed structure of the films and the bulk properties of the metal. Halliday (1954) examined thin films of copper obtained by deposition in vacuo by electron diffraction and showed that copper films consist of crystallites in the form of disks of diameter 90 Å<sup>o</sup> and thickness 15 Å<sup>o</sup>.

Schulz (1954) measured the absorption coefficient of copper films and found to vary from 2.2 to 6.22 from wavelengths  $\lambda$  4500 to 9500 Å<sup>o</sup>. Schulz and Tangherlini (1954) measured the reflectivity of copper

films at an angle of incidence  $45^\circ$  in the wavelength range of  $0.40 \mu$  to  $0.95 \mu$  and calculated the refractive index from  $R_s$  and  $R_p$  components.  $n$  varied from 0.85 to 0.13 and  $k$  varied from 2.2 to 6.22 in the wavelength range  $0.40 \mu$  to  $0.95 \mu$ . Ageing and annealing of films resulted in the increased reflectance thereby showing a higher refractive index than the fresh film.

Hill and Weaver (1958) determined optical constants of copper films of different thickness from R and T measurements for  $\lambda 5460 \text{ \AA}$  and found that the refractive index decreased with the increase of thickness, whereas  $k$  increased and became constant. Roberts (1960) studied the optical properties of solid copper in the wavelength range  $0.365 \mu$  to  $2.65 \mu$  and at temperatures  $90^\circ$ ,  $300^\circ$  and  $500^\circ\text{K}$  under vacuum ( $2 \times 10^{-5} \text{ mm}$ ) and the optical constants were evaluated by the polarimetric method. Adhav (1960) measured reflectance, transmittance, and ac conductivity of transparent films ( $d = 60 \text{ \AA}$  to  $455 \text{ \AA}$ ) deposited on quartz by evaporation in vacuo for three wavelengths  $435 \text{ m}\mu$ ,  $546 \text{ m}\mu$  and  $636 \text{ m}\mu$ ; and the optical constants were then evaluated. Payan and Rasagini (1962, 1964) measured transmission and reflection of copper films of various thickness between  $0.4 \mu$  and  $2.4 \mu$  in the wavelength range  $4000$  to  $7250 \text{ \AA}$

and the optical constants were evaluated as a function of wavelengths. Henderson and Weaver (1966) also investigated the optical properties of copper. Optical constants of copper films were obtained as a function of optical thickness by the method of Male for  $\lambda$  5460 Å. They found that  $n$  decreased with the increasing film thickness and became constant at  $n = 0.5$  for films thicker than about 1400 Å. The  $k$ -curve rose from 200 Å upto about 500 Å when it became constant at a value of  $k = 1.5$  and there was no clear maximum as observed for chromium films.

### Chromium

Chromium belongs to the VI group of the periodic table. It has normally a body centred cubic structure ( $a = 2.885$  Å) though a number of workers have reported the existence of a hexagonal phase. Bradley and Olland (1926) by X-ray diffraction found the lattice parameter of the hexagonal form to be  $a = 2.717$  Å,  $c = 4.419$  Å and  $c/a = 1.625$ .

Chromium is resistant to oxidation. Chromium films have a good adhesion to glass and are stable to mechanical action. The advantage of using a thin chromium protective under layer when preparing high

quality silver or aluminium surface mirrors by vacuum deposition have long been realised (Strong 1935, Holland 1956). Senett and Scott (1950) found that chromium films even as thin as  $20 \text{ \AA}$  were continuous and correlated the structure of evaporated films as observed by electron microscope with their optical properties.

The optical properties of chromium films have been studied by many workers. Abeles (1957) measured the reflection and the transmission of chromium films as a function of the angles of incidence and the state of polarisation of the incident light. He determined the optical constants of chromium films by the photometric method ( $R_s$ ,  $R_p$  and  $T_p$ ) and obtained 2.49 and 3.21 for  $n$ ; and 2.3 and 2.24 for  $k$  for wavelengths 546  $\mu$  and 630  $\mu$  respectively. Hill and Weaver (1958a) investigated the structure of very thin vacuum deposited chromium films by optical methods. They calculated optical constants for a series of films of varying thicknesses from R and T measurements and found that the refractive index decreased with the increase of thickness. Hill and Weaver (1958b) measured optical constants of bulk chromium metal and also evaporated films by the polarimetric method and compared the

results. Weaver and Hill (1959) studied the effects in bimetallic films of chromium and aluminium and stated that chromium films deposited on glass substrates before evaporation of aluminium not only acted as a buffer preventing the attack of the aluminium by the alkali in glass but also improved the adhesion and desirability of the aluminium. Idczak (1963) measured the transmission and reflection coefficients of chromium films for various thicknesses ranging from  $75 \text{ \AA}$  to  $1200 \text{ \AA}$  with white light and calculated the absorption coefficient. He also studied the effects of evaporation conditions and heat treatment on the optical properties of chromium films and observed no change in the optical properties with the heat treatment. Kosteik and Shklyarevskii (1964) investigated the optical properties of vacuum evaporated chromium layers in the visible region. They found that the optical constants did not change with repeated annealing. However with substrate temperature optical constants were found to increase with the substrate temperature. Henderson and Weaver (1966) found that the value of  $n$  for  $\lambda \text{ } 5460 \text{ \AA}$  decreased with the increase of the thickness until it attained a steady value of 0.57 at a thickness of about  $1100 \text{ \AA}$ , the value of  $k$  passed through a flat maximum in the range of about  $350 \text{ \AA}$  and reached a constant value of 1.8.



The maximum was not so distinct as that obtained by Hill and Weaver (1958). They suggested that the anomalous optical constants of the films were due to both the aggregated structure and a diminution of the mean free path of the free electron in the aggregate. Idczak (1967) studied the dependence of refractive index and extinction coefficient  $k$  with the wavelength in the visible region,  $n$  and  $k$  were found to increase linearly with the increasing wavelength.

Summary of published values for the optical constants of bulk and evaporated chromium is given below.

		$n$	$k$	Source
Cr. bulk	5790	2.97	4.87	Wortenbug Int. Crit. tablets
bulk	4560	3.53	4.41	Physik Chem. Tabbelex
bulk	5460	3.28	4.35	Senett and Scott (1950)
Films	5460	2.49	2.30)	Abeles (1957)
	6300	3.21	2.24)	
"	5460	0.5	1.8	Hill and Weaver (1958)
"	5460	0.57	1.8	Henderson and Weaver (1966)
" Visible region		0.4 to 0.6	1.7 to 2.0	Idczak (1967)

From the above survey, it is seen that though some investigations have been made on optical constants of copper and chromium, the reported results especially

in the latter cases differed considerably. This was apparently due to variable factors particularly for the variable conditions of evaporation, film thickness, ageing, etc. It was therefore felt necessary to reinvestigate the above optical parameters.

## (B) EXPERIMENTAL

### (a) Copper films

Copper films were deposited on glass substrates by the evaporation process in vacuo ( $\approx 10^{-5}$  torr) as described in Chapter II. Pure copper pieces (B.D.H. quality) were treated with dilute hydrochloric acid, then washed thoroughly with distilled water and finally with alcohol. They were then evaporated from a previously flashed tungsten boat in the usual way.

### (b) Chromium films

Chromium films were prepared by evaporating a piece of "spec pure" chromium from an initially flashed tungsten boat. As the m.p. of chromium is very high, higher amperage was used and the evaporation rate was also slow. Substrates were kept at about 15-20 cms. above the filament.

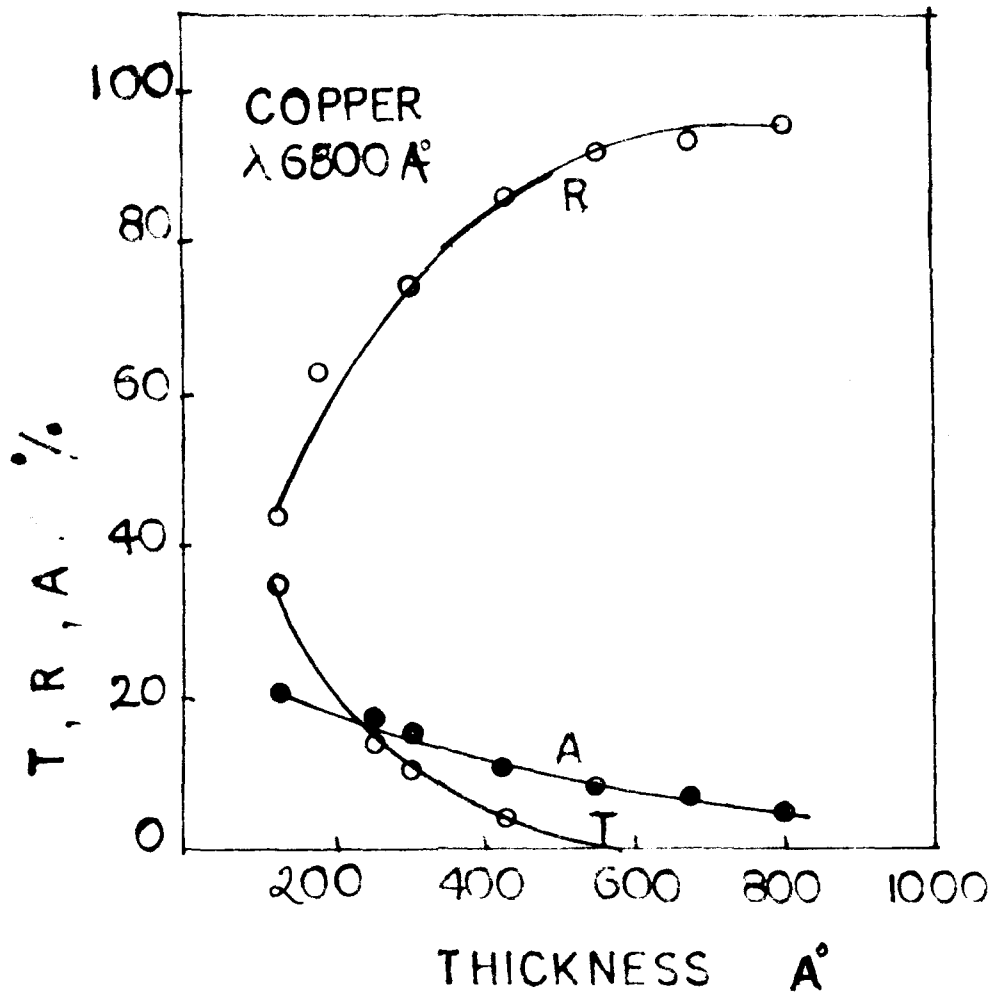


Fig. 7.

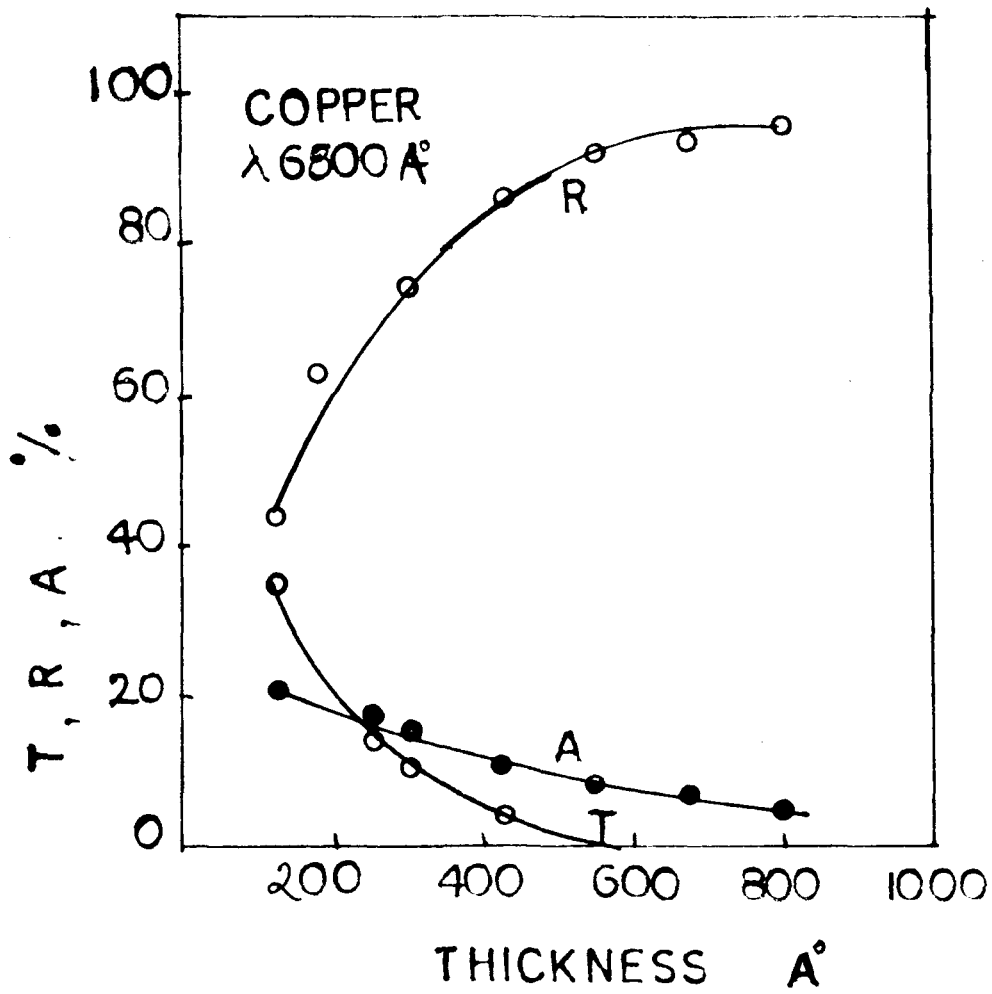


Fig. 7.

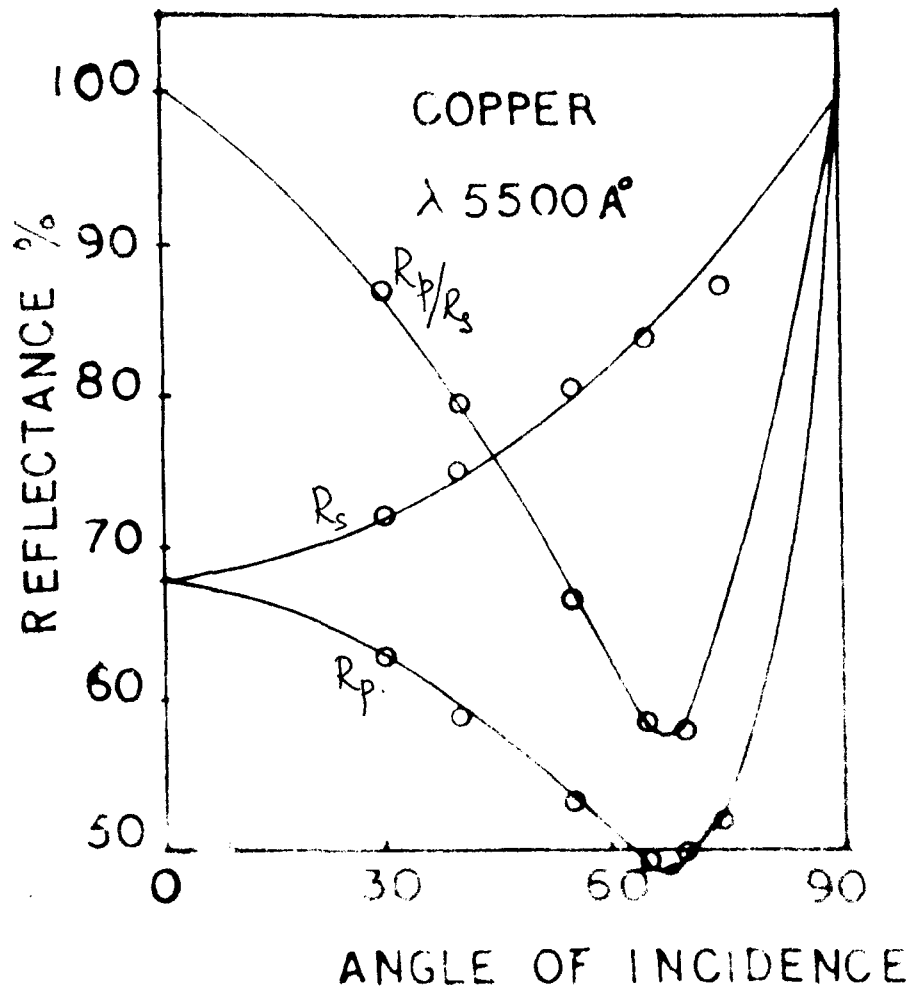


Fig. 8.

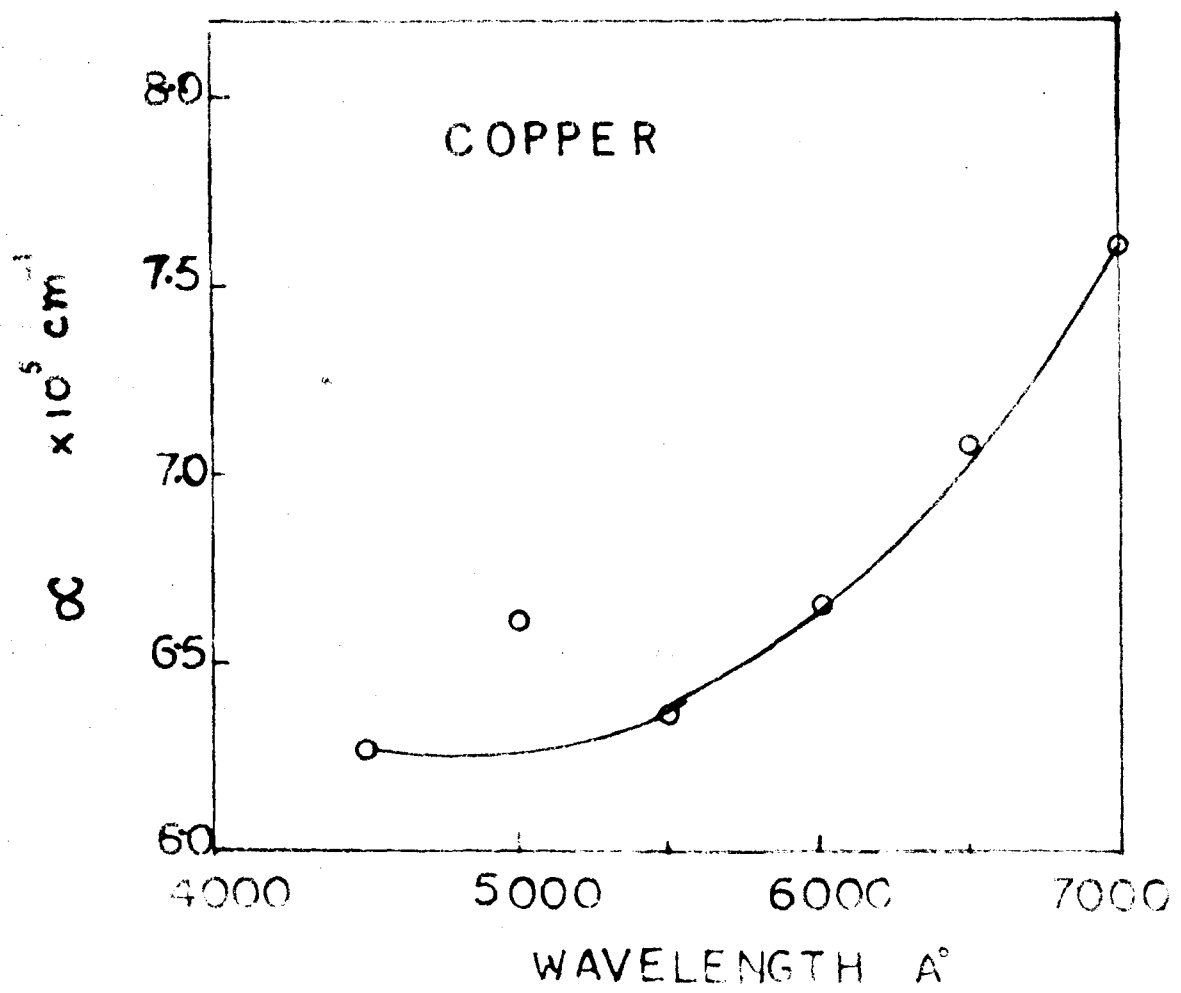


Fig. 9.

(C) RESULTS(a) Copper(i) Transmission, reflection and absorption

Fig. (5) and (6) show transmission and reflection coefficients with the wavelength for four films of different thicknesses with unpolarised light. Transmission is maximum at about  $\lambda 5500 \text{ \AA}$  and reflectance increased with wavelength. The variation of transmittance, reflectance and absorbance with the thickness of the film for  $\lambda 6800 \text{ \AA}$  is shown in Fig. (7). The transmittance decreased exponentially whereas the reflectance increased with the thickness. Fig. (8) shows the variation of  $R_s$  and  $R_p$  components with the angle of incidence. It is seen that  $R_s$  increased steadily with the angle of incidence whereas  $R_p$  decreased to reach a minimum ( $\theta = 68^\circ$ ) and then increased quite rapidly. The  $R_p/R_s$  curve cuts  $R_s$  curve at  $45^\circ$  thus conforming to homogeneity criteria  $R_s^2 = R_p$  at  $45^\circ$ .

(ii) Absorption coefficient

Absorption coefficient was calculated from the slope of  $\log T$  vs  $d$  curve for different wavelengths. The variation of absorption coefficient with the wavelength is shown in fig. (9) and the values are

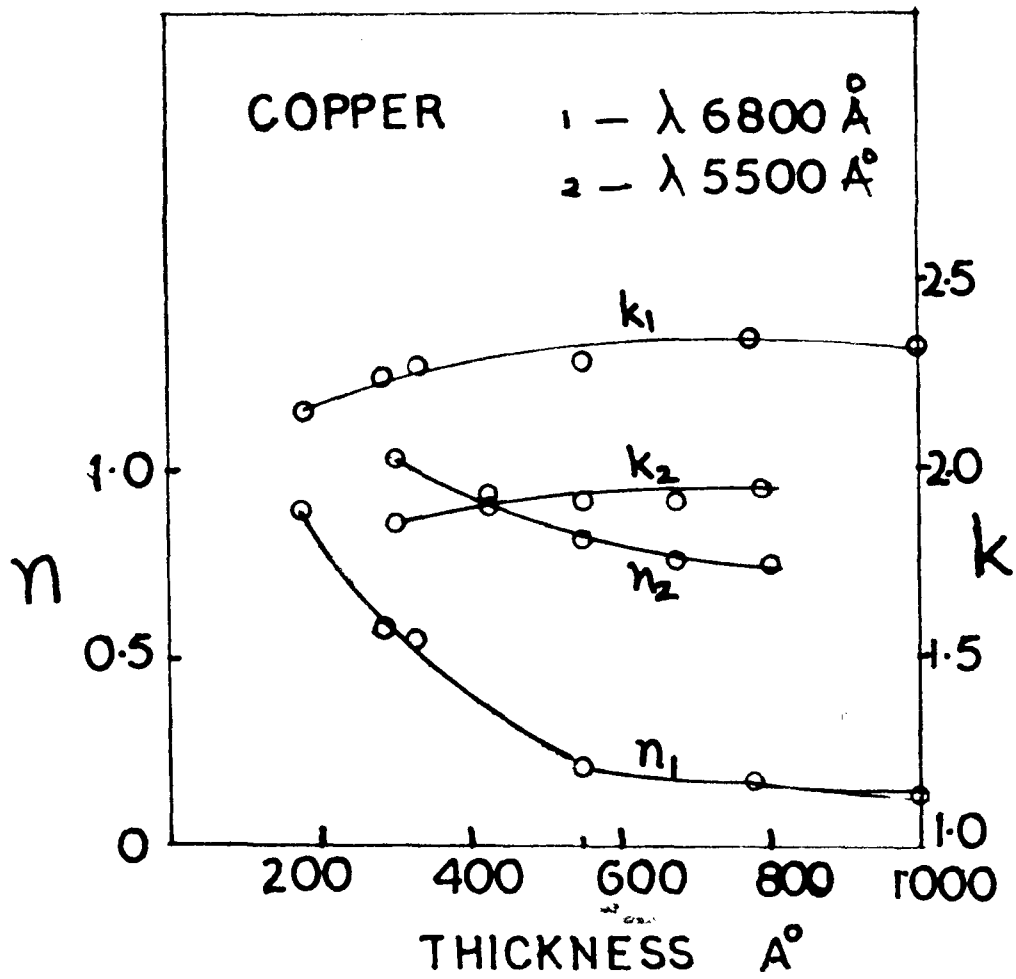


Fig. 10.



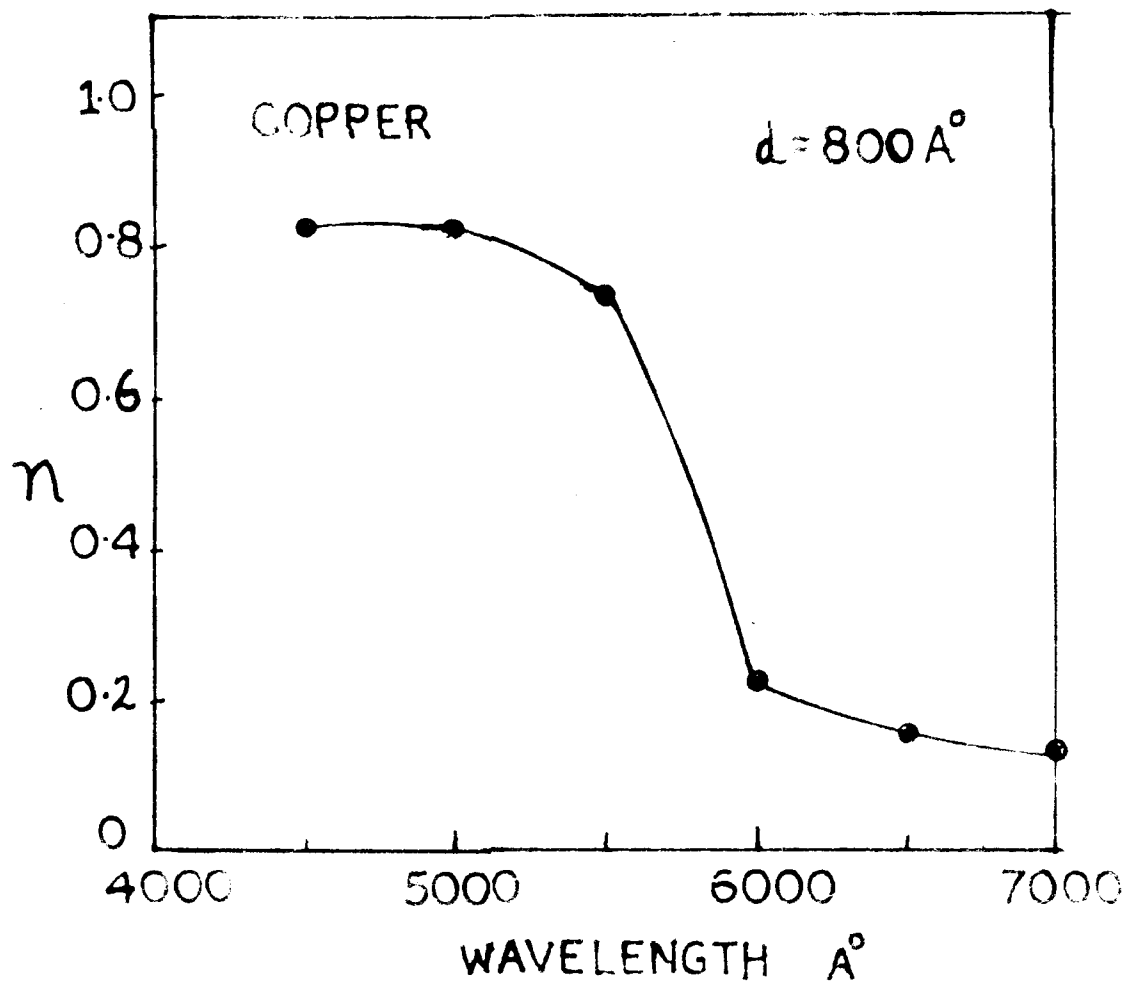


Fig. 11.

given in table 1. It is seen that the absorption coefficient increased with the wavelength ( $\lambda$  4500-7000 Å).

(iii) Optical constants

Both the refractive index and extinction coefficient were calculated from the  $R_s$  and  $R_p$  components of the reflected light at an angle  $\phi = 45^\circ$ . The variation of  $n$  and  $k$  with the thickness of the film (125 to 1000 Å) for two wavelengths  $\lambda$  5500 Å and 6800 Å was studied in details Table 2. Fig. (10) shows the variation of  $n$  and  $k$  with the film thickness. It is seen that  $n$  decreased with the increase of film thickness whereas  $k$  increased and became constant. Refractive index was however determined for various wavelengths and found to vary from 0.82 to 0.13 in the visible region ( $\lambda$  4500-7000 Å) for thickness ( $d$ ) about 800 Å (Fig. 11).

(b) Chromium

(i) Transmission, reflection and absorption

The variation of transmittance and reflectance with the film thickness for two wavelengths is shown in Fig. (12). It is seen that the transmittance decreased exponentially and the reflectance increased

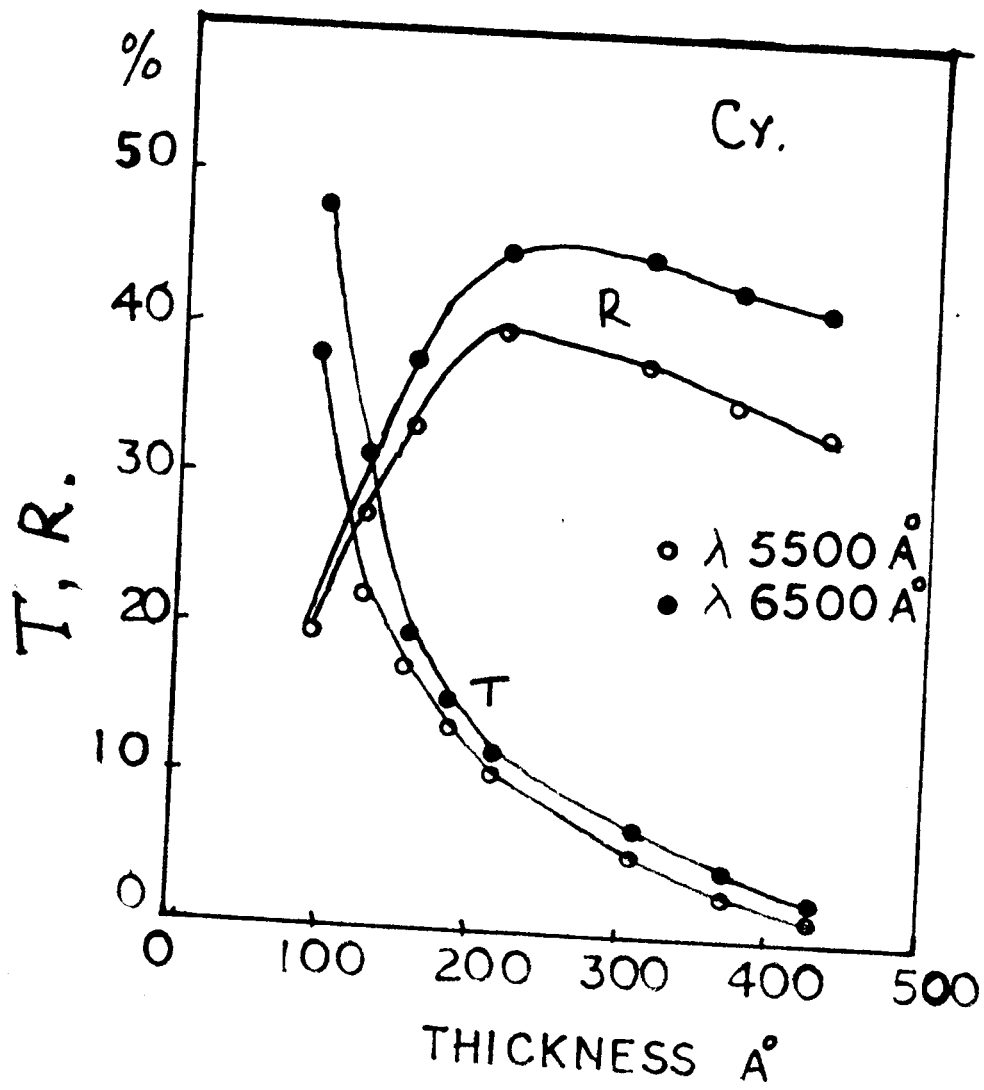


Fig. 12.

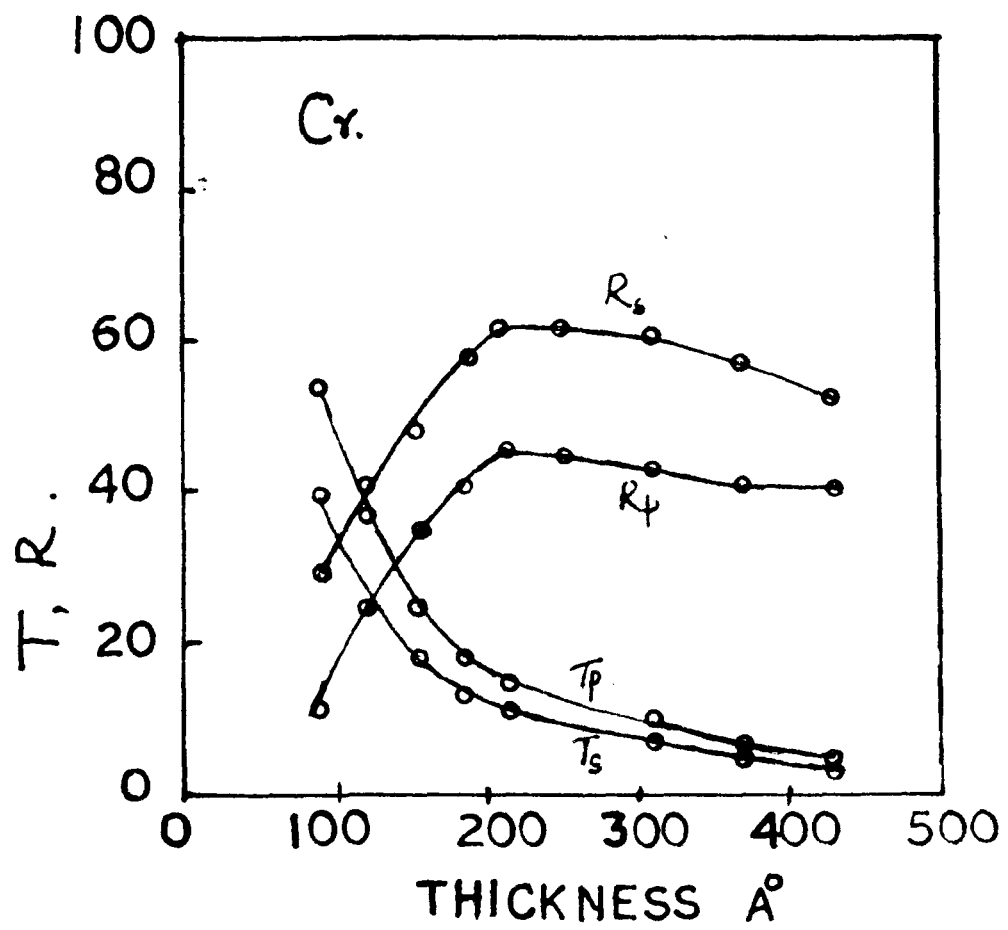
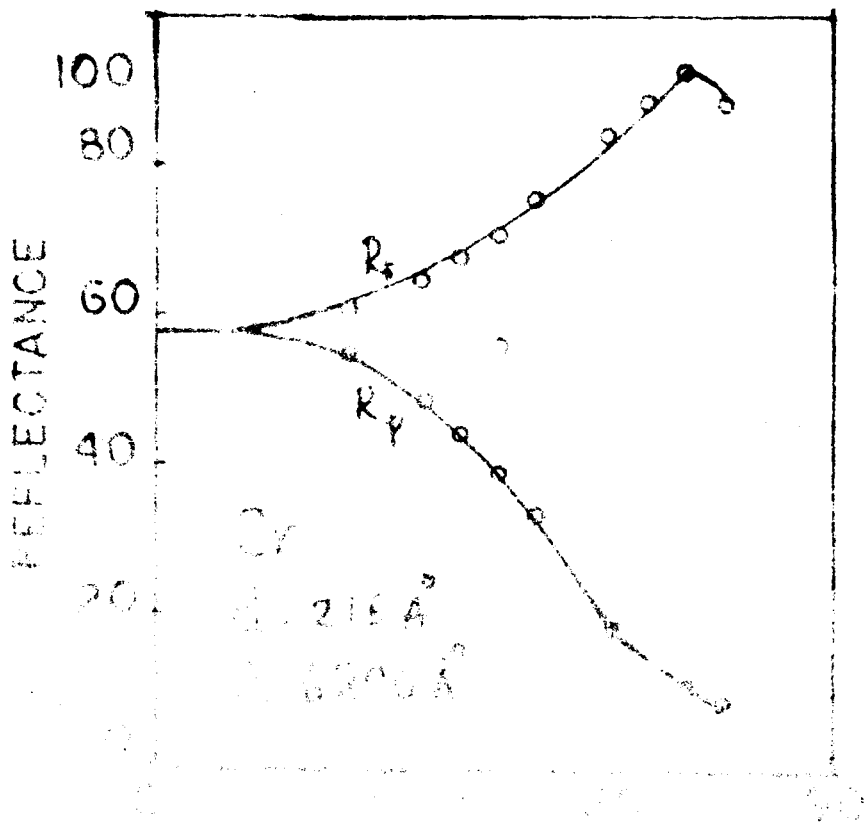
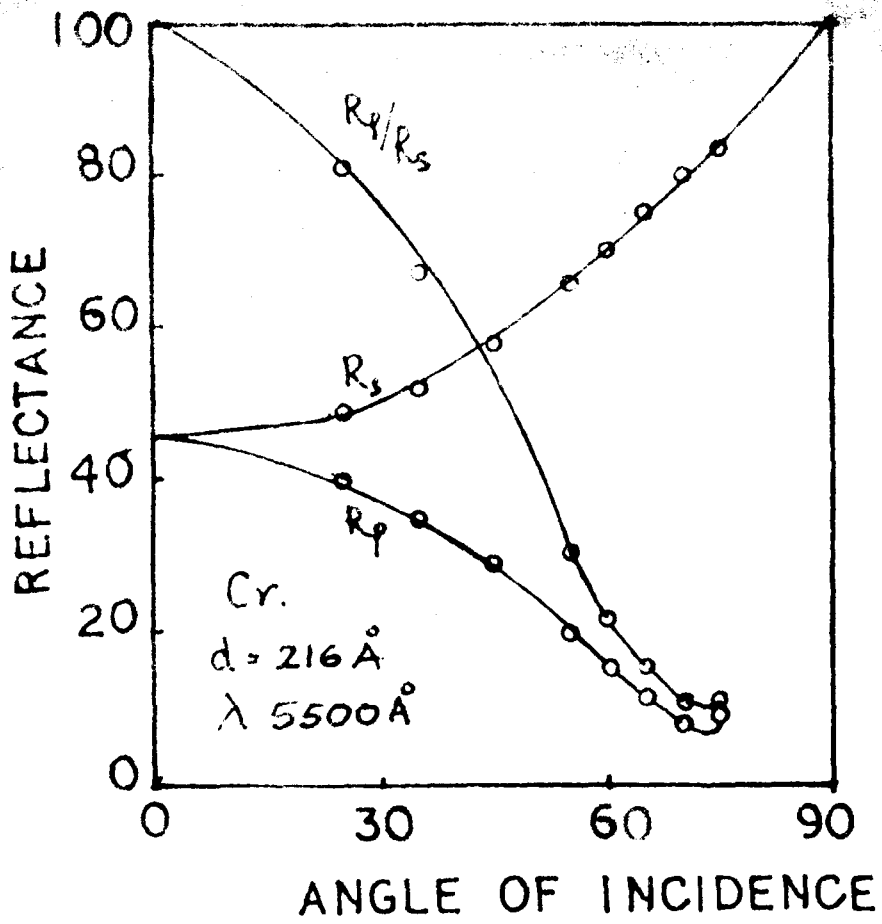


Fig. 13.



with the film thickness having a maximum at about  $200 \text{ \AA}$ .  
 Fig. (13) shows the variation of transmittance ( $T_p$  and  $T_s$ ) and reflectance ( $R_p$  and  $R_s$ ) with the film thickness for a polarised light. The variation of  $R_p$  and  $R_s$  with the angle of incidence for two wavelengths  $5500 \text{ \AA}$  and  $6800 \text{ \AA}$  is however shown in Fig. (14).

It is seen that  $R_s$  increased steadily with the angle of incidence while  $R_p$  decreased reaching a minimum and then increased.  $R_p$  (min) was found to be at  $\phi = 72^\circ.5$  for  $\lambda 5500 \text{ \AA}$  conforming to the value of refractive index  $n = 3.17$ .

#### (ii) Absorption coefficient

Absorption coefficient was calculated from the slope of  $\log T$  vs. thickness curves for different wavelengths.  $\infty$  was found to decrease with the wavelength (table 3).

#### (iii) Optical constants

Optical constants were determined from the reflected components of light  $R_s$  and  $R_p$  with the angle of incidence  $\phi = 45^\circ$ . It was observed that for thicker films which were opaque the homogeneity criterion  $R_s^2 = R_p$ . Fig. (15) shows the variation of the refractive index and extinction coefficient with the

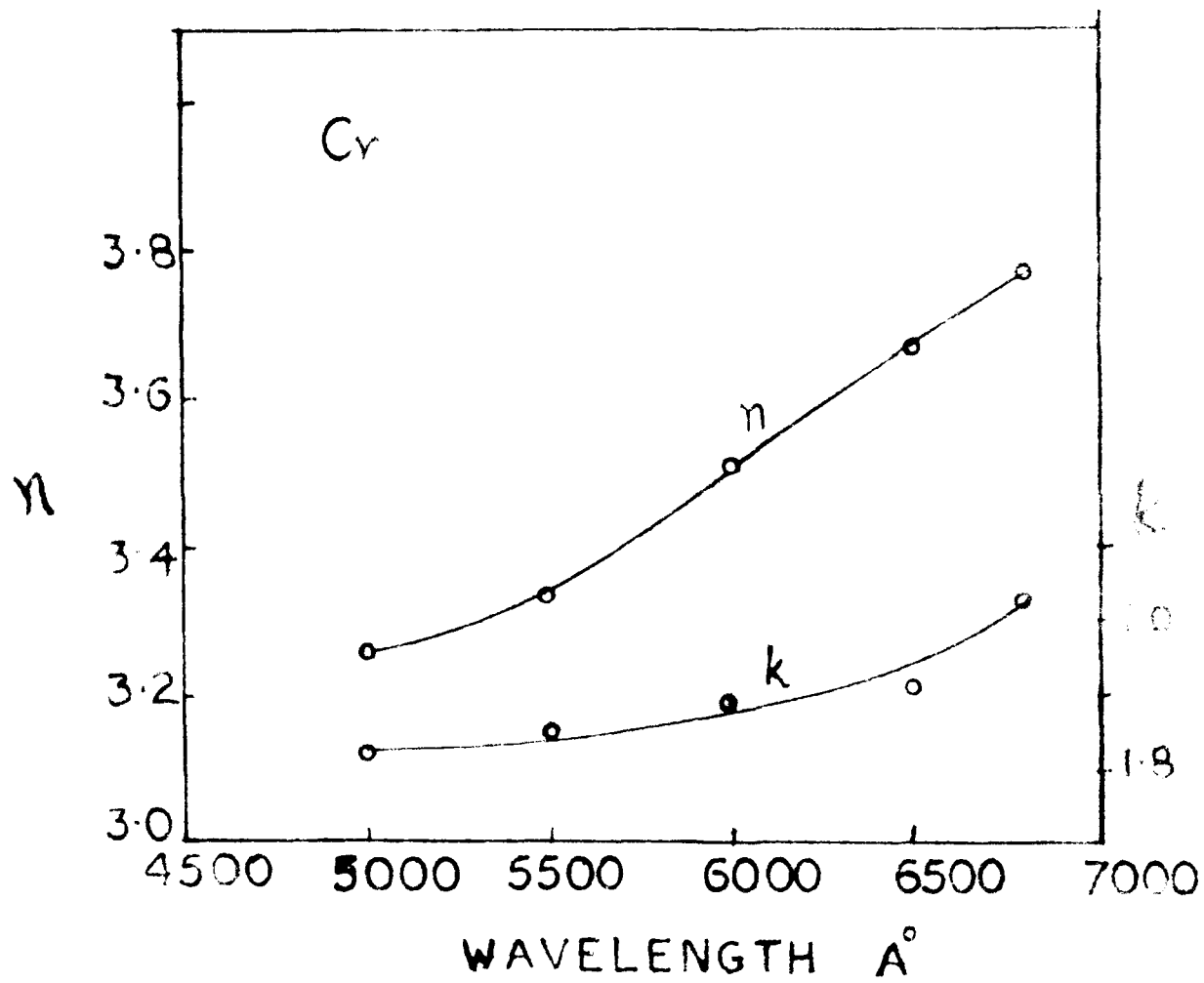


Fig. 15.

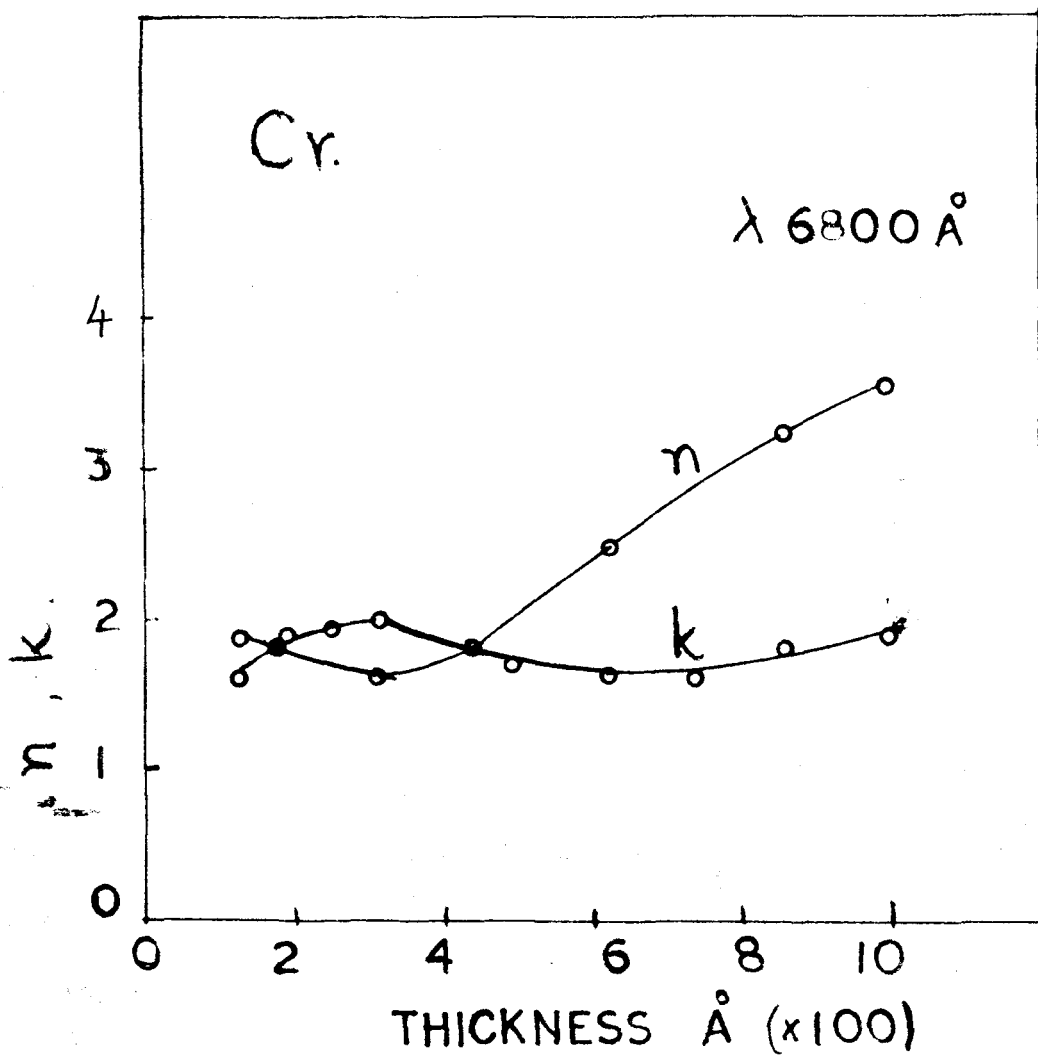


Fig. 16.



wavelength,  $n$  was found to increase from 3.23 to 3.77 and so also  $k$  from 1.82 to 2.03 for  $\lambda$  5000 Å to 6800 Å (Table 4). It was also observed that both  $n$  and  $k$  varied with the film thickness. Fig. (16) shows the variation of  $n$  and  $k$  with the thickness for  $\lambda$  6800 Å. It is seen that  $n$  had a minimum at about 350 Å and then it increased with the rise of thickness, whereas  $k$  had a maximum around 300 Å but decreasing with the further increase of thickness.  $k$ , however, increased again and the results are shown in table 5. The optical constants of chromium films deposited at higher substrate temperature ( $100^\circ\text{C}$ ) were also determined.  $n$  varied from 3.61 to 3.86 and  $k$  varied from 1.95 to 2.15 for  $\lambda$  5000 Å to 6800 Å (Table 6).

#### (D) DISCUSSION

##### (a) Copper

Optical constants of copper films were evaluated by the reflection method using  $R_s$  and  $R_p$  components at  $\phi = 45^\circ$ . It was found that the homogeneity criteria  $R_s^2 = R_p$  at  $\phi = 45^\circ$  was satisfied within the experimental error only for thick (opaque) films. Values obtained for  $n$  and  $k$  for copper films by us using the  $R_s, R_p$  method were found to agree with the

results of different workers. This agreement clearly shows that the equipment designed here was sufficiently sensitive and accurate for the studies of optical constants. It was however found that for thinner films  $n$  varied with the thickness and this variation of  $n$  with  $d$  was studied for two wavelengths  $\lambda 5500 \text{ \AA}$  and  $\lambda 6800 \text{ \AA}$ .  $n$  decreased with the increasing film thickness and became constant for thicker films, whereas  $k$  curve increased and eventually became constant. These variation in optical constants with the thickness in the low film thickness range appears to be due to the predominance of voids and discontinuities, as suggested by Rouard (1952) from the Maxwell-Garnett theory (1904). According to him a thin film of metal as composed of mixture of metal and air "particles" wherein the proportion of air particles increased as the film thickness tends to be smaller. The value of  $n$  therefore approached the value of unity for ultra thin films as  $d \rightarrow 0$ . The values obtained for  $n$  and  $k$  for different film thicknesses for  $\lambda 5500 \text{ \AA}$  agreed with the values obtained by Henderson and Weaver (1966).

(b) Chromium

It is seen from the earlier work on chromium that there is a large variation in the values of  $n$  and  $k$

for bulk and evaporated films and this might be due to the presence of its oxide. In the present study the optical constants of chromium have been evaluated by the reflection method using  $R_p$  and  $R_s$  data at  $\theta = 45^\circ$ . The values obtained for  $n$  and  $k$  were similar to bulk values. The refractive index increased with the wavelength. It was also found that  $n$  and  $k$  increased with the substrate temperature. The variation of refractive index and extinction coefficient with the film thickness have been studied for a fixed wavelength also. It was found that  $n$  initially decreased with the increase of the film thickness upto about  $400 \text{ \AA}$  and then increased to reach a steady value as the film thickness increased. The low value for  $n$  for very thin films were due to the aggregated structure and diminution of the mean free path of the electrons in the aggregate as explained by Male (1950) and Rouard (1952) using Maxwell-Garnett theory. The values obtained for  $n$  and  $k$  with film thickness agreed with the values obtained by Henderson and Weaver (1966) only for low thicknesses ( $\approx 400 \text{ \AA}$ ). Refractive index for higher thickness however decreased gradually whereas  $n$  obtained by us increased to reach a steady value approximately to that for bulk metal. Abeles (1957) also obtained a higher value of  $n$  similar to bulk metal

value using  $R_s$  and  $R_p$  data for opaque thick film.

From the above study it is now established that both  $n$  and  $k$  for Cr films can have different values depending on the film thickness as well as the wavelength,  $n$  having a minimum value ( $\sim 1.6$ ) around  $300-400 \text{ \AA}$ , but increasing rapidly with the further increase of  $d$ , but more slowly with decreasing film thickness (see table 5).  $k$  on the other hand had a maximum value around the region where  $n$  was minimum. It also tends to be lower either with the increase or decrease of film thickness. Even though  $n$  was often as great as that of bulk,  $k$  was slightly lower. Similar results were also observed for deposits formed at higher substrate temperatures. The above peculiarities observed for chromium films may be due to the transition from an aggregated to a continuous structure around  $400 \text{ \AA}$  film thickness.

COPPER FILMSTable 1

Variation of absorption coefficient and extinction coefficient with wavelength

$\lambda$ (Å)	$\alpha$ (cm <sup>-1</sup> )	k
4500	6.24x10 <sup>5</sup>	2.23
5000	6.63 x 10 <sup>5</sup>	2.64
5500	6.36 x 10 <sup>5</sup>	2.78
6000	6.63 x 10 <sup>5</sup>	3.77
6500	7.08 x 10 <sup>5</sup>	3.67
7000	7.60 x 10 <sup>5</sup>	4.23

Table 2

Variation of optical constants with thickness

$\lambda$ (Å)	Thickness	R <sub>s</sub>	R <sub>p</sub>	n	k
6800	125	0.4711	0.2553	1.80	1.83
	175	0.6488	0.4930	0.89	2.15
	275	0.7313	0.6220	0.57	2.09

Table 2 (contd.)

Variation of optical constants with thickness

$\lambda$ (Å)	Thickness	$R_s$	$R_p$	n	k
6800	325	0.7710	0.6573	0.55	2.28
	550	0.8612	0.8083	0.19	1.77
	775	0.9206	0.8507	0.17	2.35
	1000	0.9365	0.8798	0.13	2.31
5500	300	0.5491	0.3815	1.03	1.85
	425	0.5837	0.4240	0.93	1.91
	550	0.6210	0.4745	0.80	1.92
	675	0.6316	0.4903	0.75	1.90
	800	0.6507	0.51	0.74	1.97

CHROMIUM FILMSTable 3

Variation of absorption coefficient and extinction coefficient with the wavelength

$\lambda$ (Å)	$\alpha$ cm <sup>-1</sup>	k
5000	$1.02 \times 10^6$	4.06
5500	$9.8 \times 10^5$	4.29
6500	$8.58 \times 10^5$	4.44

Table 4  
Variation of  $n$  and  $k$  with  $\lambda$   
 $d$

$\lambda$ (Å)	$R_s$	$R_p$	$n$	$k$
5000	0.516	0.267	3.23	1.82
5500	0.5228	0.2738	3.34	1.85
6000	0.5355	0.2867	3.51	1.89
6500	0.5454	0.2967	3.69	1.90
6800	0.5593	0.3126	3.77	2.03

Table 5  
Variation of  $n$  and  $k$  with film thickness for  $\lambda 6800 \text{ \AA}$

No.	Thickness (Å)	$R_s$	$R_p$	$n$	$k$
1	125	0.4246	0.2047	1.92	1.59
2	185	0.4841	0.2647	1.89	1.90
3	250	0.4873	0.2702	1.83	1.91
4	310	0.5098	0.2960	1.760	2.02
5	375	0.4937	0.2864	1.610	1.90
6	433	0.471	0.25	1.92	1.83
7	494	0.5564	0.2193	2.39	1.69

Table 5 (contd.)Variation of  $n$  and  $k$  with film thickness for  $\lambda 6800 \text{ \AA}$ 

No.	Thickness ( $\text{\AA}$ )	$R_s$	$R_p$	$n$	$k$
8	618	0.4560	0.2093	2.47	1.63
9	742	0.4752	0.2266	2.95	1.59
10	865	0.5168	0.2677	3.29	1.81
11	990	0.540	0.2913	3.57	1.91

Table 6Variation of  $n$  and  $k$  with  $\lambda$  (films deposited at  $100^\circ\text{C}$ )

$\lambda$ ( $\text{\AA}$ )	$R_s$	$R_p$	$n$	$k$
5000	0.5455	0.2973	3.61	1.95
5500	0.555	0.3081	3.71	2.10
6000	0.5608	0.3147	3.74	2.07
6800	0.5684	0.3230	3.86	2.15



CHAPTER IVSTUDIES ON SELENIUM AND TELLURIUM FILMSINTRODUCTION

Selenium and tellurium are intrinsic semiconductors which crystallize in hexagonal lattices. They belong to the VI.b group of the periodic table and their free atom configurations are  $4S^2p^4$  and  $5S^25p^4$  respectively. The properties of selenium and tellurium are of great interest since the conductivities of these elements lie intermediate between metals and insulators and in fact Se is often assumed to be a semiinsulator and Te as a semimetal. Selenium exists in various allotropic forms viz. amorphous, monoclinic (red) and hexagonal (grey) selenium. Smith (1873) observed the fall of the resistance of selenium when light was incident on it and the phenomenon was understood as the photovoltaic effect. Fritts (1883) prepared the first rectifier from selenium. The crystal structures of metallic selenium and tellurium had been investigated by many workers (Slattery, 1923; Bradley 1924; Callen, 1954; Van Hippel, 1948; Asendarf, 1957) and the lattice constants of selenium <sup>and Te.</sup> are  $a = 4.34 \text{ \AA}$ ,  $c = 4.95 \text{ \AA}$  and  $a = 4.44 \text{ \AA}$ ,  $c = 5.91 \text{ \AA}$  respectively.

Amorphous selenium as produced by the vacuum evaporation absorbs strongly in the ultraviolet and short wavelengths of the visible region but becomes transparent at the red region of the visible spectrum. Optical properties of selenium have been investigated by many workers. Wood (1902) measured in the visible region the absorption coefficient and the refractive index of amorphous selenium films obtained by the cathode sputtering. Meir (1910) measured by the polarimetric method the refractive index and extinction coefficient of bulk selenium in the wavelength region  $0.257 \mu$  to  $0.668 \mu$ . Merwin and Larsen (1912) measuring on a Se prism obtained a value of 2.92 for the refractive index at a wavelength of  $0.589 \mu$  and a value of 2.716 at about  $0.67 \mu$ . Skinner (1917) and Weld (1922) determined both the refractive index and the extinction coefficient for the visible and near ultraviolet spectral region from reflectance data using a polarised light. Miller (1925) from  $R_s$  and  $R_p$  data of Se found that  $n$  varied from 3.4 to 4.4 and 2.3 to 3.1 in parallel and perpendicular positions respectively for wavelengths  $3000 \text{ \AA}$  to  $5000 \text{ \AA}$ . Becker and Schaper (1944) measured the absorption coefficient of amorphous selenium films obtained by cathode sputtering in the ~~experimental~~ spectral region  $0.70 \mu$  to  $0.58 \mu$ . Henkels (1950) obtained

activation energy 2.3 eV at absolute zero from the electrical conductivity measurements on liquid selenium. Weimer (1950) found that amorphous selenium was photoconducting possessing markedly different properties from those of either the metallic form or red monoclinic crystals and had a dark resistivity of  $> 10^{12}$  ohm cm. compared to  $10^5$  ohm-cm. for the metallic form. Gilleo (1951) studied the optical absorption and photoconductivity and also their dependence on temperature both for amorphous and hexagonal forms. Further the photoconductivity in the amorphous form was rather small whereas the hexagonal selenium had a prominent photoconducting property.

Dowd (1951) measured both absorption coefficient and refractive index of amorphous selenium in the red and infrared region and compared his results with those of Wood (1902), Meir (1910), Merwin and Larsen (1912). Gebbie and Sakar (1951) measured the absorption coefficient and refractive index of bulk selenium in the region infrared and  $n$  was found to be 2.589 at a wavelength of  $0.819 \mu$  and 2.52 at  $\lambda 1.014 \mu$ . Beyond  $2 \mu$  it attained a nearly constant value of about 2.45. Dielectric constant was found to be 6.0 for the long wavelengths. Sakar (1952) also studied the optical

properties of liquid selenium in the infrared region and upto a temperature range of  $400^{\circ}\text{C}$ , and  $n$  was found to decrease with the increase of temperature for longer wavelengths. Gebbie and Kiely (1952) measured the dielectric constant and the loss factor of amorphous selenium at a wavelength of 3 cm. and obtained a value 5.97 for  $\epsilon_1$ . Gebbie and Sakar (1951) found a value of 6.0 for  $\lambda > 3 \times 10^{-4}$  cm. and which was close to value of 6.05 obtained by Dowd (1951).

Henkels and Maczuk (1953) evaluated the activation energy (2.31 eV) from the temperature dependence of the thermoelectric power and the resistance. Hilsum (1956) studied the absorption edge of amorphous selenium and its change with temperature. He found that the edge shifted by  $2.7 \text{ \AA deg.}^{-1}$  corresponding to a change in the energy gap of  $9.7 \times 10^{-4} \text{ eV deg.}^{-1}$ . Fochs (1956) measured the energy gap of selenium from the diffuse reflection spectra and observed 1.86 eV for amorphous and 1.74 eV for metallic selenium. Kohler et al (1959) measured optical constants of evaporated selenium films by the successive approximation in the wavelength range of 0.14 to 2.5 microns.

### Tellurium

Tellurium like selenium has a highly

anisotropic crystal structure consisting of a long spiral chains of atoms of interatomic spacing ( $\approx 2.86 \text{ \AA}$ ) arranged in such a way that, in addition to the two nearest neighbours lying in the same chain each atom has four next nearest neighbours in adjacent chains. The distance of closest approach of atoms in neighbouring chains was  $3.45 \text{ \AA}$ .

Haken (1910) reported the existence of two allotropic modifications of tellurium one form stable upto  $352^\circ\text{C}$  with melting point  $452^\circ\text{C}$  and the other form stable at lower temperature. Metallic tellurium has no other modification and has been confirmed from X-ray analysis by many workers (Bradley, 1924; Slattery, 1925) and also from electron diffraction studies of thin films. Cartwright et al. (1935) investigated the effect of small impurities of common metals on the electrical conductivity, thermoelectric power and temperature resistance coefficient of pure tellurium single crystal rods and observed that the conductivity of tellurium increased as expected from the Wilson's theory (1931). Pure tellurium had a negative TCR which became less negative with the addition of copper and became positive as for metal conductors with the addition of more than 0.3% antimony.

Battom (1949, 1952) reported tellurium to be p-type semiconductor at low, as well as at high temperatures but in the samples of adequate purity there was a range of temperatures between  $+230^{\circ}\text{C}$  and  $-40^{\circ}\text{C}$  within which the sign of Hall coefficient was negative. This anomalous behaviour was also reported by earlier investigators Wold (1916), Seanton (1948).

The electrical properties of single crystals of tellurium were extensively studied by Schmidt and Wasserman (1927), Battom (1949, 1952), Fukuroi (1949, 1952), Nassbaum (1954). Results of these workers showed that tellurium was a p-type semiconductor below  $-40^{\circ}\text{C}$ , it reversed to n-type or above this temperature depending upon impurity concentration and it changed back to p-type at about  $230^{\circ}\text{C}$  the latter temperature being independent of concentration. Saturated  $R_H$  and  $\Delta E$  were found to be  $3.8 \times 10^3 \text{ cm}^3/\text{coulomb}$  and  $0.32 \text{ eV}$ . Collen (1954) on the basis of a simplified model of the tellurium lattice made some important deductions concerning the electronic band structure, infrared absorption and Hall effect. He also observed in tellurium a reversal in sign of the Hall coefficient at  $230^{\circ}\text{C}$ . Fischer et al. (1957) studied the semiconducting electrical properties of tellurium and showed that at

room temperature and above a high purity tellurium behaves as an intrinsic semiconductor with a band gap of 0.34 eV. Nassabaum et al. (1959) carried out measurements on single crystals of tellurium from 290 to 570°K at 2000 atmospheric pressure.

Ghosh (1961) studied the variation of conductivity, Hall mobility and field effect mobility with thickness and also found that the band gap was 0.34 eV. Chaudhuri (1965) studied the electrical and galvanomagnetic properties of pure single crystals of tellurium at low temperatures in the range 4.2-0.94°K. Tellurium films are used for preparing thin film transistors Weimer (1964).

Recently Goswami and his collaborators (Goswami and Jog, 1964; Deokar and Goswami, 1966; Goswami and Ojha, 1973) have carried out extensive studies on tellurium films and have shown that the parameters such as resistivity, activation energy, Hall coefficient, thermoelectric power, TCR, etc. in case of thin films are considerably dependent upon the thickness of the films, deposition conditions, annealing, temperatures, etc.

Photoconductivity and optical properties of tellurium have been investigated by many workers.

Barlott (1925) reported the existence of photoconductive effect in tellurium films and observed that the wavelength of the exciting radiation had to be less than  $4500 \text{ \AA}$ . The presence of the photovoltaic effect was observed by Bergmann and Hausler (1936) and the effect was too small to have its spectral dependence established. Moss (1949) observed photoconductivity in evaporated films of tellurium at  $195^{\circ}\text{K}$  and  $90^{\circ}\text{K}$ . The spectral response reached a maximum at 1.1 microns while the photoconductive threshold lay at about 3.5 microns. The shift of threshold with temperature was  $2 \times 10^{-4} \text{ eV/}^{\circ}\text{C}$ .

Van Dyke (1922) found that the refractive index of tellurium varied from 2.5 to 3.0 in the visible region as observed by reflection method. Miller (1925) obtained  $n$  to vary from 1.9 to 2.9 in the parallel position and 1.7 to 2.7 in the perpendicular position using a polarised light for  $\lambda$   $3000\text{-}5000 \text{ \AA}$ . The refractive index and the absorption constant of tellurium layers were also measured in the near infrared between  $3 \mu$  to  $11 \mu$  interferometrically by Moss (1952) in extrapolated to long wavelengths was found to be 4.8. The absorption constant was  $2.2 \times 10^5 \text{ cm}^{-1}$  at  $1.0 \mu$  falling rapidly with the increasing wavelength



$(5 \times 10^4 \text{ cm}^{-1}$  at 3 microns).

Hartig and Loferski (1951, 1952) measured the transmission of tellurium crystals in the infrared region and the refractive index computed from the reflected radiation yielded a value of about 5.0. Loferski (1952) found the index of refraction to be  $5.3 \pm 0.2$  at  $6 \mu$  for tellurium single crystals and this value was somewhat larger than the value found by Moss in tellurium films. Loferski (1954) also measured the variation of energy gap with temperature and found it to be  $-2 \times 10^5 \text{ eV/}^\circ\text{C}$ .

Lisitsa and Tsvelykh (1958) measured reflection and transmission of wedge films of tellurium formed on glass plate and the refractive index was calculated for the visible region. Valeev and Gisan (1965) determined the refractive index and absorption coefficient of thermally deposited tellurium layers of different thicknesses in the 2-15  $\mu$  region and  $n$  varied from 5.2 to 4.3.

It is seen from the above, that not much work has been carried out on the evaporated thin films of selenium and tellurium in the visible region. In the following, therefore, optical properties viz. transmission,

reflection, absorption, absorption coefficient, optical constants, their variation with wavelength and film thickness have been studied in detail.

(B) EXPERIMENTAL

Preparation of selenium and tellurium films

Selenium films were prepared by the slow evaporation of small pieces of "Specpure" selenium from a silica basket which was heated by a tungsten wire coiled around it, under a vacuum of the order of  $10^{-5}$  torr on suitable glass substrates. A set of about six specimens of different thicknesses was prepared at a time, as described in Chapter II. Films were red in appearance and were found to be amorphous at room temperature. These were then annealed at  $75^{\circ}\text{C}$  also in vacuo for about one hour. Optical properties of selenium films were studied both before and after annealing. Films were also deposited at higher substrate temperature ( $\simeq 100^{\circ}\text{C}$ ). These were found to be greyish in colour and nonuniform. Because of this nonuniformity of the deposits no optical properties of these films were studied.

Tellurium films were also prepared by the evaporation of small pieces of "Specpure" tellurium from

Fig. 17.

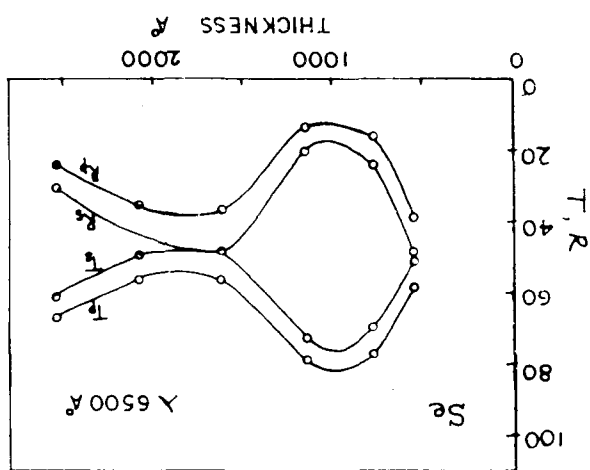
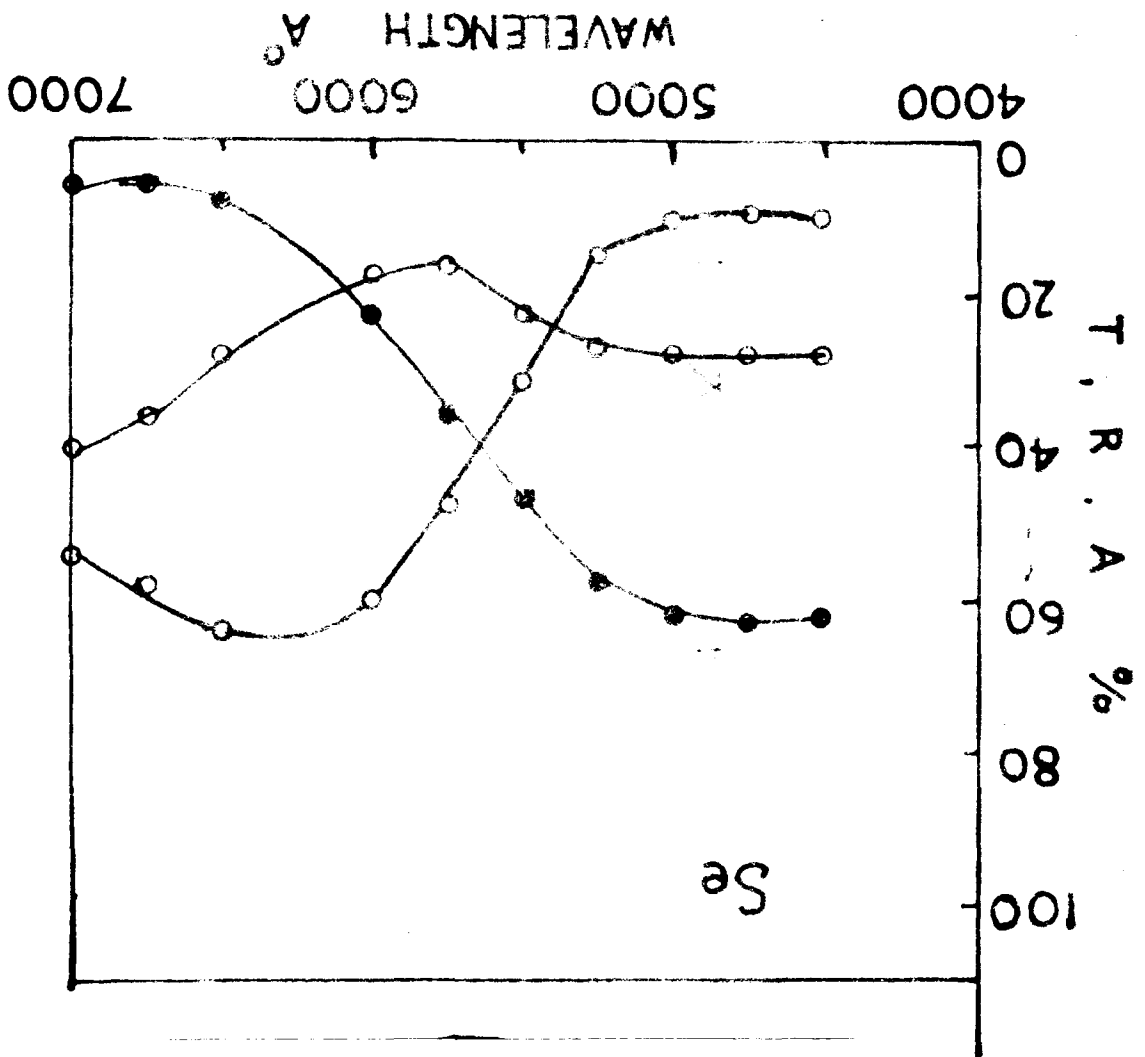


Fig. 18.

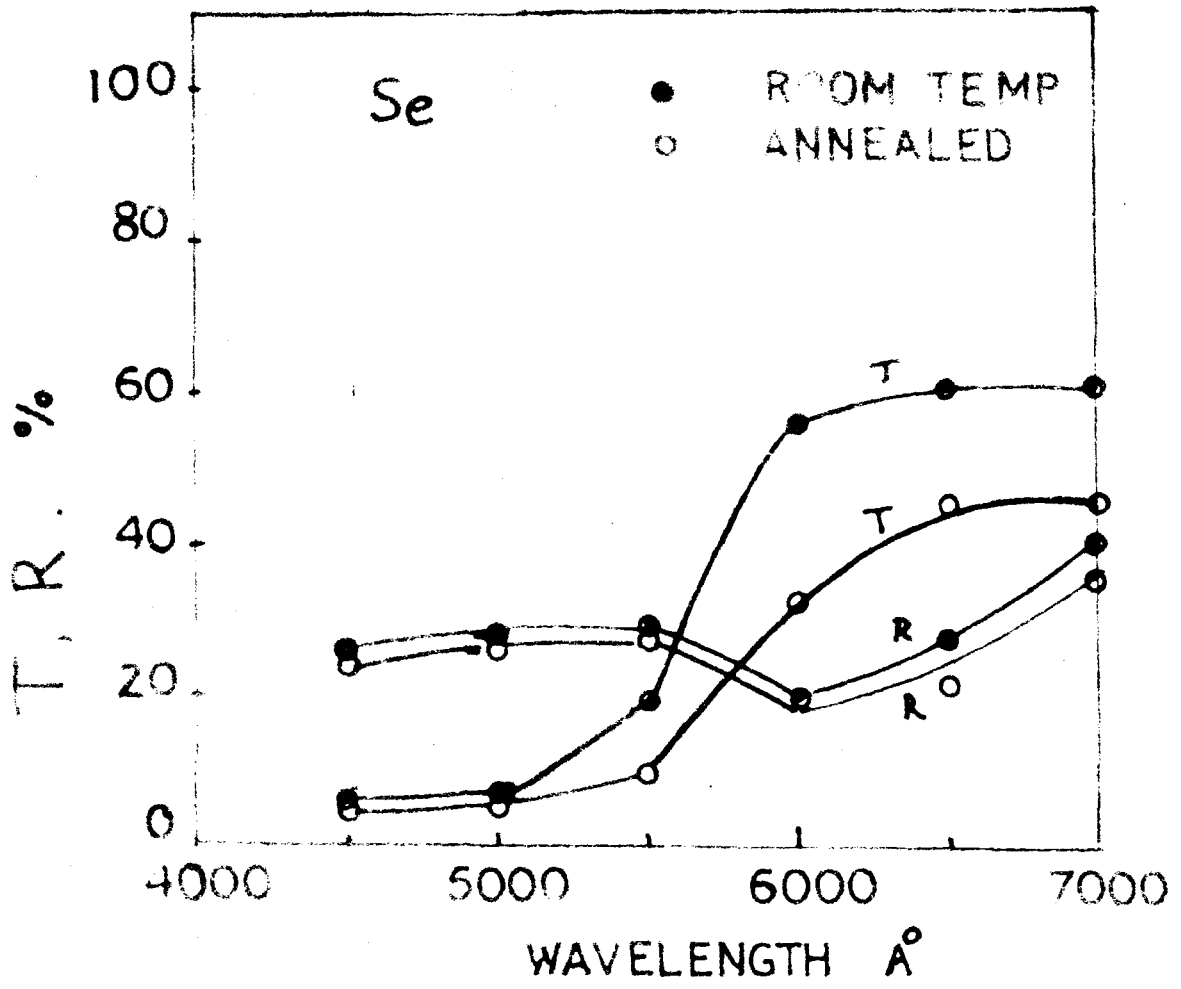


Fig. 19.

a tungsten boat in vacuo. These films were blackish in colour and they were then annealed at 75°C for about one hour also in vacuo.

### (C) RESULTS

#### (a) Selenium films

##### (i) Transmission, reflection and absorption

Fig. (17) shows the typical variation of transmittance, reflectance and absorbance of selenium film ( $d \simeq 2536 \text{ \AA}$ ) with the wavelength of incident light. It is seen that transmittance increased with the wavelength whereas absorption decreased for  $\lambda$  4500-7000  $\text{\AA}$ . The variation of transmittance ( $T_p$  and  $T_s$ ) and reflectance ( $R_p$  and  $R_s$ ) with the thickness for the polarised light ( $\lambda$  6500  $\text{\AA}$ ) is shown in Fig. (18). Maxima and minima were observed both for transmittance and reflection curves. The absorption was negligibly small. Fig. (19) which shows transmittance and reflectance of a film before and after annealing.

##### (ii) Absorption coefficient

The variation of transmittance with the thickness of the films (semilog scale) for various wavelengths is shown in Fig. (20). These curves show some

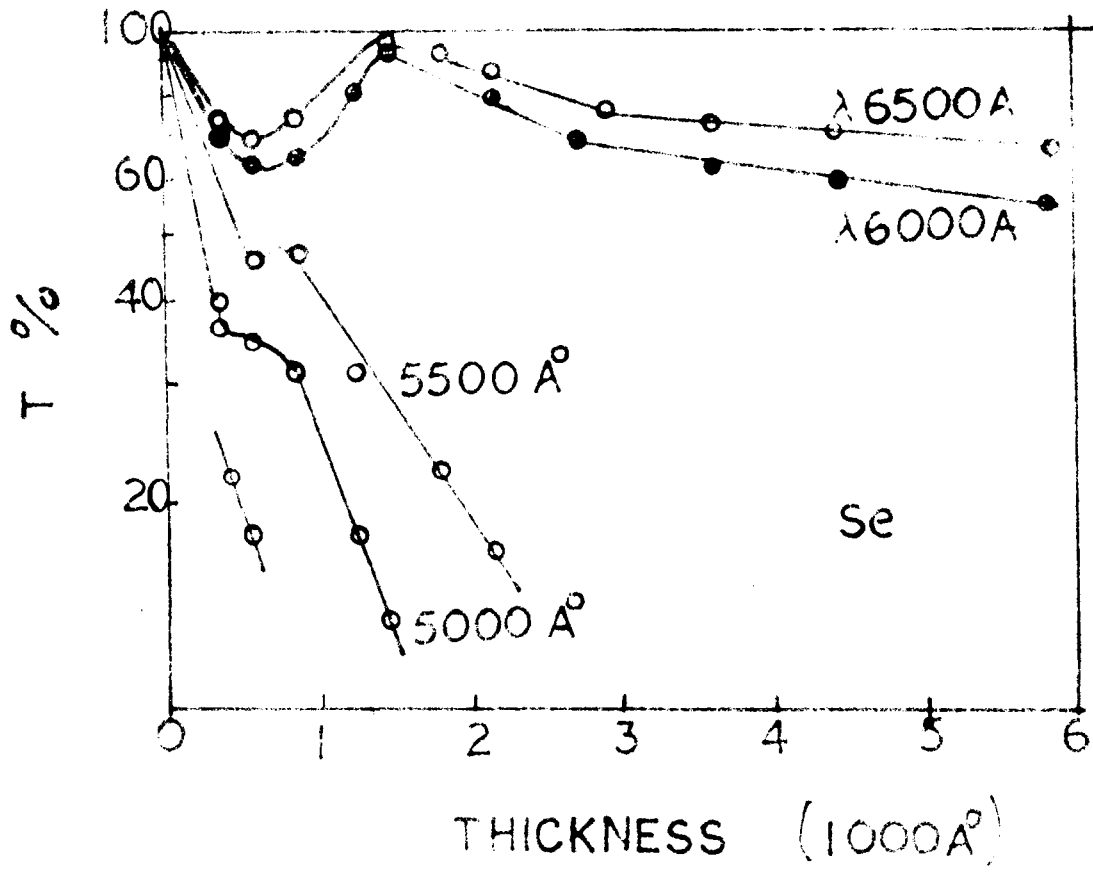


Fig. 20.

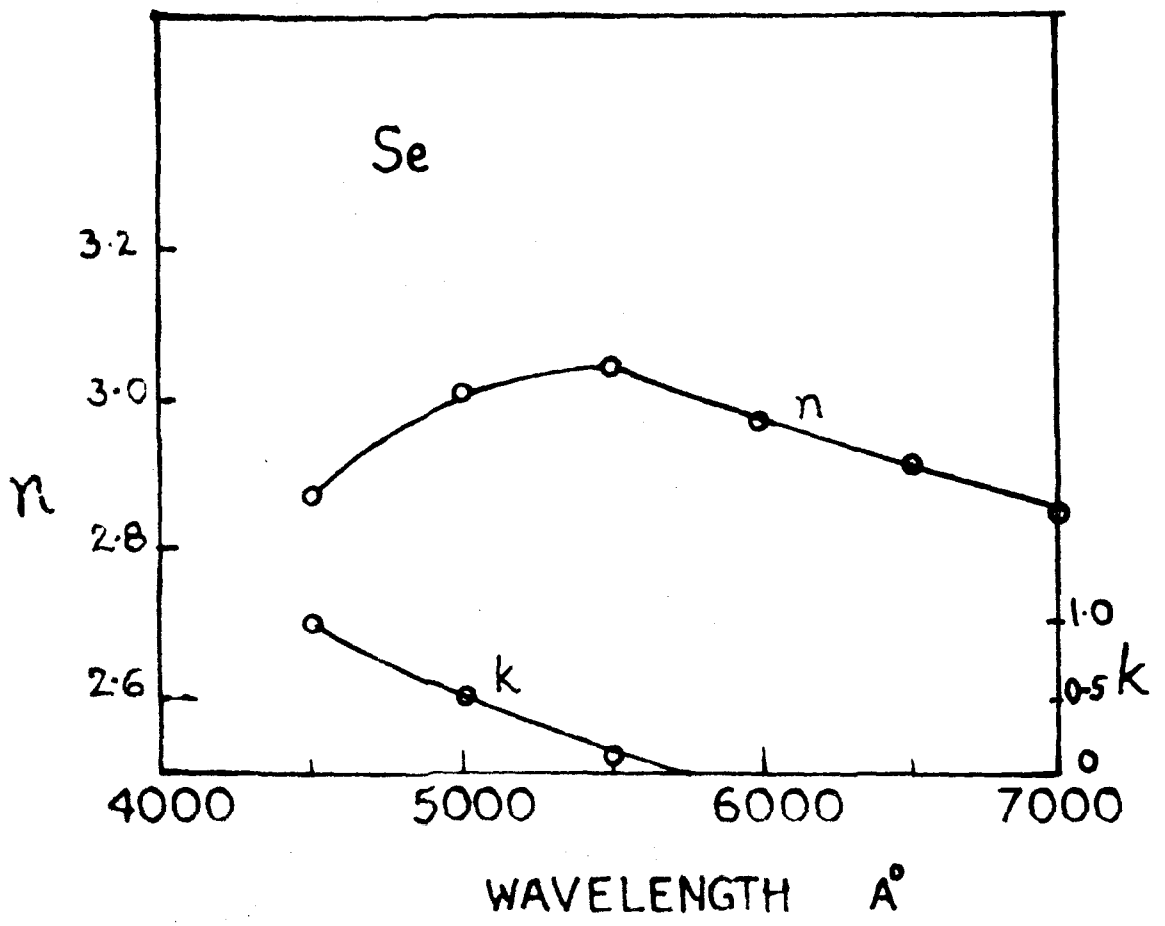


Fig. 21.

Fig. 22

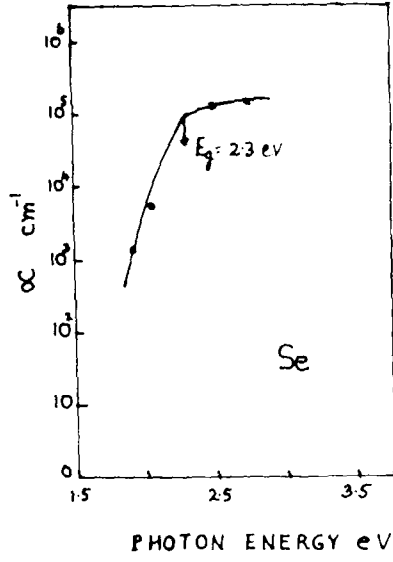


Fig. 23.

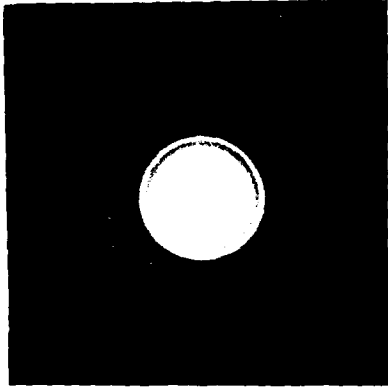
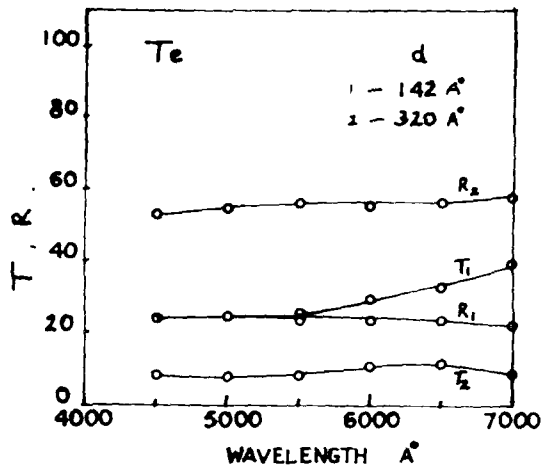


Fig. 24.





peculiarities i.e. transmittance falls exponentially (linear in semilog scale) with film thicknesses only for short wavelength of visible region, but for higher wavelengths especially in red region of the visible spectrum, peaks were observed, generally for thinner films. For thicker films ( $d > 3000 \text{ \AA}$ ) transmittance falls exponentially for all wavelengths and the absorption coefficient was calculated from the slope at that range. The variation of absorption coefficient with the wavelength and the results are given in Table 7.

### (iii) Optical constants

Optical constants  $n$  and  $k$  were determined by the reflection method.  $R_p$  and  $R_s$ , components of the reflected light at an angle  $\phi = 45^\circ$  for various wavelengths in the visible region were measured and  $n$  was evaluated from the equation (6) given in Chapter II. As the value of  $k$  was much less than unity, it was calculated from the absorption coefficient. Fig. (21) shows the variation of refractive index  $n$ , and extinction coefficient  $k$ , with the wavelength and the results are given in table 8. It is seen that refractive index varied with increase in wavelengths from 2.84 to 2.87 with a peak value 03.04 at about  $\lambda 5500 \text{ \AA}$ ,  $k$  however varied from 0.5 to a negligible value near

$\lambda$  6000 Å. It was also found that the annealed films had slightly lower refractive index than the unannealed ones.

(iv) Optical energy band gap

Optical energy band gap was determined from the plot of  $\alpha$  versus  $h\nu$  (Fig. 22). The graph showed two branches and the intersection point of these two branches (or the "corner" portion of the graph) gives the value of  $E_g$ . The band gap thus evaluated to be 2.3 eV, which agrees with the value of Stuke (1955).

(b) Tellurium films

(i) Structure

To identify the nature of film as formed at room temperature and annealed at 100°C, the electron diffraction study was made on the deposits. A typical electron diffraction transmission pattern is shown in the Fig. 23. It was found that the deposit films had a hexagonal structure  $a = 4.46$  Å,  $c = 5.93$  Å similar to those as observed by Aggarwal (1958).

(ii) Transmission, reflection and absorption

The deposits as mentioned before were blackish in colour. Fig. 24 shows transmittance, reflectance

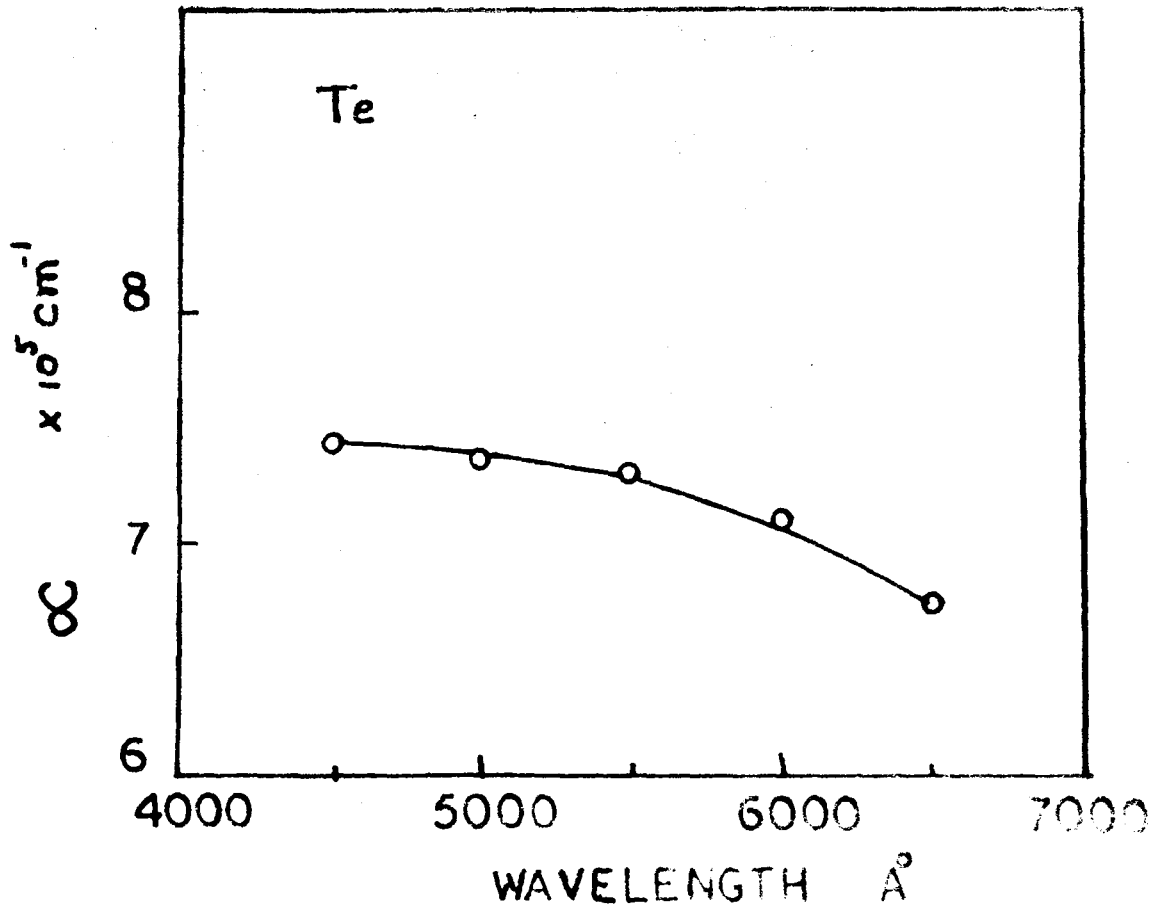


Fig. 25.

for two films ( $d = 142 \text{ \AA}$  and  $320 \text{ \AA}$ ). Transmittance increased with wavelength for very thin films, whereas reflectance was more or less same for all wavelengths. The variation of transmittance with thickness ranging between  $75 \text{ to } 450 \text{ \AA}$  were also measured for different wavelengths. It was found to fall exponentially with film thickness and there was no significant variation of transmittance between  $\lambda 4500 \text{ \AA}$  to  $\lambda 7000 \text{ \AA}$ .

### (iii) Absorption coefficient

Absorption coefficient was calculated from the slope of  $\log T$  vs  $d$  curves. The variation of the absorption coefficient with the wavelength is shown in Fig. (25). It was found that  $\alpha$  decreased though slightly from  $7.43 \times 10^5 \text{ cm}^{-1}$  to  $6.75 \times 10^5 \text{ cm}^{-1}$  with the increase of wavelengths from  $\lambda 4500\text{-}6500 \text{ \AA}$ , as shown in table 9.

### (iv) Optical constants

The optical constants were calculated from  $R_s$  and  $R_p$  components of the reflected light at an angle  $\theta = 45^\circ$ . It was however found that the homogeneity criteria  $R_s^2 = R_p$  did not hold good for tellurium films, even after annealing these films in vacuo. The inequality of the above relation however suggests that tellurium

Fig. 26.

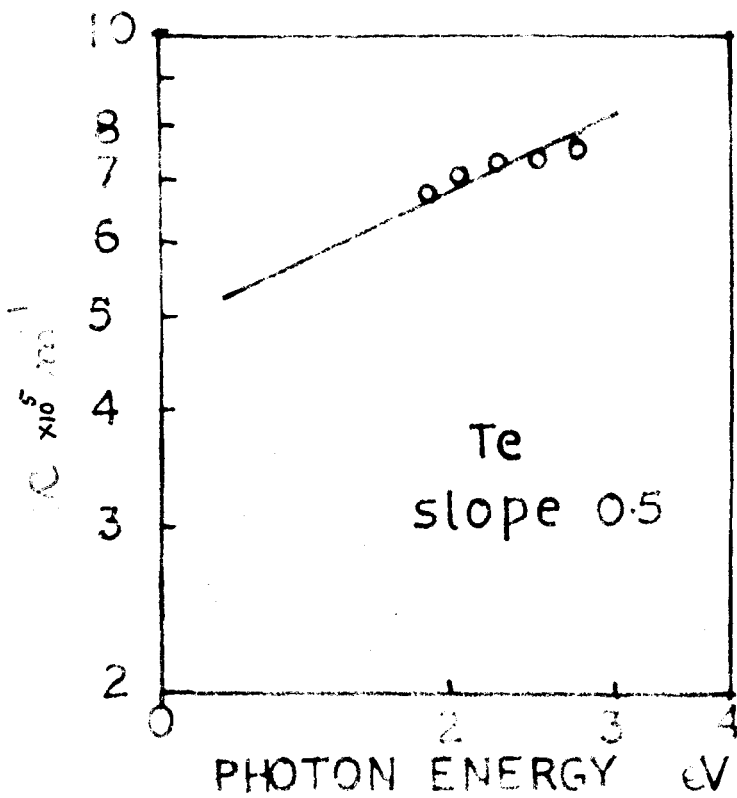
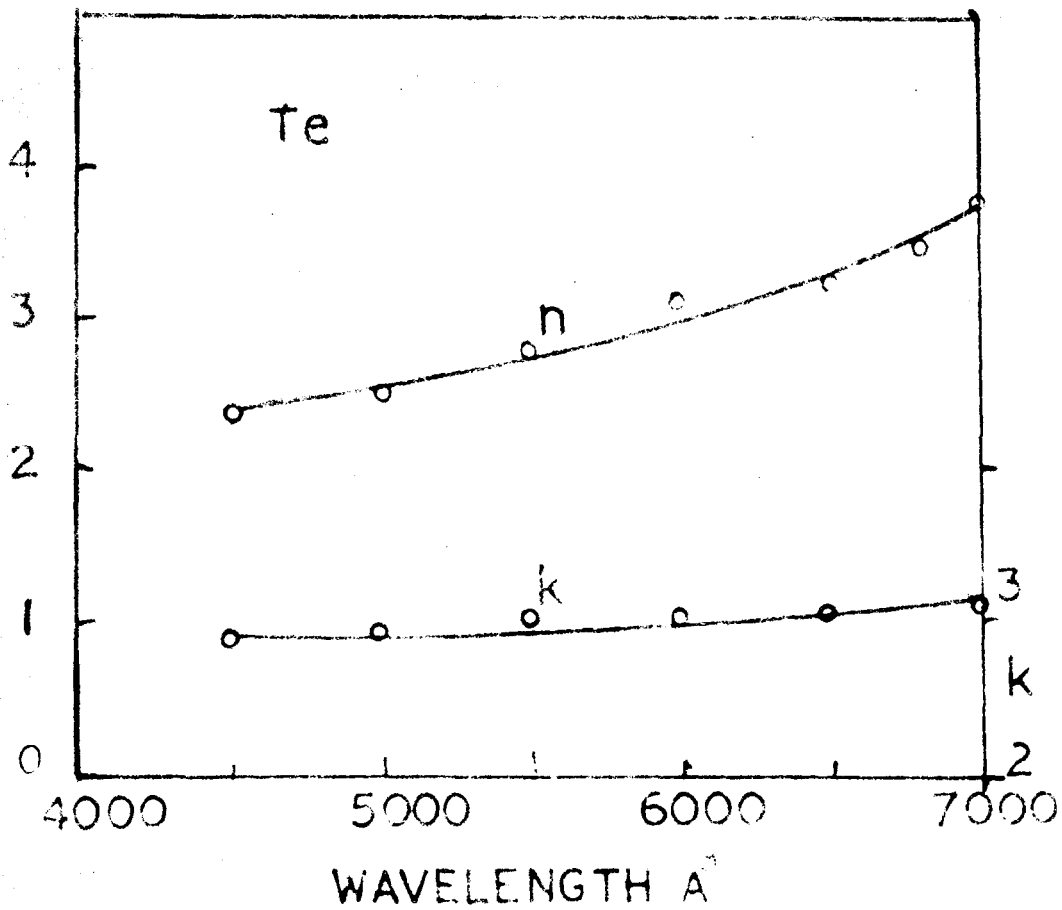


Fig. 27.

films were likely to be nonhomogeneous and probably anisotropic in optical sense. Since the formulae for  $n$  and  $k$  from  $R_s$  and  $R_p$  data are valid for all angles of incidence these parameters were calculated from the observed values. Fig. 26 shows the variation of the refractive index and extinction coefficient with the wavelength. It was found that  $n$  varied from 2.39 to 3.76 and  $k$  from 2.9 to 3.15 for the wavelengths  $\lambda$  4500 to 7000 Å (Table 10). It is remarkable to note that both  $n$  and  $k$  were quite high for all wavelengths.

#### (D) DISCUSSION

From the optical studies on selenium films, it was found that selenium absorbs strongly in the short wavelengths of visible region and became more transparent at the red region. The values obtained for the absorption coefficient in the visible spectral region agreed with the values of many other workers on selenium sputtered films. The optical energy band gap obtained from the plot of  $\alpha^{1/2}$  vs photon energy was 2.2 eV (cf Fig. 23) which was comparable with 2.2-2.3 eV from optical data of Stuke (1953) and also from the electrical measurements on liquid selenium 2.3 eV (Henkels, 1950; Henkels and Maczuzk 1953). Refractive index of selenium films were determined by using reflection method from  $R_s$  and  $R_p$  data at an angle of

incidence  $\theta = 45^\circ$ . It is seen (cf Fig. 22) that  $n$  increased with the wavelength, reached a maximum at  $\lambda 5500 \text{ \AA}$  and then decreased. The appearance of the dispersion peak in the index of refraction curve at about  $5500 \text{ \AA}$  (2.25 eV) is characteristic of the presence of an absorption edge at that energy. The value of  $n$  obtained by  $R_s$  and  $R_p$  data also agreed well with the values of Koehler et al. (1959) on selenium films obtained by normal incidence method using successive approximation. These considerations show that the  $R_s$  and  $R_p$  method which is mostly used for deriving optical constants of metals can also be utilised for the measurement of refractive index of semiconductors such as selenium, for which  $n$  is several times unity and  $k$  is less than unity.

From the optical measurements of tellurium films it is also observed that absorption coefficient decreased with the increase of wavelength in the visible region. As mentioned before even though the criterion  $R_s^2 = R_p$  at  $45^\circ$  did not hold good for tellurium films,  $n$  and  $k$  evaluated were found to be close to those value (2.5 to 3.5) obtained for bulk (Vandyke, 1922). The trend of the absorption coefficient curve with the increase of the wavelength suggests that the absorption edge is likely to be in the infra red region

and hence  $E_g$  would be in the infra red region.

It is also possible to find out the type of optical transition namely direct or indirect. The transition of electrons direct or otherwise can be determined from the slope of the curve  $\log \infty$  vs  $\log h\nu$  (Fig. 27). In the present case the slope was found to be  $1/2$ , which suggests that the transition to states in a higher band likely to be direct and allowed (Bardeen et al.1956).

In the case of selenium this method is not helpful, since the slope which was very high and in the absorption region.



Table 7

Dependence of absorption coefficient  $\alpha$ , and extinction coefficient (k) with the wavelength

$\lambda$ ( $\text{\AA}$ )	$\alpha$ $\text{cm}^{-1}$	k
4500	$1.43 \times 10^5$	0.51
5000	$1.28 \times 10^5$	0.51
5500	$8.40 \times 10^4$	0.34
6000	$7.25 \times 10^3$	0.04
6500	$2.98 \times 10^3$	0
7000	$2.0 \times 10^3$	0

Table 8

Variation of refractive index with the wavelength

$\lambda$ ( $\text{\AA}$ )	$R_s$	$R_p$	n	k
4500	0.4124	0.1619	2.87	1.0
5000	0.3959	0.1424	3.00	0.55
5500	0.3933	0.139	3.04	0.37
6000	0.3666	0.1142	2.96	0
6500	0.4633	0.2145	2.90	0
7000	0.454	0.2059	2.84	0

Table 9

Variation of absorption coefficient and extinction coefficient with the wavelength

$\lambda(\text{\AA})$	$\alpha$ ( $\text{cm}^{-1}$ )	$k$
4500	$7.43 \times 10^5$	2.66
5000	$7.37 \times 10^5$	2.93
5500	$7.30 \times 10^5$	3.19
6000	$7.10 \times 10^5$	3.39
6500	$6.75 \times 10^5$	3.50

Table 10

Dependence of  $n$  and  $k$  with the wavelength

$\lambda(\text{\AA})$	$R_s$	$R_p$	$n$	$k$
4500	0.625	0.410	2.139	2.90
5000	0.6294	0.4134	2.51	2.96
5500	0.6340	0.4156	2.79	3.06
6000	0.6296	0.4062	3.17	3.02
6500	0.6345	0.412	3.22	3.08
6800	0.6368	0.413	3.45	3.09
7000	0.6443	0.4207	3.76	3.15

CHAPTER VSTUDIES ON OXIDES OF COPPER FILMS(A) INTRODUCTION

Copper forms two definite oxides namely cuprous ( $\text{Cu}_2\text{O}$ ) and cupric ( $\text{CuO}$ ).  $\text{Cu}_2\text{O}$  (cuprite) has a simple cubic structure ( $\text{C}_3$  type), space group  $\text{P}_n 3_m$  ( $0h$ ),  $Z = 2$  with lattice parameter  $a = 4.26 \text{ \AA}$  for bulk. According to different workers (Niggili, 1922; Neuberger, 1931; Yamaguchi, 1938).  $\text{CuO}$  (tenorite) on the other hand has a monoclinic unit cell ( $a = 4.653 \text{ \AA}$ ,  $b = 3.41 \text{ \AA}$ ,  $c = 5.108 \text{ \AA}$  and  $\beta = 99^\circ 29'$ ; Tunnel et al, 1935). These oxides of copper can however be prepared by the thermal oxidation of copper in air and also by other methods.

Thermal oxidation of copper has been studied by various workers. Pilling and Bedworth (1923) made an extensive study on the oxidation of copper metal wires and reported the parabolic law at about  $700^\circ\text{C}$ . Lunholter and Kerstein (1939) studied the formation of copper oxide films by heating copper films in oxygen at temperatures in the range  $50$  to  $300^\circ\text{C}$  for various lengths of time by electron diffraction. His results revealed five zones namely  $\text{Cu}$ ,  $\text{Cu-Cu}_2\text{O}$ ,  $\text{Cu}_2\text{O}$ ,  $\text{Cu}_2\text{O-CuO}$  and  $\text{CuO}$ . Cruzon and Miley (1940) studied cuprous

cupric oxide films of different thicknesses formed by heating copper films in air at  $240^{\circ}\text{C}$  for various period of time. Cuprous films of  $d < 400 \text{ \AA}$  did not contain any cupric oxide. In the thickness range  $400 \text{ \AA}$  to  $800 \text{ \AA}$   $\text{Cu}_2\text{O}$  films contained some cupric oxide. White and Germer (1942) studied the rate of the oxidation of copper at room temperature and 20 mm. pressure by electron diffraction. Dighton and Miley (1942) found that copper was oxidised parabolically over a thickness range and then changed to a logarithmic growth rate.

Dixit and Agashe (1956) studied the oxidation of copper in air between  $150^{\circ}\text{C}$  to  $1030^{\circ}\text{C}$  and duration upto one hour by electron diffraction. Goswami and Trehan (1956, 1957, 1958) from a detailed study on the thermal oxidation of copper both single and polycrystalline at different temperatures in air, as well as in vacuo, and also from the thermal dissociation of cupric oxide to cuprous oxide came to conclusions that  $\text{Cu}_2\text{O}$  was generally formed below  $170^{\circ}\text{C}$  and at  $170^{\circ}\text{C}$ - $300^{\circ}\text{C}$  a mixture of cuprous and cupric oxide was present, and above  $300^{\circ}\text{C}$  it was mostly cupric oxide. They have also shown that  $\text{CuO}$  dissociated to  $\text{Cu}_2\text{O}$  at  $350^{\circ}\text{C}$  on heating in vacuo.

Electrical and semiconducting properties of  $\text{Cu}_2\text{O}$  have been investigated by many workers. Pfund

discovered as early as 1916 that cuprous oxide showed semiconductivity and photoconductivity. Von Auwers and Kerschbaum (1930) observed a decrease in the semiconductivity of copper oxide plates when they were heated in vacuo. Vogt (1930) studied electrical conduction, thermoelectric power, Hall constant and heat conduction between  $-70^{\circ}\text{C}$  to  $+70^{\circ}\text{C}$  of  $\text{Cu}_2\text{O}$ . Juse and Kurschetov (1932) investigated the relation between the conductivity and stoichiometric excess of oxygen, and established that the increasing deviation from the stoichiometry resulted in an enhanced conduction. Hartman (1936) investigated the electrical properties of  $\text{CuO}$  and observed a negative Hall constant and an abnormally small mobility. Augello (1942) measured the Hall constant and the conductivity of cuprous oxide and showed that the exponential law of temperature dependence was not obeyed. The departure from this law was caused by a loss of conduction holes with time and an anomalous decrease in the mean free path in the vicinity of  $100^{\circ}\text{C}$ . Fieldman (1943) studied the electrical conductivity and isothermal Hall effect in cuprous oxide. Toshihiro and Okada (1949) carried out measurements of electrical conductivity, Hall constant and thermo emf between room temperature and  $450^{\circ}\text{C}$  under a pressure of 5 to 20 mm. Hg. and magnetic field of 3000 to 4000 gauss.

Semiconducting properties of cuprous oxide were investigated by Schmidt (1954), the conductivity (K) and Hall constant (R) were measured between  $-160^{\circ}$  and room temperature. K was between  $10^{-4}$  and  $3 \times 10^{-6}$   $\text{ohm}^{-1} \text{cm}^{-1}$ , R was between  $1.8 \times 10^6$  and  $1.05 \times 10^7$   $\text{cm}^3/\text{C}$ . In most cases straight lines were obtained if  $\log K$  or  $\log R$  was plotted against  $1/T$ . Toth (1961) studied the electrical conductivity of single crystals of cuprous oxide at higher temperatures. Dahl and Switendick (1966) reported that  $\text{Cu}_2\text{O}$ , a semiconductor had a band gap of 2.17 eV. Young and Schwarz (1961) measured the electrical conductivity and the thermoelectric power of  $\text{Cu}_2\text{O}$  single crystals in the temperature range  $300^{\circ}$  to  $500^{\circ}\text{K}$ . The latter decreased only slightly with the increase of temperature whereas the former increased an activation energy was 0.26 eV. Weichmann and Kuzel (1970) made conductivity measurements of single crystals of  $\text{Cu}_2\text{O}$  from 20 to  $840^{\circ}\text{C}$  to explain the various activation energies observed at different temperatures and oxygen pressures.

Photoconductivity and optical absorption of oxides of copper have also been investigated by a number of workers. Kikoin (1938) observed a new photoelectric effect in  $\text{Cu}_2\text{O}$  when a sample of  $\text{Cu}_2\text{O}$  was placed in a magnetic field. An e.m.f. perpendicular to both the

light beam and the magnetic field was then produced. Ioffe (1937) studied the spectral distribution of the inner photo electric effect in  $\text{Cu}_2\text{O}$  and found a fundamental maximum of the photoconductivity at  $630 \text{ m}\mu$ . Semenko (1938) found a linear relationship between the photomagnetic current and the dimension of  $\text{Cu}_2\text{O}$  films. Kikoin and Simenko (1940) studied the influence of magnetic field on the photoconductivity of  $\text{Cu}_2\text{O}$ . At liquid nitrogen temperature the magnetic field however sharply reduced the photoconductivity of  $\text{Cu}_2\text{O}$ . Okada and Uno (1949) studied the inner photo effect of  $\text{Cu}_2\text{O}$  and interpreted that the peak of the photoconductivity at  $0.6 \mu$  as corresponded to a transition of electron from the full band to impurity level in the semiconductor but not to the conduction band.

Pastrnyak (1961) studied the absorption and reflection spectra of crystalline  $\text{Cu}_2\text{O}$  (bulk) in the vicinity of absorption edge at  $77^\circ\text{K}$ . The temperature dependence of the absorption coefficient  $\alpha$  in the visible region was measured ( $\alpha$  for  $\lambda 5500 \text{ \AA} = 3 \times 10^{3-2} \text{ cm}^{-1}$  and for  $\lambda 6500 \text{ \AA} = 1.5 \times 10^3 \text{ cm}^{-1}$ ). Pastrnak (1961) found that refractive index of  $\text{Cu}_2\text{O}$  (bulk) varied from about 2.7 at  $0.5 \mu$  to about 2.3 at  $12 \mu$ . Baumeister (1961) studied the relative optical absorption coefficient of polycrystalline slabs of  $\text{Cu}_2\text{O}$

at 295°, 77° and 4.2°K.

Recently optical parameters of copper oxide films have been investigated by many workers. Wieder and Czanderna (1962 and 1966) studied the oxidation of copper films and reported that a composition  $\text{CuO}_{.67}$  could be formed in 100 torr. oxygen from about 110° to 200°C for thickness upto 1085 Å depending on time and temperature. The transmittance and reflectance of  $\text{CuO}_{.67}$  and  $\text{CuO}$  films have been measured in the wavelength region 400 to 800 mμ and optical constants were determined from these data. It was found that  $n$  varied from 3.1 to 2.15 and  $k$  varied from .67 to .12 in the wavelength range 400 to 800 mμ. Czanderna and Bayko (1969) determined the optical constant of  $\text{CuO}_{.67}$  in the wavelength region 400 to 800 mμ with the help of a computer assuming a system of two absorbing layers on a transparent substrate and found that optical constants were independent of the oxide thickness. They also evaluated optical energy band gap by extrapolating the steepest portion of the absorption curve and obtained a value 2.24 eV for  $\text{CuO}_{.67}$  at room temperature compared to 2.1 eV for  $\text{Cu}_2\text{O}$  as determined from Parstrnyak's data. Recently Ladelfe et al.(1972) determined the optical constants of cupric oxide. They found that  $n$  varied from 2.45 to 2.62 and  $k$  from 0.744 to 0.132 for



$\lambda$  450-800  $\mu$ .

It is seen from the above that not much work has been carried out on optical properties of cuprous oxide ( $\text{Cu}_2\text{O}$ ) and cupric oxide ( $\text{CuO}$ ) films though recently some studies on optical properties of  $\text{CuO}$ .<sup>67</sup> have been studied. Unless the preparations of oxide films are carried out in controlled conditions, the oxide layers formed are likely to be a mixture instead of a single species. Hence some of the reported results on optical properties are likely to be thus affected. So in the following the preparations of different oxides of copper were made in controlled conditions and then their optical properties viz. transmission, reflection, optical constants, optical energy band gap, etc. have been studied as functions of film thickness, wavelength, etc. in the visible region.

#### (B) EXPERIMENTAL

The two oxides of copper namely,  $\text{Cu}_2\text{O}$  and  $\text{CuO}$  were prepared by the thermal oxidation of copper films under appropriate conditions of temperature. The methods adopted were similar to those already described by Goswami and his workers (Goswami and Trehan, 1957; Bhide, 1972). They have shown that  $\text{Cu}_2\text{O}$  was exclusively formed if copper was thermally oxidised in air at or

below 170°C. If, however, copper was heated at higher temperature say to about 200°C and a little above the layers consisted of a mixture of Cu<sub>2</sub>O and CuO. At a still higher temperature say about 300°C, the surface layers consisted of CuO only.

Copper films were deposited on glass substrates in vacuo ( $\approx 10^{-5}$  torr.) as described in Chapter II. Pure copper pieces (BDH quality) were cleaned with a dilute solution of HCl, then washed with distilled water and finally with alcohol. They were then evaporated from a previously flashed tungsten boat in the usual way in vacuo.

(a) Cuprous oxide films

The copper films thus deposited were then oxidised in air at about 150°C-160°C for about two hours in an electrically heated tubular furnace open at both ends. These films turned greenish-yellow in colour depending on film thickness and surface layers were found to be of cuprous oxide, as confirmed by electron diffraction examinations both by reflection and transmission methods.

(b) Copper oxide films

Copper films were also heated to 250°C for two

hours in air films changed to brownish red in colour. These films found to consist of a mixture of  $\text{Cu}_2\text{O} + \text{CuO}$ .

(c) Cupric oxide

Fresh copper films were heated to about  $320^\circ\text{C}$  for about 3 hours in air and the structure was confirmed by electron diffraction to be  $\text{CuO}$  only.

(C) RESULTS

(a) Cuprous oxide

Cuprous oxide films were generally greenish yellow. It was however observed that if the oxide layers were of thickness say  $> 500 \overset{\circ}{\text{A}}$ , there always remained some unreacted copper underneath the oxide film. This copper layer could not easily be oxidised in spite of repeated heating at that reaction temperature range. Consequently all experiments on  $\text{Cu}_2\text{O}$  were restricted to film thickness of about  $500 \overset{\circ}{\text{A}}$  or less.

(1) Structure

To identify the nature of the oxide films as formed at about  $150^\circ\text{C}$ , the electron diffraction study was made on the deposits. A typical electron diffraction pattern is shown in Fig. (28). Measurements of  $d$  values with graphite standard is shown in table.11.

Fig. 28

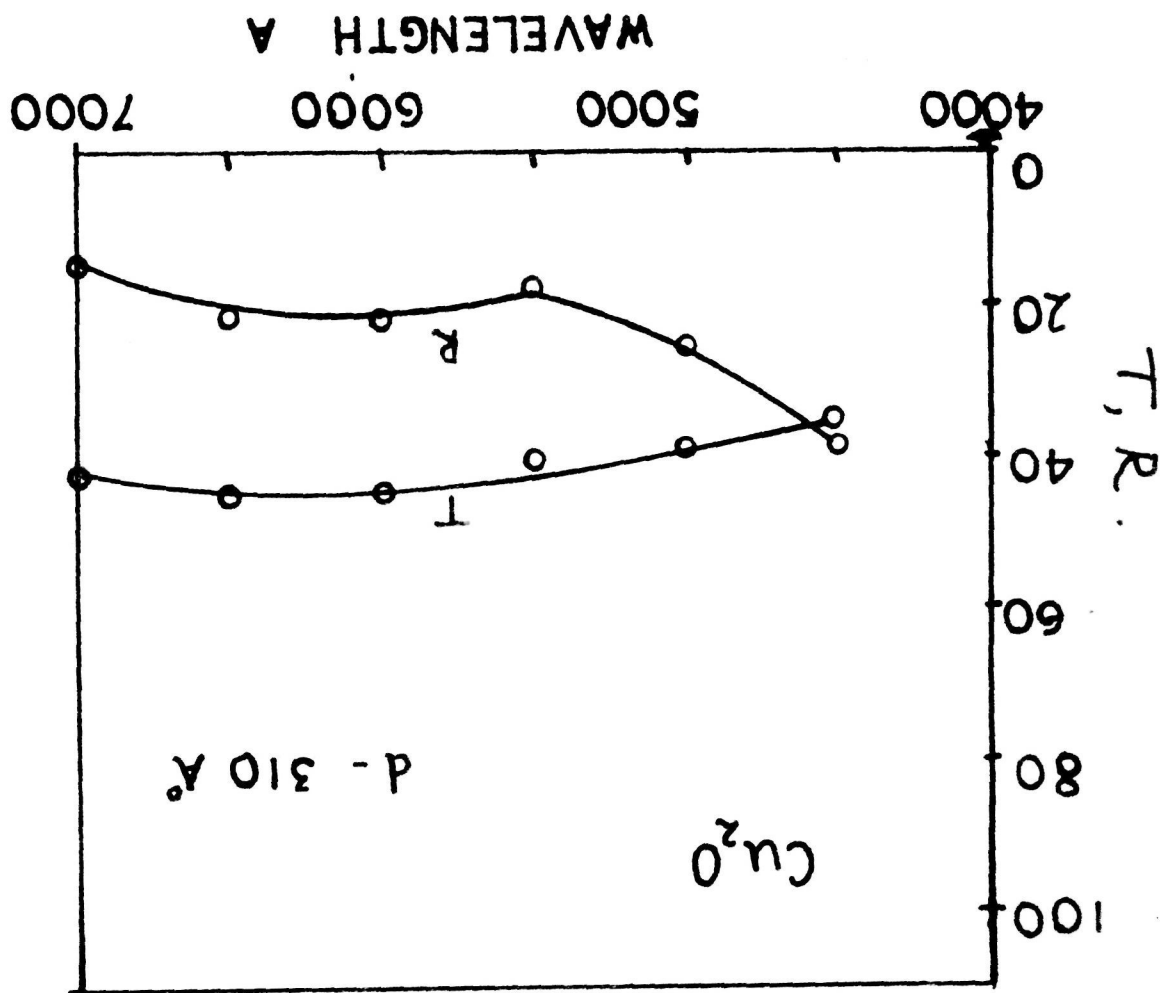


Fig. 29

It was found that the pattern corresponds to cuprous oxide having cubic structure ( $a = 4.27 \text{ \AA}$ ).

Table 11

Intensity	d in $\text{\AA}$	hkl
vf	3.02	
s	2.46	111
f	2.15	200
m	1.51	220
vf	1.27	222

s = sharp  
 m = medium  
 f = faint  
 vf = very faint

(ii) Transmission, reflection and absorption

Fig. 29 shows the typical variations of reflection, transmission of cuprous oxide film ( $d \approx 310 \text{ \AA}$ ) with the wavelength. It is seen that transmittance increased though slightly with wavelengths, whereas reflectance decreased though not uniformly. The variation of  $R_s$  and  $R_p$  components of reflected polarised light with the angle of incidence is shown

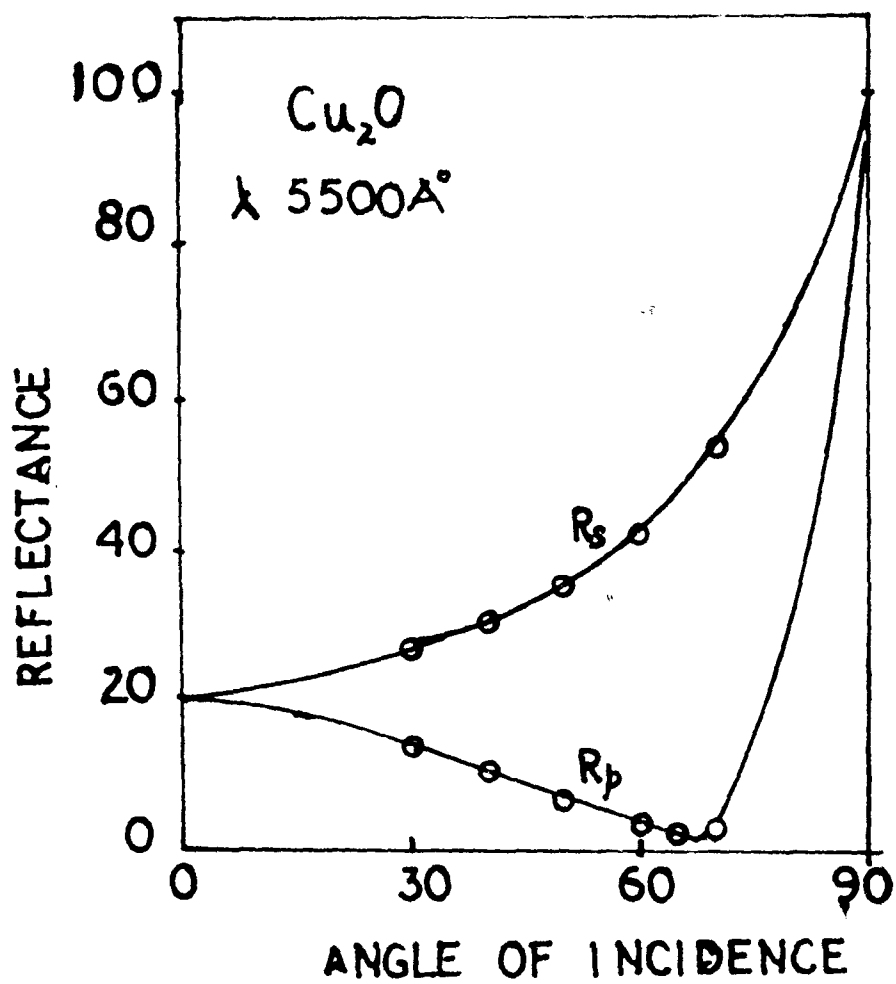


Fig. 30.

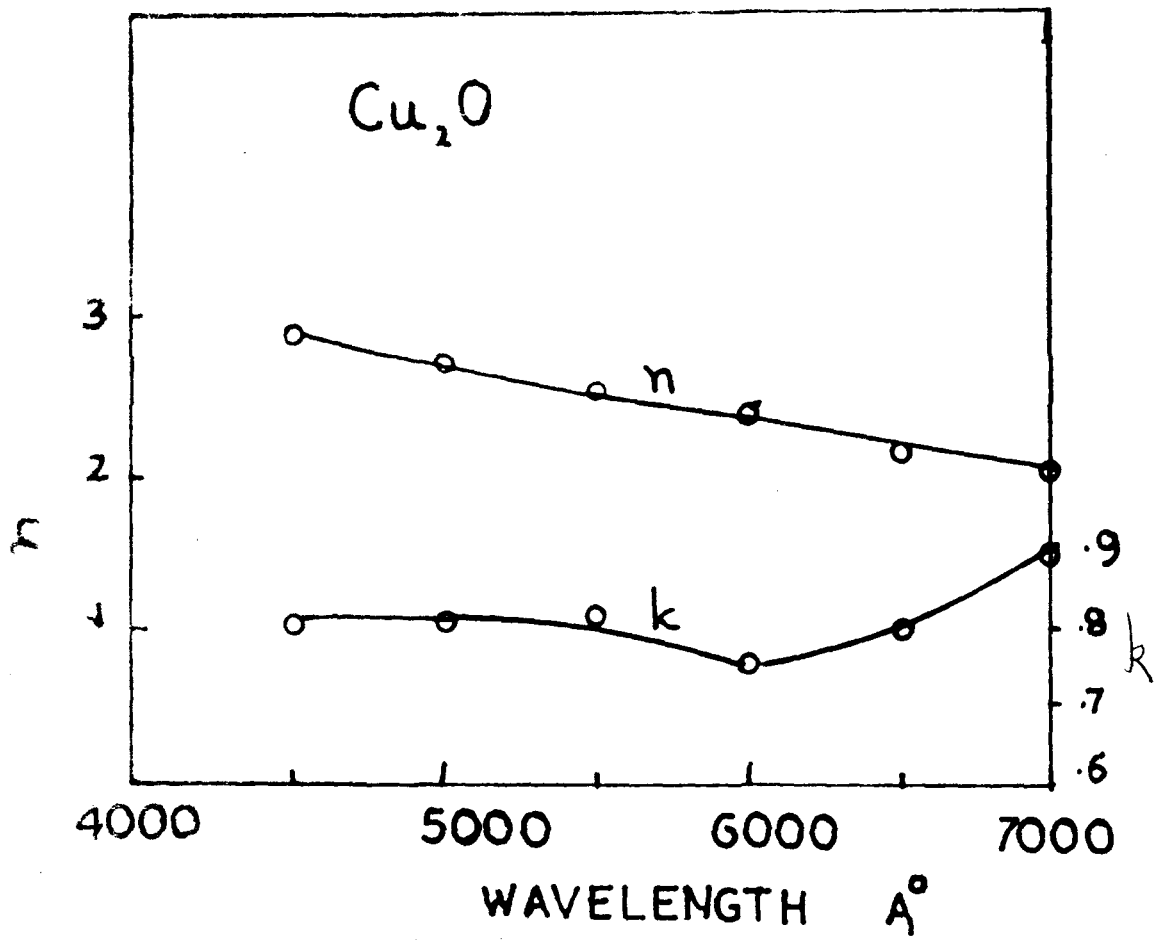


Fig. 31.

in Fig. (30). It was observed that  $R_p$  was minimum at about  $68^\circ$  for  $\lambda 5500 \text{ \AA}$  and refractive index given by  $n = \tan \phi$ , was found to be 2.48.

(iii) Absorption coefficient

The absorption coefficient was calculated from the slope of the curve  $\log T$  vs  $d$ . The dependence of the absorption coefficient and extinction coefficient with the wavelength is given in table 12. It is seen that  $\alpha$  was minimum at  $\lambda 6000 \text{ \AA}$ .

(iv) Optical constants

Refractive index was calculated from  $R_s$  and  $R_p$  components of the reflected light. It was also found that at an angle of incidence  $\phi = 45^\circ$ ,  $R_s^2 = R_p$  for all the wavelengths within the experimental error. Refractive index,  $n$  found to decrease from 2.93 to 2.02 with wavelength ( $\lambda 4500-7000 \text{ \AA}$ ).  $k$  was calculated not only from the absorption coefficient but also from  $R_s$  and  $R_p$  data. Both the values are nearly same, though the latter was a little higher. The values of  $n$  and  $k$  for various wavelengths is given in table 13 and shown in Fig. (31).



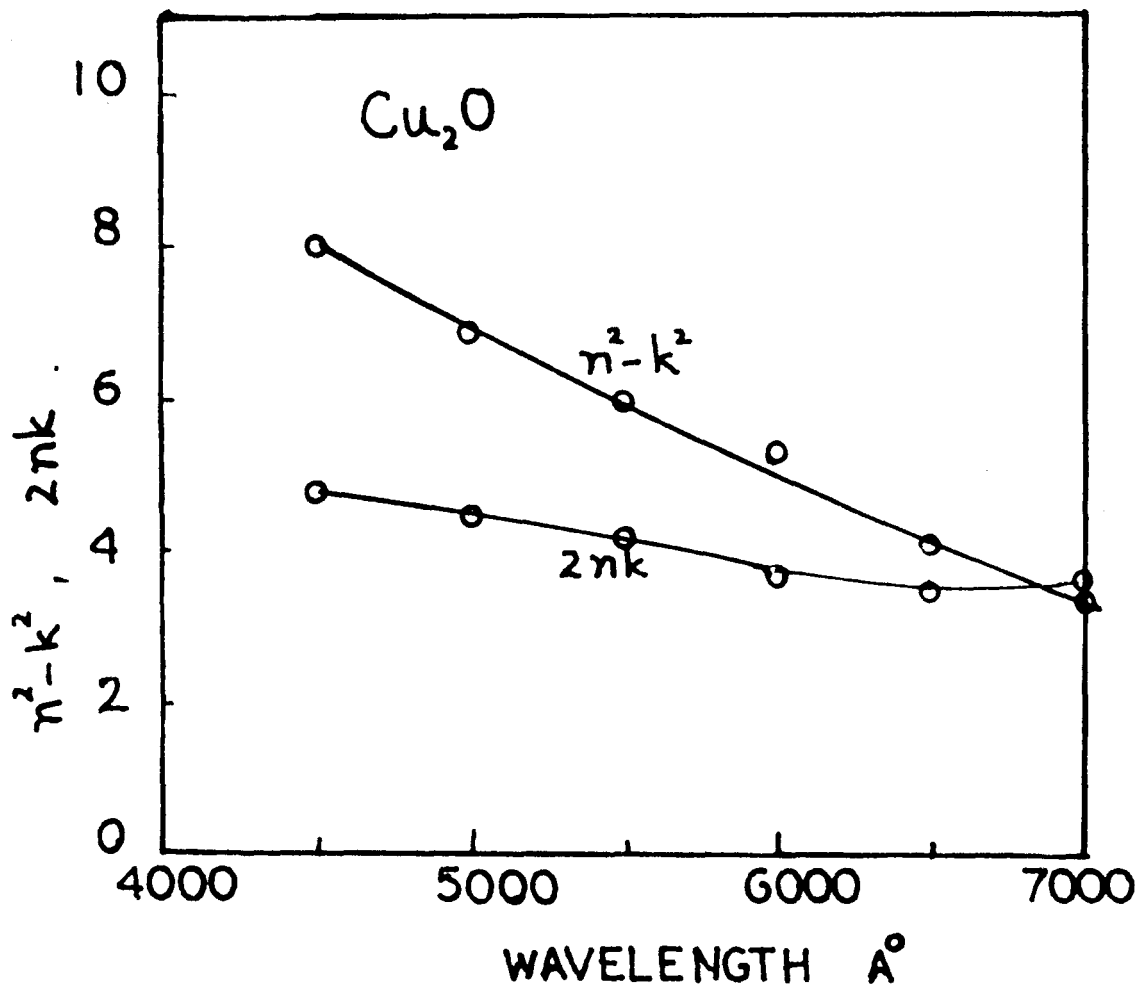


Fig. 32.

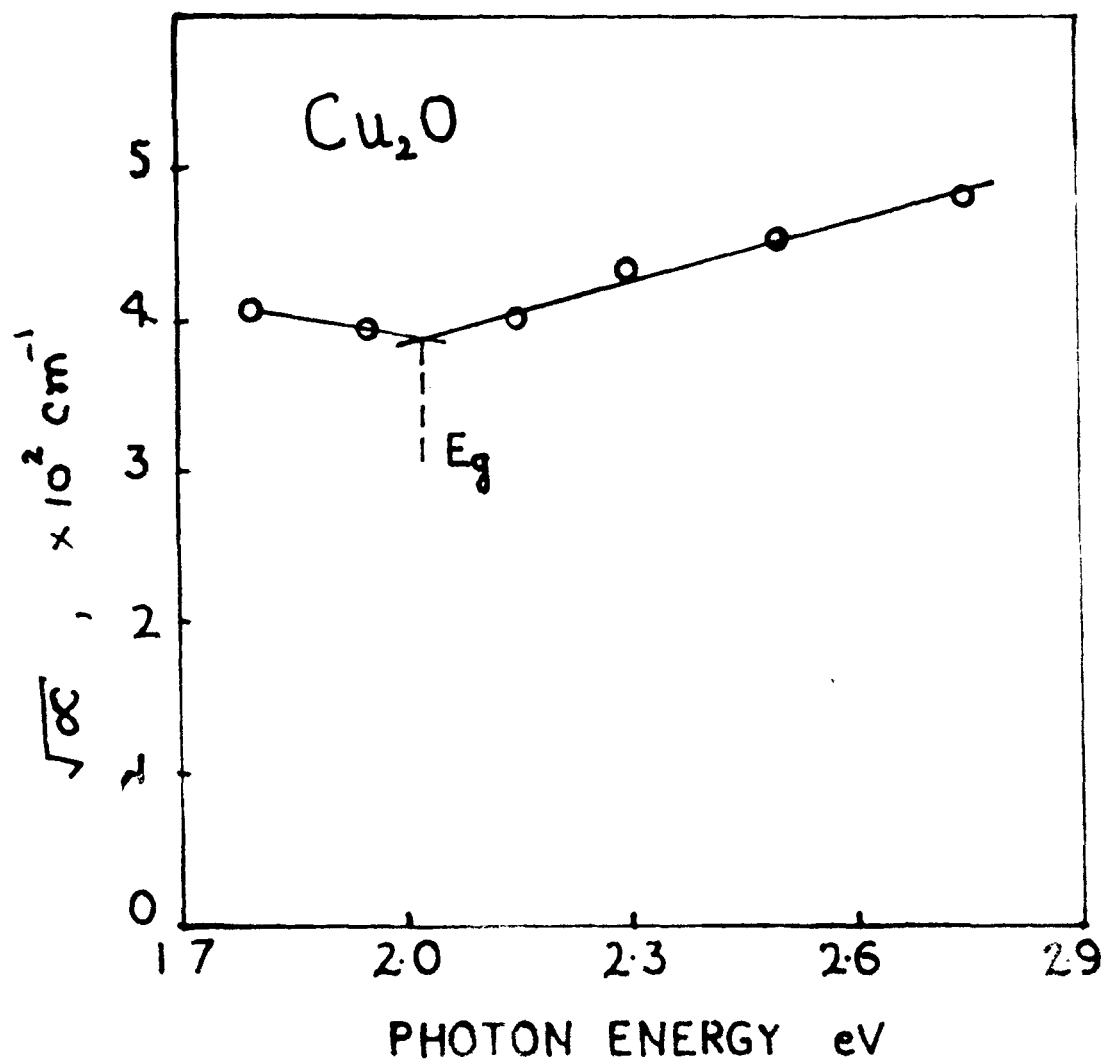


Fig. 33.

(v) Dielectric constant

It is also possible to calculate the dielectric constant for optical frequencies from the optical parameters  $n$  and  $k$ . The variation of  $\epsilon_1$  and  $\epsilon_2$  of the complex dielectric constant are shown in Fig. 32. It is seen that  $\epsilon_1 = n^2 - k^2$  varied from 7.94 to 3.27 and  $\epsilon_2 = 2nk$  varied from 4.74 to 3.64 in the visible region (Table 14).

(vi) Optical energy band gap

Optical energy band gap was determined from the plot of  $\alpha^{1/2}$  vs. photon energy (Fig. 33). The intersection point of the two straight lines of the plot gives the value of optical band gap. It is found that  $E_g$  thus obtained was 2.05 eV, which agrees with the published data of the bulk (Pastrnyak, 1961).

(b) Copper oxide(i) Structure

Oxide films of copper formed at different temperatures have been studied in detail by Goswami and Trehan (1956, '57, '58). It has been shown by them that oxides formed around 250°C consists of a mixture of the  $\text{Cu}_2\text{O}$  and  $\text{CuO}$ . Such a mixture with suitable

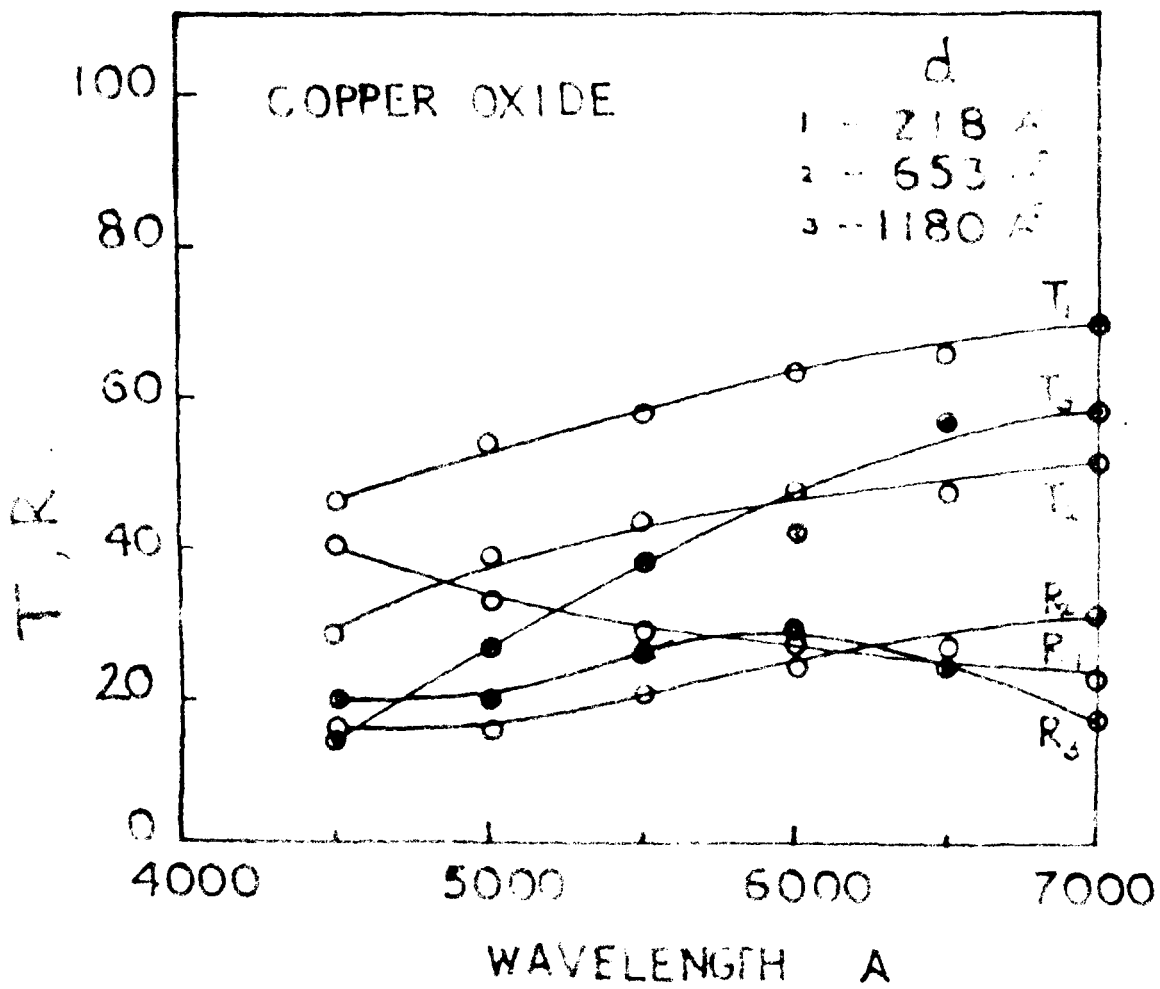


Fig. 34.

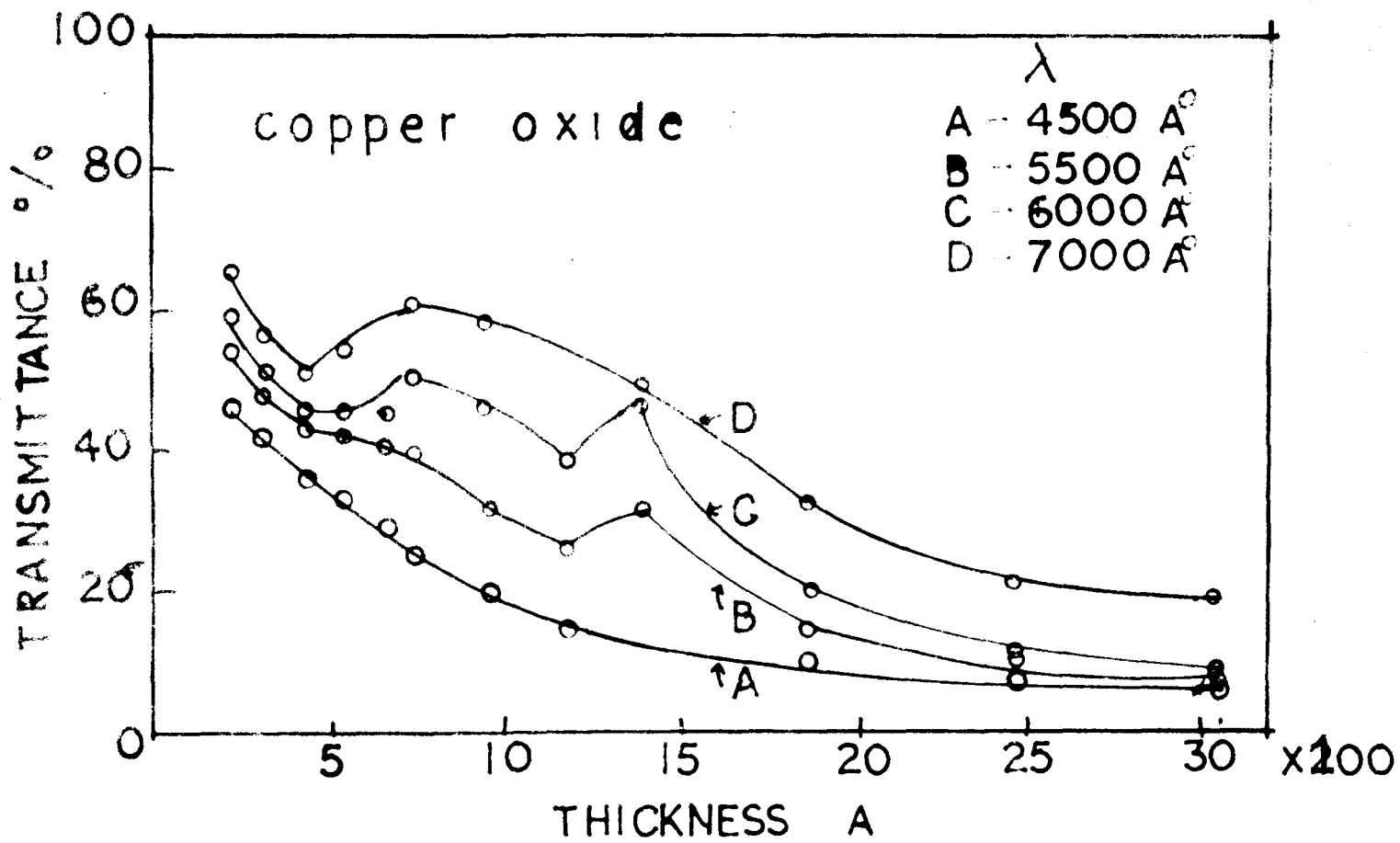


Fig 35

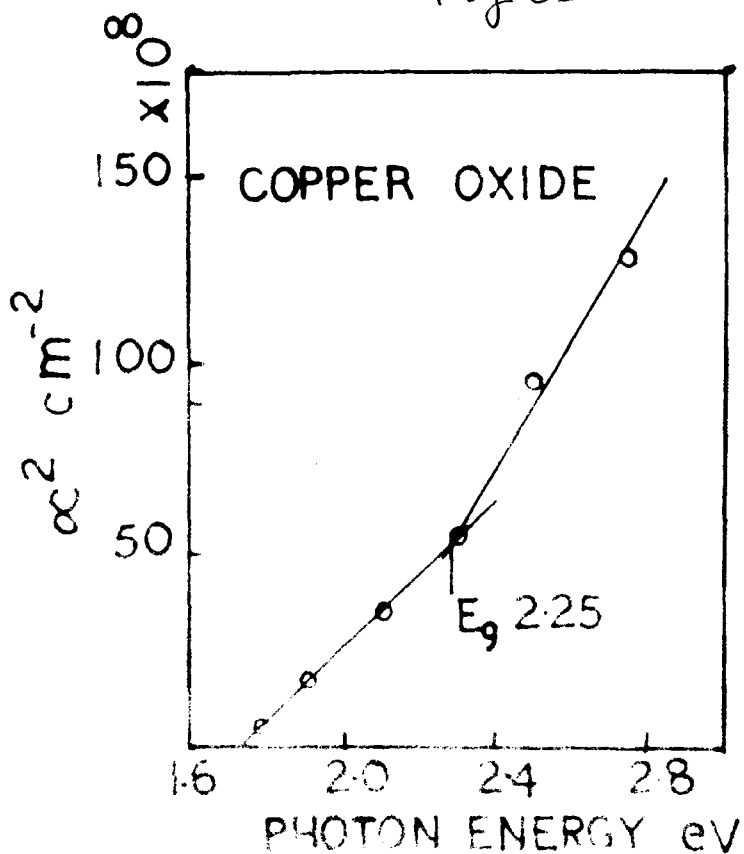
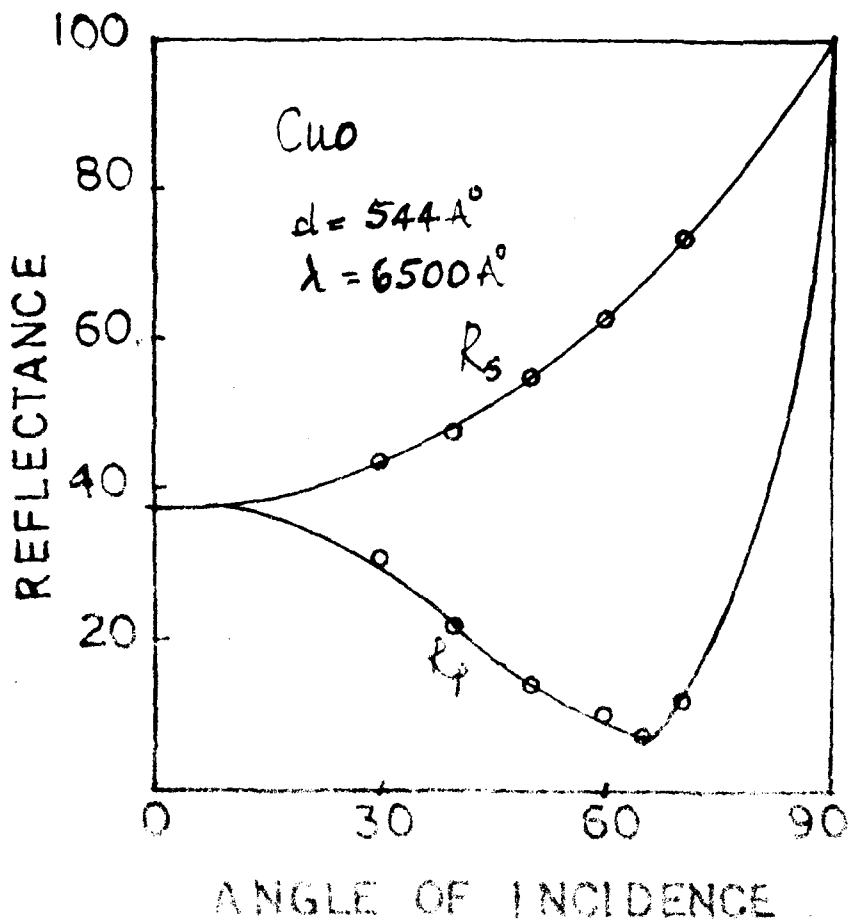
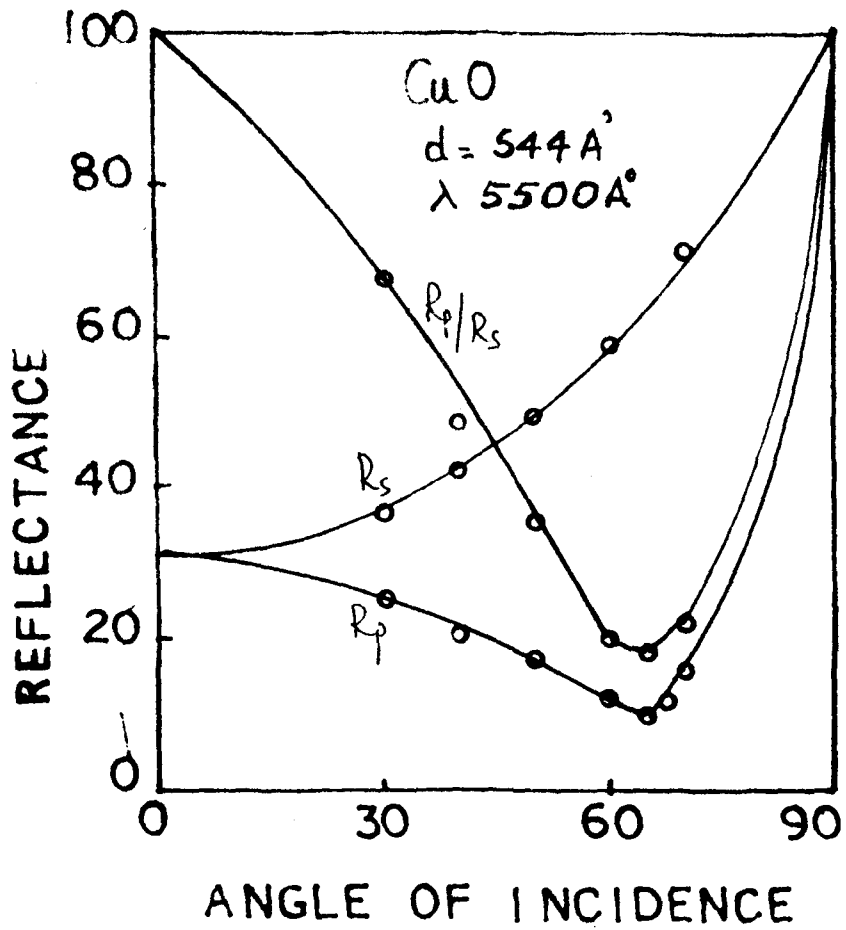


Fig. 39.

Fig. 36.



proportions of the two species of oxides will no doubt have a composition of  $\text{CuO}_{.67}$ , supposed to be a new species, as reported by various workers (Wieder and Czanderna 1962, 1966).

(ii) Transmission, reflection and absorption

Figure 34 shows transmission and reflection spectra for three films of different thicknesses ( $d = 218 \text{ \AA}$ ,  $653 \text{ \AA}$  and  $1180 \text{ \AA}$ ). These copper oxide films formed at  $250^\circ\text{C}$  showed some interesting features in its transmittance vs. thickness curves (Fig. 35). It is seen that thinner films showed interference effects for all wavelengths except for shorter wavelengths say about  $4500 \text{ \AA}$ . Interference peaks however shifted with the wavelength. Thicker films, on the other hand, showed the usual exponential fall for all wavelengths. The variation of  $R_s$  and  $R_p$  with the angle of incidence for two wavelengths  $\lambda$   $5500 \text{ \AA}$  and  $6500 \text{ \AA}$  is shown in Fig. (36).

(iii) Absorption coefficient was calculated from the transmittance vs. thickness curve. Table 15 gives variation of  $\infty$  with wavelength. It is seen that absorption coefficient varied from  $1.14 \times 10^5 \text{ cm}^{-1}$  to  $2.14 \times 10^4 \text{ cm}^{-1}$ .

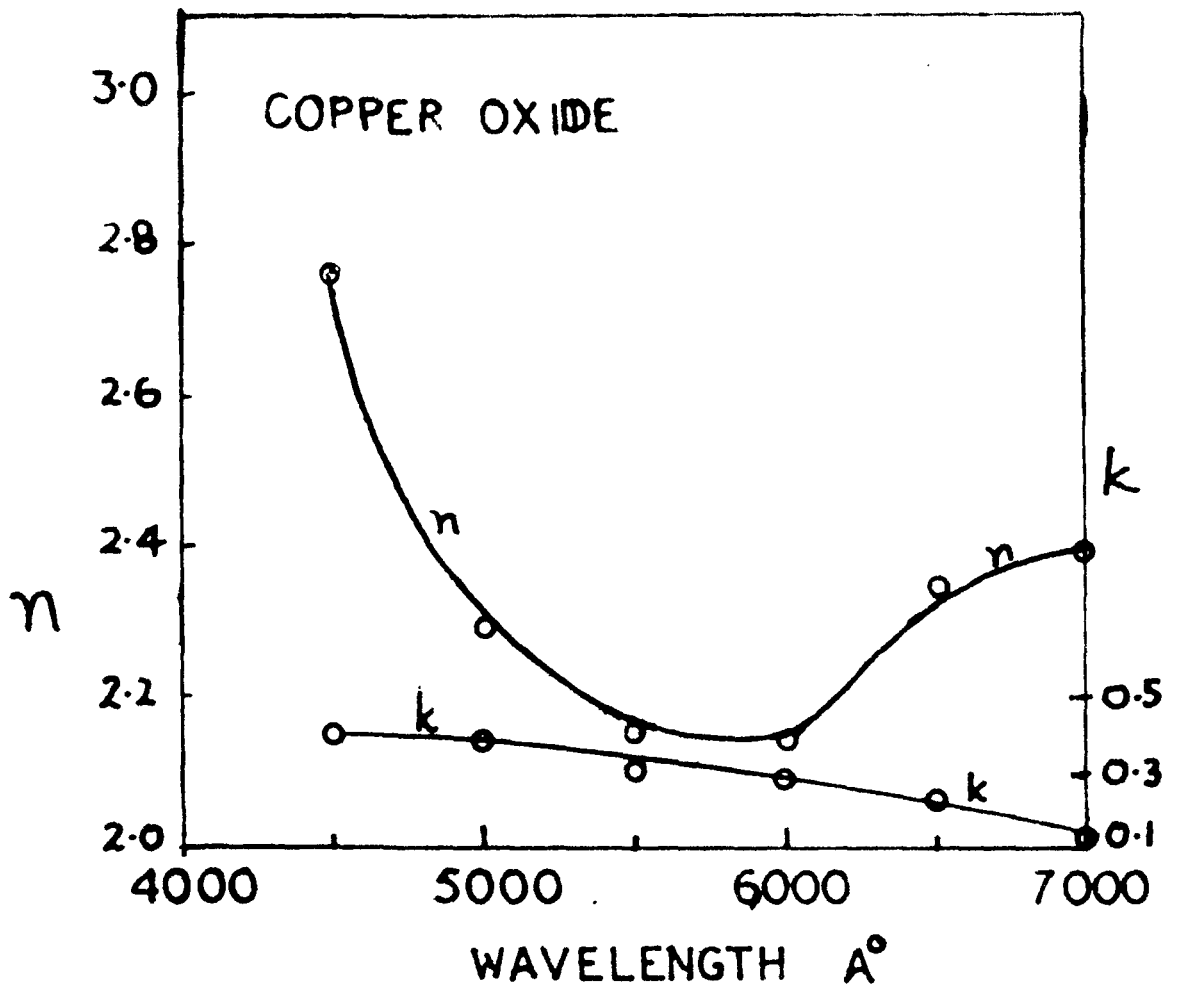


Fig. 37.



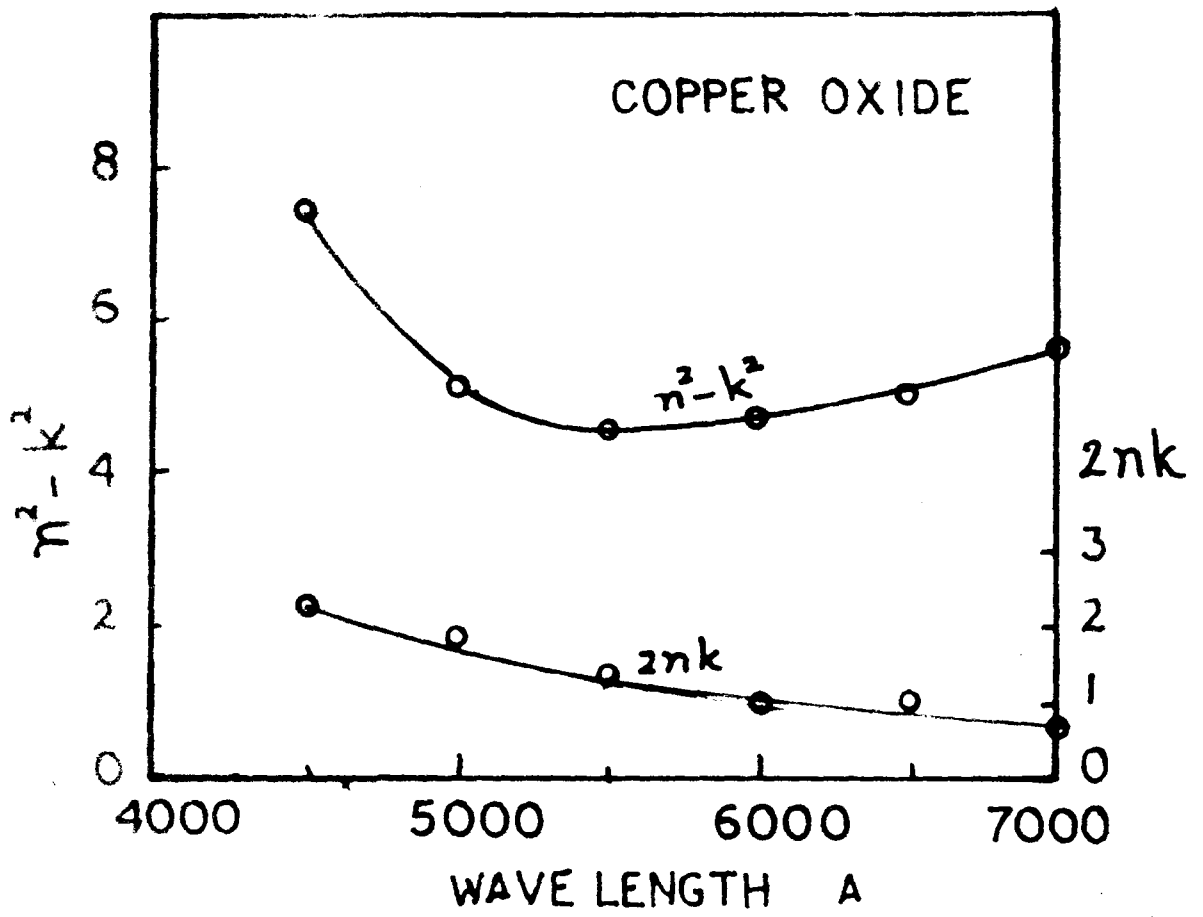


Fig 38''.

#### (iv) Optical constants

Refractive index was calculated from  $R_s$  and  $R_p$  components at an angle  $\theta = 45^\circ$ . It was found that the relationship  $R_s^2 = R_p$  at  $45^\circ$  was valid for all wavelengths. Refractive index thus calculated decreased with the increase of wavelength upto  $6000 \text{ \AA}$  and then increased as shown in the figure (37) and the values of  $n$  for various wavelengths is given in table 16. The extinction coefficient  $k$  was calculated from the absorption coefficient i.e. from the slope of transmittance vs. thickness curve, and found to vary from .41 to .12 for  $\lambda 4500-7000 \text{ \AA}$ .  $n$  was also measured for different angle of incidence. Table 17 shows the values of  $n$  for different angle of incidence i.e.  $45^\circ$ ,  $55^\circ$ ,  $65^\circ$ . All these values agree well for different  $\theta$ , thus showing that measurements at  $45^\circ$  only which also give data for homogeneity criteria is good enough for evaluation of  $n$  and  $k$ .  $n$  was found to be independent of film thickness.

#### Dielectric constant

Real part as well as imaginary part of the complex dielectric constant i.e.  $\epsilon_1$  and  $\epsilon_2$  were calculated from the optical parameters  $n$  and  $k$  (Fig. 38).  $\epsilon_1$  was found to vary from 7.45 to 2.26

fig 41.

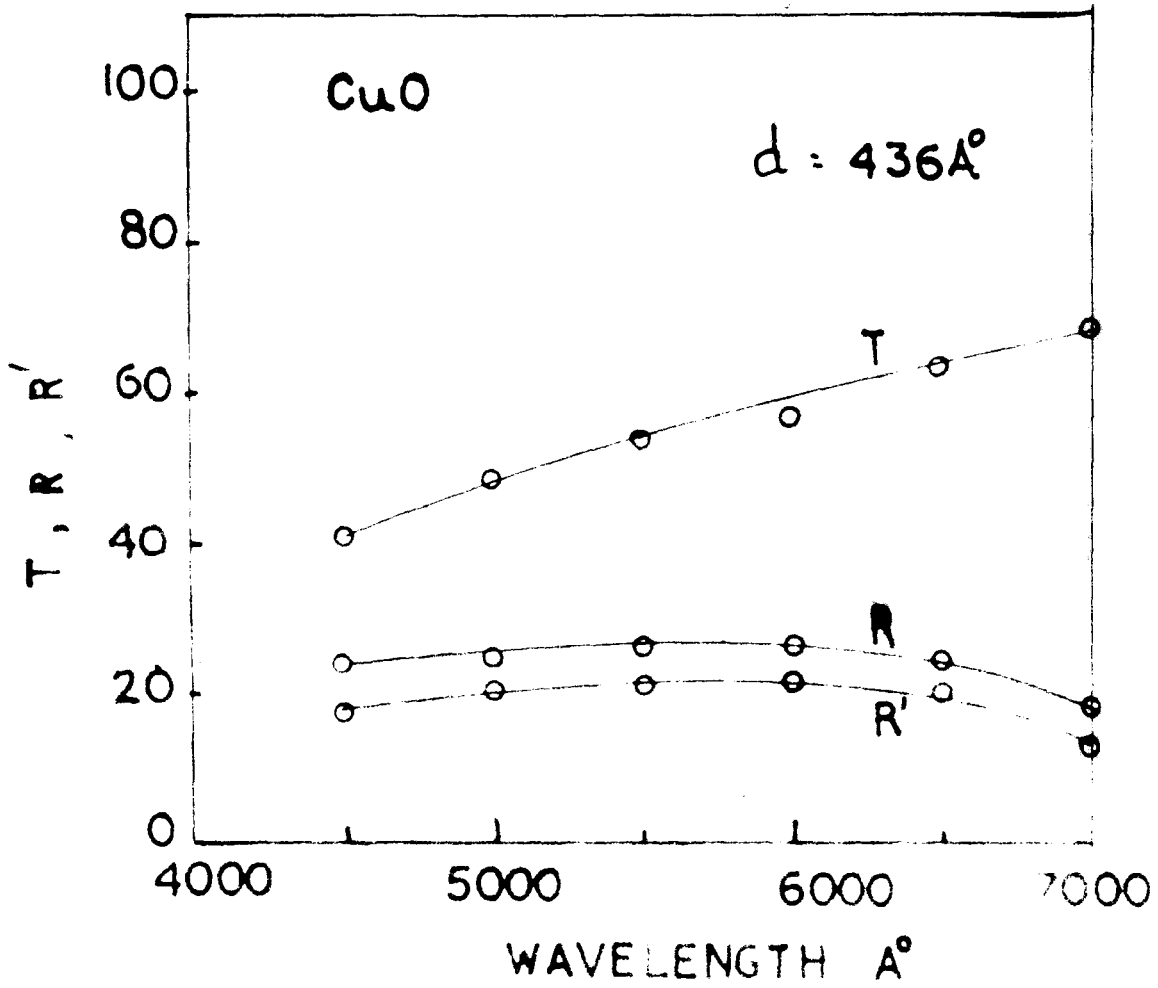
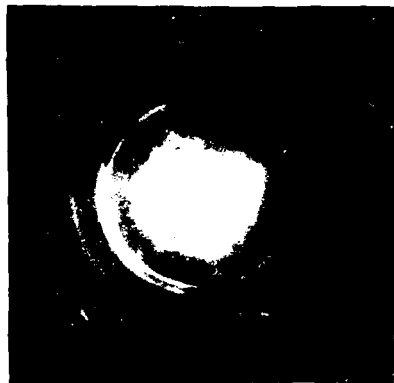


Fig. 40.



and  $\epsilon_2$  from 2.26 to 0.57 in the visible region.

### Optical energy band gap

Optical energy band gap was also determined from the plot of  $\alpha^2$  vs.  $h\nu$  (Fig. 39). The intersection point of two branches of the curve gives the value for  $E_g = 2.25$  eV which conforms to the  $E_g (= 2.24$  eV) reported by Czanderna and Bayko (1969) for  $\text{CuO}_{0.67}$ .

### Cupric oxide

#### (1) Structure

The electron diffraction transmission examination of copper films on NaCl polycrystalline tablets heated at about  $320^\circ\text{C}$  for about two hours in air yielded pattern as shown in Fig. 40. Table 18 shows  $d$  values comparing with a graphite standard. The diffraction pattern together with  $d$  values correspond to  $\text{CuO}$  reported by Goswami and Trehan (1957).

Table 18

Int.	$d$ in $\overset{\circ}{\text{A}}$	hkl
s	2.54	002 111
s	2.32	111 200

Table 18 (contd.)

Int.	d in Å <sup>o</sup>	hkl
m	1.87	$\bar{2}02$
f	1.52	113
m	1.42	$\bar{3}11, 310$

s = sharp, m = medium, f = faint

(ii) Transmission and reflection

Fig. 41 shows the typical variation of transmittance (T), reflectance (R) and reflectance from the substrate side of the film (R') with the wavelength ( $d \simeq 436 \text{ Å}^o$ ) using the normal incidence method. It is seen that transmittance increased with the wavelength whereas reflectance both R and R' had a slight tendency to decrease especially at higher wavelengths.

(iii) Absorption coefficient

Absorption coefficient was calculated from the transmittance and reflectance data at normal incidence using the equation  $T = (I-R)e^{-\alpha d}$ . The variation of absorption coefficient with the wavelength is shown in Table 19. It is seen that  $\alpha$  decreased

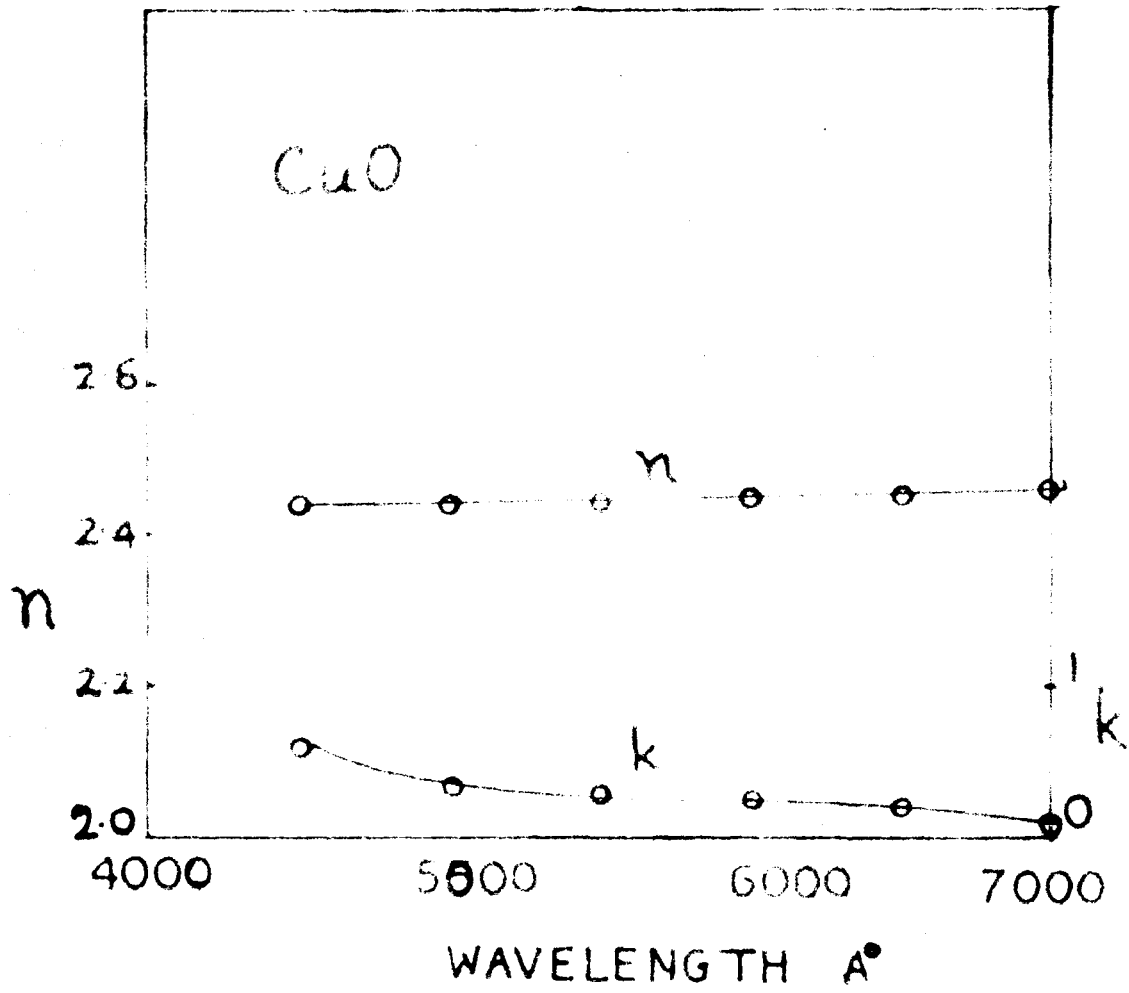


Fig 42.

with the increase of the wavelength.

(iii) Optical constants

Optical constants were evaluated from transmittance (T), reflectance (R) and reflectance from the substrate side of the film (R') using David (1937) and Wolter (1937) equations No. 7 and 8 given in Chapter II. The variation of refractive index and extinction coefficient with the wavelength is shown in figure (42) and the values are given in Table 20. It is seen that  $n$  increased only slightly with the wavelength whereas  $k$  decreased. Refractive index was also evaluated from  $R_s$  and  $R_p$  data (Table 20a). It was found that the values obtained by both the methods agreed quite well.

(iv) Dielectric constant

Dielectric constant was determined from the optical parameters  $n$  and  $k$ . The real part of the dielectric constant  $\epsilon_1 (= n^2 - k^2)$  found to vary from 5.59 to 6.44 and the imaginary part  $\epsilon_2 (= 2nk)$  found to vary from 2.79 to 0.41 for  $\lambda$  4500-7000 Å (Fig. 43).

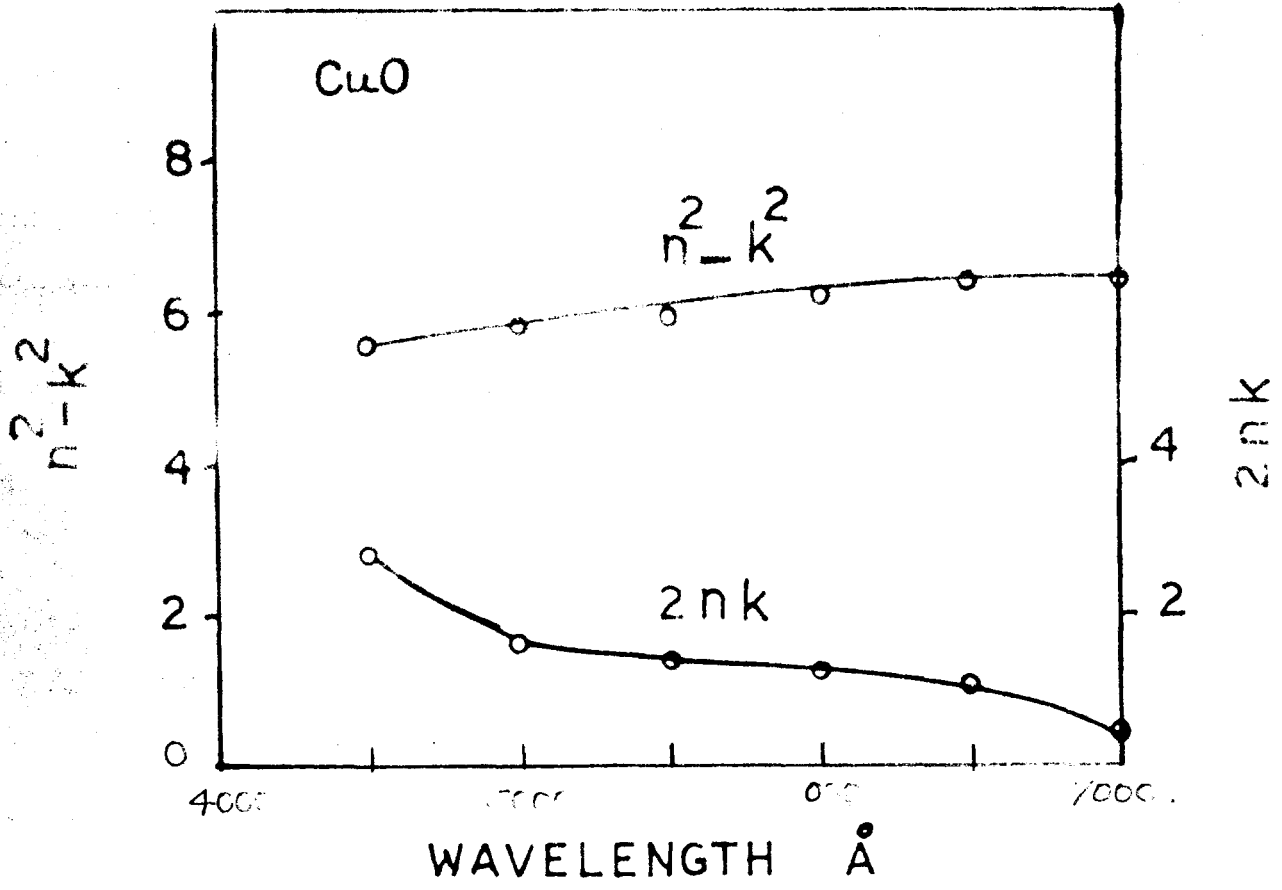


Fig. 43.

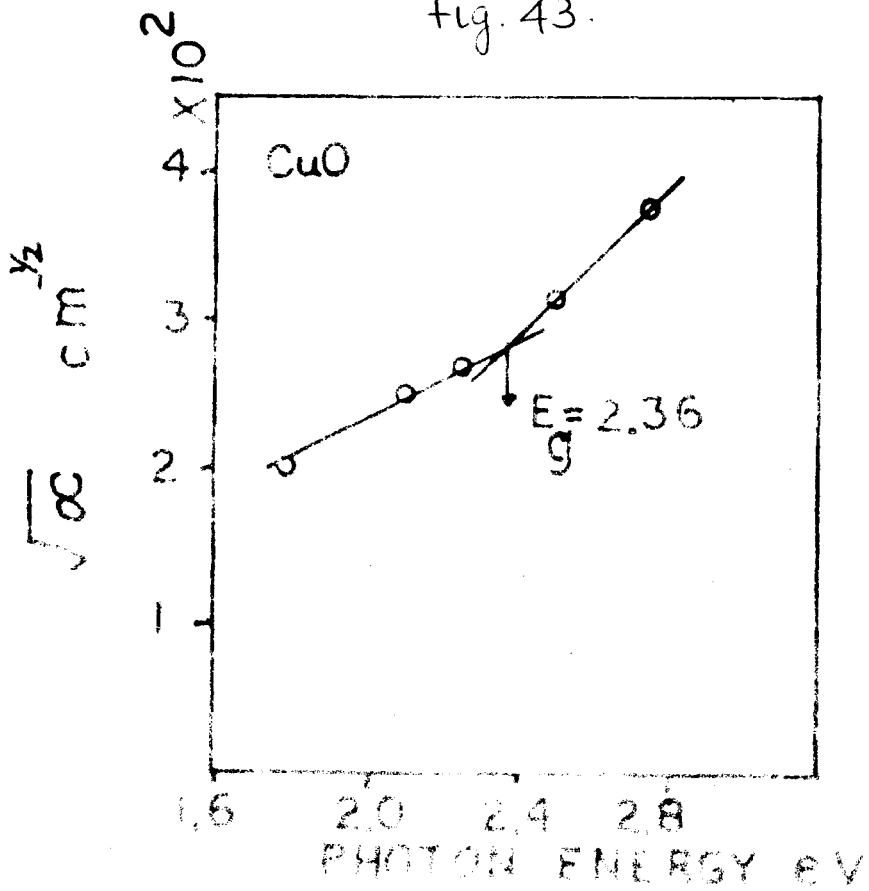


Fig. 44.



Optical energy band gap

Optical energy band gap was determined from the plot of  $\alpha^{1/2}$  vs  $h\nu$  (Fig. 44). The intersection of two branches of the curve gives the value for  $E_g$ , which was found to be  $\approx 2.36$  eV.

(D) DISCUSSION

It is seen that different oxides of copper can be prepared by thermal oxidation of copper films under appropriate conditions of temperature, as reported by Goswami and Trehan (1956, '57, '58).  $\text{Cu}_2\text{O}$  films were formed when copper films were thermally oxidised in air at about  $150^\circ\text{C}$ . At about  $200\text{-}250^\circ\text{C}$  the layers consisted of  $\text{CuO}$  along with  $\text{Cu}_2\text{O}$  and at a still higher temperature the layers consisted of  $\text{CuO}$  only.

From the electron diffraction studies it was found that cuprous oxide had cubic structure with  $a = 4.27 \text{ \AA}$ ; and  $\text{CuO}$  had a monoclinic unit cell. From the optical study on cuprous oxide ( $\text{Cu}_2\text{O}$ ) films, it was found that the refractive index decreased with the increase of wavelength similar to the observations made by Pastrnak (1961) on bulk samples. Absorption coefficient also decreased with the increase of wavelength. The optical energy band gap was found to be 2.05 eV, which is close to the bulk data 2.1 eV

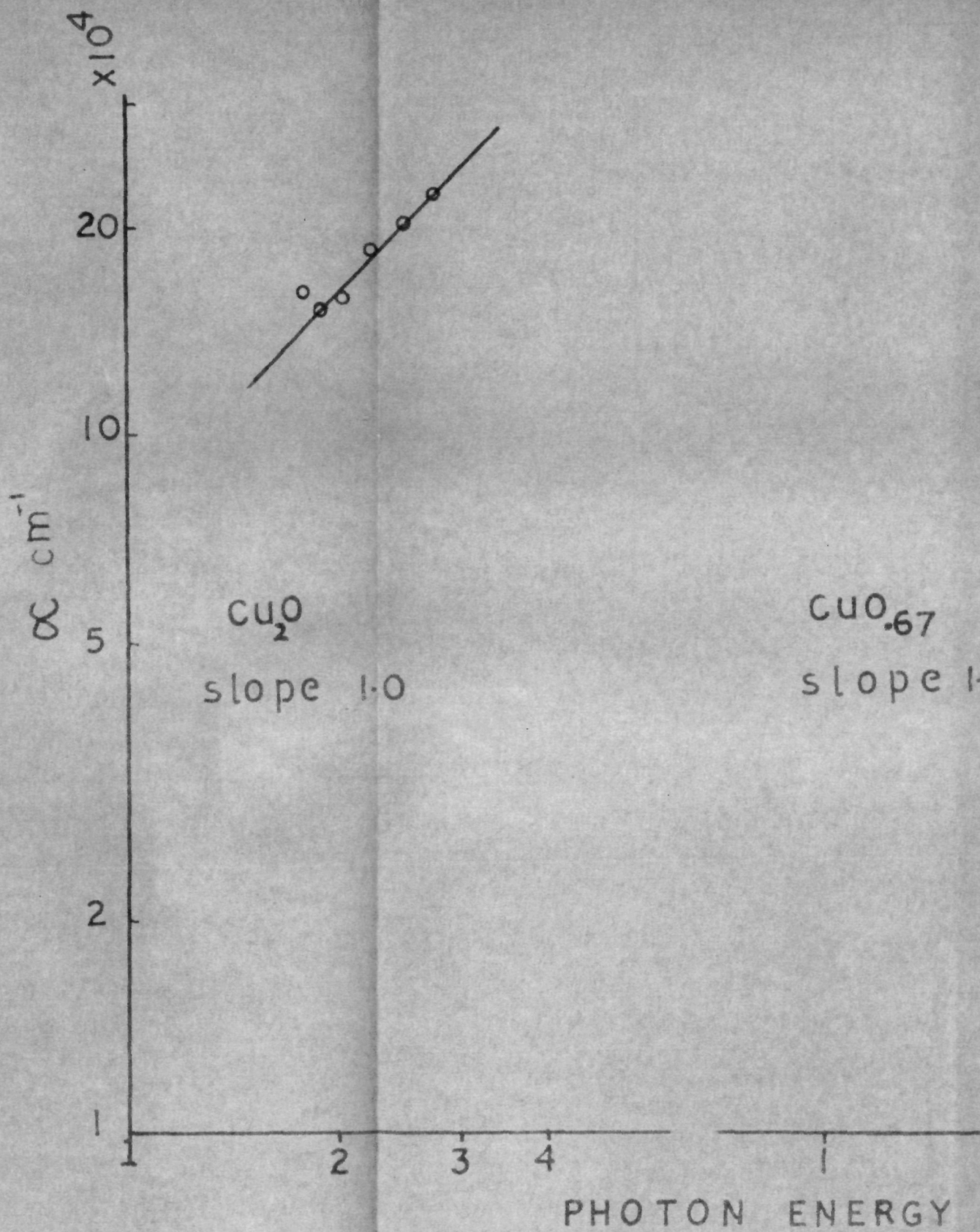


Fig. 45.

obtained by Pastrnak. The optical absorption process i.e. the effect of photon on the electrons, and their transition to higher states, whether the transitions are direct or indirect, allowed or forbidden one for  $\text{Cu}_2\text{O}$  film has also been studied. From the plot of  $\log \infty$  vs.  $\log h\nu$  (Fig. 45), the slope of which gives the power index of the equations given by Bardeen et al. (1955). Since the slope was unity, it suggests that the transition was direct but likely to be a mixture of allowed and forbidden. For allowed and forbidden transition cases the slope will respectively be 0.5 and 1.5.

From the optical studies on copper-oxide ( $\text{Cu}_2\text{O}$  and  $\text{CuO}$ ) films, it is found that refractive index decreased with the increase of wavelength with a minima at about  $\lambda 5500 \text{ \AA}$  which may be due to the presence of absorption edge. It was found that refractive index did not vary appreciably with film thickness indicating that reflection and structural properties are same throughout the film thickness range studied. Absorption coefficient decreased with the increase of wavelength the optical energy band gap was found to be 2.25 eV conforming to the value for the  $\text{Cu}_{0.67}$  composition. The slope of  $\log \infty$  vs.  $\log h\nu$  is 3/2, which indicates the transition is direct

but forbidden.

The refractive index of CuO found to increase slightly with the wavelength. Refractive index was determined from R, R' and T using David and Wolters equations and also from  $R_s$  and  $R_p$  method. The values obtained from both the methods agreed well. Absorption coefficient decreased with the wavelength and the optical energy band gap was found to be  $\approx 2.36$  eV.

From the above detailed study, not only the individual species of the oxide film of Cu namely  $Cu_2O$ , CuO and  $CuO_{.67}$  ( $Cu_2O + CuO$ ) have been identified, but also their various optical parameters, optical energy band gap, etc. have been determined and correlated with their structures. It was found that the optical energy band gap increased with the oxygen content in the oxides of copper  $Cu_2O - 2.05$  eV, copper-oxide ( $Cu_2O + CuO$ ) - 2.25 and CuO - 2.36 eV. It is also found that these parameters in most of the cases agree with the known bulk parameters.

Cuprous oxide filmsTable 12

Dependence of absorption coefficient and extinction coefficient with wavelength

$\lambda(\text{\AA})$	$\alpha (\text{cm}^{-1})$	$k$
4500	$2.25 \times 10^5$	0.81
5000	$2.03 \times 10^5$	0.81
5500	$1.87 \times 10^5$	0.82
6000	$1.57 \times 10^5$	0.75
6500	$1.55 \times 10^5$	0.80
7000	$1.65 \times 10^5$	0.90

Table 13

The variation of refractive index with the wavelength

$\lambda^0$ ( $\text{\AA}$ )	$R_s$	$R_p$	$n$
4500	0.4909	0.2442	2.93
5000	0.4908	0.2474	2.74
5500	0.4108	0.1676	2.55
6000	0.3905	0.1528	2.41
6500	0.3383	0.1148	2.15
7000	0.3125	0.098	2.02

Table 14

Variation of dielectric constant  $\epsilon_1$  and the imaginary part of dielectric constant with the wavelength

$\lambda(\text{\AA})$	$\epsilon_1$	$\epsilon_2$
4500	7.94	4.74
5000	6.85	4.44
5500	5.93	4.19
6000	5.25	3.62
6500	4.0	3.45
7000	3.27	3.64

Copper oxide filmsTable 15

Variation of  $\alpha$  and  $k$  with the wavelength

$\lambda(\text{\AA})$	$\alpha \text{ cm}^{-1}$	$k$
4500	$1.14 \times 10^5$	0.41
5000	$0.99 \times 10^5$	0.39
5500	$0.69 \times 10^5$	0.30
6000	$0.59 \times 10^5$	0.28
6500	$0.42 \times 10^5$	0.22
7000	$0.21 \times 10^5$	0.12

Table 16

Variation of refractive index with  
the wavelength

$\lambda(\text{\AA})$	$R_s$	$R_p$	$n$
4500	0.442	0.195	2.76
5000	0.367	0.1354	2.27
5500	0.355	0.1294	2.15
6000	0.334	0.1109	2.14
6500	0.3904	0.1545	2.36
7000	0.4426	0.183	2.39

Table 17

Refractive index for different  
angle of incidence ( $\lambda$  6500 $\text{\AA}$ )

$\phi$	$R_s$	$R_p$	$n$
45°	0.3694	0.1363	2.31
55°	0.4357	0.0858	2.29
65°	0.5357	0.0427	2.297

Cupric oxide filmsTable 19

Dependence of absorption coefficient with the wavelength

$\lambda(\text{\AA})$	$\alpha(\text{cm}^{-1})$
4500	$1.41 \times 10^5$
5000	$1.0 \times 10^5$
5500	$7.34 \times 10^4$
6000	$6.42 \times 10^4$
6500	$5.0 \times 10^4$
7000	$4.13 \times 10^4$

Table 20

Variation of refractive index and extinction coefficient with wavelength

$\lambda(\text{\AA})$	T	R	R'	n	k
4500	0.3693	0.323	0.3154	2.43	.56
5000	0.48	0.3073	0.30	2.44	.33
5500	0.5270	0.2834	0.2774	2.45	.29
6000	0.5606	0.2847	0.2708	2.51	.24
6500	0.5733	0.2634	0.2536	2.54	.22
7000	0.6857	0.2592	0.2346	2.54	.08



Table (20a)

Variation of refractive index<sub>p</sub> with the wavelength  
( $u \simeq 400 \text{ \AA}$ )

$\lambda$ ( $\text{\AA}$ )	$R_s$	$R_p$	$n$
5000	0.375	0.1410	2.32
5500	0.384	0.1468	2.41
6000	0.399	0.1600	2.45
6500	0.410	0.1687	2.51
7000	0.4256	0.1810	2.64

CHAPTER VISTUDIES ON SULPHIDES OF COPPER(A) INTRODUCTION

There are three types of sulphides of copper, namely covellite ( $\text{CuS}$ ), chalcocite ( $\text{Cu}_2\text{S}$ ), and deginite ( $\text{Cu}_{2-x}\text{S}$ ). Roberts and Ksanda (1929) investigated the crystal structure of covellite by the X-ray powder method and found it to be hexagonal with  $a = 3.802 \text{ \AA}$ ,  $c = 16.43 \text{ \AA}$  and  $c/a = 4.321$  (space group  $D_{6h}^4$ ,  $C_{6mm}$ ). Alsen (1931) and Oftedal (1932) obtained similar lattice parameters with  $a = 3.76 \text{ \AA}$  and  $c = 16.26 \text{ \AA}$ . Alsen also investigated the structure of low temperatures orthorhombic chalcocite and found the cell dimensions to be  $a = 11.8 \text{ \AA}$ ,  $b = 27.2 \text{ \AA}$  and  $c = 22.7 \text{ \AA}$ . Rahlf (1936) however, assigned  $a = 11.8 \text{ \AA}$ ,  $b = 26.9 \text{ \AA}$ ,  $c = 13.4 \text{ \AA}$  for the unit cell. Buerger (1941) studied the  $\text{CuS-Cu}_2\text{S}$  system and found that chalcocite above  $105^\circ\text{C}$  had a hexagonal basic structure, but below  $105^\circ\text{C}$  an orthorhombic super structure and no cubic phase was observed at least upto  $300^\circ\text{C}$ . Buerger and Buerger (1944) studied the low temperature and high temperature chalcocite and assigned the unit cell dimension as  $a = 11.94 \text{ \AA}$ ,  $b = 27.28 \text{ \AA}$ ,  $c = 13.41 \text{ \AA}$  for the low temperature chalcocite and  $a = 3.8 \text{ \AA}$  and  $c = 6.68 \text{ \AA}$  for

the high temperature form. They found the existence of a super structural symmetry relation between the high and the low temperature chalcocites above and below  $105^{\circ}\text{C}$ . Uyeda (1949) also confirmed the above results.

Rahlf (1936) studied the crystal structure of deginite  $\text{Cu}_{1.8}\text{S}$  and found it to be antiferite type ( $a = 5.564 \text{ \AA}$ ) with sulphur atoms in the face centred positions and the copper atoms in some statistical distribution.

Electrical and optical properties of the sulphides of copper have been investigated by several workers. White (1933) determined the specific heat upto  $900^{\circ}\text{C}$  of bulk cuprous sulphide and showed a region of abnormally high specific heat at  $300^{\circ}\text{C}$  above which there was no corresponding crystallographic change of state. Hirahara (1936) studied the electrical conduction and the heat capacity of bulk cuprous sulphide from room temperature to  $600^{\circ}\text{C}$ . Kozheurev (1939) measured the electrical conduction of thin films of copper sulphide prepared by passing  $\text{H}_2\text{S}$  on surfaces of  $\text{CuSO}_4$  or  $\text{Cu}(\text{NO}_3)_2$  and found the specific resistance of the film to be  $1.5$  to  $1.8 \times 10^{-2}$  ohm-cm. Cayrel (1937) studied the coefficient of absorption of cupric sulphide films formed by exposing dilute  $\text{H}_2\text{S}$  on  $\text{Cu}(\text{NO}_3)_2$  by means of a

barrier film photoelectric cell and it was about  $10^5 \text{ cm}^{-1}$  for  $\lambda = 4358 \text{ \AA}$ .

Marshall and Mitra (1965) investigated the optical properties of cuprous sulphide films and from the plot of  $\alpha^{1/2}$  vs.  $h\nu$  found that the optical energy band gap of  $\text{Cu}_2\text{S}$  to be 1.21 eV at  $300^\circ\text{K}$  and 1.26 eV at  $80^\circ\text{K}$ . Aliyarova et al (1966) found that single crystal cuprous sulphide films having an orthorhombic lattice were p-type semiconductors with carrier concentration of about  $8.5 \times 10^{19} \text{ cm}^{-3}$ , resistivity of 0.07 ohm cm. and a thermal emf of  $86 \mu\text{V}/\text{degree}$ . Sorokin et al. (1966) investigated the photoconductivity of  $\text{Cu}_2\text{S}$  and found that freshly prepared films had a low photoconductivity which depended strongly on the film thickness. For thin films ( $d < .5 \mu$ ) it was negligible but it rose with the increasing thickness in strongly absorbed light  $\lambda = 6000\text{-}7000 \text{ \AA}$  and reached saturation at thickness of the order of one micron. Absorption coefficient was calculated from the transmission and reflection of light and the optical activation energy calculated from the fundamental absorption edge was found to be 1.93. Ellis (1967) prepared  $\text{Cu}_{1.8}\text{S}$  films by the flash evaporation method and found a resistivity  $6.2 \times 10^{-4} \Omega \text{ cm}$ . and an absorption coefficient  $1.13 \times 10^3 \text{ cm}^{-1}$ .

He also reported that an useful application of  $\text{Cu}_{1.8}\text{S}$  films as conducting transparent layers.

Abdullaev et al. (1968) measured electrical conductivity, thermoelectric power and Hall effect of single crystals of p- $\text{Cu}_2\text{S}$  between  $20^\circ$  and  $600^\circ\text{C}$  and observed a sudden change in these parameters at  $125^\circ$  and  $480^\circ\text{C}$  and assumed these to be due to a structural transformation of these compounds. They found the activation energy to be 1.8 eV for the intrinsic region and 0.064 eV for the extrinsic region. Electrical and optical properties of  $\text{Cu}_2\text{S}$  films were also investigated by Selle and Maeger (1968). They reported that the thermoelectric power of  $\text{Cu}_2\text{S}$  films was about  $200 \mu\text{V}/^\circ\text{C}$  and the hole mobility was  $(7 \pm 1) \text{cm}^2/\text{V}\text{-sec}$ . Both these parameters increased as the temperature decreased. They have also measured the spectral variation of the absorption constant and the refractive index at  $295^\circ\text{K}$  and of photosensitivity at  $95^\circ\text{K}$ . The optical energy gap was found to be 1.22 eV at  $295^\circ\text{K}$  and 1.25 at  $95^\circ\text{K}$ . Nakayama (1968) studied the electrical and optical properties of  $\text{Cu}_{2-x}\text{S}$  ( $0 \leq x \leq 0.2$ ) and observed that  $\text{Cu}_{2-x}\text{S}$  was a p-type conductor and the thermoelectric power of  $\text{Cu}_2\text{S}$  was  $\simeq 60 \mu\text{V}/^\circ$ . The conductivity, mobility and carrier concentration of  $\text{Cu}_{2-x}\text{S}$  were however determined from the Hall effect and resistivity

measurements. The transmission and reflection curves of  $\text{Cu}_{1.8}\text{S}$  were plotted as a function of wavelengths (0.45-0.7  $\mu$ ). He found the optical energy band gap of  $\text{Cu}_{1.8}\text{S}$  from the plot of  $\alpha^{1/2}$  vs. wave number to be 2.3 eV and of  $\text{Cu}_2\text{S}$  was about 1.0 eV at 300°K.

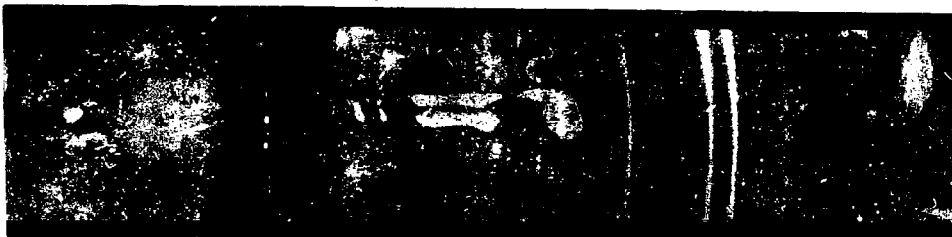
It is seen that from the above survey of literature, that not much work has been carried out on the optical properties of copper (ic and ous) sulphide films. So in the following, optical properties of cuprous and cupric sulphide films have been studied in details for transmission, reflection and absorption, absorption coefficient, optical constants and their dependence on wavelength and film thickness.

## (B) EXPERIMENTAL

### preparation of cuprous and cupric sulphide films

Thin films of cuprous sulphide were prepared by the vacuum evaporation process as described in Chapter II. Cuprous sulphide powder (blackish in colour) supplied by Albright and Wilson Ltd., England was used for evaporation. This powder was heated in a continuously evacuated system for about 2 hours at a temperature 400°C to remove the excess of sulphur, if any present, in the bulk sample. X-ray diffraction

Fig. VI.1.



X-ray pattern of Cerrous sulphide.

pattern was taken of this powder sample and the structure was ascertained to be  $\text{Cu}_{2-x}\text{S}$ . This vacuum treated powder was then evaporated from an initially flashed tungsten boat in the usual manner as described in Chapter II. A set of samples about six in number of different thicknesses were prepared at a time and their optical properties were studied both before and after annealing (usually at about  $75^{\circ}\text{C}$ ) them in vacuo. Films of cuprous sulphide obtained were brownish yellow in colour. Some films were also deposited at higher substrate temperature ( $\approx 150^{\circ}\text{C}$ ) and these films had a dark greenish appearance in contrast to those formed at room temperature (brownish). They were examined in an electron diffraction camera both by transmission and reflection techniques and their nature identified.

### (C) RESULTS

#### Cuprous sulphide films

##### (i) Structure

Deposits formed at room temperature did not yield any diffraction patterns thus indicating that these films were amorphous in nature. Films deposited at higher temperature however yielded good electron diffraction patterns. (Fig. 46 & 47) shows typical



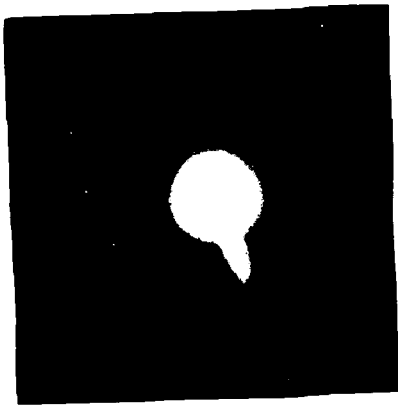


Fig. 46.

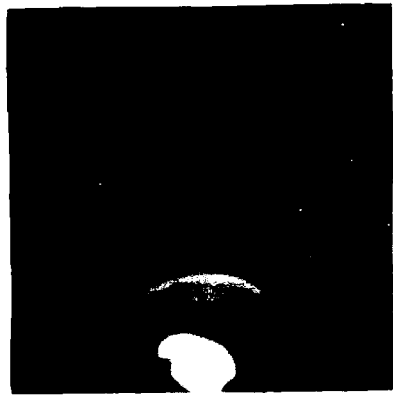


Fig. 47.

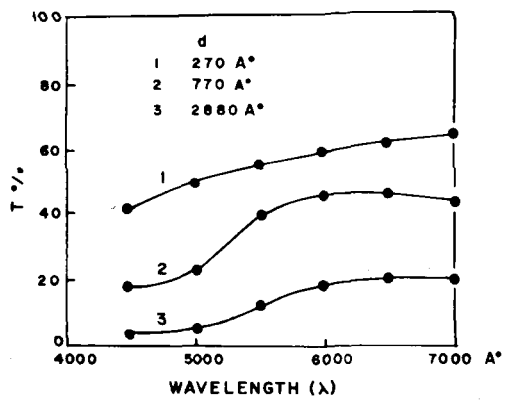


Fig. 48 a

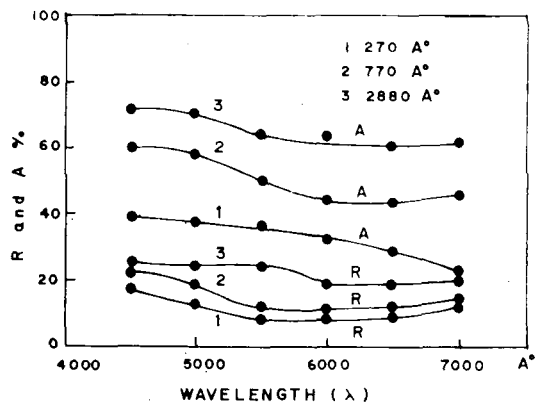


Fig. 48 b.

transmission and reflection electron diffraction pattern from graphite standard 'd' values were found which are given in table 21.

Table 21

Int.	d (Å)	hkl
f	3.16	111
vf	2.79	200
s	1.968	220
m	1.67	311
vvf	1.58	220

$$a_0 = 5.57$$

f = faint, vf = very faint, s = strong, m = medium,

vvf = very very faint

(ii) Transmission, reflection and absorption

Figs. 48a and b show the variation of transmittance and reflectance and absorptance with the wavelength for three films ( $d \approx 700 \text{ \AA}$ ,  $1360 \text{ \AA}$ ,  $2880 \text{ \AA}$ ). Transmittance increased with the wavelength whereas reflectance showed minima near about  $\lambda$  5500 to 6000  $\text{\AA}$ . The variation of transmittance ( $T_p$  and  $T_s$ ) and reflectance ( $R_p$  and  $R_s$ ) with the film thickness for the

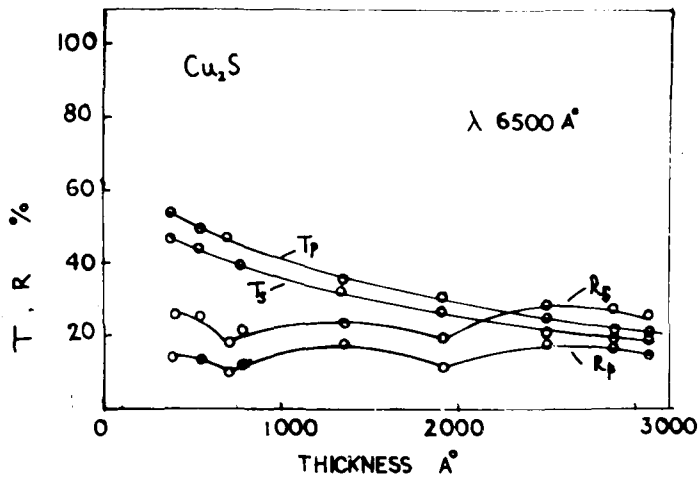


Fig 49.

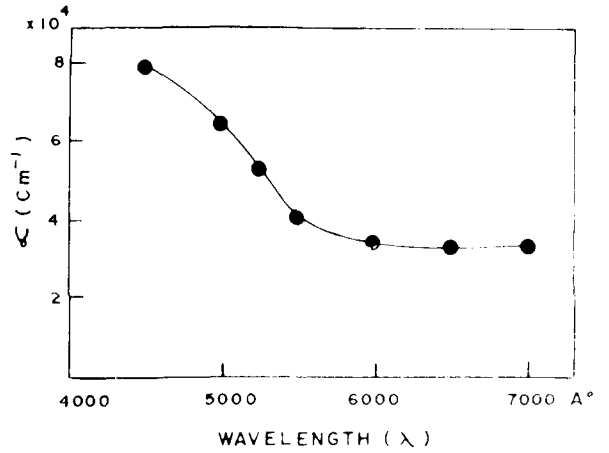


Fig. 51.

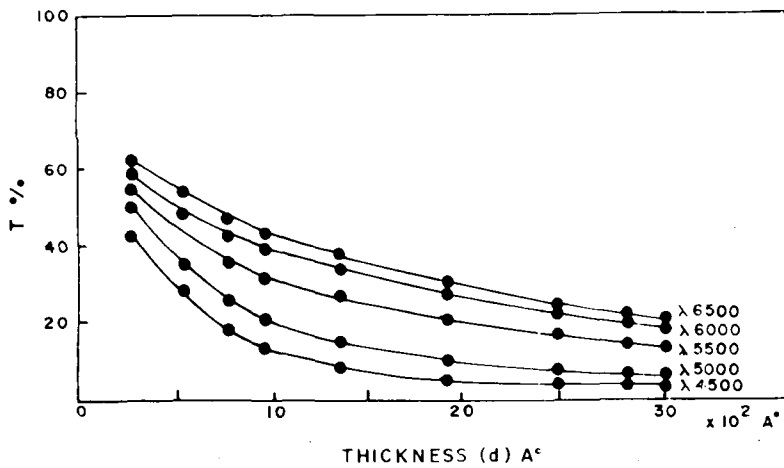


Fig. 49a.

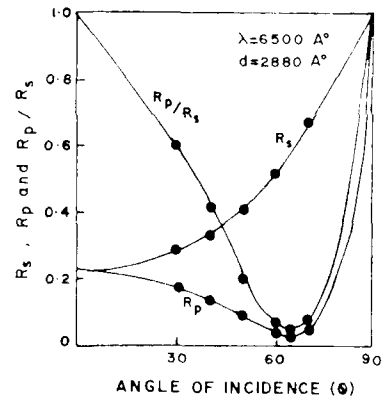


Fig. 50.

polarised beam at  $\lambda = 6500 \text{ \AA}$  is shown in Fig. 49. Both  $T_p$  and  $T_s$  decreased exponentially with the increase of thickness but reflectance showed both maxima and minima.

The variation of  $R_s$  and  $R_p$  components with the change of the angle of incidence for a film thickness  $2880 \text{ \AA}$  is shown in Fig. (50). It is seen that  $R_p/R_s$  curve intersect the  $R_s$  curve at  $45^\circ$ , thus conforming to the homogeneity condition i.e.  $R_s^2 = R_p$  at  $45^\circ$  for these films.

### (iii) Absorption coefficient

The variation of transmittance with thickness of the films for different wavelengths is shown in Fig. (51). Table (22) shows the corresponding absorption coefficient and extinction coefficient for various wavelengths. It is seen that both  $\infty$  and  $k$  decreased with the increase of wavelength.

### (iv) Optical constants

The refractive index  $n$  was evaluated from  $R_s$  and  $R_p$  components for  $\theta = 45^\circ$ , for various wavelengths and film thicknesses. A typical variation of  $n$  with the wavelength for a film thickness  $2880 \text{ \AA}$  and the values are shown in table 23. Fig. (51a) shows the variation of  $n$  with wavelengths for some films (Table 24). It is interesting to see that the refractive index curves showed a dispersion (minimum) around  $\lambda = 5500$  to  $6000 \text{ \AA}$  and more prominent for thinner films. It was

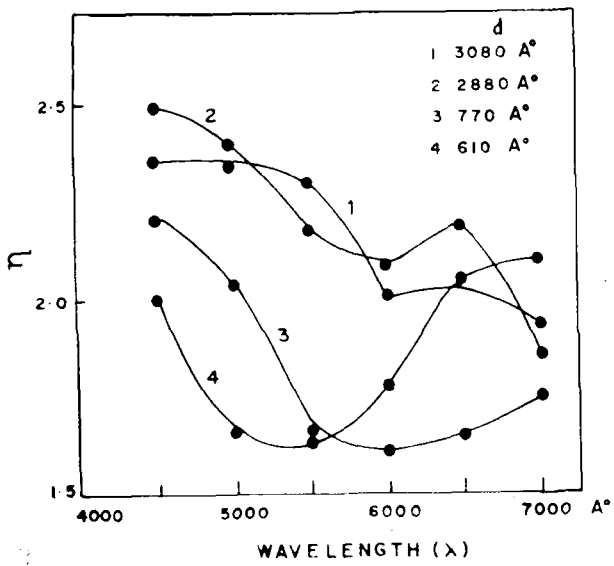


Fig. 51 a.

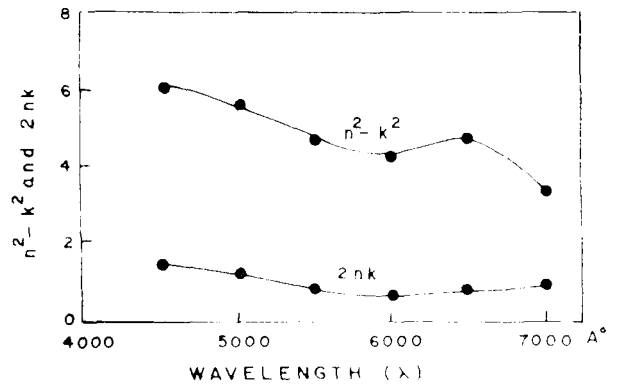


Fig. 53

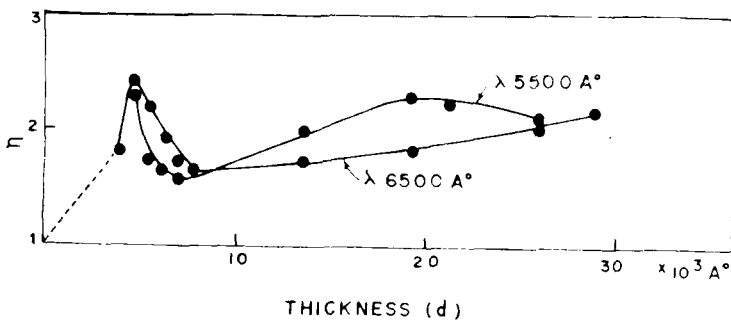


Fig. 52

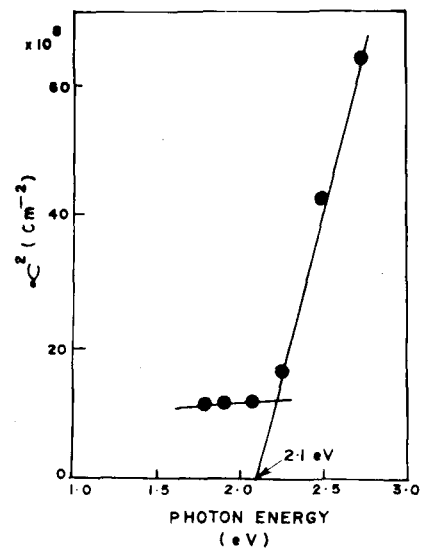


Fig. 54.

however found that  $k$  calculated from  $R_s$  and  $R_p$  was larger than those estimated from  $\mathcal{O}$ . Since  $k$  was much less than unity the values deduced from the latter were assumed to be more reasonable.

Fig. (52) shows the variation of  $n$  with film thickness ranging from 350 Å to 2500 Å obtained from two sets of evaporations for two wavelengths  $\lambda$  5500 and  $\lambda$  6500 Å. It is seen that  $n$  had a peak as well as a minimum around 400 Å and 800 Å thickness respectively.

(v) Dielectric constant

It is possible to calculate the real ( $\epsilon_1$ ) and imaginary part of the dielectric constant ( $\epsilon_2$ ) of the cuprous sulphide films from the optical parameters.

Fig. (53) shows the variation of these parameters  $\epsilon_1$  ( $=n^2 - k^2$ ) and  $\epsilon_2$  ( $=2nk$ ) with the wavelengths.  $\epsilon_1$  varied from 6.17 to 3.35 and  $\epsilon_2$  varied from 1.43 to 0.75 for wavelengths  $\lambda$  4500-7000 Å (Table 25).

(vi) Optical energy band gap

It is also possible to find the optical energy band gap  $E_g$  from the absorption coefficient. The energy dependence of the absorption coefficient ( $\mathcal{O}$ ), near the absorption edge of the fundamental absorption is given by  $\mathcal{O}^2 = h\nu - E_{opt}$  when  $\mathcal{O}^2$  vs  $h\nu$  is plotted a

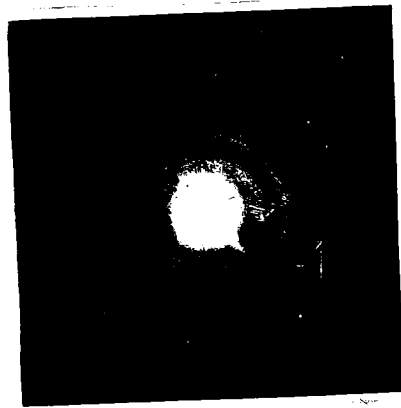


Fig. 55.

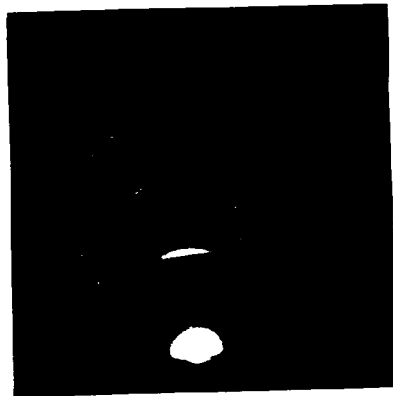


fig 56.

straight line giving a value of  $E_{opt}$  by extrapolation of  $\infty = 0$  is obtained (Macfarlane and Roberts, 1955). It was found that  $E_{opt} \simeq 2.12$  eV (Fig. 54).

### Copper sulphide films

It was observed that deposits formed at  $150^{\circ}\text{C}$  were dark greenish in colour, though the brownish films observed at room temperature were the usual type even at high temperature. Hence investigations were carried out on these green films for their structure as well as optical properties.

#### (1) Structure

Films deposited on glass and NaCl polycrystalline tablet at a temperature  $150^{\circ}\text{C}$  were examined by reflection and transmission techniques. The deposit formed on NaCl tablet yielded ring patterns (Fig. 55) and 'd' values were calculated by comparing with a graphite pattern (Table 26). A typical reflection pattern on a glass substrate is shown in Fig. 56. It is seen that thick films developed 1-d orientation  $\{110\}$  presumably of a cubic structure. The thinner films on the other hand suggested the formation of hexagonal structure ( $a = 3.792 \text{ \AA}$ ,  $c = 16.344 \text{ \AA}$ ).



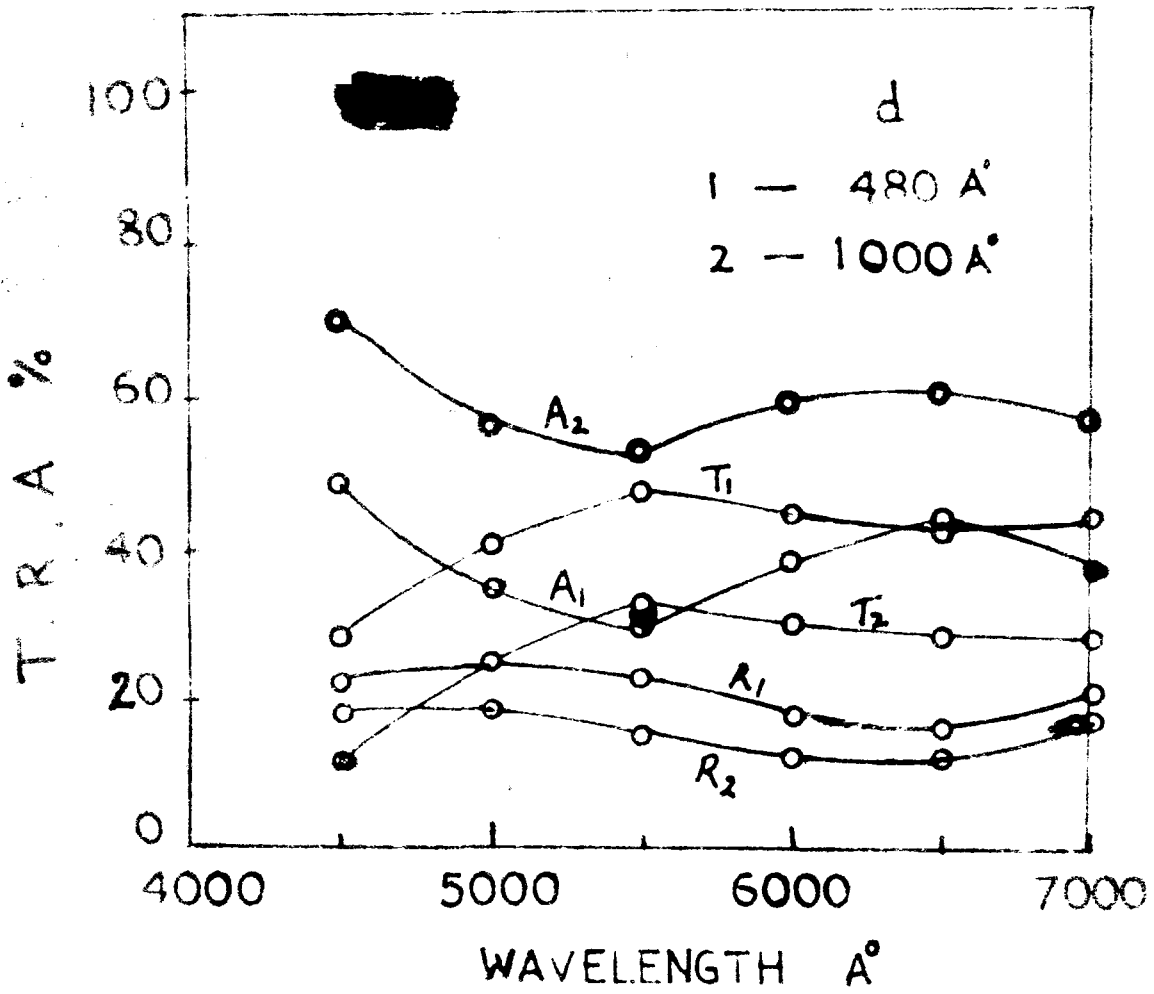


Fig. 57.

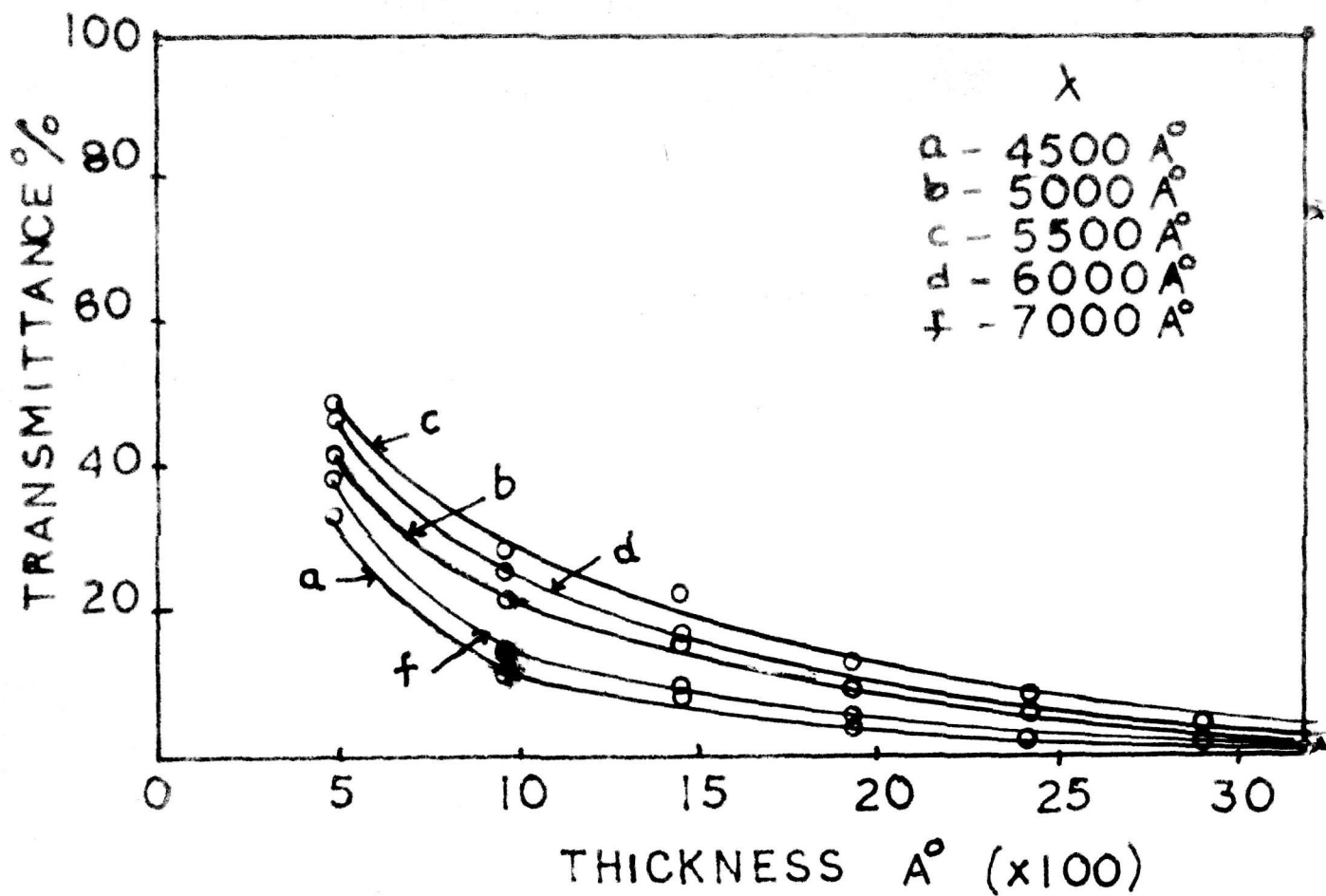


Fig. 58.

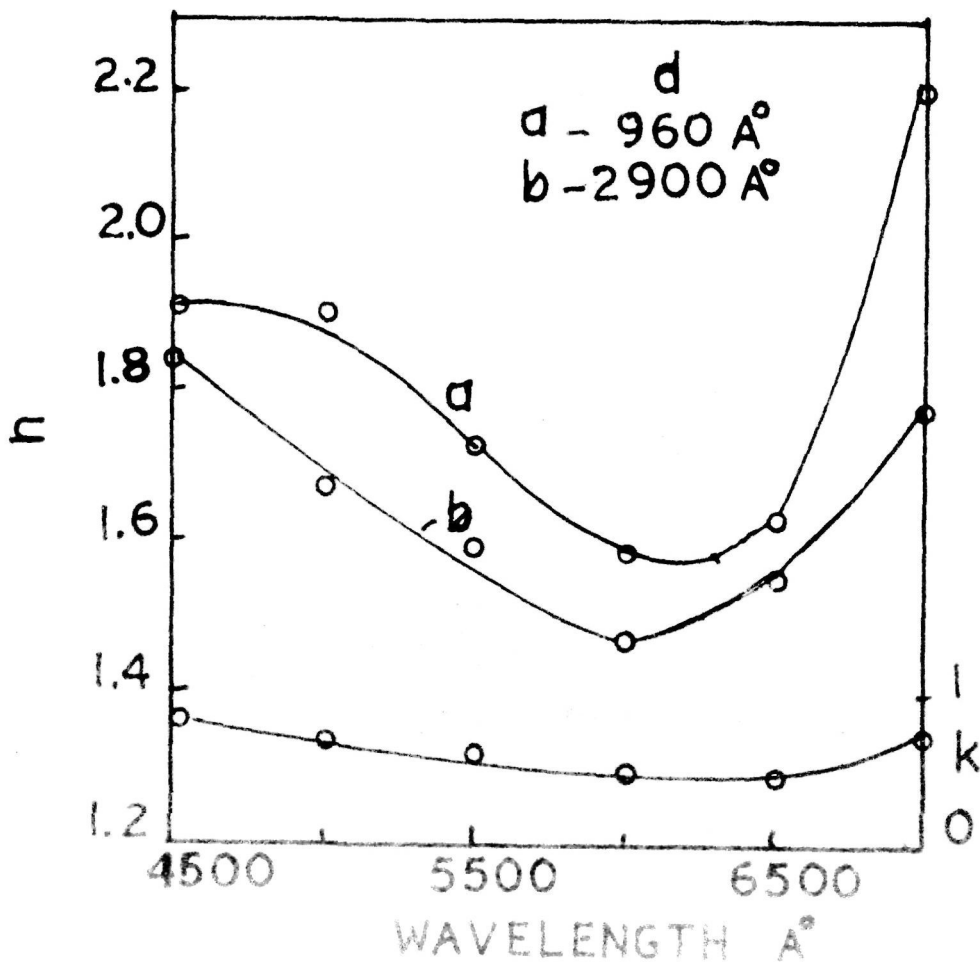


Fig. 60.

Table 26

Int.	d (Å)	hkl
ms	3.20	100
s	3.10	102
f	2.85	103
f	2.74	006
s	1.91	110
ms	1.73	108

s = strong, f = faint, ms = medium strong

(ii) Transmission, reflection and absorption

Films were greenish in colour had transmission around that region of the wavelength. Fig. (57) shows the transmittance reflectance and absorbance for a film of 480 Å and 1000 Å thickness. Absorption is seen to have minimum around  $\lambda$  5500 Å.

(iii) Absorption coefficient

Fig. 58 shows the transmittance vs. thickness for various wavelengths. Absorption coefficient was found to vary from  $1.31 \times 10^5 \text{ cm}^{-1}$  to  $1.62 \times 10^5 \text{ cm}^{-1}$

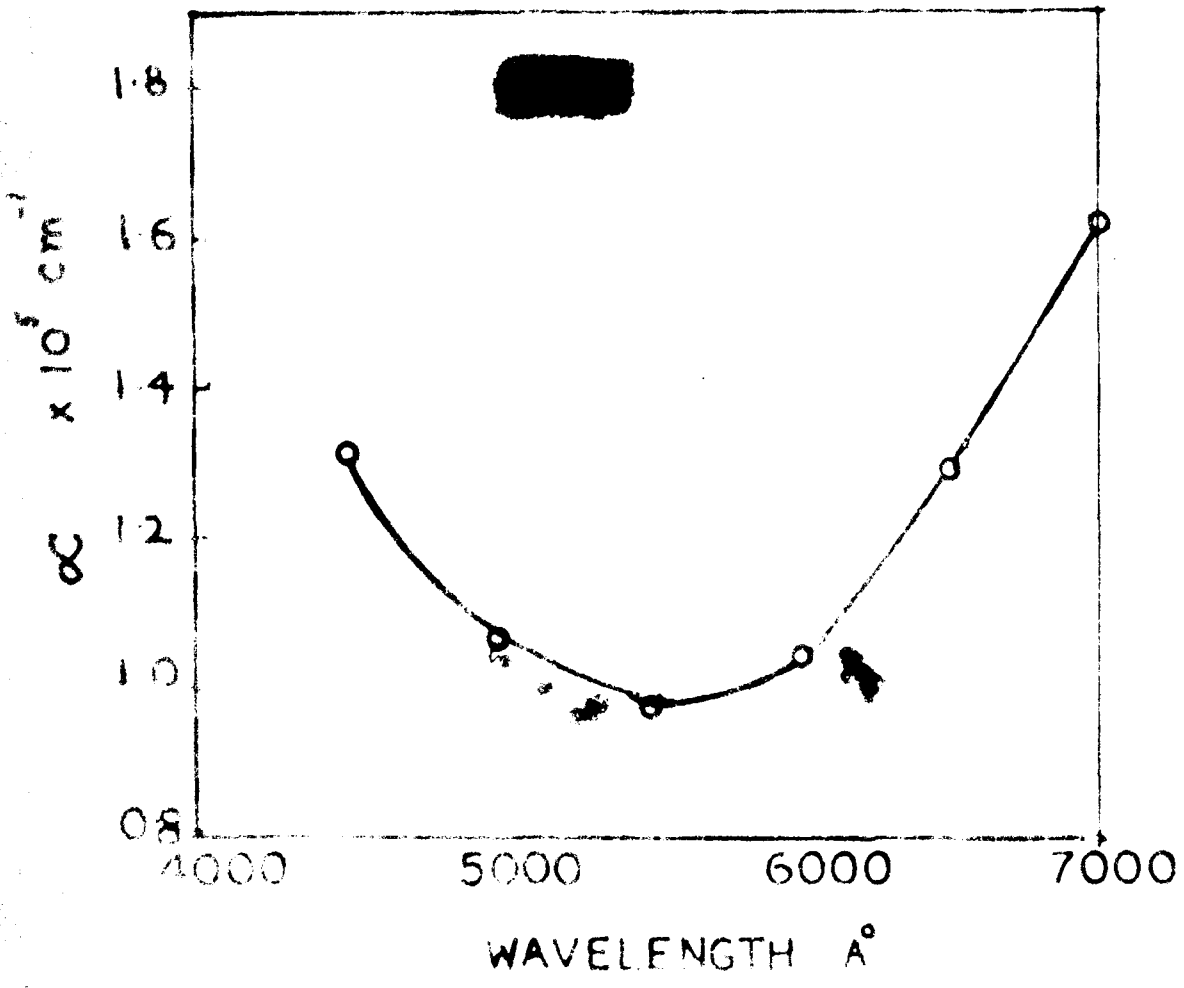


Fig. 59.

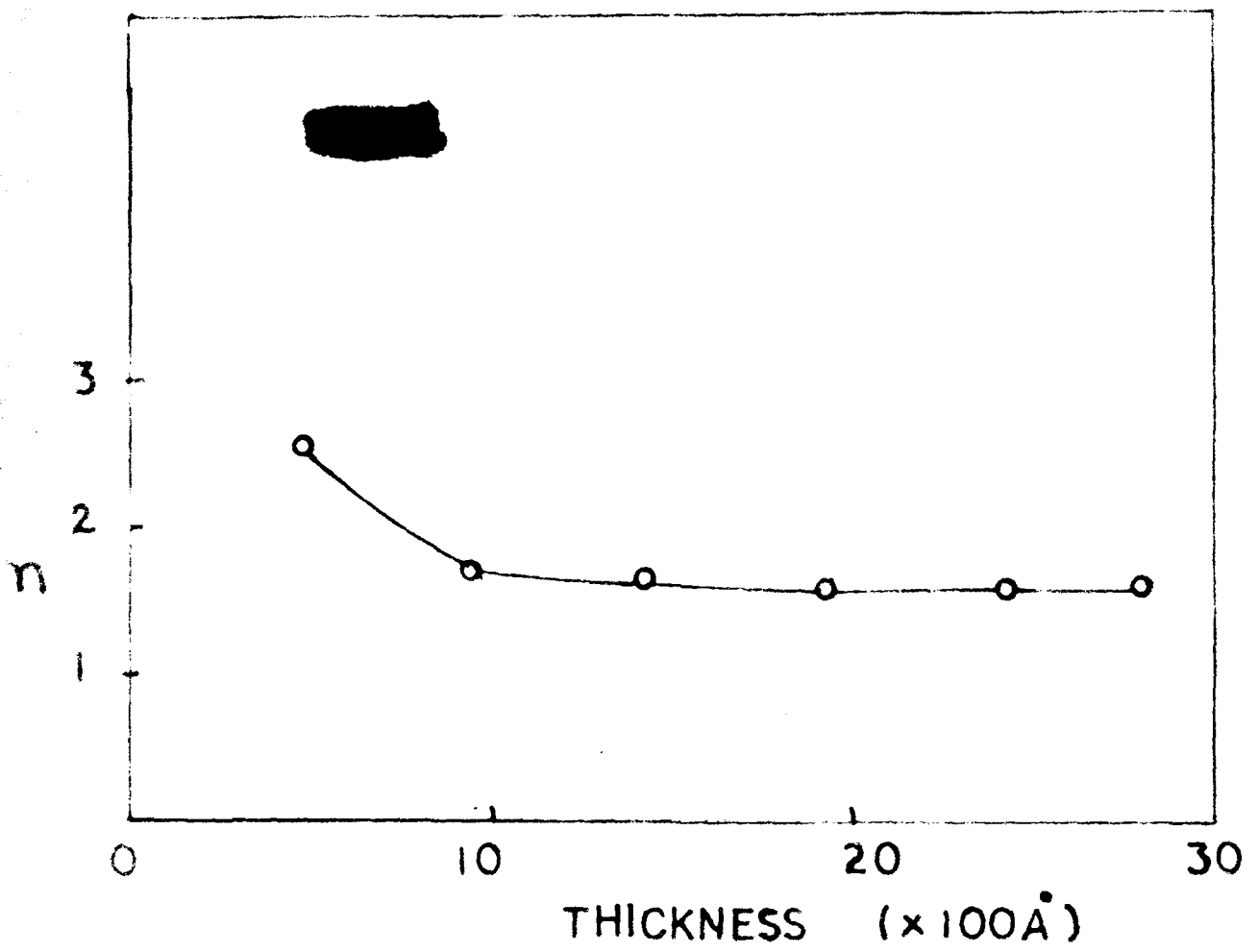


Fig. 61.

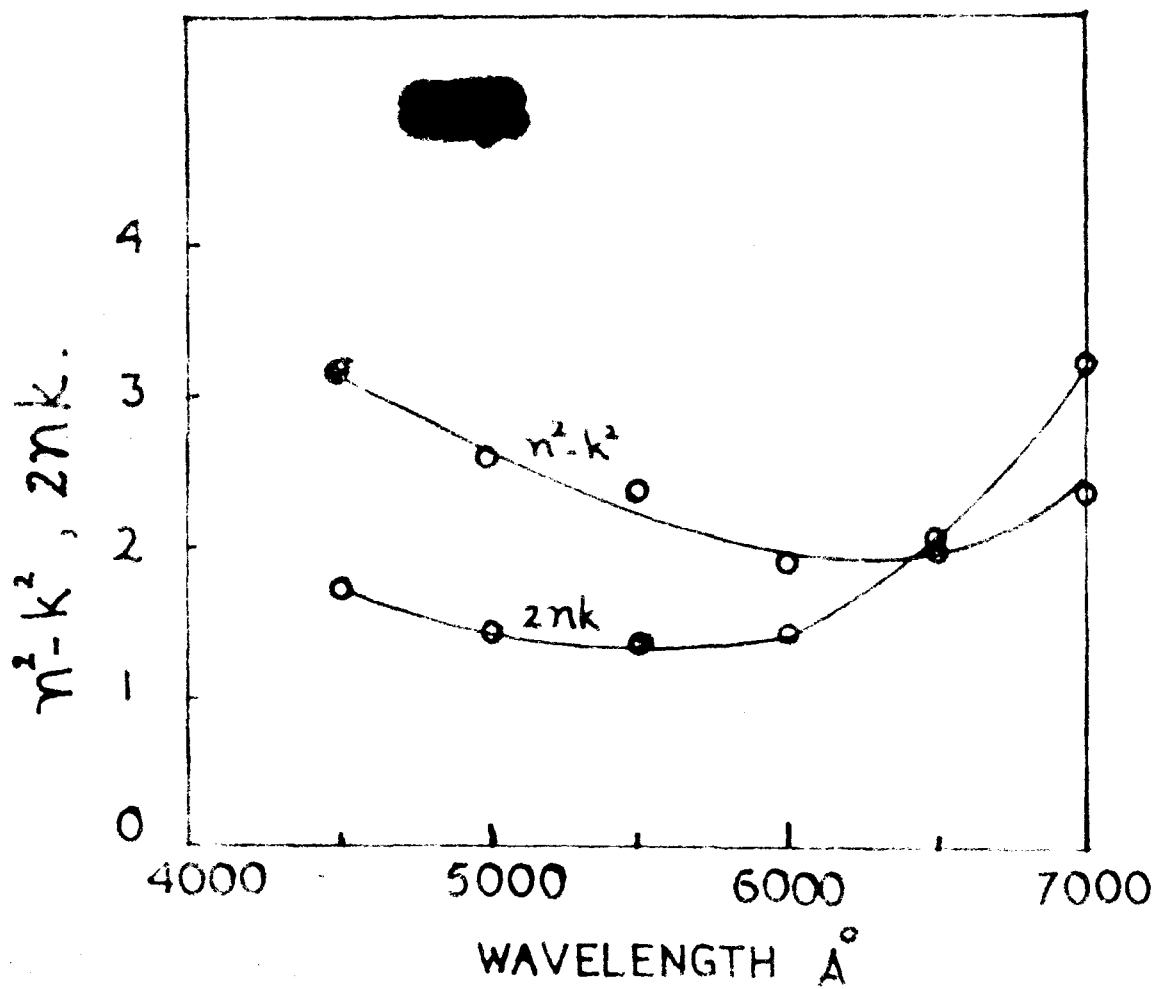


Fig. 62.

but passing through a minimum around  $\lambda 5500 \text{ \AA}$  in the visible region (Table 27 and Fig. 59).

(iv) Optical constants

Refractive index was determined from the  $R_s$  and  $R_p$  components of the reflected light at  $45^\circ$  of angle of incidence. The variation of  $n$  with the  $\lambda$  and also  $d$  were studied. For opaque film  $n$  varied from 1.84 to 1.78 with a minimum value  $\simeq 1.47$  and extinction coefficient  $k$  varied from 0.47 to 0.903 with a minimum value 0.430 at  $\lambda 5500 \text{ \AA}$  in the visible spectral region  $\lambda 4500-7000 \text{ \AA}$  (Table 28). Fig. (60) shows the variation of refractive index with the wavelength for two films ( $d = 478 \text{ \AA}$  and  $2118 \text{ \AA}$ ). Refractive index was however found to be independent of the film thickness except for very thin films (Table 29 & Fig. 61).

(v) Dielectric constant

Fig. (62) shows the variation of the real part of dielectric constant ( $\epsilon_1$ ) and imaginary part of dielectric constant ( $\epsilon_2$ ) with the wavelength. It is seen that  $\epsilon_1 (= n^2 - k^2)$  varied from 3.17 to 2.35 with a minimum value 1.91 at  $\lambda 6000 \text{ \AA}$  and  $\epsilon_2 (= 2nk)$  varied from 1.73 to 3.23 with a minimum value of 1.36 at  $\lambda 5500 \text{ \AA}$  in the visible region (Table 30).

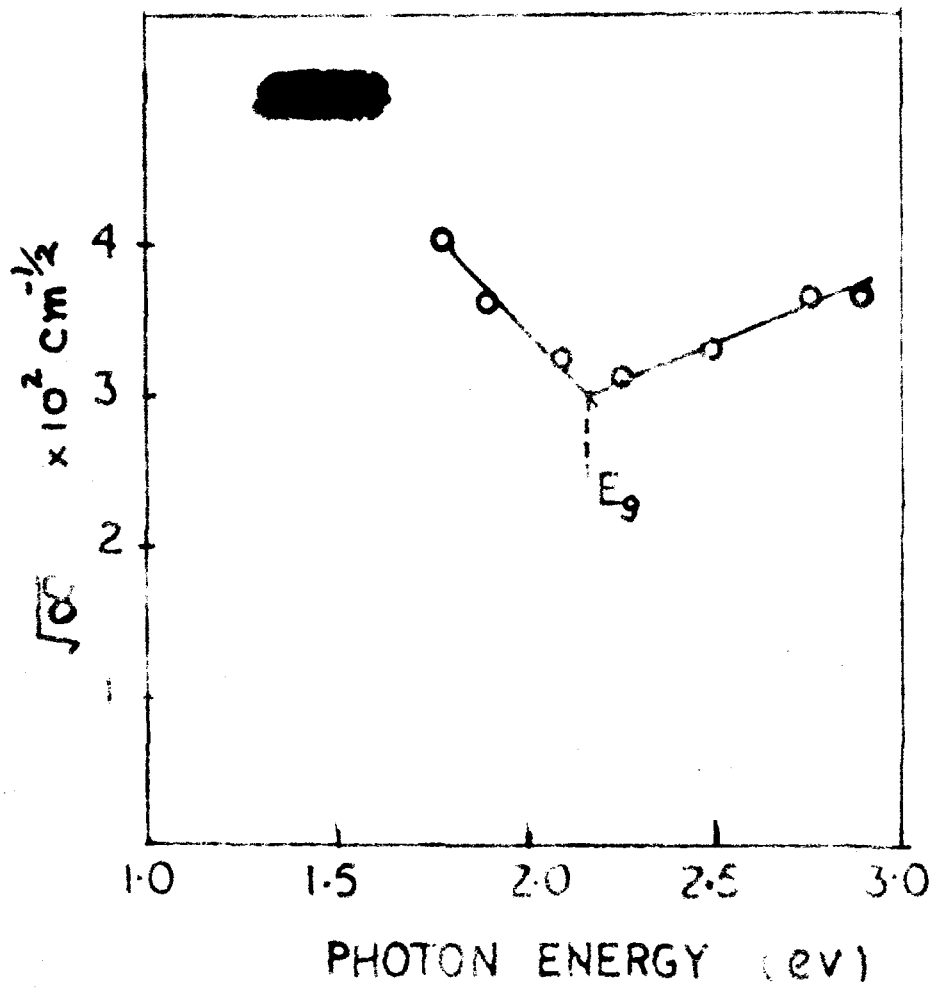


Fig. 63.



Optical energy band gap

Optical energy band gap was determined from a  $\alpha^{1/2}$  vs.  $h\nu$  plot which was given by two separate branches and the intersection point of these two lines approximately gives the value of  $E_g$ . Such a plot is shown in Fig. 63 and the band gap was evaluated to be 2.15 eV.

(D) DISCUSSION

Electron diffraction studies of the sulphide films showed that the deposits having brownish colour formed at room temperature were amorphous in nature or had a fine grained structure. An X-ray study of the bulk powder, on the other hand, showed that the sulphide are crystalline having  $a = 5.57 \text{ \AA}$  conforming to the composition  $\text{Cu}_{1.8}\text{S}$ . It is therefore presumed that the room temperature deposits would also have similar composition. Greenish deposits formed at higher substrate temperatures were crystalline in nature apparently showing the presence of two phases a cubic one for thicker films and hexagonal ( $a = 3.792 \text{ \AA}$ ;  $c = 16.344 \text{ \AA}$ ) for the thinner films. It was also found that brownish film (very thin film) at room temperature also changed to greenish one suggesting thereby that

the latter also often observed at higher substrate temperature must have occurred due to a phase change. This is borne out by the fact that the optical properties of the greenish films were different from the brownish one. It was also found that the optical properties of brownish deposits obtained at higher substrate temperature did not differ significantly from those obtained at room temperature and the diffraction pattern from these deposits conformed to cubic structure  $a = 5.57 \text{ \AA}$  corresponding to  $\text{Cu}_{1.8}\text{S}$ .

From the optical studies on brownish and greenish films, it is seen that the dispersion minima in the index of refraction curve was associated with the rapid change in the absorption coefficient in the fundamental absorption edge. The position of the minima yields a direct estimate of the energy gap. By extrapolating the linear plot of  $n^2$  vs.  $\lambda^2$  the high frequency dielectric constants may be obtained. It was found that the refractive index of brownish and greenish films varied with the film thickness. In the case of former,  $n$  had a peak as well as a minimum around 400 and 800  $\text{\AA}$  thickness respectively of the deposits. Further the refractive index had a tendency to become lower and lower with the decrease of film thickness, ultimately approaching a value of unity for ultra thin film when

$d \rightarrow 0$ . This appears to be due to the predominance of voids in the films as suggested by Male (1950) and Rouard (1952) from the Maxwell-Garnett theory. Refractive index of greenish sulphide films also decreased with the film thickness, eventually approaching a steady value for thicker films.

The optical energy band gap of brownish films was found from the plot of  $\infty^2$  vs  $h\nu$ . It was found to be 2.12 eV a value close to one reported by Nakayama (1968) for  $\text{Cu}_{1.8}\text{S}$ . Cuprous sulphide ( $\text{Cu}_2\text{S}$ ) on the other hand had a lower value  $E_{\text{opt}} = 1.26$  eV (Marshall and Mitra, 1965). The value obtained for the greenish sulphide films was 2.16 eV. It is interesting to see that the greenish film had also optical energy band gap close to that of  $\text{Cu}_{1.8}\text{S}$  film even though trend in  $\infty$  was different at least for lower wavelengths. This may be due to the presence of a new phase.

Cuprous sulphide films are used as transparent conducting layers. So, the present work provides useful data on reflection, transmission, refractive index, absorption coefficient their variation with wavelength and film thickness in the visible region.

Cuprous sulphide filmsTable 22

Variation of absorption coefficient and extinction coefficient with the wavelength

$\lambda(\text{\AA})$	$\alpha (\text{cm}^{-1})$	k
4500	$8.0 \times 10^4$	0.29
5000	$6.51 \times 10^4$	0.26
5500	$3.99 \times 10^4$	0.18
6000	$3.38 \times 10^4$	0.17
6500	$3.30 \times 10^4$	0.17
7000	$3.34 \times 10^4$	0.18

Table 23

Variation of refractive index with the wavelength

$\lambda(\text{\AA})$	$R_s$	$R_p$	n
4500	0.411	0.1702	2.50
5000	0.387	0.1498	2.40
5500	0.3479	0.1216	2.18
6000	0.3244	0.1051	2.08
6500	0.3275	0.103	2.19
7000	0.2857	0.086	1.84

Table 24

Variation of  $n$  with  $\lambda$  for four films of different thicknesses, (1) 3080 Å, (2) 2880 Å, (3) 770 Å and (4) 610 Å

$\lambda(\text{Å})$	Refractive index			
	1	2	3	4
4500	2.36	2.50	2.21	1.99
5000	2.33	2.40	2.04	1.66
5500	2.30	2.18	1.66	1.63
6000	2.00	2.08	1.60	1.78
6500	2.03	2.19	1.63	2.05
7000	1.93	1.84	1.73	2.09

Table 25

Variation of dielectric constant  $\epsilon_1$  and imaginary part of the dielectric constant  $\epsilon_2$  with wavelength

$\lambda(\text{Å})$	$n^2 - k^2$	$2nk$
4500	6.15	1.43
5000	5.69	1.22
5500	4.75	0.76
6000	4.31	0.72
6500	4.75	0.75
7000	3.35	0.95

Copper sulphide films (greenish films deposited  
at 150°C)

Table 27

Dependence of absorption coefficient and extinction  
coefficient with wavelength

$\lambda$ (Å)	$\alpha$ (cm <sup>-1</sup> )	k
4500	1.31 x 10 <sup>5</sup>	.47
5000	1.07 x 10 <sup>5</sup>	.42
5500	9.74 x 10 <sup>4</sup>	.43
6000	1.04 x 10 <sup>5</sup>	.50
6500	1.29 x 10 <sup>5</sup>	.67
7000	1.62 x 10 <sup>5</sup>	.90

Table 28

Variation of refractive index with wavelength

$\lambda$ (Å)	R <sub>s</sub>	R <sub>p</sub>	n
4500	0.2625	0.0673	1.84
5000	0.2231	0.050	1.67
5500	0.2042	0.0417	1.61
6000	0.1613	0.0262	1.47
6500	0.1704	0.0232	1.55
7000	0.2488	0.0607	1.78

Table 29

Variation of refractive index with the film thickness

No.	Thickness ( $\text{\AA}$ )	$R_s$	$R_p$	n
1.	483	0.354	0.1133	2.56
2.	960	0.236	0.0558	1.71
3.	1450	0.2151	0.0465	1.64
4.	1950	0.1917	0.0369	1.56
5.	2420	0.1936	0.0378	1.57
6.	2650	0.2042	0.0417	1.61

Table 30Variation of  $\epsilon_1$  and  $\epsilon_2$  with the wavelength

$\lambda(\text{\AA})$	$n^2 - k^2$	$2nk$
4500	3.17	1.73
5000	2.61	1.42
5500	2.38	1.36
6000	1.91	1.46
6500	1.96	2.07
7000	2.35	3.23

CHAPTER VIISTUDIES ON CUPROUS SELENIDE AND CUPROUS TELLURIDEFILMS(A) INTRODUCTIONCuprous selenide

Berzelius (1818) detected cuprous selenide in the mineral skrikuram and named it as selenkupper ( $\text{Cu}_2\text{Se}$ ). He also synthesised cuprous selenide by heating a mixture of copper and selenium to incandescence. Parkman (1861) and Margottet (1879) prepared cuprous selenide by chemical methods. Fredrich and Leraux (1908) found out the melting point of cuprous selenide as  $1113^\circ\text{C}$ . Garelli (1923) prepared  $\text{Cu}_3\text{Se}_2$  umangite from a large excess of copper and a little selenium in copper sulphate at  $40^\circ$ ; at boiling temperature  $\text{Cu}_2\text{Se}$  and  $\text{CuSe}$  were also formed in the amorphous form. Davey (1923) prepared  $\text{Cu}_2\text{Se}$  by the direct union of the elements. By X-ray diffraction study he found that  $\text{Cu}_2\text{Se}$  crystals were composed of three interpenetrating face centred cubic lattices namely two of Cu and one of Se; crystal structure was similar to that of  $\text{CaF}_2$  ( $a = 5.751 \pm .007 \text{ \AA}$ ). Hartwig (1926) also confirmed the results of Davey.



Rahlf's (1936) made detailed studies of lattice spacings of  $\text{Cu}_2\text{Se}$  and observed a high temperature form ( $a = 5.84 \text{ \AA}$  with 4 molecules per unit cell) the transition temperature of which was about  $110^\circ\text{C}$ . Boettcher et al. (1955) also studied the phase change of  $\text{Cu}_2\text{Se}$  on heating and cooling. Mole (1954) prepared a selenide of copper by the topochemical reaction of  $\text{CuCl}$  with  $\text{H}_2\text{Se}$  found it to be a cubic phase  $\text{Cu}_{2-x}\text{Se}$  ( $a = 5.76 \text{ \AA}$ ). Heyding (1966) showed that the cubic phase of  $\text{Cu}_2\text{Se}$  is not stable below  $131^\circ\text{C}$ . Ogerlec and Celustka (1966) have shown that  $\text{Cu}_{1.96}\text{Se}$  exhibited a phase transition at  $103^\circ\text{C}$ . The compound  $\text{Cu}_{2-x}\text{Se}$  has a cubic structure at room temperature when  $0.15 \leq x \leq 0.25$ .

Electrical and optical properties of cuprous selenide have recently been studied. Reinhold and Mohring (1939) measured the specific conductivity and thermal emf of  $\text{Cu}_{2-x}\text{Se}$  with different values of  $x$  ( $x = 1.96, 1.89, 1.78$  and  $1.6$ ). Abdullaev et al (1967) investigated the electrical conductivity ( $\sigma$ ), the thermo emf and the Hall constant of single crystals of  $\text{Cu}_2\text{Se}$  in the temperature range  $22$  to  $650^\circ\text{C}$ . From the temperature dependence of  $\sigma$ , the activation energy  $\Delta E$  was found to be  $1.2 \text{ eV}$  whereas the value obtained from the optical absorption edge was  $1.3 \text{ eV}$ . Thermoelectric properties (thermal emf, Hall coefficient, electronic

conduction and thermal conductivity) of copper selenide with its stoichiometric index were investigated by Raulie et al. (1970). Okamoto (1971) carried out measurements of the temperature dependence of resistivity and thermo electric power of a nearly stoichiometric cuprous selenide crystals and showed that a phase transition occurred at about 130°C. The change in electrical conduction and the thermal dilatation of cuprous selenide at its phase transition were examined by Celustka and Ogarlec (1971).

Sorokin et al. (1966) investigated the photoconductivity of cuprous selenide films. They found that freshly prepared films had a relatively low photoconductivity which increased when exposed to air at room temperature reaching a constant value. The rate of change of photoconductivity depended on the film thickness. The spectral curves of absorption coefficient and photoconductivity were also measured. The optical activation energy calculated from the fundamental absorption edge was 1.23 eV. Ellis (1967) prepared  $\text{Cu}_2\text{Se}$  by flash evaporation. He observed a resistivity of  $1.6 \times 10^{-4} \Omega \text{ cm}$  and absorption coefficient  $1.18 \times 10^3 \text{ cm}^{-1}$  and found  $\text{Cu}_{1.8}\text{Se}$  was most suitable in the application as conducting transparent layers in solar cells.

Kurdyumova (1968 and 1969) investigated the structure and optical properties of thin films of copper selenide ( $\text{Cu}_{2-x}\text{Se}$ ) deposited on single crystals of NaCl, LiF and Ge. The copper selenide films had high transparency and optical uniformity. Refractive index was calculated from the wavelength corresponding to maximum transmission and the order of interference maxima and the thickness of the film and it was found to be 2.8, 2.92 and 3.25 for wavelengths  $1.68 \mu$ ,  $0.875 \mu$  and  $0.65 \mu$  respectively. Photoconductivity of  $\text{Cu}_{2-x}\text{Se}$  films was found to increase with the exposure of the samples to air at room temperature. Electrical conductivity was also measured by him.

#### Cuprous telluride

Ford in 1903 reported a mineral richardite with a composition  $\text{Cu}_4\text{Te}_3$ . Chikashinge (1907) obtained copper and tellurium alloys by melting the elements under proper conditions. Pushin (1908) indicated that mineral richardite ( $\text{Cu}_4\text{Te}_3$ ) is the solid solution of two compounds  $\text{Cu}_2\text{Te}$  and  $\text{CuTe}$ . Tibbals (1909) prepared tellurides of copper by treating some copper salt with sodium telluride  $\text{Na}_2\text{Te}$  and the tetra telluride  $\text{Na}_4\text{Te}$ .

Thomson (1930) studied some of the phases of Cu-Te system by electron diffraction. Nowatny (1946)

determined the crystal structure of  $\text{Cu}_2\text{Te}$  (room temperature modification) to be hexagonal with a lattice constant  $a = 4.23 \text{ \AA}$ ,  $c = 7.27 \text{ \AA}$  and  $c/a = 1.71$ . Hocart and Mole (1952) studied the structure of copper tellurides formed by compressing powdered copper and tellurium at temperature upto  $250^\circ\text{C}$  by x-ray diffraction.  $\text{Cu}_{2-x}\text{Te}$  phase formed was found to be pseudocubic with  $a_0 = 10.0 \text{ \AA}$  and  $\text{Cu}_{4-x}\text{Te}$  with a tetragonal structure  $a = 3.95 \text{ \AA}$  and  $c = 6.06 \text{ \AA}$ . Anderko and Schubert (1954) reported that a high temperature phase  $\sim 640^\circ\text{C}$  of cube face centred structure  $\text{Cu}_2\text{Te}$  with a lattice constant  $a = 6.1 \pm 0.05 \text{ \AA}$  with 12 atoms in the unit cell. The phase  $\text{CuTe}$  is orthorhombic with  $a = 3.5 \text{ \AA}$ ,  $b = 4.07 \text{ \AA}$ ,  $c = 6.92 \text{ \AA}$  space group  $D_{2h}^{13} - \text{Pmmn}$ . Patzak (1956) observed that  $\text{Cu}_2\text{Te}$  became stable at room temperature with phases of varying compositions  $\text{Cu}_{2-x}\text{Te}$  ( $0 \leq x \leq 0.33$ ) and determined the periods of two hexagonal phases having complex structure  $\text{Cu}_2\text{Te}$   $a = 12.54 \text{ \AA} \approx 3a$  and  $c = 21.71 \text{ \AA} \approx 3c$   
 $\text{Cu}_5\text{Te}_3$  -  $a = 12.45 \text{ \AA} \approx 3a$  and  $c = 21.56 \text{ \AA} \approx 3c$ .

Baranova and Pinsker (1964) studied thin films of Cu-Te system for their structure and observed lattice parameter  $a = 3.10 \text{ \AA}$ ,  $b = 4.02 \text{ \AA}$  and  $c = 6.86 \text{ \AA}$  differing slightly from x-ray data. Films corresponding to a large copper content and annealed for 2 hours at

100°C showed the presence of hexagonal phases  $\beta^I$ ,  $\beta^{II}$  and  $\beta^{III}$  beside CuTe. The lattice parameter of these three phases were integral multiple of  $a = 4.24$  and  $c = 7.29 \text{ \AA}$ ,  $\beta^I - 2a$  and  $c$ ;  $\beta^{II} - 2a$  and  $3c$ ;  $\beta^{III} - 2a$  and  $5c$ . Baranova (1969) also investigated the crystal structure of thin films of the hexagonal  $\beta^{II}$  phase of the Cu-Te system by electron diffraction. The lattice parameters are  $a = 4.17 \text{ \AA}$  and  $c = 21.65 \text{ \AA}$  the space group is  $P6m2$  and the composition of this phase is  $\text{Cu}_{2-x}\text{Te}$  where  $x = 0.25 \pm .04$ .

Electrical and semiconducting properties have been investigated by a number of workers. Harbeke (1957) investigated the mechanism of electrical conductance in the Cu-Te system. He studied the electrical conduction, Hall effect and infra red absorption in bulk samples and also of thin layers of  $\text{Cu}_2\text{Te}$ . His results showed that the bulk samples of  $\text{Cu}_2\text{Te}$  to be quasi metallic conductor. Semiconducting properties were observed in vacuum evaporated thin films with the carrier concentration  $\approx 3 \times 10^{22}/\text{c.c.}$  and the mobility  $12 \text{ cm}^2/\text{V}\cdot\text{Sec}$ . The maximum of the infra red absorption of a layer  $100 \text{ m}\mu$  thick lies at  $1.8 \mu$ .

Sorokin (1965) studied the electrical properties of thin films of  $\text{Cu}_2\text{Te}$ . He reported that the preparation

of  $\text{Cu}_2\text{Te}$  films was difficult as the compound dissociated on vacuum evaporation. He found  $\text{Cu}_2\text{Te}$  to be an impurity semiconductor whose forbidden band had a width of 0.9-1.0 eV. Goswami and Nikam showed that  $\text{Cu}_2\text{Te}$  films can be deposited at higher substrate temperatures.

Braithwaite (1951) investigated the photoconductivity of  $\text{Cu}_2\text{Te}$  and later on Sorokin et al. (1966) studied the electrical conductivity and photoconductivity of  $\text{Cu}_2\text{Te}$  in details for various film thickness ranging from 0.1-1000  $\mu$ . The spectral dependence of absorption coefficient and photoconductivity was studied and the optical activation energy (1.04 eV) calculated from the fundamental absorption edge. Ellis (1967) obtained thin films of  $\text{Cu}_2\text{Te}$  by flash evaporation and found that the resistivity of  $\text{Cu}_{1.8}\text{Te}$  films increased with time. Lebrun and Bescond (1968) made a review of p-n junction photoelectric effects and suggested the possibility of thin film photocells of copper telluride and cadmium telluride.

It is seen from the above survey of literature on cuprous selenide and telluride that no systematic study on optical properties has yet been carried out so far. Since the phase compositions are dependent on the deposition condition, it is likely that their

optical properties are likely to be affected. In the following, a detailed study has been made on cuprous selenide and telluride films for their transmission reflection, absorption, absorption coefficient, optical constants, their variation with wavelength and film thickness.

### (B) EXPERIMENTAL

#### (a) Preparation of $\text{Cu}_2\text{Se}$ and $\text{Cu}_2\text{Te}$ compounds

Bulk cuprous selenide and cuprous telluride were prepared by reacting the elements in their stoichiometric ratios in vacuo. The elements were of high purity (copper B.D.H. quality and Se and Te, "Specpure" quality). Copper (cut to fine pieces) and selenium were taken in a silica tube one end of which was closed. The silica tube with their contents was then evacuated to about  $10^{-5}$  mm.Hg. and sealed and then slowly heated in an electric furnace, first at about  $300^\circ\text{C}$  for 3 hours so that the selenium could slowly react with copper metal. The temperature of the furnace was then raised by about  $50^\circ\text{C/hr}$  and the final reaction was then carried out at about  $1150^\circ\text{C}$  for 5 hours. When the reaction was over the furnace temperature was lowered to about  $800^\circ\text{C}$  and silica tube was then taken out

and immersed into cold water. The products were taken out and the x-ray pattern was taken and d-values measured. The structure corresponds to cuprous selenide.

Telluride of copper was prepared in a similar way except that the reacting temperature was about 500°C instead of 300°C. as was the case for selenium. Te slowly reacted with Cu metal. The final reaction was carried out at 1150°C for 5 hours. The composition was confirmed by x-ray diffraction.

X-ray diffraction pattern of  $\text{Cu}_2\text{Se}$  and  $\text{Cu}_2\text{Te}$  are shown in Fig. (VII.1 and VII.2). Their d values were calculated and the structure conformed to the normal values of  $\text{Cu}_2\text{Se}$  and  $\text{Cu}_2\text{Te}$ .

#### (b) Preparation of $\text{Cu}_2\text{Se}$ films

Cuprous selenide films were prepared by evaporation under vacuo (of the order  $10^{-5}$  mm. of Hg) as described in the Chapter II. Initially flashed tungsten boat was used for the evaporation. A set of 6 samples were prepared at a time, and optical properties were studied.

These films were then annealed in high vacuo for about an hour at 150°C and their optical properties



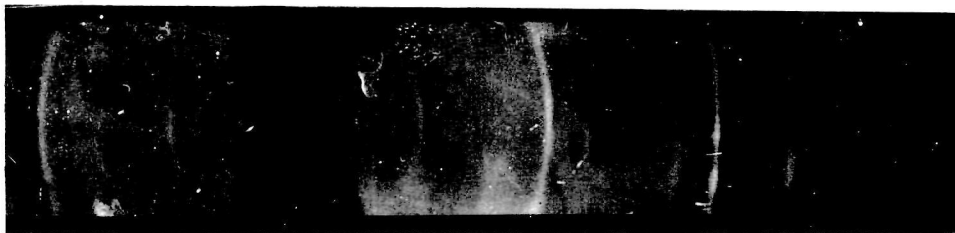
were studied.

Substrate temperature: Cuprous selenide films were also deposited at a higher substrate temperature ( $150^{\circ}\text{C}$ ) as described in Chapter II and their optical properties were investigated.

(c) Preparation of  $\text{Cu}_2\text{Te}$  films

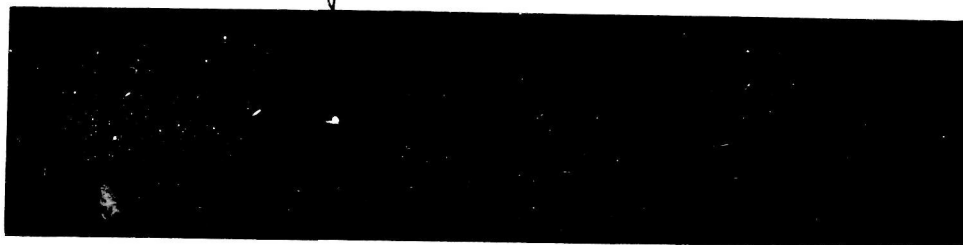
Cuprous telluride films were prepared by the flash evaporation process. Small pieces of  $\text{Cu}_2\text{Te}$  placed in a tungsten boat was evaporated for a few seconds by a sudden raising of the temperature of the filament to white hot (flash technique). The filament was then allowed to cool for a few minutes and its temperature was again raised suddenly as before. This process was repeated several times to get films of appropriate thickness on glass substrates. It was found that deposit films formed at room temperature were mostly of tellurium as was proved by electron diffraction. So films were deposited at higher substrate temperature say about  $200^{\circ}\text{C}$  and the structure was confirmed to be cuprous telluride by electron diffraction. The optical properties were then investigated for films which conformed to cuprous telluride alone.

Fig. VII. 1



X-ray pattern of Cu<sub>2</sub>Se

Fig. VII. 2.



X-ray pattern of Cu<sub>2</sub>Te.

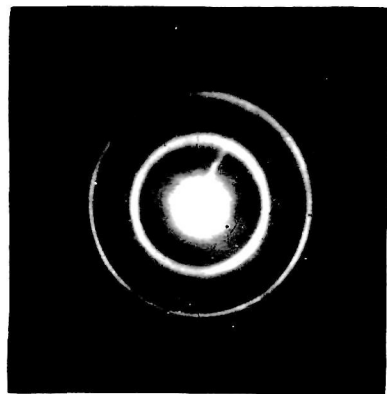


Fig. 64.

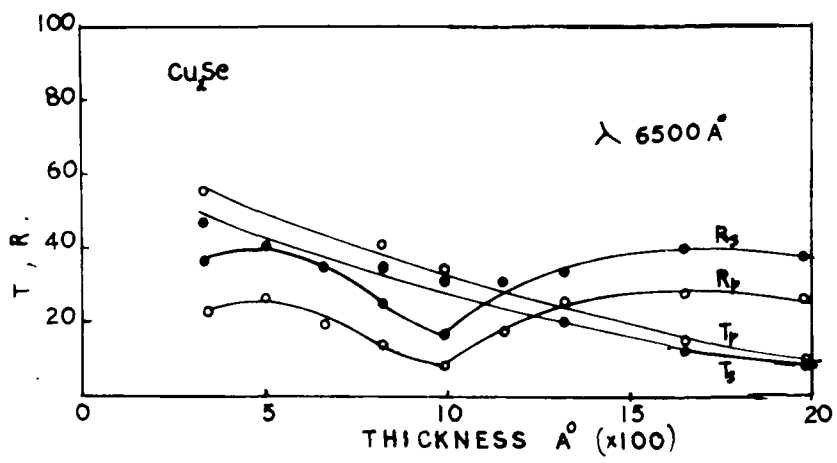
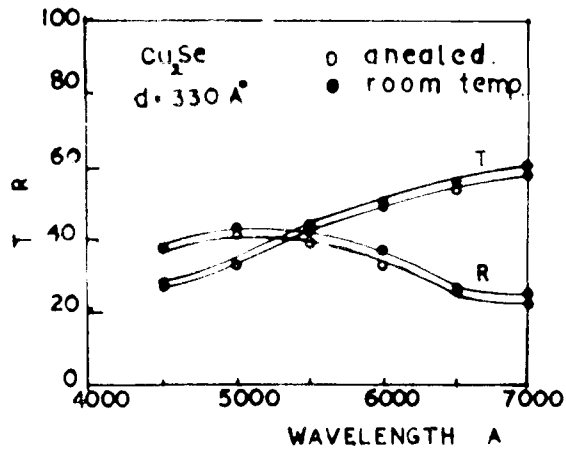
(C) RESULTSCuprous selenide films(1) Structure

Cuprous selenide films deposited on collodion at room temperature yielded ring patterns when examined in the electron diffraction camera. Fig. 64 shows a typical transmission electron diffraction pattern of the deposits formed on collodion at room temperature and the measurement of 'd' value with a graphite standard is shown in Table 31. It was found that the pattern correspond to cuprous selenide ( $\text{Cu}_2\text{Se}$ ) having a cubic structure ( $a = 5.72 \text{ \AA}$ ).

Table 31

Intensity	d in $\text{\AA}$	hkl
S	3.29	111
vs	2.04	220
f	1.73	311
vf	1.42	400
vf	1.28	420
vf	1.16	422

vs = very strong, s = strong, f = faint, vf = very faint



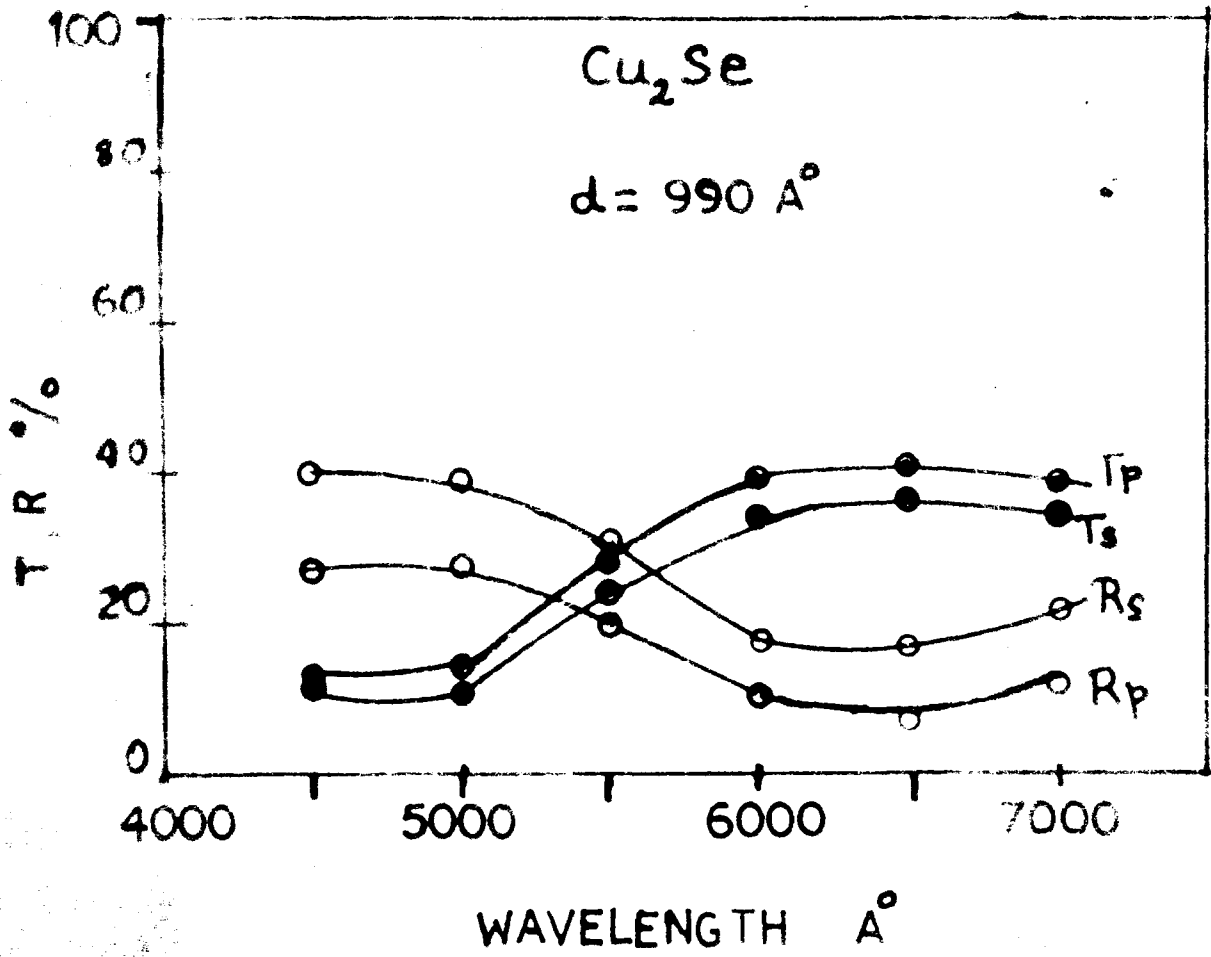


Fig. 66.

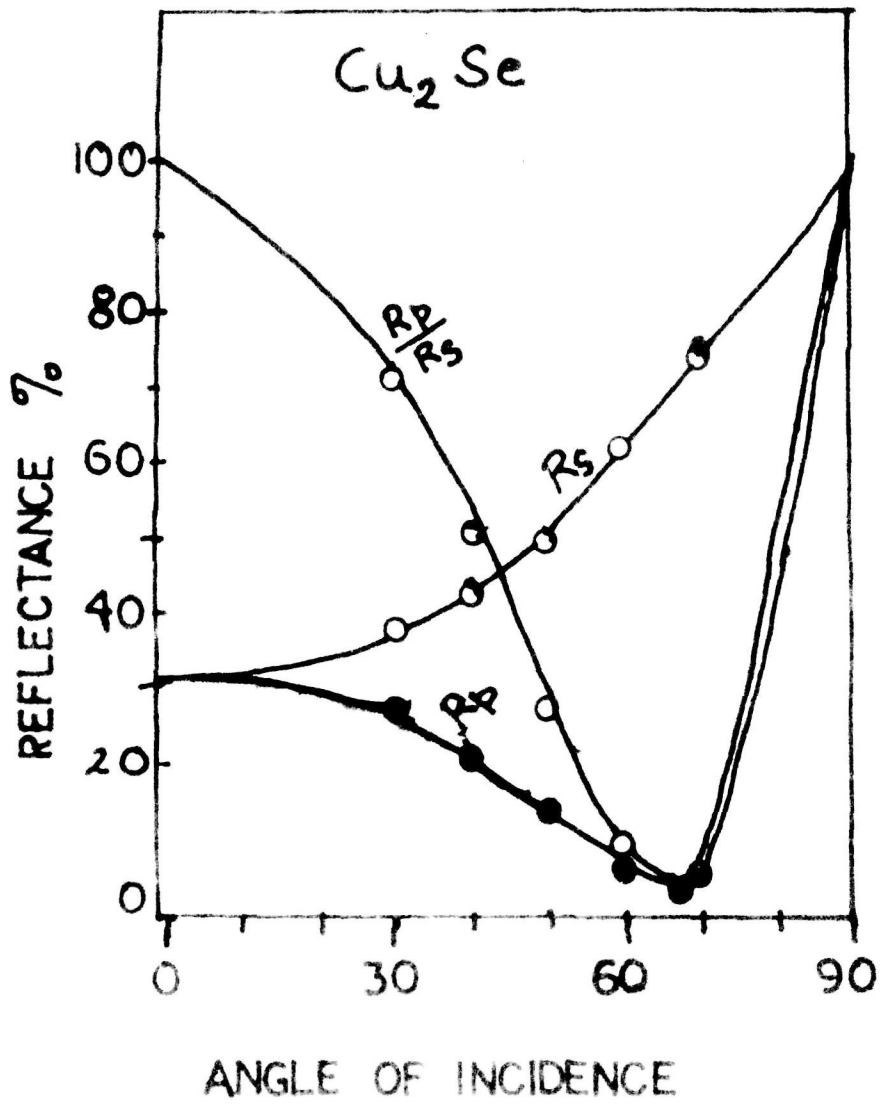


Fig. 68.

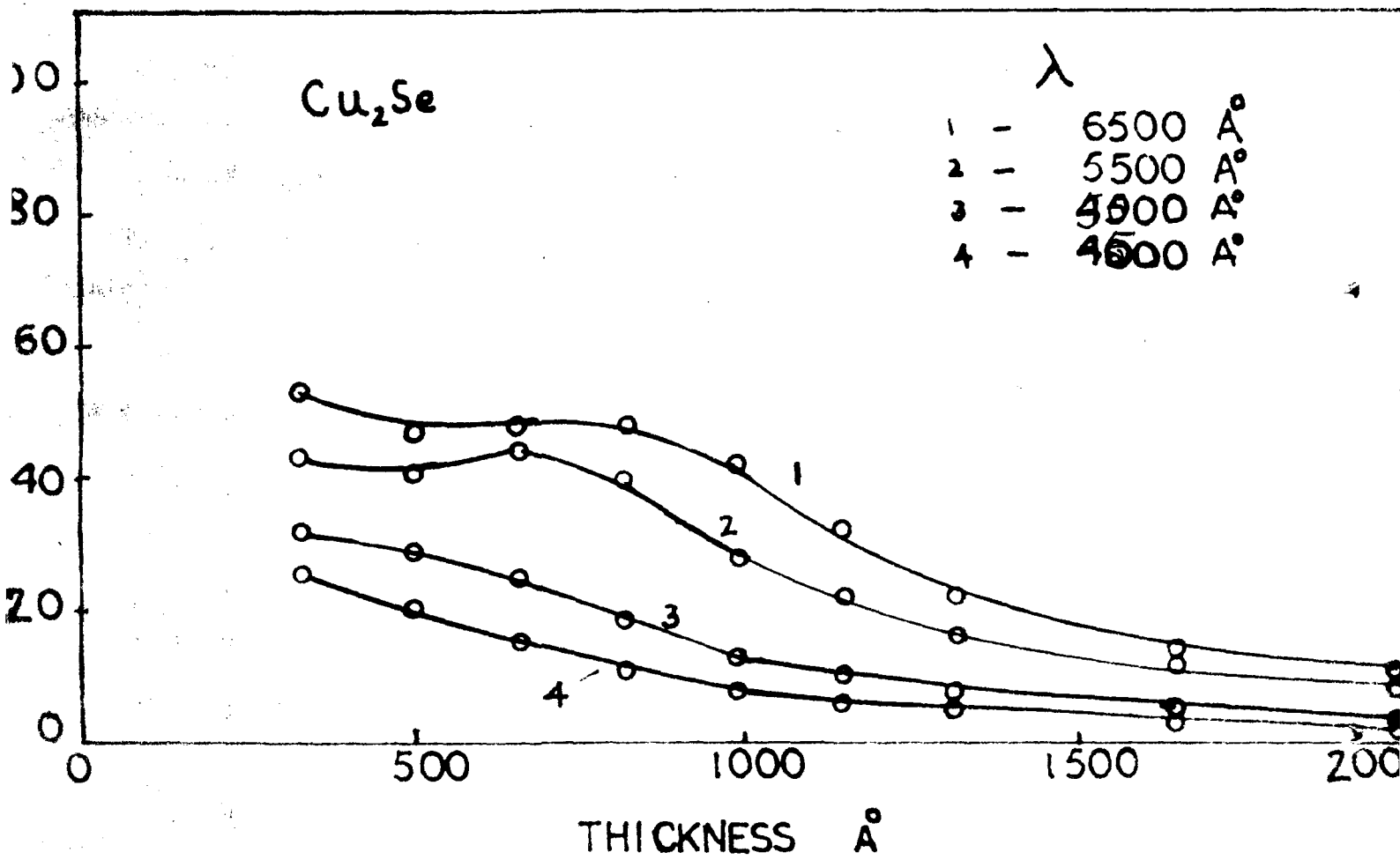


Fig. 69.

(ii) Transmission, reflection and absorption

Figure (65) shows the variation of transmittance and reflectance with the wavelength for a film ( $d \simeq 330 \text{ \AA}$ ) deposited at room temperature and of the same film annealed at  $150^\circ\text{C}$  temperature under vacuum. It was found that the films deposited at room temperature had a slightly higher transmittance and reflectance. Fig. (66) shows the variation of transmittance ( $T_p$  and  $T_s$ ) and reflectance ( $R_s$  and  $R_p$ ) with the wavelength for polarised light at an angle of incidence  $30^\circ$ . The dependence of transmittance ( $T_p$  and  $T_s$ ) and reflectance ( $R_p$  and  $R_s$ ) with the thickness of the film for parallel polarised light and perpendicularly polarised light is shown in Fig. (67). It is seen that transmittance decreased with the thickness whilst reflectance showed both maxima and minima. Variation of  $R_s$  and  $R_p$  with the angle of incidence is shown in Fig. (68).  $R_p$  is minimum at about  $67.5^\circ$  corresponding to a value of  $n = 2.41$ .

(iii) Absorption coefficient

Figure (69) shows the variation of transmittance with film thickness. It is seen that thinner films ( $d \simeq 800 \text{ \AA}$ ) showed the interference effects for all wavelengths except for  $\lambda 4500 \text{ \AA}$ . Absorption coefficient



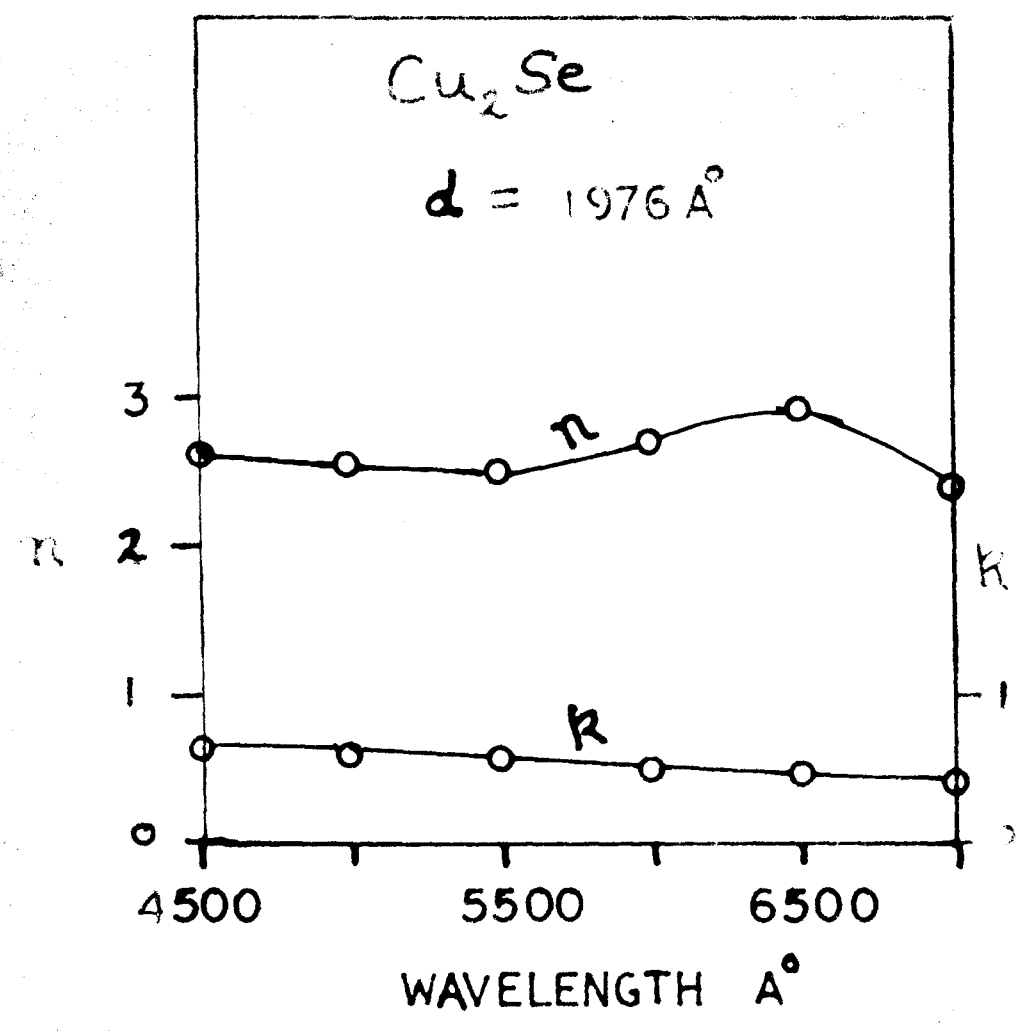


Fig.70.

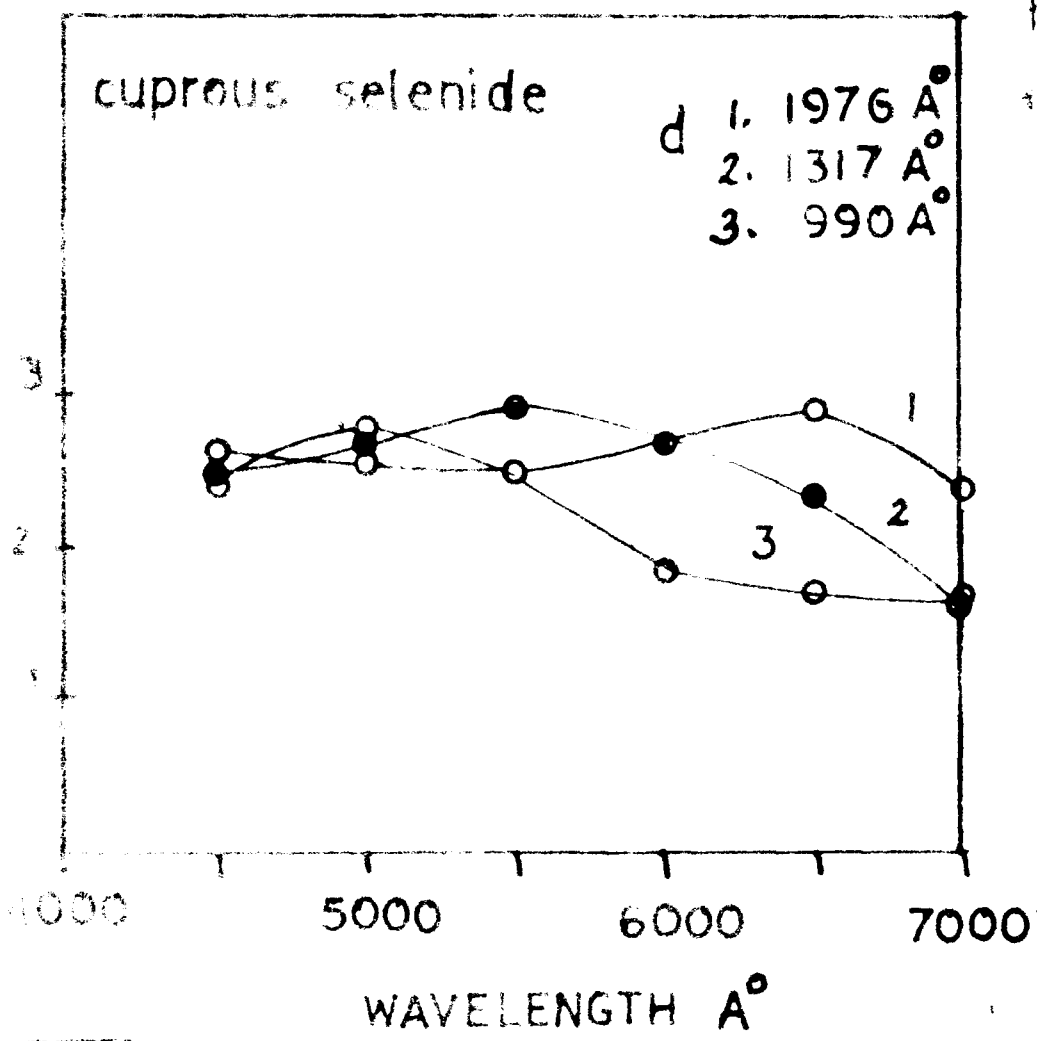


Fig. 71.

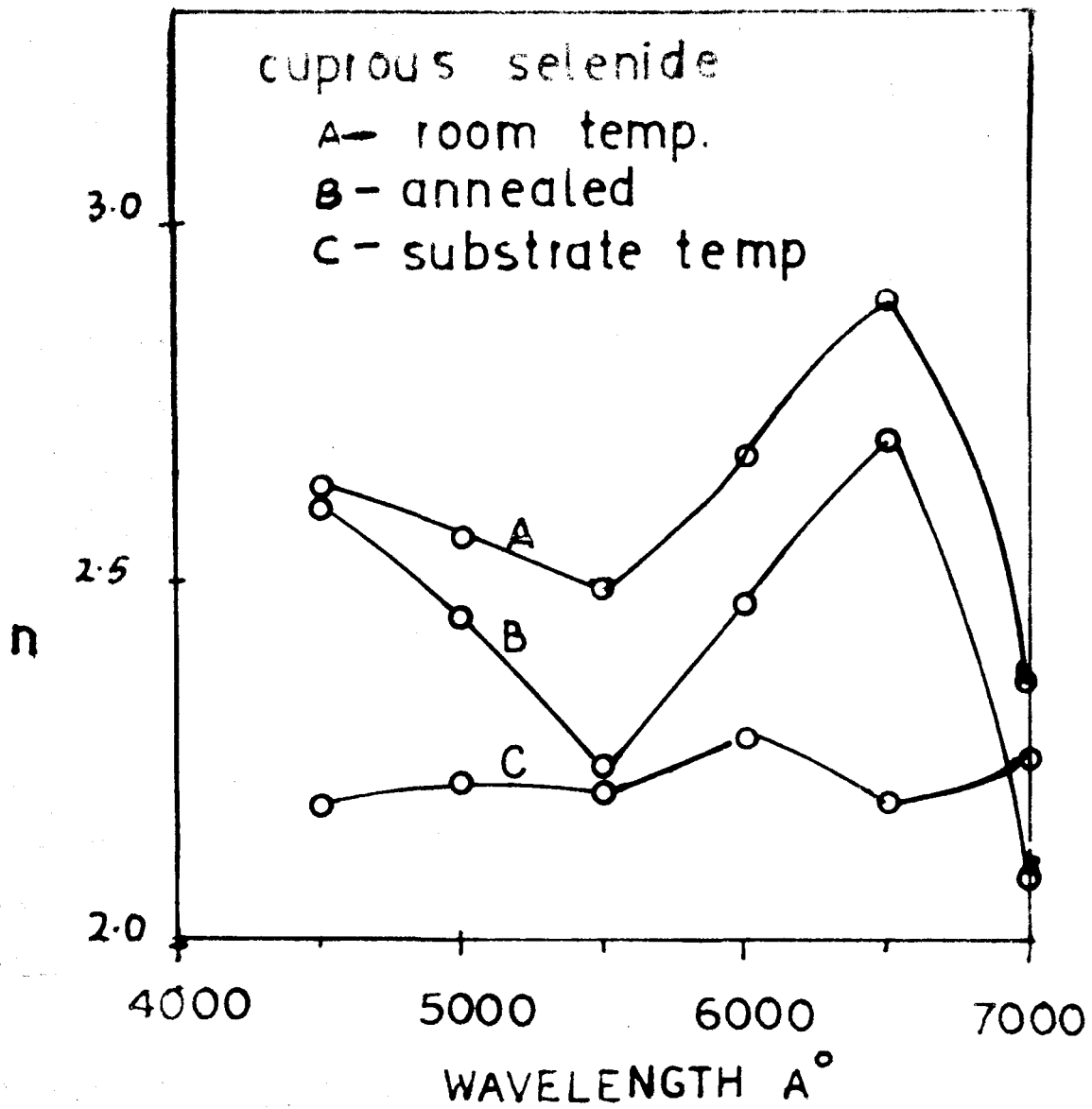


Fig. 72.

was calculated from the slope of  $\log T$  vs  $d$  curve and it was found to decrease from  $1.81 \times 10^5 \text{ cm}^{-1}$  to  $0.78 \times 10^5 \text{ cm}^{-1}$  with the increase of wavelengths (Table 32). Extinction coefficient  $k$  was calculated from the absorption coefficient and found to decrease from 0.65 to 0.43 with the increase of wavelength  $\lambda$  4500-7000 Å.

### Refractive index

The refractive index was calculated from the  $R_s$  and  $R_p$  components of the reflected light at an angle of incidence  $45^\circ$ . The homogeneity criterion  $R_s^2 = R_p$  at  $\theta = 45^\circ$  was found to be valid for all sufficiently thick films ( $d \simeq 800 \text{ Å}$ ). Table (33) shows typical values of  $n$  for various wavelengths (Fig. 70). The variation of refractive index with wavelength for three films is shown in Fig. 71 and the values are given in Table 34. It is interesting to see that peak in  $n$  shifts towards higher wavelengths with the increase of film thickness. Similar shifts with film thickness for  $n$  have been observed for oxides of Niobium and Indium by Goswami (1973) in this laboratory. Fig. (72) shows  $n$  for a film deposited at room temperature, the same film annealed in vacuo at  $150^\circ\text{C}$  and for a film deposited at a substrate temperature  $150^\circ\text{C}$  (Table 35).

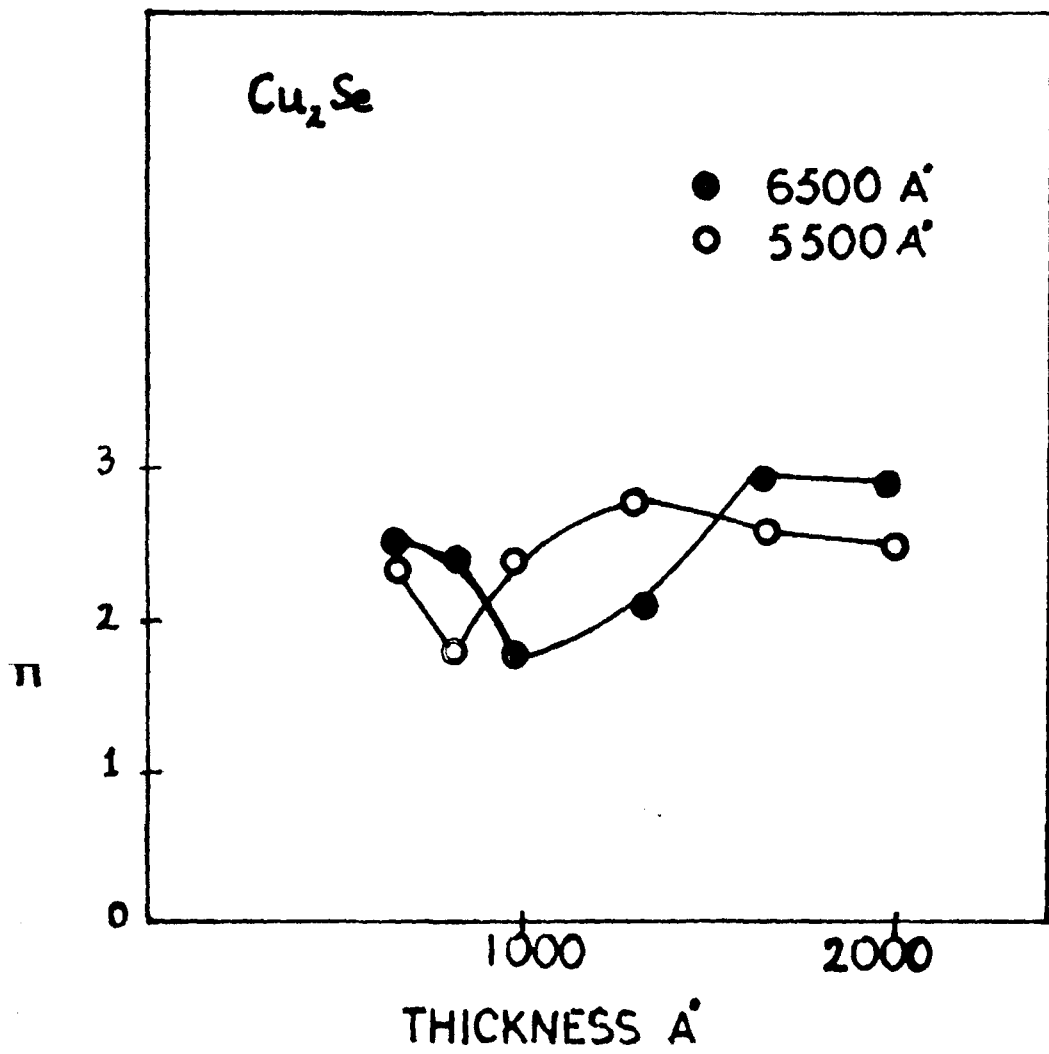


Fig. 73.

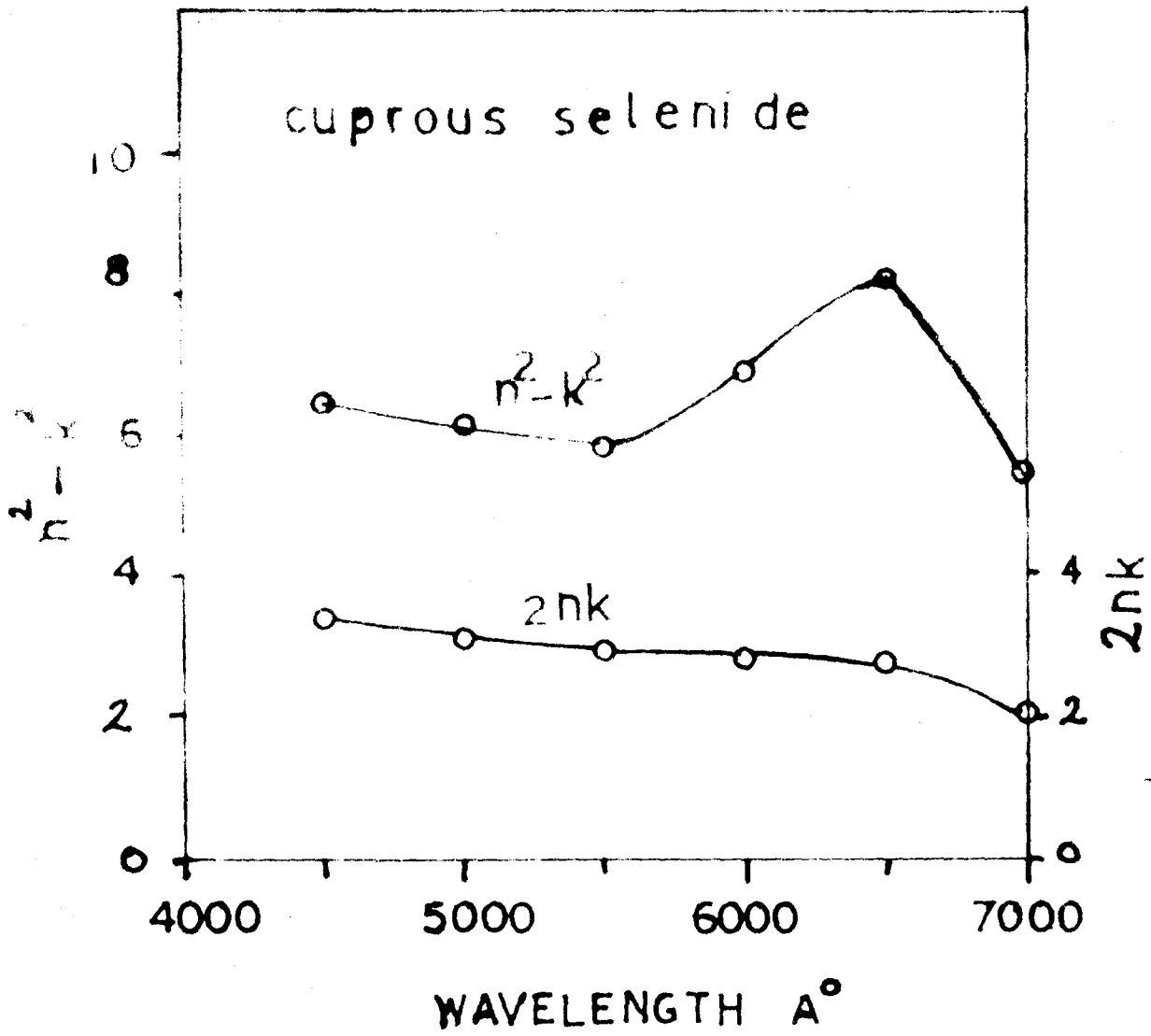


fig. 74.

Fig. (73) shows the variation of  $n$  with thickness of the films at two wavelengths  $5500 \text{ \AA}$  and  $6500 \text{ \AA}$ . A minimum value was found for  $n$  at thickness  $\approx 1000 \text{ \AA}$  and then increased and reached a steady value 2.9 for  $\lambda 6500 \text{ \AA}$ .  $n$  had a minima at about  $800 \text{ \AA}$  and then increased, for  $\lambda 5500 \text{ \AA}$ .

(v) Dielectric constant

Fig. (74) shows the variation of  $n^2 - k^2 (= \epsilon_1)$  and  $2nk (= \epsilon_2)$  with wavelengths. The value of  $k$  was however calculated from absorption coefficient. The  $\epsilon_1$  showed a peak value  $\sim 8.18$  for  $\lambda 6500 \text{ \AA}$ , whereas  $2nk$  decreased steadily from 3.4 to 2.03 with the increase of wavelength in the visible region.

Cuprous telluride films

(i) Structure

Films deposited at room temperature were found to consist mostly of tellurium. So films were deposited at a higher substrate temperature and their structure was examined by electron diffraction. Fig. (75) shows an electron diffraction transmission pattern obtained for such a film deposited at  $200^\circ\text{C}$ , 'd' values (Table 36) correspond to cuprous telluride  $\text{Cu}_2\text{Te}$ .

Fig. 75.

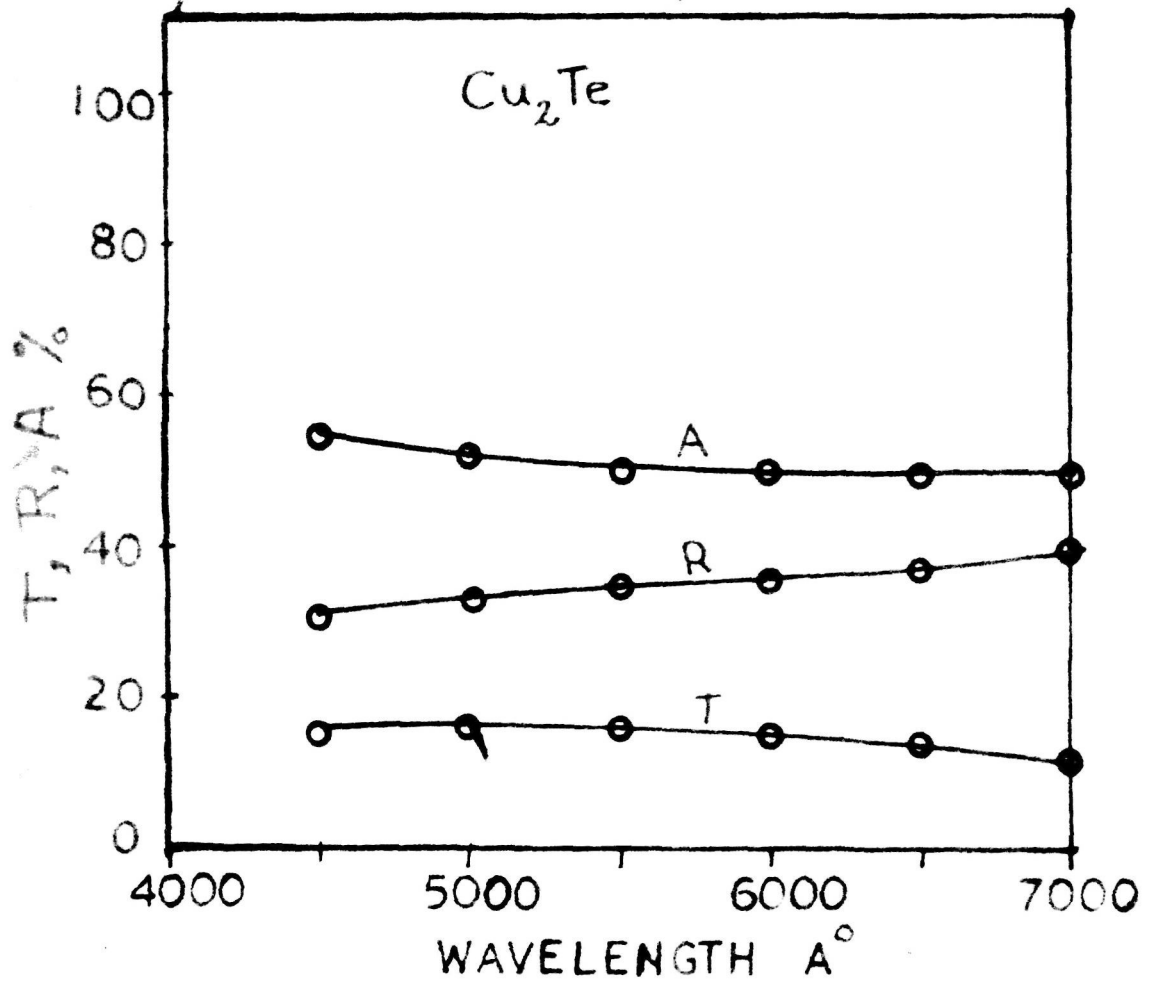


Fig. 76.



Table 36

Intensity	d in Å <sup>o</sup>	hkl
m	2.81	110
m	2.51	111
s	2.07	112
f	2.02	003
m	1.57	(122 (004
<b>F</b>	1.47	(014 (023
f	1.40	220
m	1.25	130

$$a = 3.98 \text{ Å}^{\circ}; c = 6.06 \text{ Å}^{\circ}$$

s = strong

m = medium

f = faint

(ii) Transmission, reflection and absorption

These films were blackish in colour. Fig. (76) shows the typical variation of transmittance and reflectance for cuprous telluride with wavelength for a film of thickness  $500 \text{ Å}^{\circ}$ . It is seen that the transmittance however decreased only slightly with the

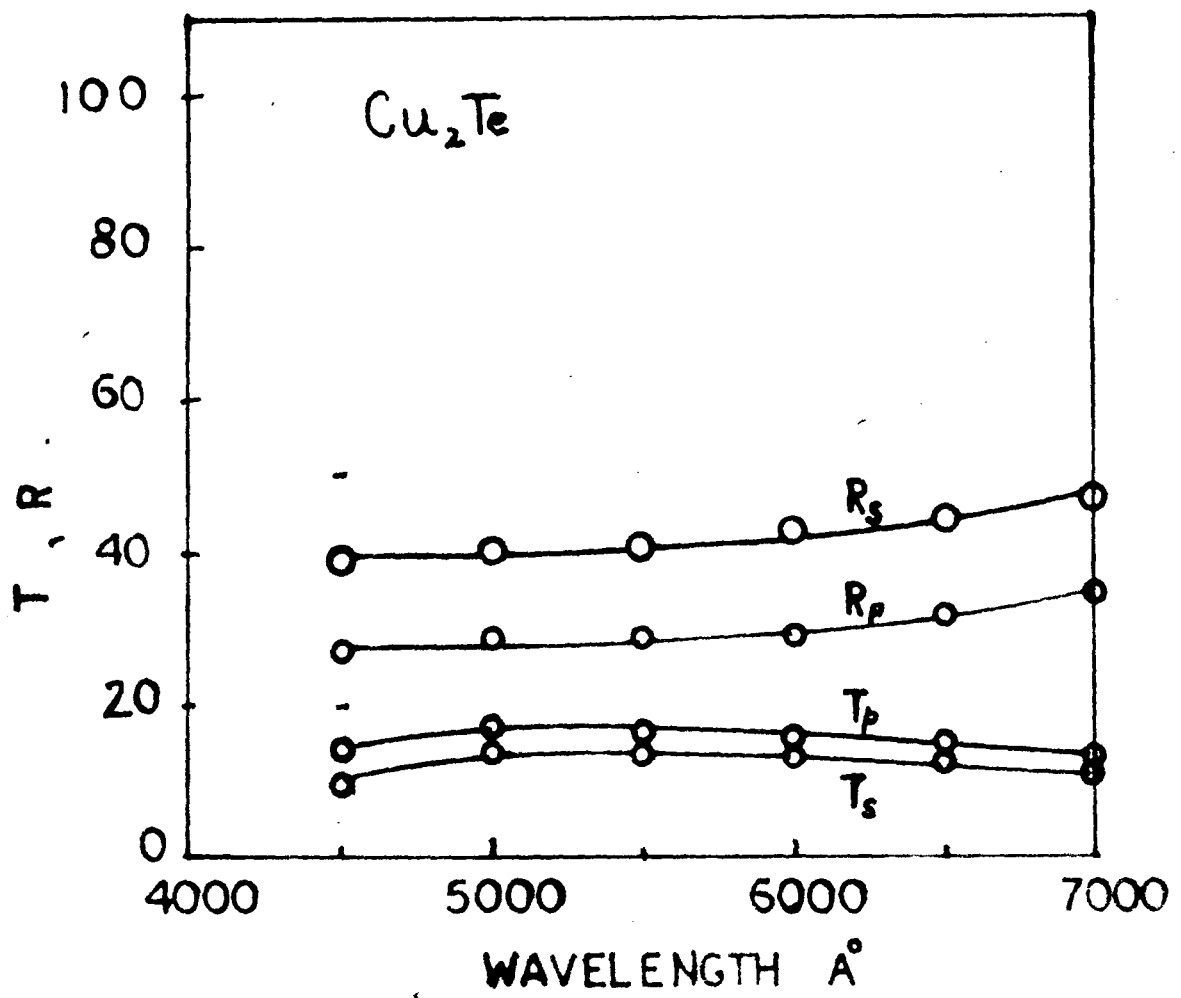


Fig. 77.

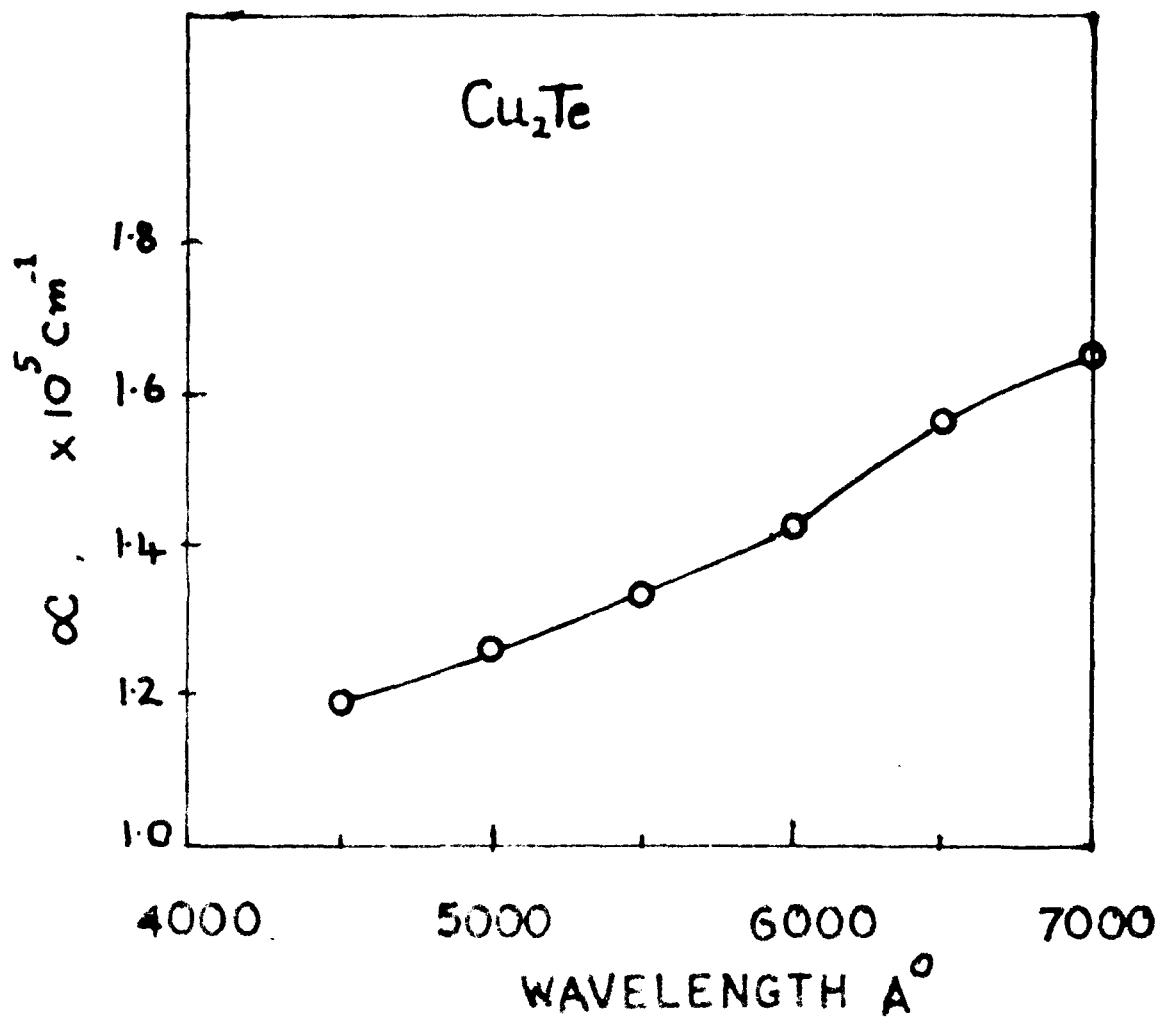


Fig. 78.

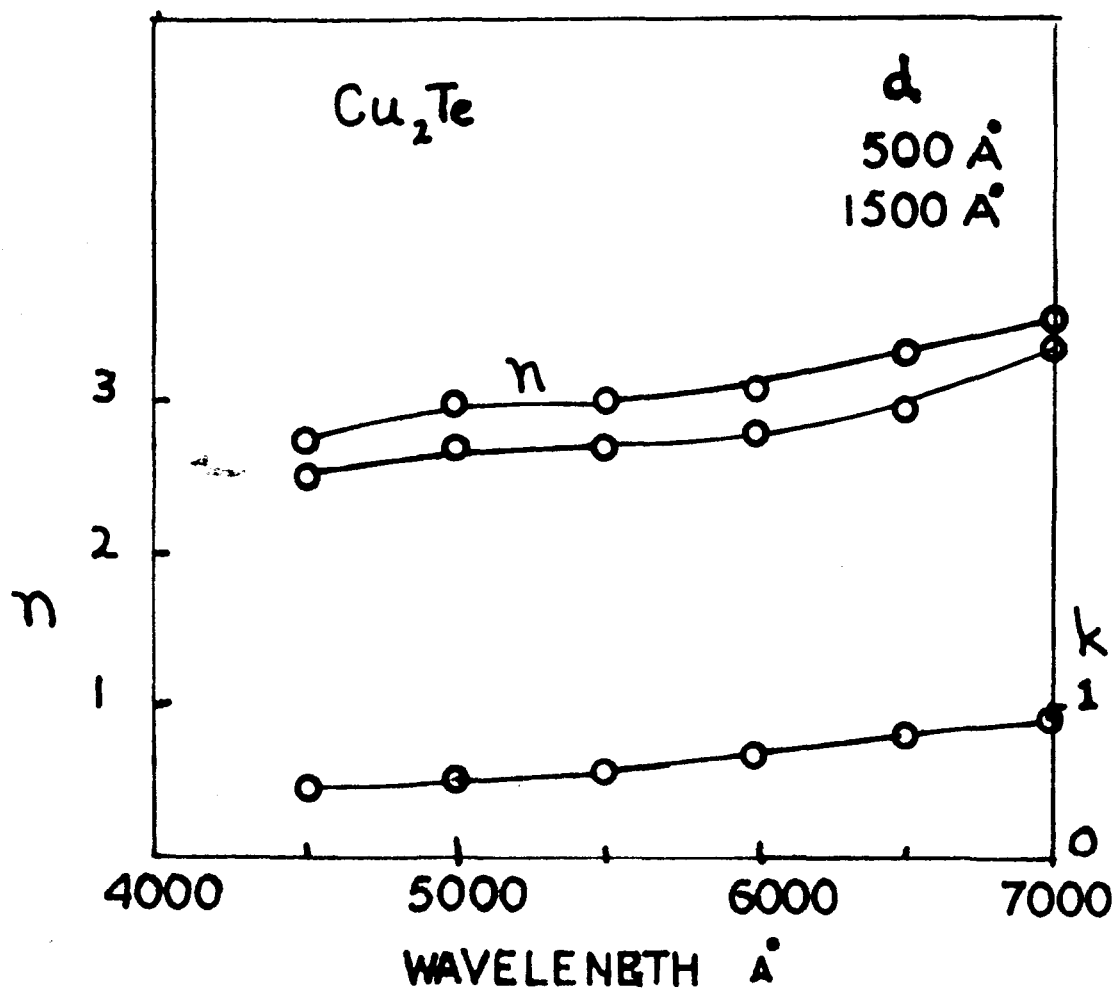


Fig. 79.

increase of wavelength whereas reflectance increased. Fig. (77) shows the typical variation of transmittance ( $T_p$  and  $T_s$ ) and reflectance ( $R_s$  and  $R_p$ ) with the wavelength for parallel and perpendicularly polarised light for film thickness.

### (iii) Absorption coefficient

Absorption coefficient was calculated in the usual way and the results are tabulated (Table 37). Fig. (78) shows the dependence of the absorption coefficient with the wavelength. It is seen that  $\alpha$  increased slightly with wavelength i.e. from  $1.19 \times 10^5 \text{ cm}^{-1}$  to  $1.65 \times 10^5 \text{ cm}^{-1}$  for  $\lambda 4500-7000 \text{ \AA}$ . The extinction coefficient ( $k$ ) was calculated from the absorption coefficient. It was found to vary from 0.45 to 0.9 in the visible region ( $\lambda 4500-7000 \text{ \AA}$ ).

### (iv) Optical constants

The refractive index was calculated from  $R_s$  and  $R_p$  components of the reflected light at  $45^\circ$  angle of incidence. It was found that homogeneity criteria  $R_s^2 = R_p$  at  $45^\circ$  agreed for all films. The variation of refractive index with wavelength was also studied in details for various films thickness ranging from  $500 \text{ \AA}$  to  $1600 \text{ \AA}$ . Typical variations of refractive index with

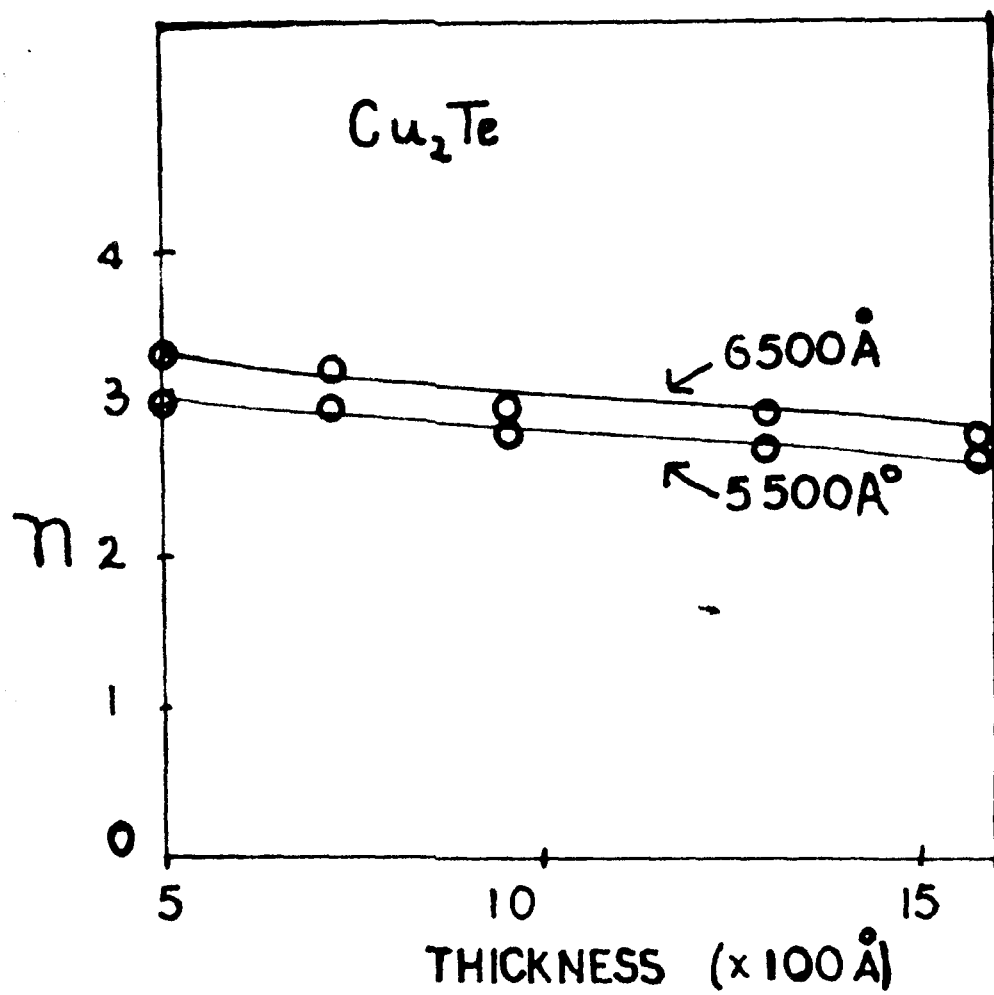


Fig. 80.

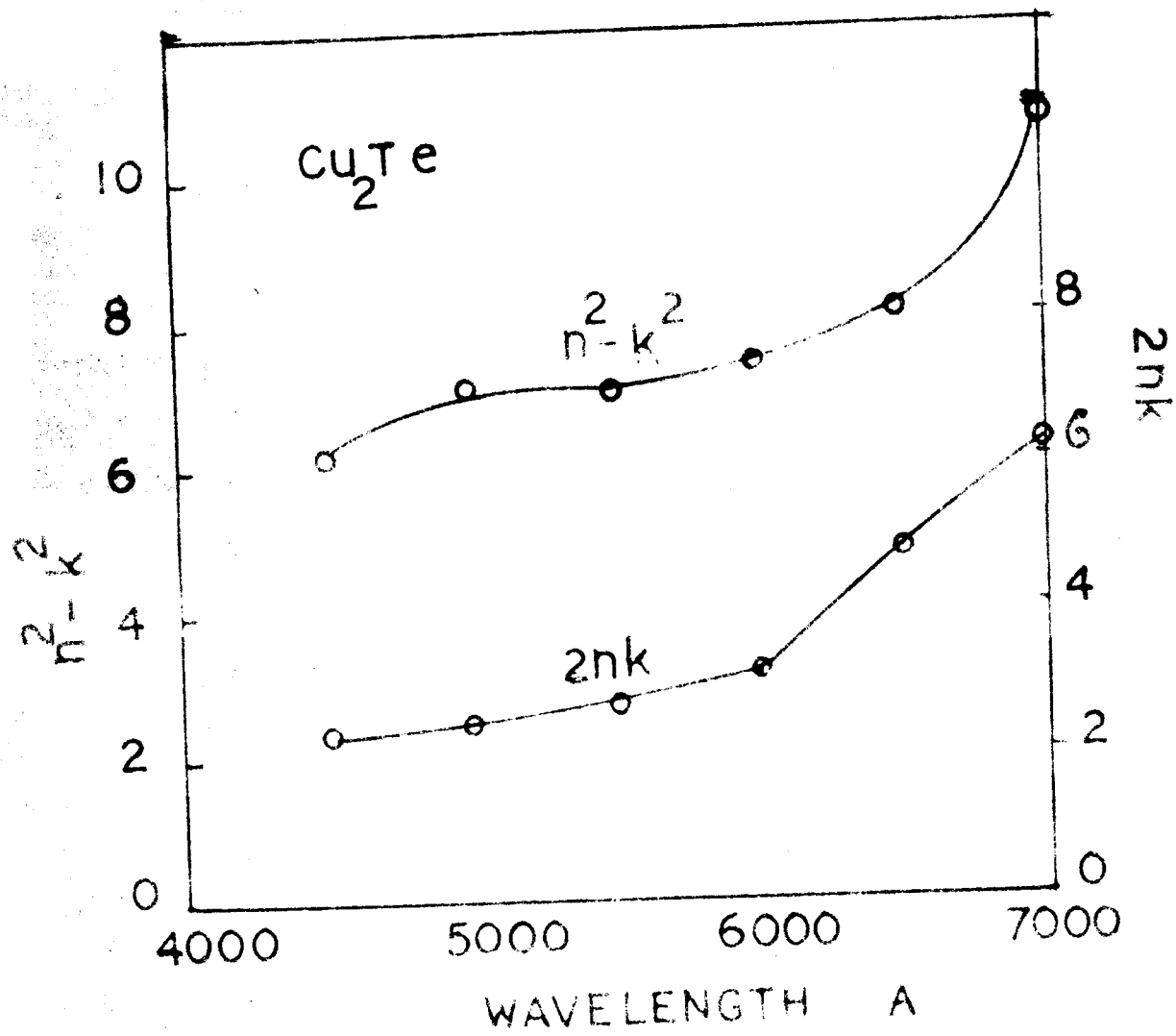


fig. 81.

wavelengths is shown in Fig. 79 for two films ( $d \simeq 500$  and  $1500 \text{ \AA}$ ). For an opaque film of thickness  $1300 \text{ \AA}$ ,  $n$  increased from 2.52 to 3.4 in the visible region ( $\lambda 4500-7000 \text{ \AA}$ ) and the values of  $n$  are given in Table 38. The same type of variation of the refractive index was observed for different film thicknesses. Extinction coefficient  $k$  was calculated from the absorption coefficient and it was found to vary from 0.45 to 0.92 for  $\lambda 4500-7000 \text{ \AA}$ .

It was, however, observed that the refractive index was found to change with the change in the film thickness. Figure (80) shows the variation of  $n$  with thickness for two wavelengths ( $\lambda 6500 \text{ \AA}$  and  $\lambda 5500 \text{ \AA}$ ; table 39). For  $\lambda 6500 \text{ \AA}$ ,  $n$  decreased from 3.34 to 2.73 and for  $\lambda 5500 \text{ \AA}$ , from 3.02 to 2.62 for film thicknesses ranging from  $500 \text{ \AA}$  to  $1600 \text{ \AA}$ .

(v) Dielectric constant

Fig. (81) shows the variation of  $\epsilon_1 = (n^2 - k^2)$  and absorption  $\epsilon_2 = (2nk)$  with the wavelength. It is seen that  $\epsilon_1$  varied from 6.15 to 10.7 and  $\epsilon_2$  varied from 2.27 to 6.26, both however increased with the wavelength in the visible region ( $\lambda 4500-7000 \text{ \AA}$ ).



(D) DISCUSSION

From the electron diffraction studies of the selenide and telluride of copper, it was found that the films obtained by vapour phase method conformed to  $\text{Cu}_2\text{Se}$  ( $a = 5.72 \text{ \AA}$ ) and  $\text{Cu}_2\text{Te}$  ( $a = 3.98 \text{ \AA}$  and  $c = 6.06 \text{ \AA}$ ). These results clearly showed that cuprous selenide and telluride can be vacuum deposited through the latter was possible only at a higher substrate temperature. Recently Goswami and coworkers (Goswami and Goswami, 1971); Goswami, Rao & Prabhat Singh) showed that at suitable substrate temperatures even films of group III-V compounds could be deposited even though they are reported to dissociate in vacuo during deposition.

From the studies of optical properties of cuprous selenide films it is seen that  $n$  not only depends on the wavelength but also on the deposition condition such as substrate temperature and annealing (cf Fig. 72). Refractive index,  $n$  decreased when the films were annealed and also when they were deposited at higher temperature. This was due to the decrease in reflectance ( $R_s$  and  $R_p$ ) of films deposited at higher substrate temperature compared to those formed at room temperature. The decrease of  $R$  and  $n$  at higher substrate temperature seems to be associated with

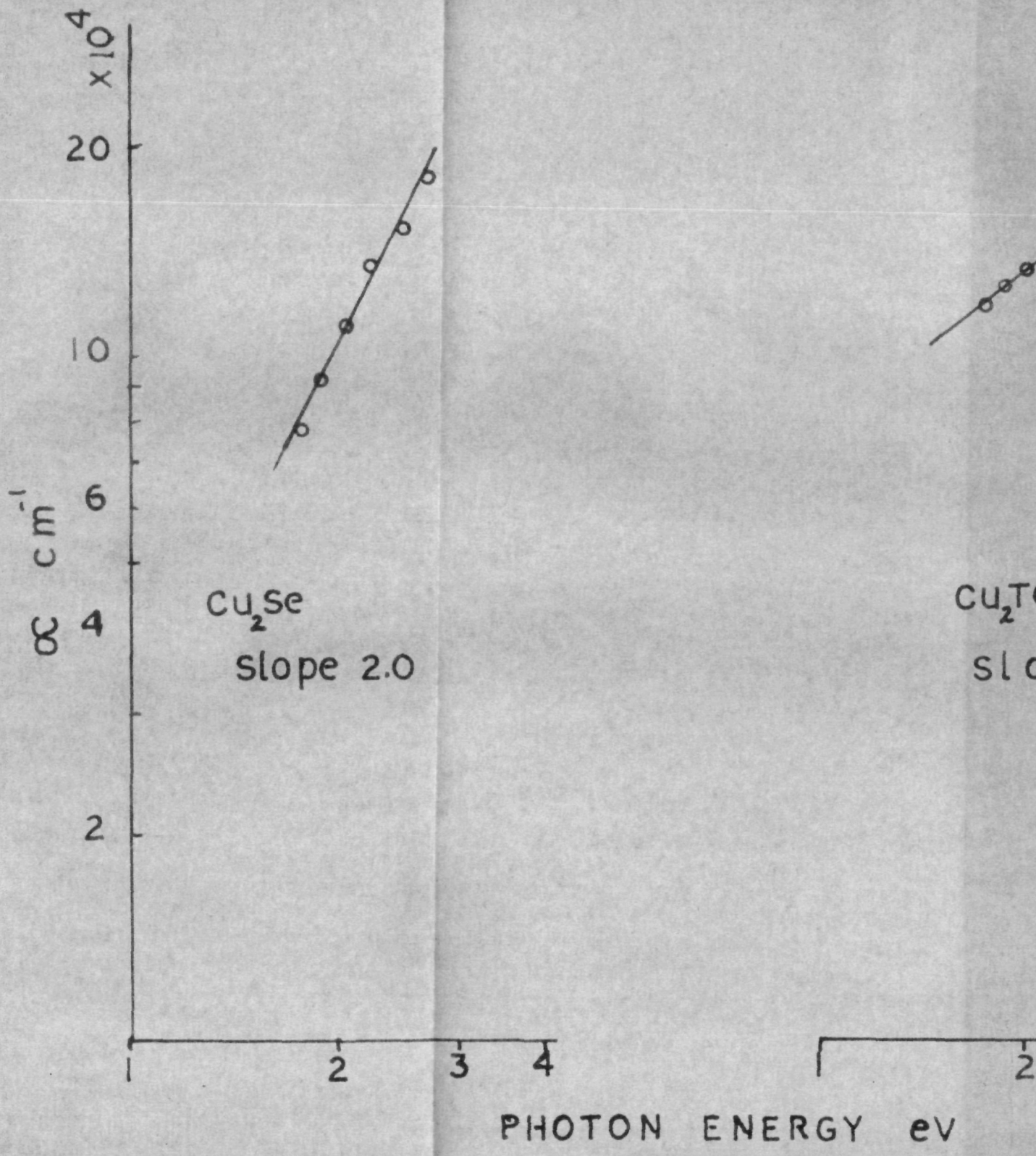


fig 82

the crystal size of the deposit films. It was found that refractive index of cuprous selenide varied with the thickness of the film. Refractive index decreased with the increase of film thickness and then increased to reach a steady value for thicker films. From the optical studies on cuprous telluride films, it is seen that the optical constants increased with the wavelength. Absorption coefficient also increased with the wavelength. Very thin films had higher refractive index,  $n$  decreased and reached a steady value as the thickness increased. The explanation for these optical behaviour is same as given in earlier cases.

It is also possible to find out the absorption process of light and the transition of electrons or carrier from lower to higher energy levels in the semiconductor. In the present case of cuprous selenide on plotting  $\log \alpha$  against  $\log h\nu$  (Fig. 82) it was found that the trace was a straight line the slope of which was found to be 2.0. As mentioned earlier it is possible to find out the type of transition namely direct or indirect taking place from the slope of the above curve according to the equations given by Bardeen and others (1956). The power index of the equation as observed from the slope determines the

nature of transition. Since the slope was about 2 it may be concluded that the transition was indirect but allowed. For cuprous telluride films however the slope was found to be 0.75 which according to equation of Brooks (1955) and Bardeen et al. (1956) suggest that direct transition took place and the phenomenon might be accompanying with a little of forbidden one, since for the ideal case of direct transition the power index would have been 0.5. Since the absorption edge was beyond the visible region the optical energy band gap would hence be in the infra red region, as observed by other workers.

Cuprous selenide filmsTable 32

Dependence of absorption coefficient and extinction coefficient with the wavelength

$\lambda(\text{\AA})$	$\alpha \text{ cm}^{-1}$	$k$
4500	$1.81 \times 10^5$	0.65
5000	$1.53 \times 10^5$	0.61
5500	$1.35 \times 10^5$	0.59
6000	$1.09 \times 10^5$	0.52
6500	$0.92 \times 10^5$	0.48
7000	$0.78 \times 10^5$	0.43

Table 33

Variation of refractive index with wavelength

$\lambda(\text{\AA})$	$R_s$	$R_p$	$n$
4500	0.4225	0.1783	2.62
5000	0.4179	0.1754	2.56
5500	0.3954	0.1550	2.49
6000	0.4260	0.1802	2.68
6500	0.4502	0.2006	2.90
7000	0.3763	0.1410	2.36

Table 34

Refractive index with the wavelength for three films

$\lambda(\text{\AA})$	Refractive index		
	$d \simeq 1976 \text{\AA}$	$d \simeq 1317 \text{\AA}$	$d \simeq 988 \text{\AA}$
4500	2.62	2.46	2.44
5000	2.56	2.66	2.79
5500	2.49	2.93	2.50
6000	2.68	2.73	1.83
6500	2.90	2.36	1.74
7000	2.36	1.67	1.60

Table 35Variation of refractive index with wavelength  
(substrate temp.  $150^{\circ}\text{C}$ )

$\lambda(\text{\AA})$	$R_s$	$R_p$	$n$
4500	0.347	0.1206	2.18
5000	0.3506	0.1225	2.22
5500	0.3555	0.1272	2.21
6000	0.364	0.132	2.29
6500	0.351	0.124	2.19
7000	0.3583	0.1278	2.26

Cuprous telluride filmsTable 37

The variation of absorption coefficient with the wavelength

$\lambda(\text{\AA})$	$\alpha \text{ cm}^{-1}$	$k$
4500	$1.19 \times 10^5$	0.45
5000	$1.26 \times 10^5$	0.50
5500	$1.33 \times 10^5$	0.58
6000	$1.43 \times 10^5$	0.68
6500	$1.57 \times 10^5$	0.81
7000	$1.65 \times 10^5$	0.92

Table 38

Typical variation of refractive index with wavelength

$\lambda(\text{\AA})$	$R_s$	$R_p$	$n$
4500	0.4105	0.169	2.52
5000	0.4321	0.1859	2.71
5500	0.4451	0.1995	2.70
6000	0.4559	0.2087	2.80
6500	0.4742	0.2252	2.96
7000	0.5290	0.2803	3.40

Table 39

Variation of  $n$  with  $d$  for two wavelengths  $5500 \text{ \AA}$ <sup>o</sup>  
and  $6500 \text{ \AA}$ <sup>o</sup>

$\lambda(\text{\AA})$ <sup>o</sup>	$d(\text{\AA})$ <sup>o</sup>	$R_s$	$R_p$	$n$
6500	500	0.5126	0.2621	3.34
	730	0.5166	0.2693	3.15
	950	0.4657	0.2166	2.92
	1300	0.4742	0.2252	2.96
	1570	0.4506	0.2049	2.72
5500	500	0.4731	0.229	3.02
	730	0.4815	0.2318	3.04
	955	0.4521	0.2046	2.805
	1300	0.4451	0.1995	2.705
	1570	0.4340	0.190	2.62



CHAPTER VIIISTUDIES ON INDIUM ARSENIDE FILMS(A) INTRODUCTION

Indium arsenide is a semiconductor belonging to III-V compounds. Materials from this group of compounds in particular provide films with the desirable properties of electrical mobility and refractive index and found suitable for use in Hall effect devices, thin film transistors and optical interference filters, etc. Applications of InAs as Hall generators has been investigated by many workers (Kuhrt, 1954; Hartel, 1954; Weiss, 1961). Brady and Kunig (1966) and Kunig (1968) described the fabrication of InAs thin film transistors; the device characteristics were analysed and related to the material properties. Hilsum (1957) found that this material was useful for the construction of photocells. Cox et al. (1961) developed vacuum deposited multilayer infra red antireflection coatings of InAs for the  $\mu$  to  $15 \mu$  region.

Sul'man and Ukhanov (1965), Johnson (1966) and others found the lattice constant of InAs to be  $a = 6.063 \text{ \AA}$ .

Electrical and semiconducting properties of InAs have been investigated by many workers and numerous literatures are available on these aspects. Folberth et al.(1954) for example found that the band width of the forbidden zone to be 0.47 eV at absolute zero with a temperature dependence of  $-4.5 \times 10^{-4} \text{ eV/}^{\circ}\text{K}$ . The electron mobility at room temperature was 30,000 sq. cm/V. Sec. and it followed approximately  $T^{-3/2}$  law. The ratio of mobilities was 150 at  $300^{\circ}\text{K}$  and increased with the rising temperature. Harman et al.(1956) measured the Hall coefficient and resistivity as a function of temperature. A room temperature mobility of 30,000  $\text{cm}^2/\text{V}.\text{Sec.}$  was obtained for a donor concentration of about  $1.7 \times 10^{16}/\text{cm}^3$ . Nasledov and Khalilov (1956) also investigated the electrical properties of InAs.

Group III-V compounds such as indium arsenide generally dissociate during their thermal evaporation. Alternative to the direct evaporation Gunther (1958 and 1961) employed the "3 temperature gradient" i.e. the two elements were evaporated at temperature  $T_1$  and  $T_2$  and deposited at a third temperature  $T_3$  on a suitable substrate.  $T_1$  and  $T_2$  were chosen so that there was an excess of more volatile compound in the vapour phase and  $T_3$  was chosen so that only molecules of the desired compound were deposited while excess of atoms of the volatile

element were re-emitted into the vapour phase. He measured Hall mobilities up to  $13,000 \text{ cm}^2/\text{v. sec.}$  and Hall constant up to  $100 \text{ cm}^3/\text{C. Sec.}$  Both the Hall constant and mobility increased with the grain size of the polycrystalline layer. Dixon (1959) measured the Hall constant and resistivity as a function of carrier concentration for zinc doped single crystal InAs (p-type) at temperature ranging from  $4.2^\circ$  to  $500^\circ\text{K.}$  He observed anomalous electrical properties for smaller carrier concentration.

The electrical and galvanomagnetic properties of the epitaxial InAs films investigated by McCarthy (1967) showed good agreement with the corresponding temperature dependent parameters of bulk crystalline InAs. Vlasov and Semiletov (1968) studied the electrical properties of epitaxial films of InAs and observed a strong dependence of electron mobility and carrier concentration on the thickness of the film. For thickness  $\sim 20 \mu\text{m}$  the mobility amounted to  $17,000 \text{ cm}^2/\text{v. sec.}$  and the concentration  $\sim 1.7 \times 10^{16} \text{ cm}^{-3}$ . Howson (1968) prepared InAs films by the "three temperature process" and studied the electrical properties. Aliev (1969) measured the electrical conductivity, thermoelectric power, magnetothermoemf and transverse Nerst-Ettingshausen coefficient of n-type InAs samples ( $n = 1.7 \times 10^{18} - 6 \times 10^{19} \text{ cm}^{-3}$ ) at  $90^\circ$ ,

200° and 300°K in fields upto 21 Koe. Jha and Korgaonkar (1972) studied the electrical properties of d.c. sputtered InAs films. The sputtered film of InAs showed a Hall mobility of  $7 \text{ cm}^2/\text{v. sec.}$  The low mobility was due to highly disordered structure and impurities present.

The optical properties and the optical energy band gap of bulk InAs have been studied by many workers. Most of the optical work has been carried out in the infra red region. Talley and Enright (1954), Hilsun (1957) and Dixon (1957) showed that InAs to be a promising detector for the infra red region using either photoconductive or photoelectromagnetic effects. The photovoltaic effect (Talley and Enright, 1954) was observable even at room temperature, but was much stronger ( $\sim \times 1000$ ) at liquid nitrogen temperature. The hole mobility derived from Hall effect and conductivity measurement at room temperature was  $10^2 \text{ cm}^2/\text{volt. sec.}$ , while the electron mobility was  $10^4 \text{ cm}^2/\text{volt. sec.}$  Hilsun (1957) also observed photoconductive (PC) and photoelectromagnetic (PEM) effect in a purified InAs crystal (2) at room temperature. The material was n type with  $3 \times 10^{16} \text{ cm}^{-3}$  and an electron mobility  $24000 \text{ cm}^2/\text{v. sec.}$  The carrier life time deduced from the ratio of the photoconductive to photoelectromagnetic voltages was  $0.2 \mu \text{ sec.}$  Dixon (1957

also reported photoelectromagnetic effect in InAs. He found that the magnitude of PEM current was dependent upon the photon flux, magnetic induction, life time and mobilities of the electrons and holes, temperature and surface recombination velocity.

Morrison (1961) studied the optical properties of polished bulk samples of Indium Arsenide in the spectral region 0-6 eV and the variation of optical constants with photon energy (0-6 eV). Sulman and Ukhanov (1965) investigated the optical forbidden band with and the dependence of the effective electron mass on the electron density in InAs films. The effective mass was however calculated from the reflection coefficient for light of certain wavelengths. Potter (1966) reported optical properties of InAs evaporated on to a heated glass substrate as being similar to those of the bulk material. Howson (1968) investigated optical properties of the thin films of Indium Arsenide in the wavelength region 0.7 to 5.0  $\mu\text{m}$  and calculated the optical constants from interference fringes. He found that the refractive index decreased as the substrate temperature increased from 4.0, at 3.5  $\mu\text{m}$  for films produced at ambient temperature to 3.0 for those prepared at the highest temperature of 400°C. He also studied the absorption coefficient at various substrate temperatures.

It is seen from the above survey of literature that though a few investigations have been made on films no systematic study has yet been made on optical properties in the visible region. In the following, therefore, a detailed investigation has been made on InAs films for their transmittance, reflectance, absorption coefficient, optical constants, their variation with wavelength and thickness of the film.

## (B) EXPERIMENTAL

### (1) Preparation of bulk Indium Arsenide

Indium arsenide was prepared by reacting the elements in their stoichiometric ratio (1:1) under vacuo. Pure indium (99.99%) and arsenic (99.99%) were taken in a silica tube one end of which was closed. Silica tube with the elements was then evacuated to about  $10^{-5}$  mm. of Hg. and sealed; and heated in an electric furnace. The temperature was raised slowly at the rate of  $75^{\circ}\text{C}$  per hour upto  $1000^{\circ}\text{C}$  and maintained at that temperature for about 8 hours and cooled to about  $300^{\circ}\text{C}$  and then quenched in cold water. X-ray diffraction pattern was taken to identify the compound formed and the structure was confirmed ( $a = 6.053$ , ZnS type) together with a little  $\text{In}_2\text{O}_3$  ( $a = 10.12$  bcc).

Fig. VIII.1.



X-ray pattern of InAs.

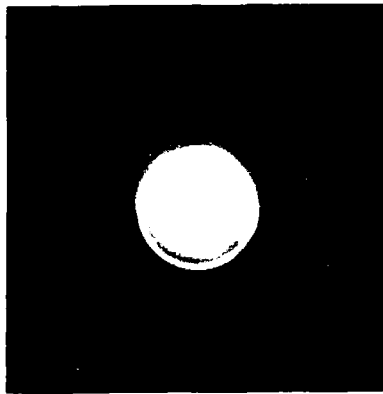


fig. 83.

(ii) Preparation of Indium Arsenide films

Barua and Goswami (1966), Goswami and Goswami (1973) have recently reported that it is possible to deposit group III-V compounds by the thermal evaporation method under certain conditions without adopting the triple temperature technique. Indium arsenide films were prepared by evaporation process as described in Chapter II. Tungsten boat was used for evaporating the bulk compound. All the films deposited at room temperature were annealed at  $100^{\circ}\text{C}$  for about one hour and their optical properties were studied.

(iii) Substrate temperature

Indium arsenide films were also deposited at a higher substrate temperature  $150^{\circ}\text{C}$  and the effect of substrate temperature on the optical properties were investigated.

(C) RESULTS

(1) Structure

Deposits of indium arsenide formed at room temperature were amorphous in nature or had a fine grained structure. With the increase of substrate temperature the deposits become crystalline and sharp



fig. 84.

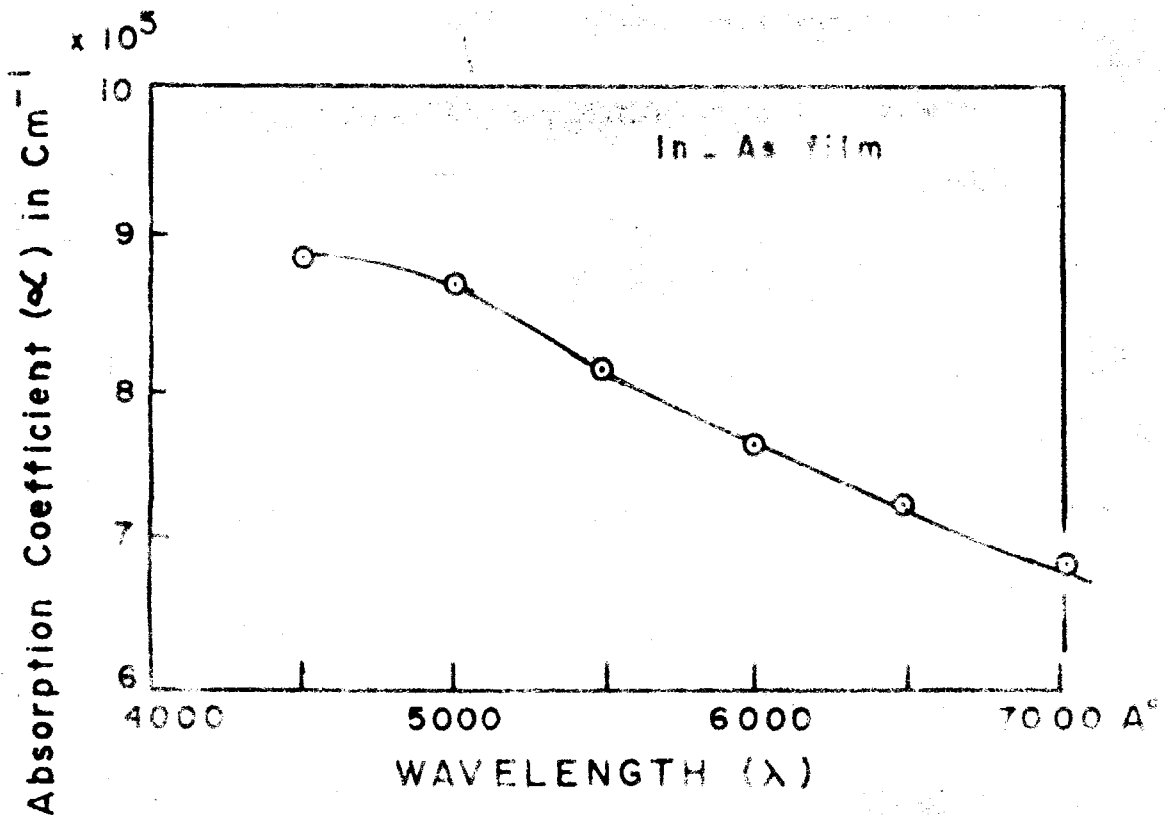
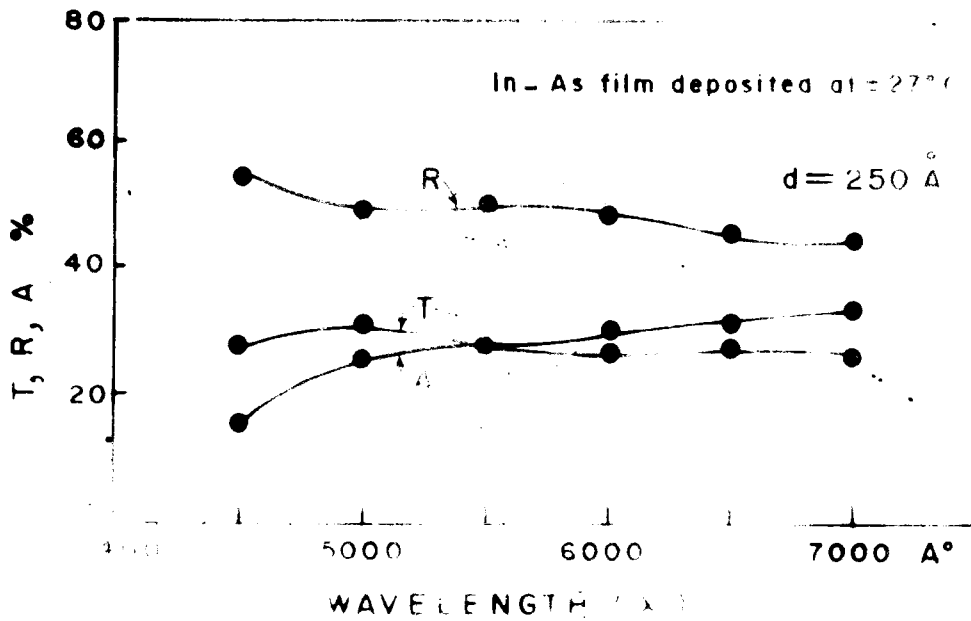


Fig. 85.

diffraction patterns were obtained. Fig. (83) shows a typical electron diffraction pattern of InAs films formed at higher substrate temperature. It is seen that these deposits had the normal ZnS type of structure with  $a = 6.05$ .

(ii) Transmission, reflection and absorption

Fig. (84) shows the typical variation of transmittance, reflectance and absorbance of a film ( $a \approx 250 \text{ \AA}$ ) deposited at room temperature, with the wavelength. It is seen that absorption increased with the wavelength. Films become opaque, blackish in colour at about  $350 \text{ \AA}$  thickness.

(iii) Absorption coefficient

Absorption coefficient evaluated for transparent films showed that this parameter varied from  $8.9 \times 10^5 \text{ cm}^{-1}$  to  $6.5 \times 10^5 \text{ cm}^{-1}$  with the increase of wavelength from  $\lambda 4500$  to  $7000 \text{ \AA}$ . The variation of absorption coefficient with the wavelength is shown in Fig. (85) and the results are tabulated (Table 40).

(iv) Optical constants

Refractive index and extinction coefficient were evaluated from  $R_s$  and  $R_p$  components of the reflected

Fig. 86.

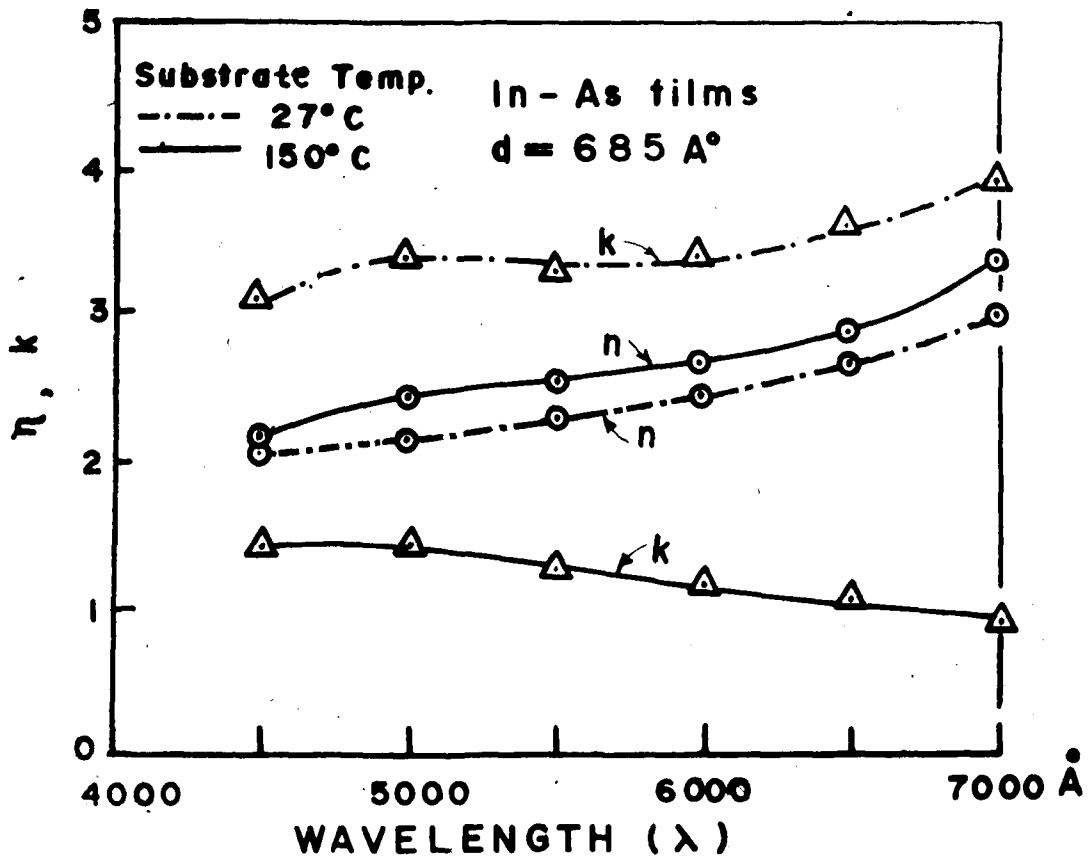
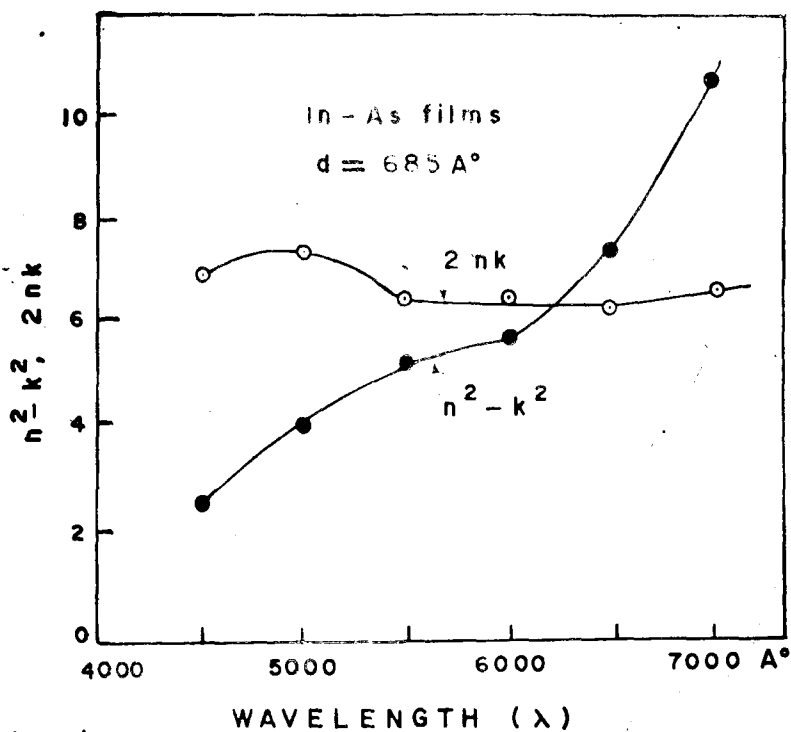


Fig. 87.



light for different wavelengths at an angle of incidence  $\theta = 45^\circ$ .  $n$  and  $k$  were determined for films deposited at room temperature and also at higher substrate temperature ( $t_s$ ) about  $150^\circ\text{C}$ . Results are given in tables (41) and (42) and Fig. (86). It is interesting to see that there is only a slight variation of  $n$  for two substrate temperatures, but  $k$  varied considerably being less at higher  $t_s$ . There was no appreciable change in the refractive index with the film thickness which are opaque.

(v) Dielectric constant

Fig. (87) shows the variation of dielectric constant  $n^2 - k^2$  and absorption  $2nk$  with  $\lambda$  and results are shown in table (43). It is seen that the dielectric constant varied from 2.56 to 10.7; and absorption  $2nk$  varied from 6.86 to 6.58 with a peak value around  $\lambda 5500 \text{ \AA}$ .

(D) DISCUSSION

The above study shows that it is possible to deposit indium arsenide films having ZnS type of structure by the thermal evaporation method without adopting the triple temperature technique. Similar observations were also made for GaP as deposited earlier

by Goswami and Goswami (1973). It is also seen that the deposits formed at  $t_s$  below  $120^\circ\text{C}$  were mostly amorphous in nature but became crystalline at higher  $t_s$ .

From the optical measurements made on deposits formed at room and higher temperature, it is seen that  $n$  remained more or less constant but  $k$  slightly decreased with the increase of substrate temperature. This appears to be associated with the crystal growth process of these films. The optical properties for bulk indium arsenide have recently been studied by Morrison (1961) in the far infra red and ultraviolet region. On a comparison of these values with those of films studied in the visible region, it can be seen that though  $n$  was similar for both films and bulk,  $k$  however slightly differed and this is more prominently shown in the  $n^2 - k^2$  and  $2nk$  curves. For the bulk, the former varied from 10 to 11 compared to 2.56 to 10.7 for films and the latter 13 to 17 compared to 6.86 to 6.58 for films though the trend in both the cases is similar. The peak value of  $2nk$  observed around  $\lambda 5500 \text{ \AA}$  for bulk was also observed for thin films.

It is also possible to study the effect of light on the electron transport process in the material. On plotting  $\log \propto$  against  $\log h\nu$  straight line graph

was obtained and the slope was found to be 0.75 which follows an equation given by Brooks (1956) conforming to direct transition mostly allowed with a little of forbidden transition.

As indium arsenide is used in many devices such as photocells, infra red films, etc. the present study provides useful data on transmission, reflection, refractive index, absorption coefficient, their variation with wavelength and film thickness.

Indium Arsenide FilmsTable 40

Variation of absorption coefficient and extinction coefficient with the wavelength

$\lambda(\text{\AA})$	$\alpha (\text{cm}^{-1})$	k
4500	$8.98 \times 10^5$	3.22
5000	$8.67 \times 10^5$	3.45
5500	$8.07 \times 10^5$	3.53
6000	$7.63 \times 10^5$	3.64
6500	$7.24 \times 10^5$	3.74
7000	$6.81 \times 10^5$	3.80

Table 41

Variation of n and k with the wavelength (films were deposited at room temperature and annealed at 100°C for one hour)

$\lambda(\text{\AA})$	$R_s$	$R_p$	n	k
4500	0.6667	0.4671	2.10	3.15
5000	0.6628	0.4591	2.29	3.40
5500	0.6600	0.454	2.39	3.20
6000	0.6780	0.4737	2.73	3.49
6500	0.6905	0.4887	2.93	3.68
7000	0.7127	0.5182	3.11	4.00

Table 42

Variation of  $n$  and  $k$  with wavelength (films deposited at temperature  $150^{\circ}\text{C}$ )

$\lambda(\text{\AA})$	$R_s$	$R_p$	$n$	$k$
4500	0.4324	0.20	2.22	1.54
5000	0.4316	0.1909	2.50	1.47
5500	0.410	0.1666	2.59	1.24
6000	0.4136	0.1683	2.66	1.22
6500	0.4186	0.1677	2.89	1.06
7000	0.4602	0.2027	3.41	0.97

Table 43

Variation of  $\epsilon_1$  and  $\epsilon_2$  with the wavelength

$\lambda(\text{\AA})$	$\epsilon_1$	$\epsilon_2$
4500	2.56	6.86
5000	4.09	7.35
5500	5.17	6.42
6000	5.59	6.49
6500	7.23	6.13
7000	10.70	6.58



CHAPTER IXSUMMARY AND CONCLUSIONS

In the present study on the optical properties of vacuum deposited films, an attempt has been made to determine the different optical parameters and their dependence on the film thickness and the wavelength of the incident light. Effects of various factors, such as substrate temperature and the annealing of deposit films etc., on the optical properties have also been studied in greater details. It has also been found that grain growth, crystal size, surface asperities which are governed by vacuum deposition conditions considerably influence the optical properties of the deposited films. A simultaneous study of the film by the electron diffraction technique offered a means to identify the nature of the film and also to correlate the structural and optical properties.

In order to investigate the optical properties, a spectrophotometer was designed and fabricated in this laboratory. This was then standardised and calibrated to evaluate the optical constants of thin films using the  $R_s$  and  $R_p$  method at oblique incidence.  $n$  and  $k$  were evaluated at various angle of incidence ( $\theta$ ),

such as  $45^\circ$ ,  $55^\circ$ ,  $65^\circ$  and it was found that there was no appreciable change in  $n$  and  $k$  with  $\theta$ . Therefore the optical constants were evaluated from  $R_s$  and  $R_p$  components of reflected light at a fixed angle of incidence,  $\theta = 45^\circ$ , which also served as a test for the homogeneity of the film satisfying the relation  $R_s^2 = R_p$  within the experimental error. The measurements were straight forward and the use of the homogeneity criterion  $R_s^2 = R_p$  also ensured that the results were correct and not affected by inhomogeneities due to structure. This method was found suitable even for semiconductors and other compounds. The optical properties of metals (Cu and Cr) and semiconductors such as elemental (Se and Te), oxidic ( $Cu_2O$ , CuO and  $Cu_2O + CuO$ ), chalcogenides ( $Cu_2S$ ,  $Cu_2Se$  and  $Cu_2Te$ ) and III-V compounds (InAs) have been studied in details.

In the case of copper films,  $n$  was found to decrease from 0.82 to 0.13 whereas  $k$  increased from 2.23 to 4.23 with the increase of the wavelength in the visible region ( $\lambda$  4500 Å - 7000 Å). Both  $n$  and  $k$  varied with the film thickness and reached a steady value when the deposits were sufficiently thick. For chromium films, the values obtained for  $n$  and  $k$  were similar to bulk values. The refractive index increased from 3.23 to 3.77 with the wavelength

(5000 Å - 7000 Å). It was also found that the optical constants varied with the film thickness and reached a steady value similar to that of the bulk as the film thickness increased. It was found that,  $n$  increased with the substrate temperature.

The variation of optical constants of copper and chromium with the film thickness appears to be due to the presence of discontinuities and voids expected in thin films, this tends to lower the optical constants.

For selenium films  $n$  increased with the wavelength, reached a maximum at  $\lambda$  5500 Å and then decreased. A peak in the index of refraction appears to be associated with the rapid change in the absorption coefficient near the fundamental absorption edge. Absorption coefficient was found to decrease with the increase of wavelength (4500 Å - 7000 Å). These films were however quite transparent in the red region, hence  $k$  was very low. The optical energy band gap was found to be 2.3 eV. Tellurium films were found to be nonhomogeneous and anisotropic, since  $R_s^2 = R_p$  did not hold good at  $\theta = 45^\circ$ .  $n$  varied from 2.40 to 3.76 in the visible region and  $\infty$  was found to decrease with the increase of wavelength. The absorption of light is accompanied by the direct and allowed transitions.

Studies made on different oxides of copper showed formation of two distinct species  $\text{Cu}_2\text{O}$  (ous) and  $\text{CuO}$  (ic) and a third one which was found to be  $\text{CuO}_{.67}$  (a mixture of  $\text{Cu}_2\text{O}$  and  $\text{CuO}$ ) by different conditions of oxidation. The optical constants were evaluated in each case for different wavelengths and film thickness. Optical constants were found to be independent of film thickness. It was found that the optical energy band gap increased with the oxygen constant in the oxides of copper namely, 2.05 for  $\text{Cu}_2\text{O}$ , 2.25 for  $\text{CuO}_{.67}$  and 2.36 for  $\text{CuO}$ . The optical transition of these oxides of copper films were found to be direct.

Electron diffraction study of cuprous sulphide films showed that the deposits formed at room temperature were amorphous or had a fine grained structure. The diffraction pattern of the deposits obtained at a higher substrate temperature conform to cubic structure, ( $a = 5.57 \text{ \AA}$ ) corresponding to  $\text{Cu}_{1.8}\text{S}$ . It was found that the refractive index of the sulphide film decreased from 2.50 to 1.84 with the increase of wavelength and showed a dispersion minima around  $\lambda 6000 \text{ \AA}$ , which may be due to the presence of absorption edge at that energy. The optical energy

band gap was found to be 2.12 eV (Goswami and Rao B.V., 1973). The variation of refractive index with the film thickness appears to be due to the predominance of voids, discontinuities <sup>etc.</sup> in thin films as suggested by Rouard (1952) from the Maxwell Garnett theory.

From the electron diffraction studies of the selenide and telluride of copper, it was found that the deposits conformed to  $\text{Cu}_2\text{Se}$  ( $a = 5.72 \text{ \AA}$ ) and  $\text{Cu}_2\text{Te}$  ( $a = 3.98 \text{ \AA}$  and  $c = 6.06 \text{ \AA}$ ). From the optical studies on  $\text{Cu}_2\text{Se}$  films, it was found that  $n$  was dependent on the deposition condition, such as substrate temperature and annealing in vacuo.  $n$  was found to vary from 2.62 to 2.36 with a peak at  $\lambda 6500 \text{ \AA}$  in the wavelength region  $\lambda 4500-7000 \text{ \AA}$ .  $n$  was also found to vary with the film thickness. From the absorption studies it was found that the optical transition ~~was~~ was indirect and allowed. From the optical studies on cuprous telluride films, it was found that the optical constants increased ( $n$ , from 2.52 to 3.40 and  $k$  from 0.45 to 0.92) with the wavelength  $4500 \text{ \AA} - 7000 \text{ \AA}$ .

Indium arsenide deposits had normal ZnS type structure with  $a = 6.05 \text{ \AA}$  at higher substrate temperature. Deposits formed at room temperature were amorphous or had a fine grained structure. The

refractive index was similar for both bulk and films,  $k$  however, slightly differed (Goswami, Rao B.V. and Prabhat Singh, 1973). From the absorption studies the optical transition was found to be direct.

The above study of the optical properties in the visible region gives some insight into the absorption of electromagnetic radiation and consequent changes caused, and also about electronic transport process and band gap of thin films. It also shows that the absorption process in thin films unlike the case of semiconducting properties were similar to bulk materials though the inherent defects present in these films may cause some minor modification in their magnitude. In fact the thin film optical constants can at least be taken as an approximate measure of bulk material, where their determination is difficult because of the preparation difficulties in suitable crystalline form. Further, the present study had to be restricted to the visible region because of limitation of the equipment and consequently some of the data concerning the absorption edge lying in the infra red or ultraviolet region could not be studied. A detailed study embracing infrared, visible and ultraviolet region of metals, semiconductor and insulator along with the electron

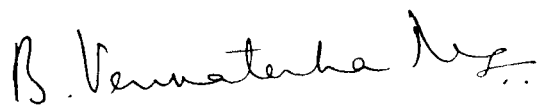
diffraction and electron microscopic study would throw a coherent picture regarding the process involving the absorption of electromagnetic waves.

### ACKNOWLEDGEMENTS

The author is extremely grateful to Dr. A. Goswami, Ph.D.(London), D.Sc.(London), Assistant Director, National Chemical Laboratory, Poona for his guidance, supervision, encouragement and keen interest throughout the work and his kindness in giving an opportunity to work in his "Electron Diffraction and Thin Film Division".

The author is thankful to the Director, National Chemical Laboratory, Poona for the permission to work as a guest worker and also to the Director, Armament Research and Development Establishment, Poona for the permission to work at NCL for the degree.

He also thanks his colleagues in the "Electron Diffraction and Thin Film Division" for their kind cooperation.



(B. VENKATESHA RAO)



REFERENCES

1. Abdullaev, G.B., Aliyarova, Z.A. and Asadov, G.A. (1967) Phys. Status. Solidi (Ger.) 21, 461.
2. Abdullaev, G.B., Aliyarova, Z.A., Zamanova and Asladev, G.A. (1968) Phys. Status. Solidi (Ger.) 26, 65
3. Abeles, F. (1950) J. Phys. Rad. 11, 310.
4. Abeles, F. (1957) J. Opt. Soc. Am. 47, 473.
5. Abeles, F. (1958) J. Phys. Radium 19, 327.
6. Adhav, R.S. (1960) Canad. J. Phys. 38, 1570.
7. Aggarwal, P.S. (1958) Ph.D. Thesis, Poona University.
8. Aliev, S.A. (1969) Fiz. Tekh. Paluprovodnikov (USSR) 3, 44.
9. Aliyarova, Z.A., Zamanova, E.N. (1966) Slozhnye Poluprov. Akad. Nauk. Azerb. SSR. Inst. Fiz 119 (Russ.).
10. Alsen, N. (1931) Geol. Fören Förh 53, 111.
11. Anderko, K. and Schubert, K. (1954) Z. Metallk 45, 371.
12. Asendorf, R.H. (1957) J. Chem. Phys. 27, 11.
13. Augello, S.J. (1942) Phys. Rev. 62, 371.
14. Avery, D.G. (1950) Phil. Mag. 41, 1018.
15. Avery, D.G. (1952) Proc. Phys. Soc. (Lond.) B65, 425.
16. Avery, D.G. (1953) Proc. Phy. Soc. Lond. B66, 133.
17. Baranova, R.V. and Pinskar, Z.G. (1964) Soviet Phys. Crystallography 9, 83.

18. Bardeen, J. Blatt, F.J. and Hall, L.H.  
(1954/6) Photoconductivity Conference; Wiley,  
N.Y.
19. Barlott (1925), Phys. Rev. 26, 247.
20. Barua, K.C. and Goswami, A. (1967) Ind. J.  
Pure and Appl. Phys. 5, 480.
21. Battom, V. (1949) Phys. Rev. 75, 1310.
22. Battom, V. (1952) Science 115, 570.
23. Baumeister, P.W. (1961) Phys. Rev. 121, 359.
24. Becker, A. and Schaper, J. (1944) Z. Phys.  
122, 49.
25. Bergmann and Hausler (1936) Z. Physik 100, 50.
26. Berzelius (1818) Acad. Handl. Stokkholm 39, 13.
27. Bhide, R.D. (1972) Ph.D. Thesis. Poona Univ.  
27a. Boettcher et al (1955) Z. Angew Phys. 7, 478.
28. Bode, H.W. (1945) Network Analysis of  
Feedback Amplifier Design, Van Nostrand,  
London and New York.
29. Bor, J. Hobson, A. and Wood, C. (1939) Proc.  
Phys. Soc. Lond. 51, 932.
30. Bradley, A.J. (1924) Phil. Mag. 48, 477.
31. Bradley, A.J. and Ollard, E.F. (1926) Nature,  
117, 122.
32. Brady, T.P. and Kunig (1966) Appl. Phys.  
Letter (USA), 9, 259.
33. Braithwaite, J.G.N. (1951) Proc. Phys. Soc.  
Lond. B64, 274.
34. Brattain, W.H. and Briggs, H.B. (1949)  
Phys. Rev. 75, 1705.
35. Brooks, H. (1955) Advances in Electronics and  
Electron Phys. Vol. 7; Academic Press, N.Y.

36. Buckel, W. and Hilsch, R. (1954) Z. Phys. 138, 109.
37. Buerger, N.W. (1941) Econ. Geol. 36, 19.
38. Buerger, M.J. and Buerger, N.W. Am. Mineral 29, 55.
39. Cartwright, C.H. and Schwarz, M.H. (1935) Proc. Roy. Soc. 148A, 648.
40. Cayrei Jean (1937) Comp. rend. 205, 488.
41. Celustka, B. and Ogerlec, Z. (1971) J. Phys. and Chem. Solids 32, 1449.
42. Chaudhari, N. (1965) Ind. J. Pure Appl. Phys. 3, 50.
43. Chikashinge, M. (1907) Zeitanorg Chem. 54, 50.
44. Collen, H.B. (1954) J. Chem. Phys. 22, 518.
45. Cox, J.T., Hass, G. and Jacobus, G.J. (1961) J. Opt. Soc. Am. 51, 714.
46. Cruzon, C.G. and Miley, H.A. (1940) J. Appl. Phys. 11, 631.
47. Czanderna, A.W. and Boyko, F.L. (1969) J. Vac. Sc. and Tech. 6, 746.
48. Dahl, J.P. and Switendick, A.C. (1966) J. Phys. Chem. and Solids 27, 931.
49. Davey, W.P. (1923) Phys. Rev. 21, 380.
50. David, E. (1937) Z. Phys. 106, 606.
51. Deokar, V.D. and Goswami, A. (1966) Proc. Int. Symp. on 'Basic problems in thin film physics' Clausthaus Gottingen p. 653.
52. Deokar, V.D. and Goswami, A. (1966) Ind. J. Pure and Appl. Phys. 4, 288.
53. Dexter, D.L. (1956) Phys. Rev. 101, 48.
54. Dighton, A.L. and Miley, H.A. (1942) Trans. Elect. Chem. Soc. 81, 321.

55. Dixit, K.R. and Agashe, V.V. (1955) Z. Naturf. 10a, 152.
56. Dixon, J.R. (1957) Phys. Rev. 107, 374.
57. Dowd, J.J. (1951) Proc. Phys. Soc. (Lond.) B64, 783.
58. Drude, P. (1891) Wied. Ann. 43, 126.
59. Drude, P. (1894) Ann. d. Physik 51, 77.
60. Dunholter, H. and Kerstein, H. (1939) J. Appl. Phys. 10, 523.
61. Ellis, S.G. (1967) J. Appl. Phys. 38, 2906.
62. Fan, H.Y. (1956) Rep. Progr. Phys. 19, 107.
63. Fieldman (1943) Phys. Rev. 64, 113.
64. Finch, G.I. and Wilman, H. (1937) Ingt. Exact. Nature, 16, 353.
65. Fischer, G. White, G.K. and Woods, S.P. (1957) Phys. Rev. 106, 480.
66. Fochs, P.D. (1950) J. Opt. Soc. Am. 40, 623.
67. Fochs, P.D. (1956) Proc. Phys. Soc. Lond. B69, 70.
68. Folberth, O.G., Madelung, O. and Weiss (1954).  
Z. Naturforsch. 9a, 954.
69. Ford, W.E. (1903) Amer. Journ. Science (4), 15, 169.
70. Fredrich, K. and Leraux, A. (1908) Met. 5, 355.
71. Fukuroi, T. Tanuma, S. and Tabisawa, S. (1949) Sci. Rep. Res. Insts. Tohoku Univ. A1. 365, 375.
72. Fukuroi, T. Tanuma, S. and Muto (1954) Sci. Repts. Res. Inst. Tohoku Univ. 6A, 18.
73. Gebbie, H.A. and Sakar, E.W. (1951) Proc. Phys. Soc. (Lond.) B64, 360.

74. Gebbie, H.A. and Kieley, D.G. (1952) Proc. Phys. Soc. (Lond.) B65, 553.
75. Gerelli, F. (1923) Atti. acca. Sci. Torino 58, 297; Rec. trav. Chim. 42, 818.
76. Ghosh, S.K. (1961) J. Phys. Chem. Solids 19, 61.
77. Gilileo, M.A. (1951) J. Chem. Phys. 19, 1291.
78. Goswami, A. and Jog, R.H. Ind. J. Pure and Appl. Phys. 2, 407.
79. Goswami, A. and Goswami, N.N. (1973) Ind. J. Pure and Appl. Phys. 11.
80. Goswami, A. and Ojha, S.M. (1973) Thin Solid Films 16, 187.
81. Goswami, A. and Trehan, Y.N. (1956) Trans. Faraday Soc. 52, 358.
82. Goswami, A. and Trehan, Y.N. (1957) Proc. Phys. Soc. Lond. B70, 1005.
83. Goswami, A. and Trehan, Y.N. (1958) Trans. Faraday Soc. 54, 1703.
84. Goswami, Amit. P. (1973) Ph.D. Thesis, Poona University.
85. Goswami, A. and Rao, B.V. (1973) Ind. J. of Pure and Appl. Phys. (accepted for publication).
86. Goswami, A., Rao, B.V. and Prabhat Singh (1973) Ind. J. Pure and Appl. Phys. (under publication).
87. Gunthur, K.G. (1958) Z. Naturforsch 139, 1081.
88. Gunthur, K.G. and Freller, H. (1961) Z. Naturforsch (Germany) 16a, 279.
89. Haken, W. (1910) Ann. Phys. 32, 291.
90. Hall, J.F. and Furgusson, W.F.C. (1955) J. Opt. Soc. Am. 45, 74.

91. Halliday, J.S., Rymer, T. B. and Wright, K.H.R. (1954) Proc. Roy. Soc. A225, 546.
92. Harbeke, G. (1957) Abhandl. Braunsch. Wiss. Gesell 9, 180.
93. Harman, T.C., Goering, H.L. and Beer, A.C. (1956) Phys. Rev. 104, 3562.
94. Hartel (1954) Siemens - Z.28 No.8, 376.
95. Hartig, P.A., Loferski, J.J. and Miller (1961) Phys. Rev. 83, 876.
96. Hartig, P.A., Loferski, J.J. and Miller, R.F. (1952) Phys. Rev. 86, 652.
97. Hartig, P.A. and Loferski, J.J. (1954) J. Opt. Soc. Amer. 44, 17.
98. Hartman (1936) Z. Physik. 102, 709.
99. Hartwig, W. (1926) Z. Kristallogr. 64, 503.
100. Hass, G. (1942) Kolloid Z., 100, 230.
101. Hass, G. and Thun, R.E. (1964) 'Physics of Thin Films' Vol. 2. Academic Press, Newyork and London p.324.
102. Heavens, O.S. (1955) 'Optical Properties of Thin Solid Films' Butterworths, London.
103. Heavens, O.S. (1964) Physics of Thin films. 2, Academic Press, Newyork and London p.193.
104. Henderson, G. and Weaver, C. (1966) J. Opt. Soc. Am. 56, 1551.
105. Henkels, H.W. (1950) J. Appl. Phys. 21, 725.
106. Henkels, H.W. and Maczuk, J. (1953) J. Appl. Phys. 24, 1056.
107. Heyding, R.D. (1966) Canad. J. Chem. 44, 1233.
108. Hill, R.M. and Weaver, C. (1958a) Trans. Far. Soc. 54, 1140.

109. Hill, R.M. and Weaver, C. (1958b) Trans. Far. Soc. 54, 1464.
110. Hilsum, C. (1956) Proc. Phys. Soc. Lond. B69, 506.
111. Hilsum, C. (1957) Proc. Phys. Soc. Lond. B70, 1011.
112. Hirahara, E. (1936) J. Phys. Soc. Japan 2, 211.
113. Hocart, R. and Mole, R. (1952) C.R. Acad. Sci. Paris 234, 111.
114. Holland, L. (1958) "Vacuum Deposition of Thin Films" Chapman and Hall Ltd., London.
115. Howson, R.P. (1968) Brit. J. Appl. Phys. 1, 15.
116. Howson, R.P. (1968) *ibid* 1, 939.
117. Humphreys-Owen, S.P.F. (1960) Proc. Phys. Soc. Lond. 77, 949.
118. Iaczak, E.F. (1963) Optics and Spectroscopy, 15, 54.
119. Iaczak, E.F. (1967) Optics and Spectroscopy, 22, 504.
120. Ioffe, A.V. (1937) Physik Z., Sowjeet Union 11, 241.
121. Jha, K.N. and Korgaonkar, A.V. (1972) Thin Solid Films 9, 133.
122. Johnson, J.E. (1966) J. Appl. Physik. 37, 2188.
123. Juse, W. and Kurtschetow, B.W. (1932) Physik, Zeits Sowjetunion, 2, 453.
124. Kickoin, I.K. (1938) J. Exptl. Theoret. Phys. (USSR) 8, 826.
125. Kikoin, I.K. and Simenko, D.L. (1940) J. Exptl. Theoret. Phys. (USSR) 1030.
126. Koehler, W.F., Odenchantz, F.K. and White, W.C. (1959) J. Opt. Soc. Am. 49, 109.

127. Kostyeik, V.P. and Shklyarevskii, I.N. (1964) Optics and Spectroscopy 16, 165.
128. Kozheurov, V.A. (1939) Colloid, J. (USSR) 5, 45.
129. Kretzmann, R. (1940) Ann. Physik. 37, 303.
130. Kroliskowski, W.P. (1969) Phys. Rev. 185, 882.
131. Kuhrt, F. (1954) Siemens - Z. 28, 370.
132. Kunig, H.F. (1968) Solid State Electronics 11, 335.
133. Kurdyumova, R.N. (1968) Kristallografiya USSR 13, 796 Eng. translation in Soviet Phys. Cryst. (USA).
134. Kurdyumova, R.N. (1969) Soviet Phys. Cryst. 13, 689.
135. Ladelfe, A., Czanderna, A.W. and Biegan, J.R. (1972) Thin Solid Films 10, 403.
136. Lebrun, J. and Bescond, F. (1968) Onde Elect. (France) 48, 351.
137. Lisitsa, M.P. and Tsvelykh, N.G. (1958) Optics and Spectroscopy 19, 62.
138. Loferski, J.J. (1952) Phys. Rev. 87, 904.
139. Loferski, J.J. (1954) Phys. Rev. 93, 707.
140. Lu, S.S. and Chang, Y.L. (1941) Proc. Phys. Soc. Lond. 53, 517.
141. Macfarlane, G.G. and Roberts, V. (1955) Phys. Rev. 98, 1865.
142. Male, D. (1950) C.R. Acad. Sci. Paris. 230, 1349.
143. Male, D. (1954) Ann. Chim. Paris 9, 145.
144. Margottet (1879) Recherches, Surles Sul Furesles Seleniures etles tellures metallique, Paris.



145. Marshall, R. and Mitra, S.S. (1965) *J. Appl. Phys.* 36, 3882.
146. Mayer, H. (1959) *Structure and Properties of Thin Films* p.225, Wiley, Newyork.
147. Mayer, H. (1961) *Symposium on Electronics and Magnetic Properties of Thin Layers*, Louvin, Belg.
148. Maxwell-Garnett, J.C. (1904) *Trans. Roy. Soc. Lond.* 203A, 385.
149. McCarthy, J.P. (1967) *Solid State Electronics* 10, 649.
150. Meir, W. (1910) *Ann. Phys. Lpz.* 31, 1017.
151. Merwin, H.E. and Larsen, E.S. (1912) *Amer. J. of Science* 34, 42.
152. Miller, R.F. (1925) *J. Opt. Soc. Am.* 10, 621.
153. Minor, R.S. (1904) *Ann. der. Phys.* 10, 193.
154. Mole, R. (1954) *Ann. Chim. (Paris)* 9, 145.
155. Motts, N.F. and Jones, H. (1936) *Properties of metals and alloys*, Oxford Univ. Press.
156. Morrison, R.E. (1961) *Phy. Rev.* 124, 314.
157. Moss, T.S. (1949) *Proc. Phys. Soc. Lond.* A62, 264.
158. Moss, T.S. (1952) *Proc. Phys. Soc. Lond.* B65, 62.
159. Moss, T.S. (1959) *Optical Properties of Semiconductors*, Butterworth Scientific Publications, 1959.
160. Murmann, H. (1933) *Z. Phys.* 80, 161.
161. Nakayama, N. (1968) *J. Phys. Soc. Jap.* 25, 290.
162. Nasledov, D.N., A. Yu. Khalilov (1956) *Zhur. Tekh. Fiz.* 26, 251.
163. Nassbaum, A. (1954) *Phys. Rev.* 94, 337.

164. Neuberger, M.C. (1931) Z. Krist. 77, 169.
165. Niggili, P. (1922) Z. Krist. 57, 253.
166. Nowatny, H. (1946) Z. Metallik, 37, 40.
167. Nozieres, P. and Pines, D. (1958) Phys. Rev. 109, 741, 762, 1062.
168. Oftegal, I. (1932) Z. Krist. 83, 9.
169. Ogerlek, Z. and Celustka, B. (1966) J. Phys. Chem. Solids 27, 615.
170. Okada, T. and Uno, R. (1944) J. Phys. Soc. Japan 4, 351.
171. Okamoto, K. (1971) Jap. J. Appl. Phys. 10, 508.
172. Parkman (1861) Amer. Journ. Sci. (2) 33, 334.
173. Pashley, D.W. (1959) J. Inst. Met. 87, 419.
174. Pastrnyak, I. (1961) Sov. Phys. Solid State 3, 633.
175. Pastrnak, J. (1961) Czech. J. Phys. 11, 374.
176. Patzek, L. (1956) Z. Metallik 47, 418.
177. Payan, R. and Rasagini, G. (1962) C.R. Acad. Sci. (France) 254, 1272.
178. Pfound, A.H. (1916) Phys. Rev. 7, 289.
179. Piccard, R.G. and Duffendeck, C.S. (1943) J. Appl. Phys. 14, 291.
180. Pilling, N.B. and Bedworth, R.F. (1923) J. Inst. Met. 29, 529.
181. Pinsker, Z.G. (1953) "Electron Diffraction" (Butterworth, London).
182. Potter, R.F. (1966) Appl. Opt. 5(1), 35.
183. Puschin, N.A. (1908) Journ. Russ. Phys. Chem. Soc. 39, 13.
184. Rahlf, P. (1936) Z. Phys. Chem. (B), 31, 157.

185. Ramazanov, K.A. (1962) Soviet Physics Solid State 3, 1640.
186. Reinhold, H. and Mohring, H. (1937) Z. Physik. Chem. B38, 221.
187. Roberts, S. (1960) Phys. Rev. (1960) 118, 1509.
188. Roberts, H.S. and Ksanda, C.J. (1929) Am. J. Sci. 17, 489.
189. Robin, S. (1952) J. Phys. Raa. 13, 493.
190. Rose, A.J. (1946) C.R. Acad. Sci. Paris, 222, 805.
191. Rosenfield, L. (1951) "Theory of Electrons" North Holland Publishing Co. Amsterdam.
192. Rouard, M.P. (1952) Comp. Rend. 235, 1587.
193. Roulie, R. Sudres, M. Mahene, J. (1970) Rev. Chim. Miner (France) 7, 713.
194. Saker, E.W. (1952) Proc. Phys. Soc. Lond. B65, 785.
195. Scanton (1948) Ph.D. thesis, Purdue Univ.
196. Schmidt, P. (1954) Ann. Physik. 14, 265.
197. Schridt and Wasserman (1927) Zeitz. f. Physik. 46, 653.
198. Schopper (1952) Z. Physik. 131, 215.
199. Schulz, L.G. (1954) J. Opt. Soc. Am. 44, 540.
200. Schulz, L.G. and Tangherlini, F.R. (1954) J. Opt. Soc. Am. 44, 362.
201. Selle, V. and Maege, J. (1968) Phys. Status Solidi (Ger) 30, 153.
202. Senett, R.S. and Scott, G.D. (1950) J. Opt. Soc. Am. 40, 203.
203. Semenko, D.L. (1938) J. Exptl. Theoret. Phys. USSR 8, 836.

204. Skinner (1917) Phys. Rev. 9, 148.
205. Slattery, M.K. (1923) Phys. Rev. 21, 378.
206. Slattery, M.K. (1925) Phys. Rev. 25, 333.
207. Smith, W. (1873) Nature 7, 303.
208. Sorokin, G.P. (1965) Soviet Phys. J. USA 4, 92.
209. Sorokin, G.P. Yu. M. Papshev and P.T. Oush (1966) Soviet Phys. Solid State 7, 1810.
210. Stewart, R.W. (1948) Canad. J. Res. 26, 230.
211. Strong, J. (1935) Rev. Sci. Instrum. 16, 143.
212. Stuke, J. (1953) Z. Phys. Lpz. 134, 194.
213. Sulman, S.G. and Yu. I. Ukhencv (1965) Soviet Phys. Solid State 7, 768.
214. Talley, R.M. and Enlight, D.P. (1954) Phys. Rev. 95, 1092.
215. Thomson, G.P. and Cochrane, W. (1939) "Theory and Practice of Electron Diffraction" MacMillan, London.
216. Thomson, G.P. (1930) Proc. Roy. Soc. 128A, 649.
217. Tibbals, C.A. (1909) Bull Univ. Wisconsin, 274 and J. Amer. Chem. Soc. 31, 902.
218. Tolansky, S. (1948) "Multiple Beam Interferometry" Lond. Oxford Univ. Press.
219. Tool, A. (1910) Phys. Rev. 31, 1.
220. Toth, R.S., Kilkson, R. and Trivich, D. (1961) Phys. Rev. 122, 482.
221. Toshihiro and Okeda (1949) Bussuron Kenkyu (Researches on Chem. Phys.) No.19, 15.
222. Tunnel, G., Pesnjak, E. and Ksanda, C.J. (1935) Z. Krist. A90, 120.

223. Ueda, R. (1949) J. Phys. Soc. Japan 4, 287.
224. Valeev, A.S. and Gisan, M.A. (1965) Optics and Spectroscopy, 19, 62.
225. VanDyke, G.D. (1922) J. Opt. Soc. Am. 6, 917.
226. Van Rippel, A. (1948) J. Chem. Phys. 16, 372.
227. Van Vachten, J.A. (1969) Phys. Rev. 182, 891.
228. Vasicek, A. (1947) J. Opt. Soc. Am. 37, 145.
229. Vlasov, V.A. and Semiletov, S.A. (1968) Kristallografiya (USSR) 12, 734.
230. Vogt, W. (1931) Ann. Physik. 7, 183.
231. Voigt, W. (1910) Phys. Zeit 2, 303.
232. Von Auwers and Kerchbaum (1930) Ann. Phys. Lpz. 7, 129.
233. Wait, G.R. (1922) Phys. Rev. 19, 615.
234. Weaver, C. and Hill, R.M. (1959) Phil. Mag. 4, 1107.
235. Weichmann, F.L. and Kuzel, R. (1970) Canad. J. of Phys. 48, 63.
236. Weimer, P.K. (1950) Phys. Rev. 79, I, 171.
237. Weimer, P.K. (1964) Proc. I.E.E.E. 52, 608.
- 237a. Weiss, H. (1961) Solid State Electronics 1, 225.
238. Weld, R.D. (1922) J. Opt. Soc. Am. 6, 67.
239. Weld, R.D. (1961) Solid State Electronics 1, 225.
240. Wemple, S.H. and DiDomenico, D. (1971) Phys. Rev. 53, 1338.
241. White, W.P. (1933) J. Am. Chem. Soc. 55, 1047.
242. White, A.H. and Germer, L.H. (1942) Trans. Elect. Chem. Soc. 81, 305.

- 243. Wieder, H. and Czanderna, A.W. (1962) J. Phys. Chem. 66, 816.
- 244. Wieder, H. and Czanderna, A.W. (1966) J. Appl. Phys. USA 37, 184.
- 245. Wilson, A.H. (1931) Proc. Roy. Soc. 133A, 458.
- 246. Williams, R.C. and Backus, R.C. (1949) J. Appl. Phys. 20, 98.
- 247. Wold, P.S. (1916) Phys. Rev. 7, 163.
- 248. Wolter, H. (1937) Z. Phys. 105, 269.
- 249. Wood, R.W. (1902) Phil. Mag. 3, 607.
- 250. Young, A.P. and Schwarz, C.M. (1969) J. Phys. Chem. Solids 30, 249.
- 251. Yamaguchi, T (1938) Proc. Phys. Math. Soc. Japan 20, 230.